

COUPLING OF CO<sub>2</sub> AND CS<sub>2</sub> WITH NOVEL OXIRANES:  
POLYCARBONATE VS. CYCLIC CARBONATE PRODUCTION

A Dissertation

by

STEPHANIE JO WILSON

Submitted to the Office of Graduate Studies of  
Texas A&M University  
in partial fulfillment of the requirements for the degree of

DOCTOR OF PHILOSOPHY

Approved by:

Chair of Committee,	Donald J. Darensbourg
Committee Members,	Timothy R. Hughbanks
	Hong-Cai Joe Zhou
	Nicole S. Zacharia
Head of Department,	David H. Russell

August 2013

Major Subject: Chemistry

Copyright 2013 Stephanie Jo Wilson

## ABSTRACT

Polycarbonates are a type of engineering thermoplastic that have countless uses in modern society. Currently, the major industrial production of polycarbonates involves the polycondensation of a diol and phosgene or phosgene derivative. Though there are many advantages to this process, it creates large amounts of waste and requires dangerous chemicals in order to proceed. Over the past four decades, the coupling of CO<sub>2</sub> and epoxides has grown into a viable, greener alternative for the production of select polycarbonates. The byproduct of this reaction, cyclic carbonates, also have use as polar, high boiling solvents.

This dissertation will be divided into three parts. First, the coupling of indene oxide and CO<sub>2</sub> to form poly(indene carbonate) and *cis*-indene carbonate will be discussed. Poly(indene carbonate) has the highest T<sub>g</sub> yet reported for polymers derived CO<sub>2</sub>/epoxides coupling, up to 138 °C. Polycarbonate production requires the use of (salen)Co(III) catalysts and low temperatures, though some cyclic carbonate production is still observed. Selective production of poly(indene carbonate) has been achieved through the use of bifunctional cobalt(III) complexes. The effects of temperature and cosolvent choices on polymer production will be thoroughly discussed.

Though polycarbonate is the kinetic product from the coupling of CO<sub>2</sub> and epoxides, the thermodynamic product is cyclic carbonate. There are six potential mechanisms that yield this undesired byproduct, though there is limited research into which pathways are the most active during polymerization reactions. Temperature-

dependent kinetic studies were performed to obtain the activation parameters for the direct, polymer-free coupling of cyclopentene oxide, indene oxide, 1,2-butylene oxide, and styrene oxide with CO<sub>2</sub> utilizing (salen)CrCl/*n*Bu<sub>4</sub>NCl to yield their corresponding cyclic carbonates. Additionally, the metal-free backbiting of the singly-coupled styrene oxide/CO<sub>2</sub> intermediate was simulated utilizing the halohydrin 2-chloro-1-phenylethanol.

Finally, the coupling of cyclopentene oxide with carbon disulfide to yield poly[thio]carbonates and cyclic [thio]carbonates utilizing (salen)CrCl/PPNX will be discussed. In each reaction, scrambling of the oxygen and sulfur atoms in both the polymeric and cyclic product is observed. Long reaction times lead to increased amounts of [thio]ether linkages and therefore polymers with lower glass transition temperatures. Insights into both the coupling and scrambling mechanisms will be presented.

## DEDICATION

I dedicate this dissertation to my wonderful family. My parents, Mary Jo and Rick, have never failed in their support for me in the classroom, on the volleyball court, or in every other aspect of life. Thanks to my brother and sister, sister-in-law, nieces, and nephew for their faith and encouragement. I love you all very much.



## ACKNOWLEDGEMENTS

First and foremost, I would like to thank my advisor, Prof. Don Darensbourg. What started as a summer internship transformed into an exciting world full of science, learning, and teaching. Don, I would especially like to thank you for your patience, guidance, and for sharing many helpful conversations and needed laughs about anything from my confusing results to the antics of freshman chemistry students. I have never regretted my decision to come and work for you. I would also like to thank Professors Timothy Hughbanks, Hongcai (Joe) Zhou, and Nicole Zacharia for serving on my dissertation committee, and Professor Marcetta Darensbourg for her support with my research. You have each helped to make me a better scientist, and I appreciate your help and guidance. My research and stipend have largely been funded by the Department of Energy Office of Science Graduate Student Fellowship (DOE-SCGF). This fellowship has provided me with countless opportunities, and I am extremely grateful for its honor.

Science has always fascinated me. As a young girl, I was obsessed with the ideas of dinosaurs and outer space. I am fairly certain that if it were not for the sheer amount of physics involved in astronomy, I would have gone into that field. But, it was Chemistry & AP Chemistry with Mr. Dan Wunderlich that won me over. Eventually, a polymer class with Dr. Brian Mullen evolved into a summer internship with GE Plastics, and I had found an exciting new world that I could not wait to explore.

I have always had phenomenal support from my family and friends. My parents Jo and Rick are absolutely wonderful. They have always been so giving, loving, and

encouraging in every aspect of my life. My sister Jessica, brother Kyle, sister-in-law Aimée, and my wonderful nieces and nephew Michelle, Elizabeth, and Jacob help to keep me grounded and remind me of the important things in life. My extended family of aunts, uncles, cousins, and the late great Leona Chinn have always believed in me. I would like to thank the Meadows and Otter Creek extended families for your kindness over the years. Liesl Goecker and Rondrell Moore were some of the first and most wonderful friends I ever made. These are each that special brand of friendship, where miles and months can pass without contact, and the minute you catch up it is as if not a single day has passed. High school pals Alison, Whitney, Kim, Andrea, Brooke, Sammy, etc. provided me with an abundance of laughter and happy memories.

Admittedly, I had no idea what I wanted to do when it came to applying to college. I was fortunately recruited to play volleyball at the University of Southern Indiana. I cannot imagine a better place for me than USI – I was blessed with incredible teammates (Go Eagles!), wonderful friends, and phenomenal professors who truly cared about their students' education. Drs. Shelly Blunt and Adrian Gentle deserve particular praise. Neither of you have any idea what your support in school and now friendship has meant to me. I hope to one day be as great as of an educator as you. Also, thanks to Dr. Evan Millam for giving the most accurately awful description of graduate school.

Jill (Myrick) Scheirer and Molly (Rahman) Steftenagel quickly transformed from my college roommates into my best friends. Every bit of college was better because the two of you were in it. I am so happy to be moving back closer to you both. I cannot leave out Tim Scheirer, the guy who so proudly became our friend all thanks to *The*

*Sound of Music*. Rock on, Timmy. My chemistry friends Emily Kraft, Stephanie (Schenk) Bates, Lauren Adcock, and Brian Bates know how to throw the very best dinner parties in the Midwest. I do not know how many bottles of wine we consumed, but I do know that a good time was had by all.

Though we may not have known each other in the happiest of times in our lives, I am eternally grateful to my Texas A&M friends and colleagues for bringing life and fun to these past four years. I can say without doubt that the D.J. Darensbourg research group is [one of] the best in the department. Together with past and current members Dr. Jeremy Andreatta, Dr. Osit Karroonnirun, Dr. Shawn Fitch, Dr. Adriana Moncada, Dr. Adolfo Horn, Dr. Guang-Peng Wu, Dr. Bo Li, Dr. Fu-Te Tsai, Chris Costanzo, Erica Shepp, Samuel Kyran, Yuraima Fonseca, Andrew Yeung, Joanna Chung, and Yanyan Wang, I have shared countless conversations (intellectual and otherwise), breakfast tacos, kolaches, birthday cake, and wonderful, laughter-filled memories. Dr. Sheng-Hsuan Wei in particular has been an invaluable friend and comrade-in-arms during the entirety of my graduate school career. I must thank my friends in the M.Y. Darensbourg group, with particular thanks to Jason Denny, Dr. Scott Brothers, and Tiffany Pinder. The phenomenal Ethel Mejia, Sandy Manning, Julie Zercher, Will Seward, and Dr. Yohannes Renzom have answered countless questions and been invaluable during my time at A&M.

Away from work, Michael Eller and the rest of the softball crew provided me with so many laughs, meaningless conversations, and a reason to sit outside and enjoy a beer on nice Texas evenings. Sam Timpa has kept me sane during our tenure in charge

of Phi Lambda Upsilon. Georgette Lang understands that guacamole sometimes needs just a bit/lot more garlic. Nick Fox is one of those wonderful friends who will always be there to listen when you need it most. Mary and Shep Poland have been incredibly kind and supportive and provided me with countless escapes away from the doldrums of graduate school. And, my dog Rudy “Rudebaker” Wilson has given me wonderful excuses to go for long walks, take trips to the park, or snuggle up on the couch.

In addition to my larger group of friends, a few more people deserve specific shout outs – the people who have been my closest confidants during my tenure at A&M. Dr. Jen Hess helped to guide me through my first two years with laughter, mixed drinks, ‘90s music, and 5:00 AM trips to Snook. Brian Eoff has been an amazing friend who thankfully understands little to nothing about chemistry. Danielle Crouthers (along with her wonderful fiancée Justin) has been my dearest friend, without whom I am not sure I would have survived graduate school. And last, but certainly not least, I want to thank my best friend in the whole world, Dr. Ross Poland. They say to never date within your research group, and ignoring that advice was the best decision I have ever made.

Finally, thanks to the casts, writers, and crews of *Psych*, *How I Met Your Mother*, *Parks and Recreation*, *Arrested Development*, *Twin Peaks*, and *Third Rock from the Sun*, the people behind [google.com/news](http://google.com/news), TAMU’s Aggie Athletics, Dash Harris, the state of Louisiana for being just the way it is, bluebonnets, H.E.B., NASA’s Astronomy Picture of the Day, Misty May Treanor and Kerri Walsh Jennings, Queen, the Houston Rockets, the Indianapolis Colts and Pacers, the New York Mets, The Muppets (particularly Rowlf), Mika, and Netflix.

## NOMENCLATURE

$A_i$	Absorbance at time = infinity
$A_t$	Absorbance at time = t
ATR	Attenuated Total Reflectance
A.U.	Absorbance units
$CDCl_3$	Deuterated Chloroform
CHC	Cyclohexene Carbonate
$CH_2Cl_2$	Dichloromethane
CHO	Cyclohexene Oxide
$cm^{-1}$	Wavenumbers
$CO_2$	Carbon Dioxide
COS	Carbonyl Sulfide
CPC	Cyclopentene Carbonate
CPO	Cyclopentene Oxide
$CS_2$	Carbon Disulfide
Deg.	Degrees
DBU	1,8-diazabicycloundec-7-ene
DMC	Double Metal Cyanide
DNP	2,4-dinitrophenoxide
DSC	Differential Scanning Calorimetry
$E_A$	Activation Energy

eqn	Equation
FT-IR	Fourier Transform-Infrared Spectroscopy
GC-MS	Gas Chromatography-Mass Spectrometry
HCl	Hydrochloric Acid
IC	Indene Carbonate
IO	Indene Oxide
IR	Infrared Spectroscopy
$k_{\text{obs}}$	Observed Rate Constant
MeOH	Methanol
MHz	megahertz
MPa	megapascals
$M_n$	Number-Average Molecular Weight
$M_w$	Weight-Average Molecular Weight
$n\text{Bu}_4\text{N}$	tetra- <i>n</i> -butyl ammonium
NMR	Nuclear Magnetic Resonance
PC	Propylene Carbonate
PDI	Polydispersity Index
PCHC	Poly(cyclohexene carbonate)
PO	Propylene Oxide
PPC	Poly(propylene carbonate)
ppm	parts per million
PPN	Bis(triphenylphosphine)iminium

R.T.	Room Temperature
(salen)CoY	<i>N,N'</i> -bis(3,5-di- <i>tert</i> -butylsalicylidene)-1,2-cyclohexanediamino cobalt(III) 2,4-dinitrophenoxide
(salen)CrCl	<i>N,N'</i> -bis(3,5-di- <i>tert</i> -butylsalicylidene)-1,2-cyclohexanediamino chromium(III) chloride
t	time
T	Temperature
<i>t</i> Bu	<i>tert</i> -butyl
TBD	1,5,7-triabicyclo[4,4,0] dec-5-ene
TGA	Thermogravimetric Analysis
$T_d$	Onset Polymer Decomposition Temperature
$T_{d50}$	Temperature at which 50% of the polymer has decomposed
$T_g$	Glass Transition Temperature
$T_m$	Melting Temperature
TOF	Turnover Frequency
XRD	X-ray Diffraction
X	Halogen or Pseudohalogen
Y	2,4-dinitrophenoxide

## TABLE OF CONTENTS

	Page
ABSTRACT .....	ii
DEDICATION .....	iv
ACKNOWLEDGEMENTS .....	v
NOMENCLATURE.....	ix
TABLE OF CONTENTS.....	xii
LIST OF FIGURES.....	xiv
LIST OF TABLES .....	xxi
CHAPTER I INTRODUCTION AND LITERATURE REVIEW.....	1
Industrial Production of Polycarbonates .....	1
Carbon Dioxide as a C1 Feedstock .....	4
Catalytic Coupling of CO <sub>2</sub> and Epoxides.....	6
Recent Efforts to Expand CO <sub>2</sub> /Epoxides Copolymerization Process .....	10
Traditional Metal Catalysts .....	11
Chain Transfer.....	13
Notable Recent Catalytic Developments .....	15
Cyclic Carbonate Production .....	19
Kinetics and Thermodynamics of Epoxides/CO <sub>2</sub> Coupling.....	21
Poly(Cyclohexene Carbonate) .....	23
Sulfur-Containing Polymers and Cyclic (Thio)carbonates .....	24
Carbon Disulfide/Oxirane Coupling Reactions .....	25
Physical Methods for the Characterizations of Coupling Products .....	26



	Page
CHAPTER II SYNTHESIS OF POLY(INDENE CARBONATE) FROM INDENE OXIDE AND CO <sub>2</sub> : A POLYCARBONATE WITH A RIGID BACKBONE.....	29
Introduction.....	29
Experimental.....	31
Results and Discussion.....	36
Conclusions.....	56
Future Work.....	57
CHAPTER III KINETICS OF CYCLIC CARBONATE FORMATION UTILIZING (SALEN)CrCl .....	60
Introduction.....	60
Experimental.....	63
Results and Discussion.....	73
Conclusions.....	96
Future Work.....	98
CHAPTER IV COPOLYMERIZATION OF CYCLOPENTENE OXIDE AND CARBON DISULFIDE: SELECTIVITY FOR POLYMER VS. CYCLIC [THIO]CARBONATES .....	100
Introduction.....	100
Experimental.....	102
Results and Discussion.....	112
Conclusions.....	136
Future Work.....	138
CHAPTER V SUMMARY AND CONCLUSIONS .....	141
REFERENCES.....	148
APPENDIX A .....	158
APPENDIX B .....	160
APPENDIX C .....	181
APPENDIX D .....	188
APPENDIX E .....	191

## LIST OF FIGURES

FIGURE		Page
I-1	Schematic representing the typical industrial phosgene-based process for BPA-polycarbonate production .....	3
I-2	CO <sub>2</sub> as a starting material for chemical transformations .....	5
I-3	Epoxides that have been successfully copolymerized with CO <sub>2</sub> as of May 2013 .....	9
I-4	Traditional (salen)M(III)X catalyst with PPNX and <i>n</i> Bu <sub>4</sub> NX onium salt cocatalysts.....	12
I-5	Skeletal representation and crystal structure of ( <i>R,R</i> )- <i>N,N'</i> -bis(3,5-di- <i>tert</i> -butylsalicylidene)-1,2-cyclohexanediaminochromium(III) chloride, commonly referred to as (salen)CrCl.....	12
I-6	Refractive Index trace (GPC, 1 mL/min THF eluent) of bimodal poly(indene carbonate) sample .....	14
I-7	Two methods for copolymer production, through ( <i>a</i> ) direct initiation or ( <i>b</i> ) chain transfer. For clarity, the metal has not been included.....	14
I-8	Nozaki's cobalt catalyst with attached piperidenyl arms is capable of shuffling protons between polymer chains and attached amines .....	16
I-9	Highly active cobalt catalyts containing four appended quarternary amine arms from Lee and coworkers. Y = 2,4-dinitrophenoxide .....	17
I-10	Modified (salen)Co(III)X complexes from Lu and coworkers .....	19
I-11	Possible coordination modes, <i>trans</i> - and <i>cis</i> -, for (salen)Co(III)X complexes.....	19
I-12	Six mechanisms by which <i>trans</i> - and <i>cis</i> -cyclic carbonates can be produced.....	21
I-13	Free energy reaction coordinate diagram for the coupling of epoxides with CO <sub>2</sub> .....	22

FIGURE		Page
I-14	High pressure ASI® ReactIR 1000 system setup utilized by the D.J. Darensbourg labs at Texas A&M University.....	27
I-15	ReactIR™ ic10 system for ambient pressure measurements purchased from Mettler Toledo.....	27
II-1	Thermal ellipsoid representation of ( <i>IS,2R</i> )-indene oxide (left) and dihydronaphthalene oxide (right) with ellipsoids at 50% probability surfaces. Hydrogen atoms have been omitted for clarity. Bond angles and lengths are identical for the ( <i>IR,2S</i> )-indene oxide enantiomer.....	37
II-2	Catalyst system for the copolymerization of indene oxide and CO <sub>2</sub> . <i>N,N'</i> -bis(3,5-di- <i>tert</i> -butylsalicylidene)-1,2-cyclohexanediamino cobalt(III)-2,4-dinitrophenoxide, (salen)CoDNP, (1) and PPN-2,4-dinitrophenoxide, PPNDNP.....	38
II-3	Thermal ellipsoid representation of <i>cis</i> -indene carbonate with ellipsoids at 50% probability surfaces. All hydrogens have been omitted for clarity except H1 and H2 to display the <i>cis</i> - nature of the product. Inset image is looking down the C2-C1 bond, displaying the torsion in the five-membered cyclic ring. O1-C1-C2-O2 dihedral angle = 14.187°; O4-C11-C12-O5 torsion dihedral = 8.252°.....	40
II-4	Relevant data from the second cycle of the DSC thermogram of the polymer sample from Table II-2, entry 3. T <sub>g</sub> = 134 °C.....	44
II-5	TGA curve of polymer sample from Table II-2, entry 3.....	44
II-6	Carbonate O-(C=O)-O peak in the <sup>13</sup> C NMR of poly(indene carbonate) samples from Table II-2 entry 1 (green), entry 2 (blue), and entry 3 (red). CDCl <sub>3</sub> , 125 MHz.....	45
II-7	Bifunctional catalysts 2 with -NEt <sub>2</sub> Me arm (top left), 3 with -NCy <sub>2</sub> Me arm (top right), and 4 with appended TBD group (bottom left) were generously donated by the Xiao-Bing Lu Group of Dalian University of Technology in Dalian, China. Bifunctional catalyst <b>5</b> bearing the out of pocket Co(III) metal center was generously donated by Dr. Bun Yeoul Lee of Ajou University in Suwon, South Korea.....	48

FIGURE		Page
II-8	Proposed polymerization mechanism by bifunctional catalysts. The electrostatic attraction between the free polymer anion and the ammonium salt prevents polymer backbiting to cyclic carbonate .....	52
II-9	Potential backbiting reactions for the formation of <i>cis</i> -indene carbonate .....	53
II-10	$M_n$ of poly(indene carbonate) vs $T_g$ displaying dependence of the thermal transition on the molecular weight of these species.....	54
II-11	$^1\text{H}$ NMR of purified poly(indene carbonate) sample. Bulk polymer signals can be observed at 6.2 and 5.5 ppm. X's signals can be observed at 5.9 and 4.7 ppm. 500 MHz, $\text{CDCl}_3$ .....	55
II-12	$^{13}\text{C}$ NMR of the carbonate $\text{O}(\text{C}=\text{O})\text{O}$ purified poly(indene carbonate) sample. Bulk polymer signal can be observed at 154.4 ppm. X can be observed at 155.8 ppm. 125 MHz, $\text{CDCl}_3$ .....	55
III-1	Six potential mechanisms for <i>in situ</i> backbiting to form cyclic carbonate .....	62
III-2	O-C-C-O dihedral angles of various cyclic carbonates. (a) <i>cis</i> -cyclopentene carbonate – $0.347^\circ$ , (b) <i>cis</i> -1,4-dihydronaphthalene carbonate – $2.005^\circ$ , (c) <i>cis</i> -indene carbonate #1 – $8.252^\circ$ , (d) <i>cis</i> -indene carbonate #2 – $14.188^\circ$ , (e) styrene carbonate – $21.667^\circ$ , (f) <i>trans</i> -cyclohexene carbonate – $23.98^\circ$ , (g) ethylene carbonate – $24.287^\circ$ , (h) ethylene carbonate – $28.326^\circ$ , (i) <i>trans</i> -cyclohexene carbonate – $29.717^\circ$ .....	74
III-3	Product growth traces for the coupling of alicyclic epoxides and $\text{CO}_2$ utilizing <i>in situ</i> ATR-FTIR spectroscopy. (a) 99% selective PCHC growth at $1750\text{ cm}^{-1}$ and < 1% <i>trans</i> -CHC at $1810\text{ cm}^{-1}$ as confirmed by $^1\text{H}$ NMR. (b) 100% selectivity for CPC at $1804\text{ cm}^{-1}$ as confirmed by $^1\text{H}$ NMR. Reaction conditions: 500 eq. epoxide (15 mL), 1 eq. (salen)CrCl, 2 eq. PPNN <sub>3</sub> , 3.4 MPa $\text{CO}_2$ , 80 °C, 3 hours...	78
III-4	Kinetic plots of $\ln[(A_i - A_t)/A_t]$ vs. time for <i>cis</i> -cyclopentene carbonate production. Observed rate constants are $5.80 \times 10^{-5}\text{ s}^{-1}$ at 43 °C (red), $12.8 \times 10^{-5}\text{ s}^{-1}$ at 53 °C (blue), $23.5 \times 10^{-5}\text{ s}^{-1}$ at 63 °C (yellow), and $63.8 \times 10^{-5}\text{ s}^{-1}$ at 73 °C (purple).....	80

FIGURE		Page
III-5	Arrhenius plot of <i>cis</i> -cyclopentene carbonate production in the presence of (salen)CrCl/ <i>n</i> Bu <sub>4</sub> NCl. $R^2 = 0.989$ .....	81
III-6	Thermal ellipsoid representation of <i>cis</i> -cyclopentene carbonate with ellipsoids at 50% probability surfaces. At right, looking down the plane created by C2-C1-C3-C5 to show the near-planarity of the cyclic carbonate ring ( $O1-C1-C2-O2 = 0.347^\circ$ ).....	81
III-7	Changing shape of <i>cis</i> -indene carbonate $\nu_{CO_3}$ during the course of the reaction at 45 °C, 6.0 g indene oxide, 6.0 mL toluene. As the concentration of indene carbonate increases, the shoulder at 1793 $cm^{-1}$ becomes the dominant peak.....	83
III-8	Kinetic plots of $\ln[(A_i - A_t)/A_t]$ vs. time for <i>cis</i> -indene carbonate production, where $A_i$ and $A_t$ represent the absorbance of the cyclic stretch at 1815 $cm^{-1}$ at time equals infinity and $t$ , respectively. Observed rate constants are $1.85 \times 10^{-5} s^{-1}$ at 31 °C (red), $5.66 \times 10^{-5} s^{-1}$ at 40.5 °C (blue), $26.0 \times 10^{-5} s^{-1}$ at 51 °C (yellow), and $82.6 \times 10^{-5} s^{-1}$ at 59 °C (purple).....	83
III-9	Arrhenius plot of <i>cis</i> -indene carbonate production in the presence of (salen)CrCl/ <i>n</i> Bu <sub>4</sub> NCl. $R^2 = 0.993$ .....	84
III-10	Kinetic plots of $\ln[(A_i - A_t)/A_t]$ vs. time for butylene carbonate production, where $A_i$ and $A_t$ represent the absorbance of the cyclic stretch at 1815 $cm^{-1}$ at time equals infinity and $t$ , respectively. Observed rate constants are $2.76 \times 10^{-4} s^{-1}$ at 69 °C (red), $4.82 \times 10^{-5} s^{-1}$ at 78 °C (blue), $8.64 \times 10^{-5} s^{-1}$ at 87 °C (purple).....	85
III-11	Arrhenius plot of 1,2-butylene carbonate production in the presence of (salen)CrCl/ <i>n</i> Bu <sub>4</sub> NCl. $R^2 = 0.999$ .....	85
III-12	Kinetic plots of $\ln[(A_i - A_t)/A_t]$ vs. time for styrene carbonate production. Observed rate constants are $4.31 \times 10^{-5} s^{-1}$ at 25 °C (red), $13.9 \times 10^{-5} s^{-1}$ at 33 °C (blue), $38.0 \times 10^{-5} s^{-1}$ at 43 °C (yellow), and $66.4 \times 10^{-5} s^{-1}$ at 49 °C (purple).....	88
III-13	Arrhenius plot of styrene carbonate production in the presence of (salen)CrCl/ <i>n</i> Bu <sub>4</sub> NCl. $R^2 = 0.998$ .....	88

FIGURE		Page
III-14	Thermal ellipsoid representation of styrene carbonate with ellipsoids at 50% probability surfaces. At right, looking down C8-C7 bond to show torsion in cyclic carbonate ring ( $O1-C8-C7-O3 = 21.667^\circ$ ) .....	89
III-15	$^1H$ NMR of 2-chloro-1-phenylethanol (blue) and 2-chlorophenylethanol immediately following the addition of 1.4 eq DBU displaying clean, quantitative deprotonation (red). Red signals from 1-3 ppm are from DBU. Toluene- $d_8$ , 300 MHz .....	91
III-16	<i>In situ</i> ATR-FTIR monitoring of the backbiting of 2-chloro-1-phenylethanol under 1 atm $CO_2$ . Inset images show the production of white DBU•HCl precipitate during the course of the reaction .....	92
III-17	FT-IR traces of styrene carbonate production at $1815\text{ cm}^{-1}$ from the DBU-initiated backbiting of 2-chloro-1-phenylethanol under 1 atm $CO_2$ pressure.....	93
III-18	Quantitative formation of styrene carbonate (black) after the addition of 100 psi $CO_2$ to 2-chloro-1-phenylethoxide solution (red). The reaction is estimated to have completed in less than 2 minutes .....	95
III-19	Expected reactivity trend of bromo- and chlorohydrins for base-initiated backbiting to styrene carbonate.....	96
III-20	Energies of activation for various backbiting reactions to styrene carbonate .....	98
IV-1	At left, three-dimensional stack plot of the reaction of azide ( $2000\text{ cm}^{-1}$ ) with $CS_2$ . $CS_2$ was added after 3 minutes. After ~2 hours, the reaction was heated to $80\text{ }^\circ C$ , and the growth of thiocyanate was observed at $2055\text{ cm}^{-1}$ . At top right, traces of the disappearance and growth peaks of free $N_3^-$ (red), and $SCN^-$ (blue). Bottom right, zoomed in view from 0-2.75 hours reaction time.....	116
IV-2	Trace of the -O-(C=O)-S- monothiocarbonate polymer at $1712\text{ cm}^{-1}$ displaying peak growth after 6 hours. Reaction loading is (salen)CrCl:PPNCl:cyclopentene oxide: $CS_2 = 1:2:1500:3000$ .....	117
IV-3	Carbonate region of the $^{13}C$ NMR of poly[thio]carbonate from Table IV-3, entry 2. $CDCl_3$ , 125 MHz .....	119

FIGURE		Page
IV-4	FT-IR of poly[thio]carbonate from Table IV-3, entry 2. CH <sub>2</sub> Cl <sub>2</sub> solvent .....	120
IV-5	Thermal ellipsoid representation of <i>trans</i> -cyclopentene trithiocarbonate with ellipsoids at 50% probability surfaces. Inset image is looking down the S1-C4 plane to show torsion caused by <i>trans</i> -configuration. S2-C2-C2'-S2' angle = 46.44° .....	124
IV-6	Calculated local minima for cyclopentene carbonate (OOO) species: <i>cis</i> -boat, <i>cis</i> -chair, and <i>trans</i> - .....	126
IV-7	Calculated relative enthalpies for cyclopentene carbonate isomers in kcal/mol .....	127
IV-8	Calculated relative enthalpies for cyclopentene trithiocarbonate isomers in kcal/mol .....	127
IV-9	Calculated relative enthalpies for cyclopentene thiocarbonate isomers in kcal/mol .....	128
IV-10	Calculated relative enthalpies for cyclopentene dithiocarbonate isomers in kcal/mol .....	129
IV-11	Proposed mechanism for scrambling in the coupling of cyclopentene oxide and CS <sub>2</sub> .....	132
IV-12	Time lapsed <sup>13</sup> C NMR of the reaction between cyclopentene oxide (red) and <i>trans</i> -cyclopentene trithiocarbonate (purple) to produce cyclopentene sulfide (green) and <i>cis</i> -cyclopentene carbonate (blue) in toluene- <i>d</i> <sub>8</sub> . Broadening of cyclopentene oxide's carbon at 56.3 ppm is likely due to ring-opening and ring-closing of the epoxide .....	134
IV-13	Time lapsed <sup>13</sup> C NMR of the reaction between cyclopentene sulfide (green) and <i>cis</i> -cyclopentene carbonate (blue) in toluene- <i>d</i> <sub>8</sub> . Cyclopentene (orange) is the first observable product .....	135
IV-14	Proposed mechanism for observed scrambling between cyclopentene oxide and <i>trans</i> -cyclopentene trithiocarbonate .....	136
IV-15	Proposed scrambling occurring in the coupling of CO <sub>2</sub> and cyclopentene oxide .....	139

FIGURE	Page
V-1 Idealized representation for atmospheric CO <sub>2</sub> sequestration and use as a starting material for the production of value-added polycarbonates.....	146



## LIST OF TABLES

TABLE		Page
I-1	Published kinetic barriers for CO <sub>2</sub> /epoxide coupling reactions .....	23
II-1	Production of <i>cis</i> -indene carbonate .....	39
II-2	Production of poly(indene carbonate) .....	43
II-3	Copolymerization of indene oxide and CO <sub>2</sub> utilizing bifunctional catalysts .....	49
III-1	X-ray crystallographic data for various cyclic carbonates .....	75
III-2	X-ray crystallographic data for propylene carbonates .....	76
III-3	Observed first order rate constants for the DBU-initiated backbiting of 2-chloro-1-phenylethanol under 1 atm CO <sub>2</sub> pressure .....	93
III-4	Summary of cyclic carbonate activation parameters .....	97
IV-1	Azide stretching frequencies in tetrachloroethylene .....	112
IV-2	Reaction of cyclopentene oxide with CS <sub>2</sub> with (salen)CrCl and PPNN <sub>3</sub> in a 300 mL stainless steel Parr reactor .....	114
IV-3	Reaction of cyclopentene oxide with CS <sub>2</sub> with (salen)CrCl and PPNCl in a 25 mL stainless steel Parr reactor .....	118
IV-4	Coupling reactions of cyclopentene sulfide with CS <sub>2</sub> .....	123
IV-5	Coupling reactions of cyclopentene sulfide with CO <sub>2</sub> .....	123
IV-6	Conditions needed for O/S scrambling utilizing a purified mix of cyclic [thio]carbonate materials utilizing (salen)CrCl and <i>n</i> Bu <sub>4</sub> NCl...	131
IV-7	Conditions needed for O/S scrambling utilizing <i>trans</i> -cyclohexene trithiocarbonate and cyclohexene oxide .....	131

# CHAPTER I

## INTRODUCTION AND LITERATURE REVIEW\*

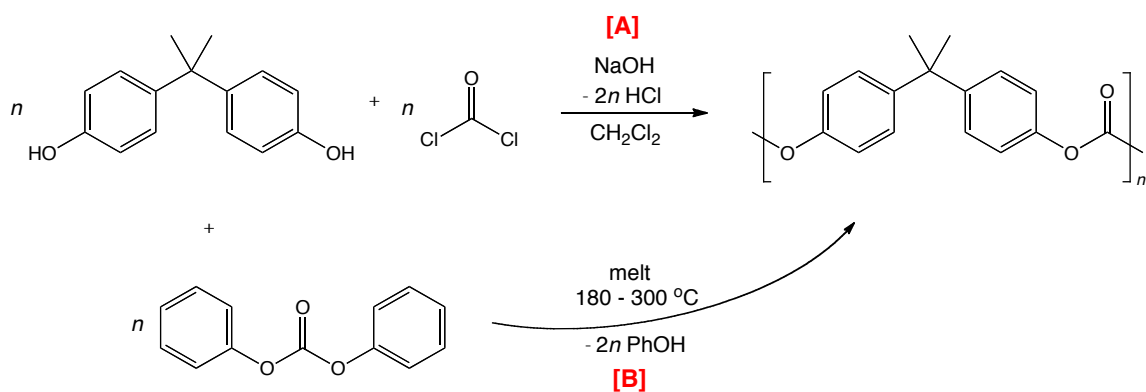
### **Industrial Production of Polycarbonates**

The most common type of polycarbonate in the market today, bisphenol-A (BPA) polycarbonate, has numerous useful physical and mechanical properties, including high transparency to visible light, tensile strength of ~75 MPa, and a high glass transition temperature ( $T_g$ ) of 145-150 °C.<sup>1</sup> BPA polycarbonate is used as a raw material in many applications including compact and blu-ray discs, automotive/airplane interiors, window panes, sunglasses, surgical devices, et al.<sup>2</sup> Demand for BPA polycarbonate was estimated to be approximately 360 metric tons in 2011, and it is expected to remain a valuable commodity in the coming decades.<sup>3</sup>

Industrially, BPA polycarbonate and other polycarbonates are typically produced through the polycondensation of a diol and phosgene (Scheme I-1, route A). Though this phosgene process has been heavily optimized over the years since its creation, it has several drawbacks. Phosgene is a highly toxic gas that gained infamy for its use as a chemical weapon in World War I. Phosgene's LC50 is 360.0 mg/m<sup>3</sup> (30.0 minutes), and the American Conference of Industrial Hygienists, ACIH, has set the human exposure limit to 0.1 ppm.<sup>4</sup> Bisphenol-A is a known endocrine disruptor,<sup>5</sup> and trace amounts of

---

\*Portions reprinted (adapted) from “What’s New with CO<sub>2</sub>? Recent Advances in its Copolymerization with Oxiranes.” Darensbourg, D.J.; Wilson, S.J. *Green Chem.* **2012**, *14*, 2665-2671. Reproduced by permission of The Royal Society of Chemistry. <http://dx.doi.org/10.1039/c2gc35928f>.



**Scheme I-1.** Industrial routes for the production of BPA polycarbonate with (a) phosgene and (b) diphenylcarbonate.

bisphenol-A can be found within the finished plastic. This free bisphenol-A can leach into food or drink, and, as a result, BPA polycarbonate's use in the food storage industry has greatly decreased over the past decade. The whole polymer production process requires a large amount of solvent, some 10x  $\text{CH}_2\text{Cl}_2$  and 10-100x water compared to the amount of BPA polycarbonate produced, w/w (Figure I-1).<sup>6</sup> The use of chlorine gas and chlorinated starting materials can also lead to corrosion to the industrial equipment, saline waste, and various impurities and deformities in the produced polycarbonate materials.

Recently, a greener and more sustainable commercial route has been developed by the Asahi Kasei Corp. (Japan) which involves a phosgene-free production of BPA polycarbonate from bisphenol-A and diphenyl carbonate (Scheme 1, route B).<sup>6</sup> This synthetic route provides several advantages. Diphenyl carbonate can be isolated as a pure solid, allowing for the removal of the chlorinated byproducts that can cause discoloration and physical deformities in the polymer. It can be produced utilizing

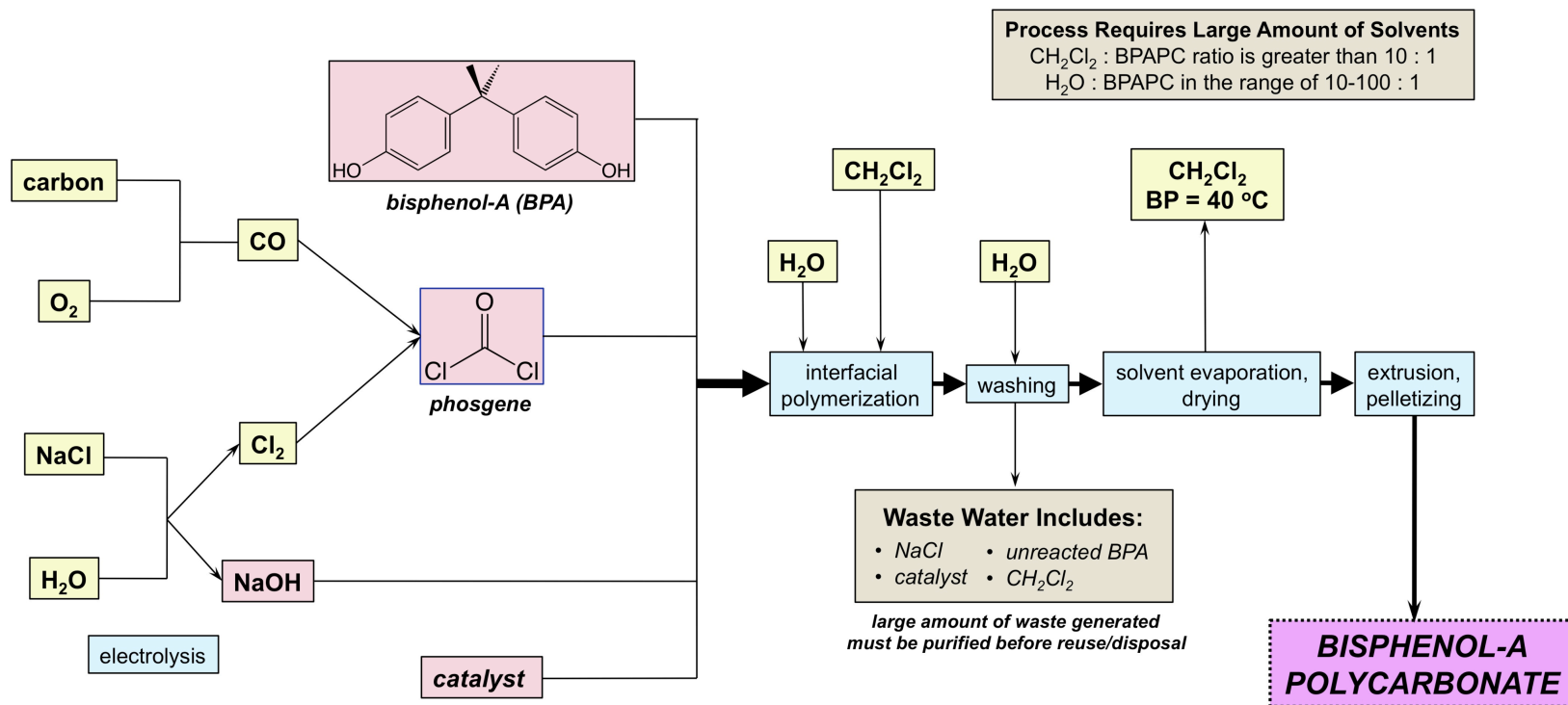


**Figure I-1.** Schematic representing the typical industrial phosgene-based process for BPA-polycarbonate production. Adapted from Reference 6.

carbon dioxide as a starting material,<sup>7</sup> and the polymerizations can be done under melt conditions without added solvent, base, or catalyst.

### **Carbon Dioxide as a C1 Feedstock**

Carbon dioxide, CO<sub>2</sub>, is the most abundant waste produced by humans.<sup>8</sup> Seeing as it is carbon in its most oxidized form, CO<sub>2</sub> is generally regarded as an inert compound and is therefore not often employed in chemical reactions. In order to activate CO<sub>2</sub> to become a viable starting material for chemical synthesis, a large energy input is required. However, CO<sub>2</sub> is inexpensive, abundant, non-toxic, non-corrosive, non-flammable, can exist as a supercritical fluid above its critical point (31.1 °C, 7.38 MPa), and is vulnerable to nucleophilic attack and various electron-donating reagents.<sup>9</sup> As such, it represents a strong candidate to be a C1 feedstock to produce value-added materials. It is worth noting however that the high-purity CO<sub>2</sub> required by some of these processes could drive up the cost of this otherwise cheap material due to the need for added purification steps.

There are four generally accepted ways by which CO<sub>2</sub> can be transformed into useful chemicals:<sup>9</sup>

1. To employ high-energy starting materials (e.g. H<sub>2</sub>, compounds with ring strain, organometallics, oxygenated platform molecules, et al.) and/or catalysts for the transformations (Figure I-2).
2. To shift the equilibrium to the left by removing a particular product (via Le Châtlier's Principle).
3. To supply extra energy via light or electricity.

4. To form low-energy synthetic targets (e.g. organic carbonates, lactones).  
 Currently, CO<sub>2</sub> is being employed in the industrial synthesis of urea,<sup>10</sup> methanol,<sup>11</sup> aspirin,<sup>12</sup> and various cyclic carbonates and polycarbonates (*vide infra*).

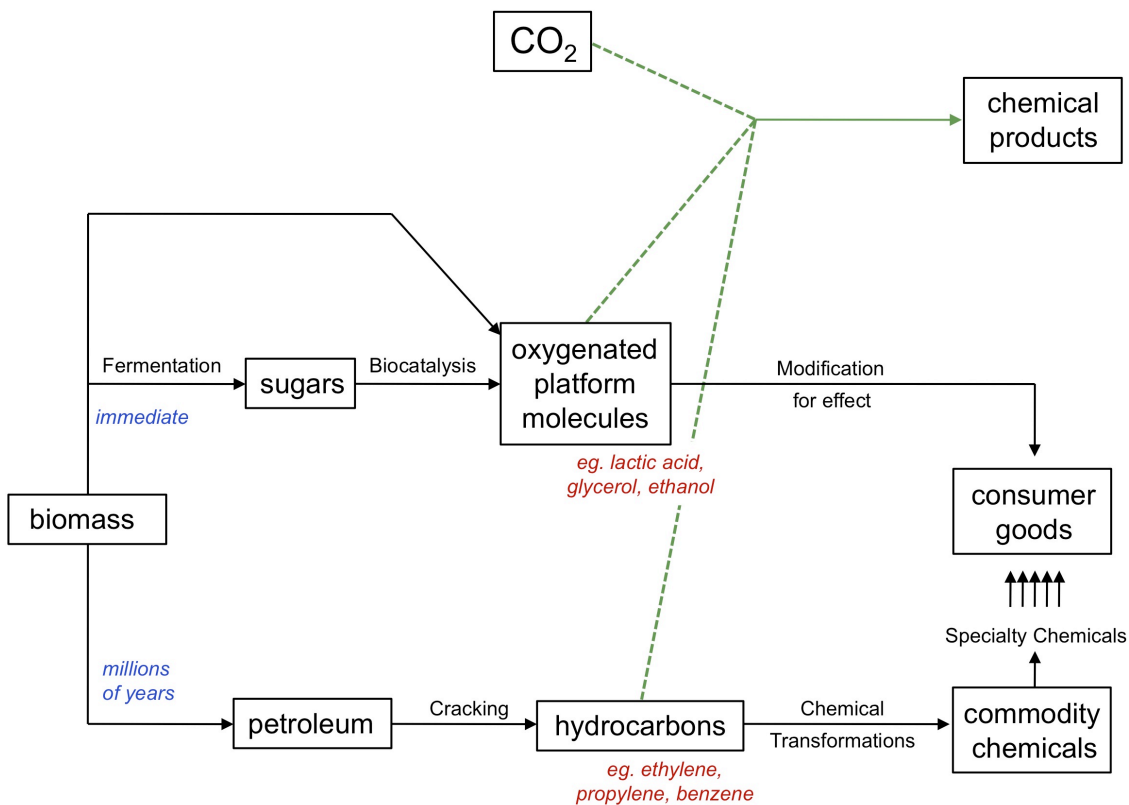


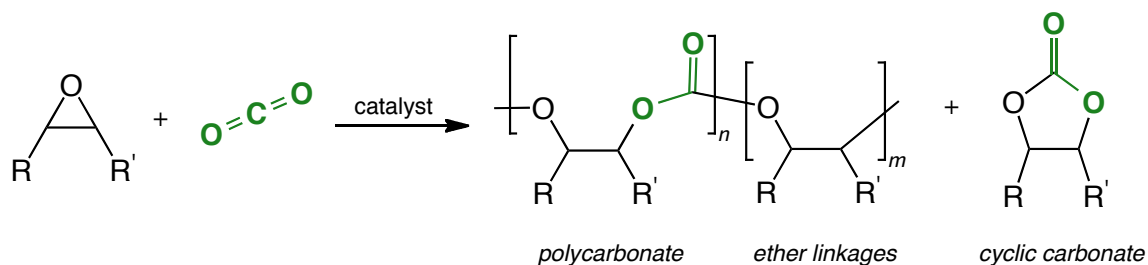
**Figure I-2.** CO<sub>2</sub> as a starting material for chemical transformations.

Along with water vapor and methane, carbon dioxide is well known as one of the chief greenhouse gases. Thus, it is understandable to believe that utilization of CO<sub>2</sub> in chemical transformations can help to counteract the growing atmospheric problem. However, it is estimated that only 7-10% of the annually emitted carbon dioxide could be recycled into value-added chemicals.<sup>8</sup> Regardless, the abundance, low cost, and

ability of CO<sub>2</sub> to replace toxic reagents still make it a very attractive starting material for chemical transformations.

### Catalytic Coupling of CO<sub>2</sub> and Epoxides

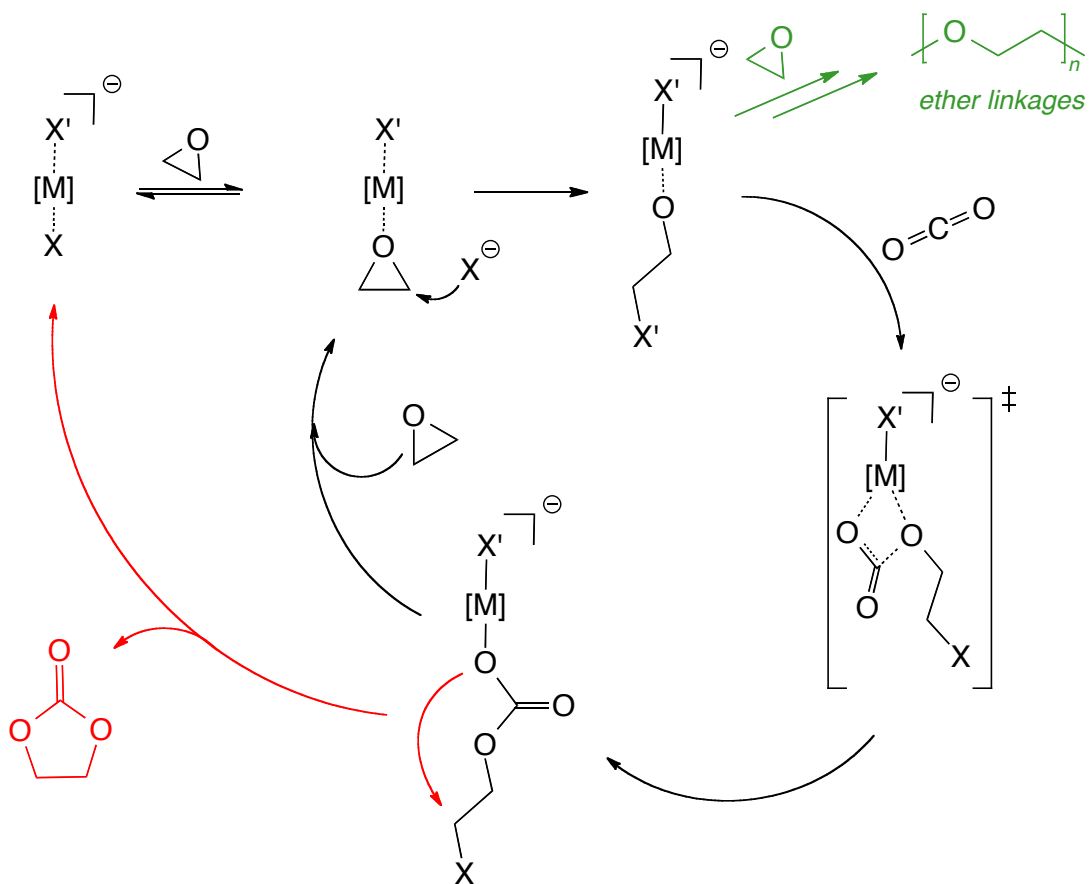
In 1969, Shohei Inoue, Hideomi Koinuma, and Teiji Tsuruta published an extremely influential set of papers in *Die Makromolekulare Chemie* and *Polymer Letters* in which they described the first successful production of polycarbonates from the catalytic coupling of epoxides and CO<sub>2</sub> (Scheme I-2).<sup>13,14</sup> Utilizing catalytic amounts of diethylzinc and water, Inoue was able to produce a random polymer blend of poly(propylene carbonate-*co*-propylene oxide) from propylene oxide and CO<sub>2</sub>. As will be discussed later, the fact that this chemistry worked at all is a feat to be lauded. Water and alcohols often act as chain transfer agents and thereby decrease the polymer's molecular weight, and extreme drying measures are often taken to limit water's presence within the reaction mixture.



**Scheme I-2.** Generalized schematic of epoxides and CO<sub>2</sub> coupling.

The accepted mechanism for polycarbonate production from the coupling of epoxides and CO<sub>2</sub> can be seen in Scheme I-3. Epoxide coordination to the metal is

followed by nucleophilic ring-opening, concerted insertion of CO<sub>2</sub>, and further epoxide coordination and ring-opening by the now nucleophilic polymer chain end. In continuing around this mechanism, polycarbonates can be formed. In addition to polycarbonate, two byproducts of the reaction are also possible. Ether linkages can be formed from successive ring-openings of epoxide without CO<sub>2</sub> insertion (green), and cyclic carbonates are formed either from the initial coupling of a single epoxide with CO<sub>2</sub> or from backbiting from preformed polymer chains (red).

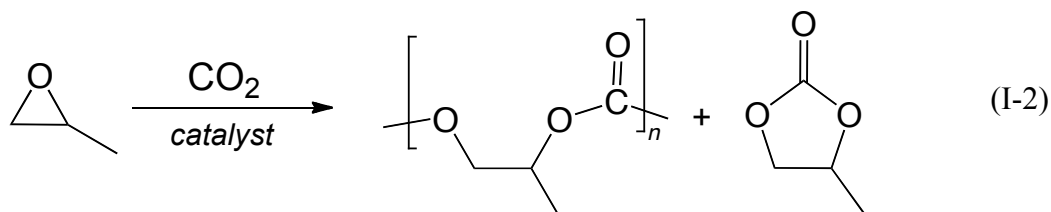
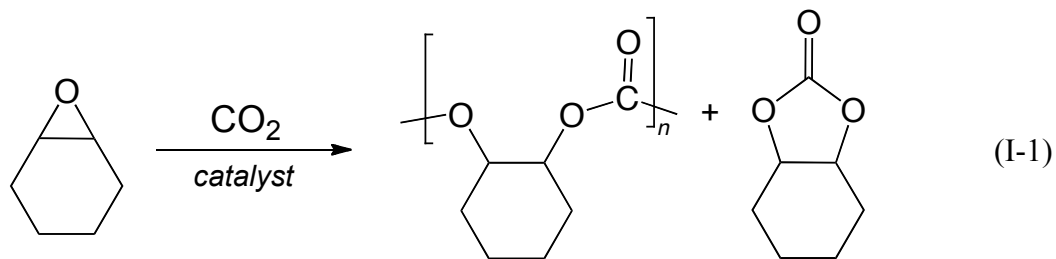


**Scheme I-3.** Generalized mechanism for the production of polycarbonates (black), ether linkages/polyether (green), and cyclic carbonate (red). X can be either the initiating nucleophile or a growing polymer chain.



For many years, cyclohexene oxide (CHO) and propylene oxide (PO) have been the main epoxide sources for copolymerization with CO<sub>2</sub> to afford polycarbonates (eqn I-1 and I-2, respectively). In general, poly(cyclohexene carbonate) (PCHC) is easy to selectively form using a wide variety of catalysts and temperatures. It has a relatively high T<sub>g</sub> of ~115 °C, but its brittle nature has not yet allowed it to be commercialized for any products without being copolymerized with a more mechanically friendly monomer such as propylene oxide.<sup>15</sup>

Unlike the easy to synthesize poly(cyclohexene carbonate), poly(propylene carbonate) (PPC) requires more developed systems and/or reaction conditions to avoid



formation of the cyclic carbonate byproduct. PPC also has excellent mechanical properties that make it an attractive material for widespread use, though it is marred by a low T<sub>g</sub> of only ~37 °C. PPC contains 44% CO<sub>2</sub> by weight, and it burns cleanly and

gently in air without emitting harsh residues. It is already finding use as a coating for metal foodstuff containers and finishes for wood or other materials,<sup>16</sup> and it may have use as a biomimetic scaffold for tissue engineering.<sup>17</sup> PPC production has been commercialized by Novomer<sup>18</sup> and Empower Materials<sup>15</sup> in the United States and SK<sup>19</sup> in Korea, while other companies such as Sumitomo, Bayer, China Blue Chemical, and Henan Tianguan have also begun research in the area.<sup>20</sup> In 2012 in cooperation with BASF, Siemens announced the development of PPC-containing polymers that will be commercialized for vacuum cleaner parts.<sup>21</sup>

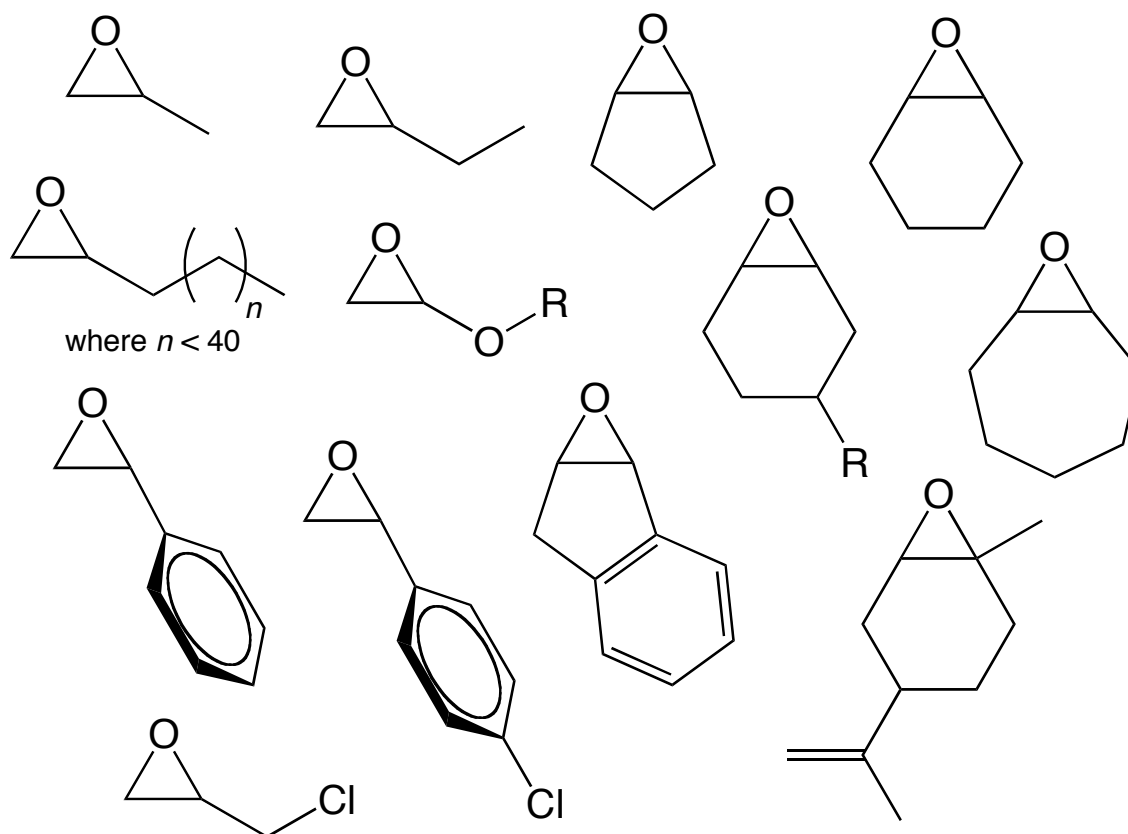


**Figure I-3.** Epoxides that have been successfully copolymerized with CO<sub>2</sub> as of May 2013.

## Recent Efforts to Expand CO<sub>2</sub>/Epoxides Copolymerization Process

Though PCHC and PPC are the most commonly polymers for CO<sub>2</sub>/epoxides copolymerization investigations, many other systems have also been explored (Figure I-3). Several alicyclic and aliphatic epoxides have proven capable of undergoing copolymerization with CO<sub>2</sub>, though several systems deserve particular praise. Monomers such as 1-butene oxide,<sup>22</sup> 1-hexene oxide,<sup>22,23</sup> and other long chained 1-alkylene oxides<sup>23b</sup> have been successfully copolymerized with CO<sub>2</sub>. Two separate recent reports from Grinstaff<sup>24</sup> and Frey<sup>25</sup> showed the coupling of a protected glycidyl ethers with CO<sub>2</sub> to ultimately yield the biodegradable poly(1,2-glycerolcarbonate).

Derivatives of CHO including [2-(3,4-epoxycyclohexyl)ethyl]-trimethoxysilane<sup>26</sup> (Darensbourg) and several different cyclohexene oxides that had been functionalized at the monomer's 4-position (Coates) have also been successful.<sup>27</sup> Cycloheptene oxide and cyclopentene oxide have had limited success with zinc<sup>28</sup> and cobalt<sup>29</sup>-based catalysts. Limonene oxide has long been a target because it is directly derived from limonene, a renewable starting material found in the peels of oranges and other citrus fruits. In 2004, Coates and coworkers successfully synthesized poly(limonene carbonate) utilizing a  $\beta$ -diiminate zinc acetate catalyst.<sup>30</sup> Xiao-Bing Lu and coworkers have produced highly (98%) isotactic PCHC has been produced by the use of triply (*S,S,S*)-chiral cobalt(III) complexes with salen-type ligands.<sup>31</sup> This is the first polycarbonate sample produced by CO<sub>2</sub>/epoxides coupling with crystalline domains in the polymer sample,  $T_m = 216$  °C. The authors suggest that crystalline polycarbonates may offer greater versatility as far as commercialization is concerned.

Epoxides bearing electron-withdrawing groups have long been desired as starting materials. In particular, the production of poly(styrene carbonate) ( $T_g = 80\text{ }^\circ\text{C}$ ) from styrene oxide and  $\text{CO}_2$  has become a very hot topic. Though Inoue had limited success with its synthesis,<sup>13</sup> most standard catalysts of the past several decades have been wholly ineffective for its production, with only a few low-yielding exceptions.<sup>32</sup> Instead, (salen)Co(III)X complexes have proven quite good for selective poly(styrene carbonate) synthesis.<sup>33</sup> Recently, Chisholm and coworkers employed chromium(III) tetraphenylporphyrin chloride/PPNCl<sup>34</sup> for the production of poly(styrene carbonate), though yield, turnover frequency, and polymer/cyclic selectivity were all lower than what is generally observed for cobalt complexes. Poly(epichlorohydrin-co- $\text{CO}_2$ ) ( $T_g = 31\text{ }^\circ\text{C}$ , atactic) has also been selectively formed by cobalt systems,<sup>35</sup> and highly isotactic semi-crystalline polymer ( $T_g = 42\text{ }^\circ\text{C}$ ,  $T_m = 108\text{ }^\circ\text{C}$ ) has been recently synthesized utilizing highly developed (salen)Co(III) complexes.<sup>36</sup> Lastly, and particularly relevant to this thesis, Darensbourg and Wilson successfully coupled  $\text{CO}_2$  and indene oxide to form poly(indene carbonate), the polycarbonate with the highest  $T_g$  yet produced from this process ( $T_g$  of up to  $138\text{ }^\circ\text{C}$ ).<sup>37</sup>

### **Traditional Metal Catalysts**

To date, the most successful systems for  $\text{CO}_2$ /epoxides coupling have typically involved a (salen)M(III)-based catalyst with some sort of added onium salt cocatalyst (Figure (I-4)). The D.J. Darensbourg group has long utilized (salen)Cr(III)Cl and (salen)Cr(III)N<sub>3</sub> with bis(triphenylphosphine)iminium (PPNX) or tetrabutylammonium

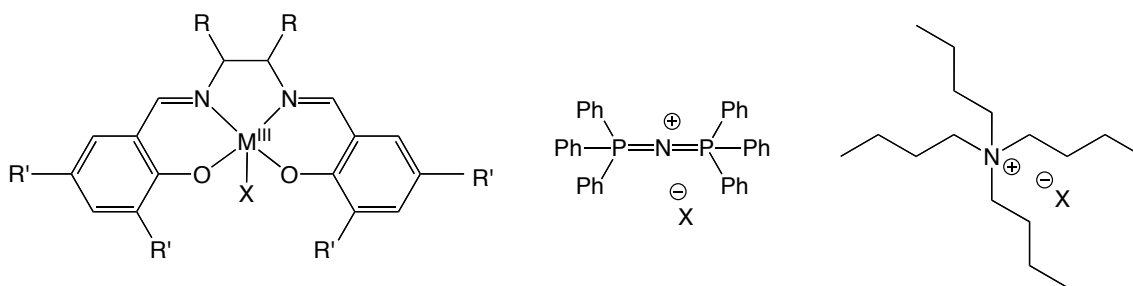


**Figure I-4.** Traditional (salen)M(III)X catalyst with PPNX and  $n\text{Bu}_4\text{NX}$  onium salt cocatalysts.

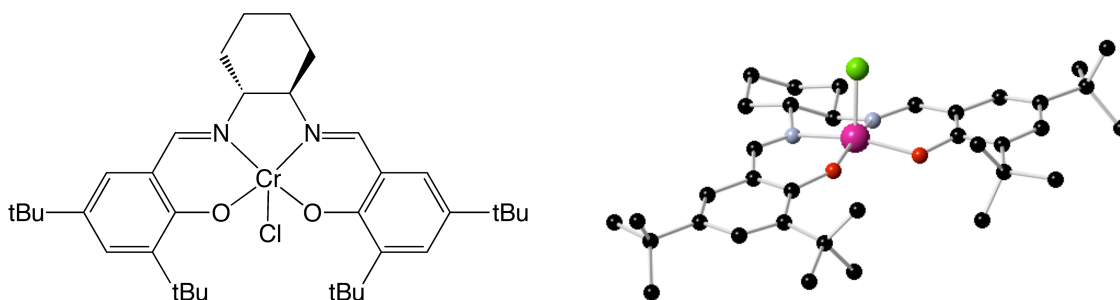


**Figure I-5.** Skeletal representation and crystal structure of *(R,R)*-*N,N'*-bis(3,5-di-*tert*-butylsalicylidene)-1,2-cyclohexanediaminochromium(III) chloride, commonly referred to as (salen)CrCl.<sup>38</sup>

$(n\text{Bu}_4\text{NX})$  salt cocatalysts, where X is a halogen or pseudohalogen (Figure I-5).<sup>39</sup> These catalysts have been structurally characterized<sup>38,40</sup> and represent well-defined systems for  $\text{CO}_2$ /epoxides coupling. The main problem with (salen)Cr(III)X systems is their propensity to produce cyclic carbonate for systems other than cyclohexene oxide.<sup>41</sup>

For systems without an added cocatalyst, a bimetallic pathway is preferred. Catalysts such as Coates' zinc  $\beta$ -diiminate,<sup>30,28b, 42</sup> Rieger's linked (salen)Cr(III),<sup>43</sup> Lee's heteronuclear zinc complexes,<sup>44</sup> and Williams' bimetallic systems<sup>45</sup> have also proved effective for selective copolymerization reactions. Despite desires to make

generalizations as to the effectiveness of various catalyst/cocatalyst combinations for all types of epoxide/CO<sub>2</sub> systems, it has become increasingly apparent that the chemical and structural nature of a given epoxide heavily influences its ability to copolymerize with CO<sub>2</sub>.

### **Chain Transfer**

Along with desired chain propagation, the polymerization process can be hindered by various chain transfer processes. Chain transfer occurs when the activity of the growing polymer chain is transferred to another species, effectively stopping further growth of that chain. For the copolymerization of CO<sub>2</sub> and epoxides, water,<sup>45d</sup> alcohols, diols,<sup>46</sup> and other materials bearing acidic protons<sup>47</sup> can act as chain transfer agents.

The GPC traces of most polycarbonates produced from the coupling of CO<sub>2</sub> and epoxides are bimodal in nature, meaning that there are two main distributions of polymer chain lengths produced during the reaction (Figure I-6). One mode belongs to X-poly-OH, whereby the initiator X<sup>-</sup> starts a chain, propagation occurs, and the chain is terminated by hydrolysis. If no chain transfer occurs, the number of these species should be equal to the number of initiators present in the reaction. In the other case, the acidic proton from a chain transfer agent can “cap” a growing polymer chain, effectively stopping further propagation. In addition, a new anionic initiator from which propagation can occur has been created (Figure I-7). In this manner, RO-poly-OH and HO-poly-OH chains are generated. Chain transfer, when uncontrolled, can lead to shorter overall chain lengths and broad molecular weight distributions.

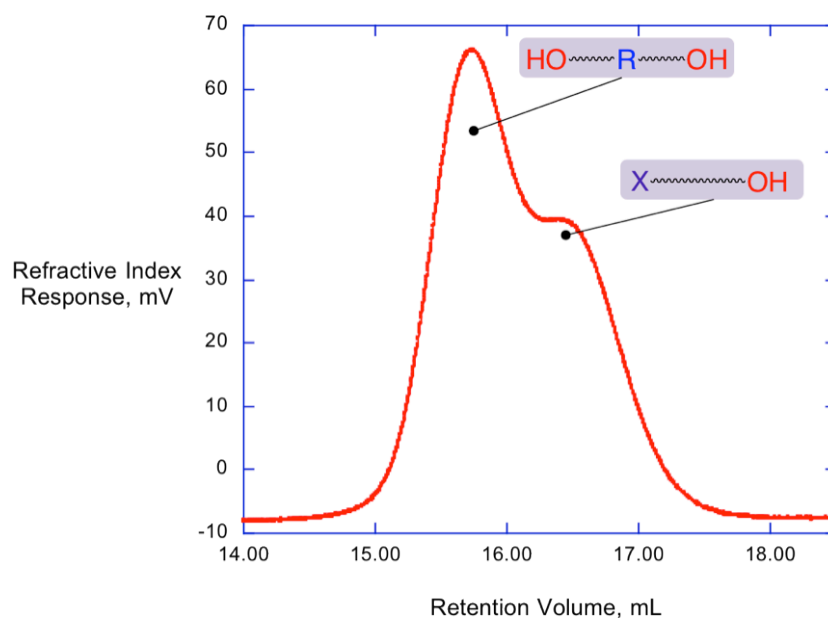


**Figure I-6.** Refractive Index trace (GPC, 1 mL/min THF eluent) of bimodal poly(indene carbonate) sample.

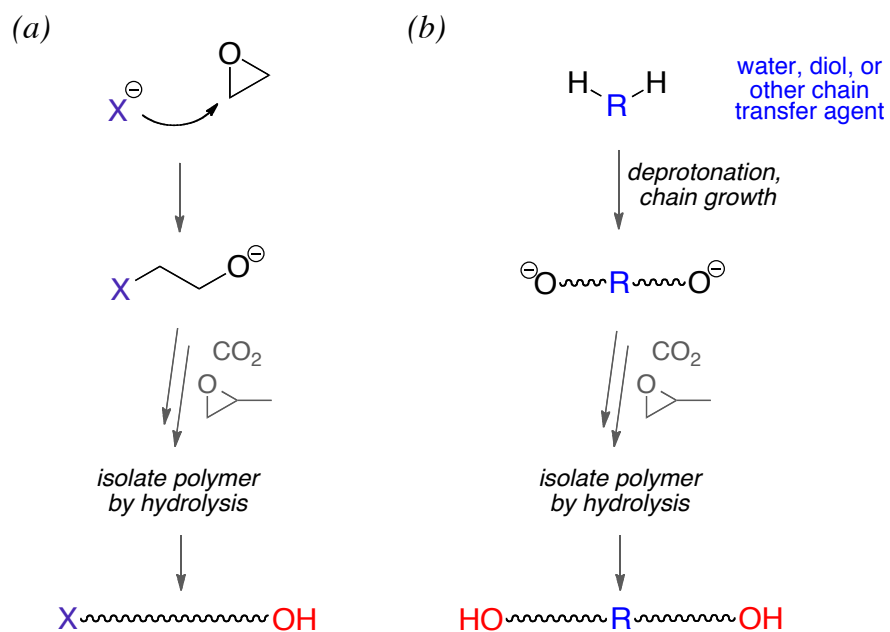


**Figure I-7.** Two methods for copolymer production, through (a) direct initiation or (b) chain transfer. For clarity, the metal has not been included.

Despite their propensity to lower polymer molecular weight, chain transfer processes can sometimes be desirable. An immortal polymerization occurs when there is rapid and reversible chain transfer.<sup>48</sup> As such, the system is able to handle the addition of chain transfer agents while retaining good control, i.e. narrow molecular weight distributions.

### **Notable Recent Catalytic Developments**

Though it had initially been overlooked due to stability issues between active cobalt(III) and inactive cobalt(II), (salen)Co(III)X complexes exploded in the mid-2000s as excellent catalysts for the selective copolymerization of propylene oxide with CO<sub>2</sub>. The Coates and Lu groups were able to produce poly(propylene carbonate) with >99% selectivity at room temperature in neat propylene oxide from various (salen)Co(III)X complexes and onium salt cocatalysts.<sup>49</sup> In each case, the yields were typically held below 50% however, as the increased viscosity of the solution at higher conversions would eventually lead to increased backbiting to cyclic propylene carbonate. At this point it is worthy of note that cyclic carbonates are not only detrimental in that they consume available monomer but also that they can block the metal center from incoming epoxide, as cyclic carbonates are better ligands than epoxides.<sup>50</sup>

In 2006, Nozaki and coworkers published the first example of cobalt catalysts with aminated arms appended at the 3-position of the salen ligand for CO<sub>2</sub>/epoxides coupling (Figure I-8).<sup>23a</sup> The complex's piperidinyl arms allow for controlled chain transfer reactions, whereby a proton shuffles between the amine and free polymer chains in solution. At increased (~80%) conversions, it was able to maintain 96% selectivity



for copolymer production when reactions were run in neat PO. Even at the comparatively high temperature of 60 °C where most contemporary catalysts would only produce cyclic propylene carbonate, 90% selectivity for PPC production was maintained, though the yield remained low at 34%. When the reaction was run in a dimethoxyethane cosolvent, 20 equivalents (to 1 equivalent catalyst) of the chain transfer agent methanol was added, and 95% selectivity for polymer was maintained, though the polymer's molecular weight dropped dramatically.

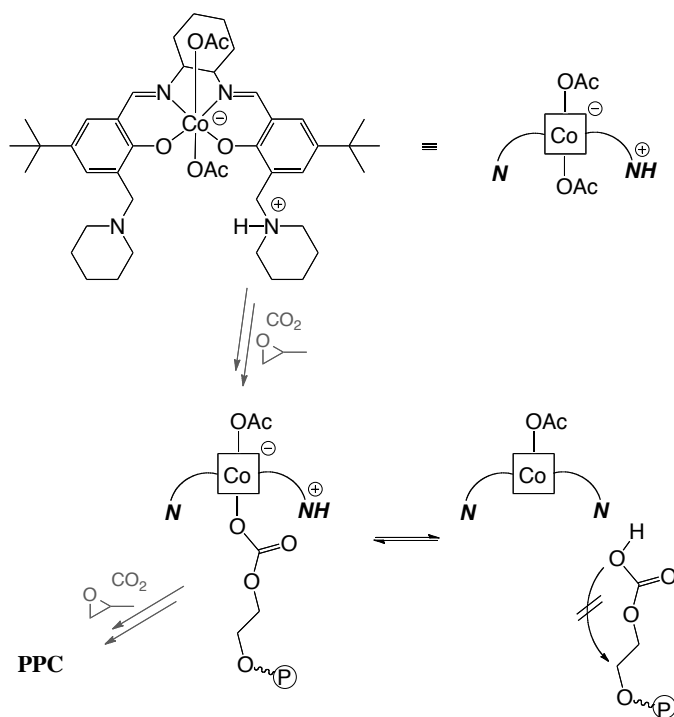


**Figure I-8.** Nozaki's cobalt catalyst with attached piperidene arms is capable of shuffling protons between polymer chains and attached amines.

The ability of Nozaki's catalyst to shuffle protons between the amines and the growing polymer chains opened up an entirely new branch of ligand design, whereby a

single complex serves the combined purposes of both the catalyst and the cocatalyst. As time has gone on, increasingly complex (salen)Co(III)X catalysts have been synthesized, and all have gone on to have resounding success for the production of poly(propylene carbonate) and other polymers which were once thought inaccessible.

Lee's superactive complexes featuring four quaternary ammonium salts have proven to be some of the most active catalysts to date (Figure I-9). Interestingly, both the structure and the activity of the complex rely heavily on the nature of the substituent at the 3-position of the phenyl rings. If it is a *tert*-butyl group, the cobalt remains locked in the typical salen tetradentate pocket and the catalytic activity is high (TOF  $\approx$  1300 h<sup>-1</sup>), though in the same realm of other catalysts.<sup>51</sup> If instead a methyl group is placed at the 3-position, the cobalt no longer coordinates through the imine nitrogens and sits outside of the salen pocket, instead coordinating to four 2,4-dinitrophenoxide moieties.<sup>52</sup> This unusual binding mode allows for greatly increased activity and stability, with TOF

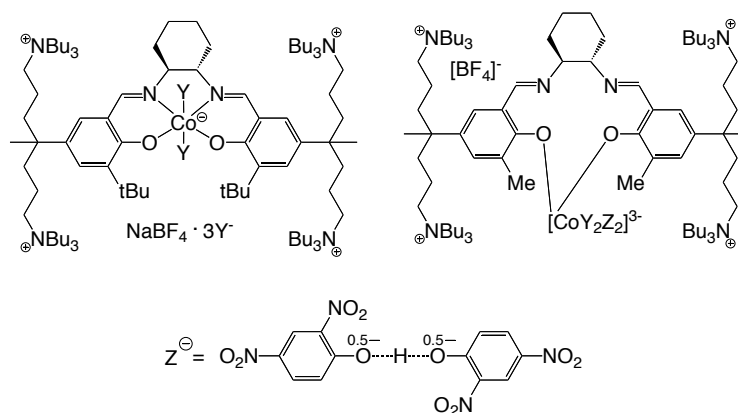


**Figure I-9.** Highly active cobalt catalysts containing four appended quaternary amine arms from Lee and coworkers. Y = 2,4-dinitrophenoxide.

of  $>20000\text{ h}^{-1}$  at  $80\text{ }^{\circ}\text{C}$ , reaching  $M_n$  of up to  $300,000\text{ g/mol}$ . Later improvements involved exchanging the 2,4-dinitrophenoxides for 2,4-dichlorophenoxides or 4-nitrophenoxides for increased laboratory safety.<sup>53</sup>

Similarly great activity has been found utilizing the asymmetric (salen)Co(III)X complexes synthesized by Lu et al. featuring an appended bulky amine or quaternary ammonium salt at the 3-position of one phenyl ring, respectively (Figure I-10).<sup>54</sup> The cobalt catalyst featuring an appended 1,5,7-triabicyclo[4,4,0] dec-5-ene (TBD) sterically hindered base and acetate as the coordinating anion, is able to operate at temperatures as high as  $100\text{ }^{\circ}\text{C}$ , reaching TOF of  $10900\text{ h}^{-1}$  while maintaining 97% selectivity for polymer. Appended  $-\text{NEt}_2\text{Me}^+$  quaternary ammonium salt and 2,4-dinitrophenoxide anion (abbreviated DNP or Y) was slightly less effective than the TBD complex for PPC production, with TOF of  $3900\text{ h}^{-1}$  at  $90\text{ }^{\circ}\text{C}$  while maintaining 95% selectivity for polymer. Both of these systems have also proven to be very effective for other epoxide/ $\text{CO}_2$  copolymerizations including the productions of poly(styrene carbonate),<sup>33b</sup> poly(epichlorohydrin-co- $\text{CO}_2$ ),<sup>35</sup> and poly(indene carbonate).<sup>55</sup>

The popular counter ion and initiator 2,4-dinitrophenoxide can bind in a  $\kappa^2$  fashion and therefore instill a twisted geometry of the salen ligand whereby the two open coordination sites are *cis*- to one another (Figure I-11).<sup>56</sup> This differs from the traditional (salen) *trans*- coordination considered for most salen complexes, particularly (salen)Cr(III)X complexes. A recent report has shown that  $\text{CO}_2$  can insert into the Co-O

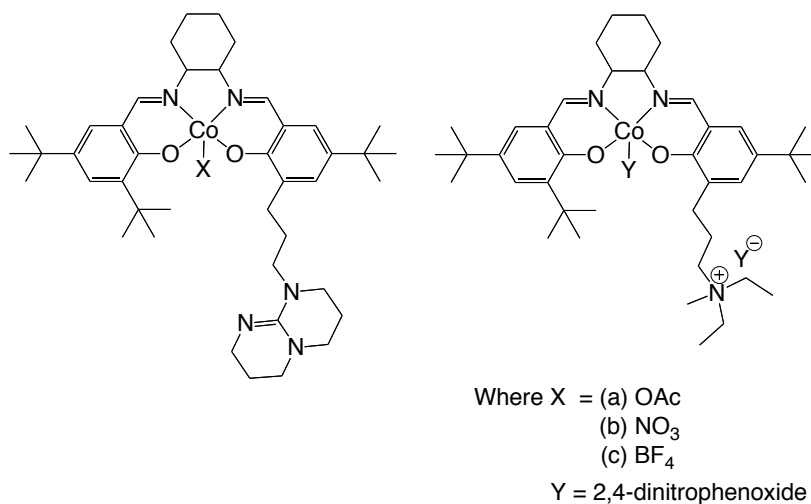


**Figure I-10.** Modified (salen)Co(III)X complexes from Lu and coworkers.

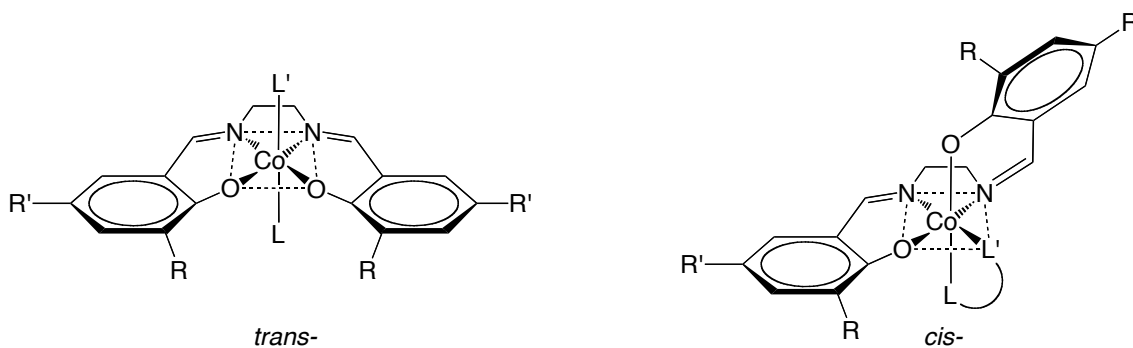


**Figure I-11.** Possible coordination modes, *trans-* and *cis-*, for (salen)Co(III)X complexes.

phenoxide bond of the (salen)CoDNP complex operating in the *cis-* configuration.<sup>57</sup> The authors suggest that this activation step may be important in initiating polymerization.

### Cyclic Carbonate Production

Cyclic carbonates have wide use as green solvents, gasoline additives, electrolytes for lithium batteries, and raw materials for polyurethane synthesis, et al.<sup>58</sup> In fact, several research groups across the globe are working diligently toward the selective

production of cyclic carbonates from epoxides and CO<sub>2</sub>, whereby polycarbonate or polyether production is an undesired byproduct.<sup>58-59</sup> This chemistry is led in part by the North group at Newcastle University. They utilize bimetallic aluminum salen complexes with *n*Bu<sub>4</sub>NBr cocatalyst to selectively produce cyclic carbonates at ambient temperature.<sup>60</sup>

The research in the D.J. Darensbourg group has instead focused on selective polycarbonate production, though cyclic carbonate byproduct is often produced concomitantly (Scheme I-2). In this manner, cyclic carbonate can form by one of six different mechanisms (Figure I-12).<sup>61</sup> Both metal-bound and metal-free alkoxide polymer chain end backbitings will produce 5-membered cyclic carbonates with *trans*-configuration (Pathways **a** and **f**, respectively). Conversely, metal-bound and metal-free polymer carbonate chain end backbiting reactions will produce cyclic carbonates with *cis*- configuration (Pathways **b** and **e**, respectively). *Cis*- cyclic carbonates can also be produced by carbonate backbiting prior to polymer propagation, i.e. immediately following initial epoxide ring-opening and CO<sub>2</sub> insertion (metal-bound Pathway **c** and metal-free Pathway **d**). In each of these cases, R and R' represent the respective side chains for the epoxide starting material. For aliphatic epoxides such as propylene and styrene oxide, no distinctions can be made between *trans*- and *cis*- cyclic carbonates, and thus we are unable to directly assign whether alkoxide or carbonate backbiting is most active. The distinction between the geometric isomers is prevalent instead for alicyclic epoxides such as cyclohexene oxide, cyclopentene oxide, and indene oxide.

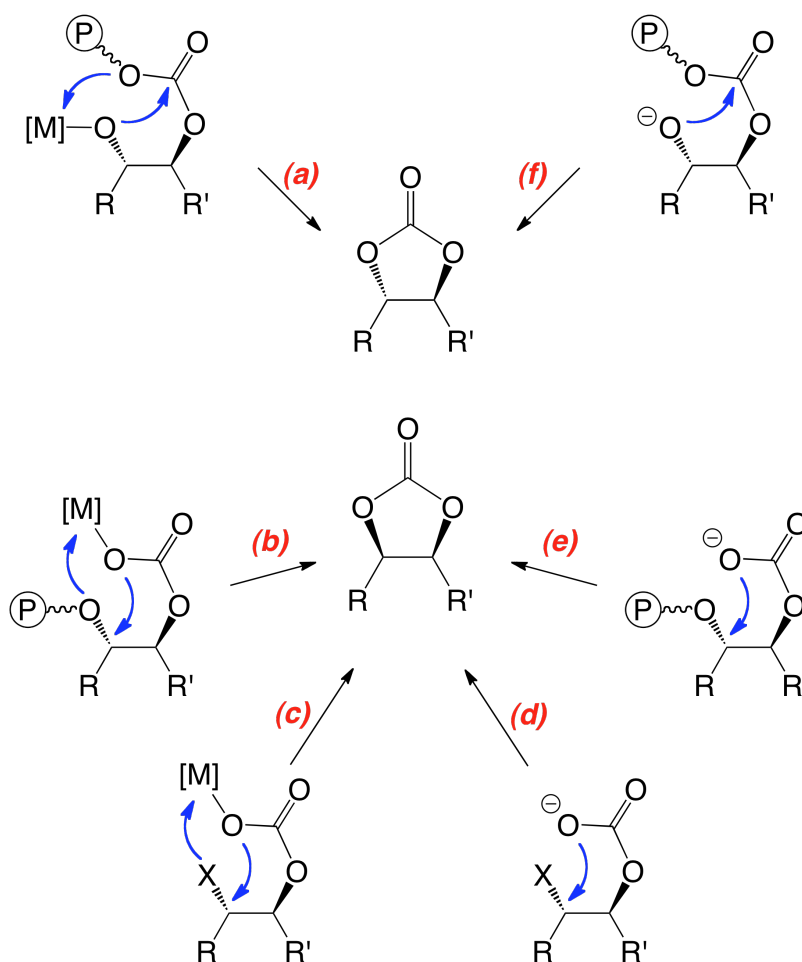


**Figure I-12.** Six mechanisms by which *trans*- and *cis*-cyclic carbonates can be produced.

### Kinetics and Thermodynamics of Epoxides/CO<sub>2</sub> Coupling

Polycarbonates are the kinetic product of the coupling of CO<sub>2</sub> and epoxides, cyclic carbonates are the thermodynamic product (Figure I-13). Several studies have been accomplished in which the kinetic barriers to polymer and cyclic carbonate formation were experimentally determined (Table I-1). In general, coupling barriers are highly dependent on the choice of catalyst system. Relative to chromium, cobalt

catalysts tend to decrease activation barriers to both products and increase the difference between barriers ( $\Delta E_A$ ). It is worth noting that in each of these studies, no distinction was made as to which of the cyclic carbonate production pathways were operative. Instead, cyclic carbonate was defined as coming from either polycarbonate or carbonate initiators.

In 2012, Darensbourg and Wei published a kinetic study monitoring the anion-initiated depolymerization of various polycarbonates produced from the coupling of  $\text{CO}_2$  and epoxides.<sup>62</sup> The rate of depolymerization was highly dependent on the basicity of the anion initiator, with  $\text{N}_3^- > \text{Cl}^- \gg \text{Br}^-$ . Kinetic activation barriers for the azide-initiated depolymerization of polycarbonates under argon atmosphere were determined to be poly(styrene carbonate) (46.7 kJ/mol) < poly(epichlorohydrin-*alt*- $\text{CO}_2$  carbonate) (76.2 kJ/mol) < poly(propylene carbonate) (80.5 kJ/mol).

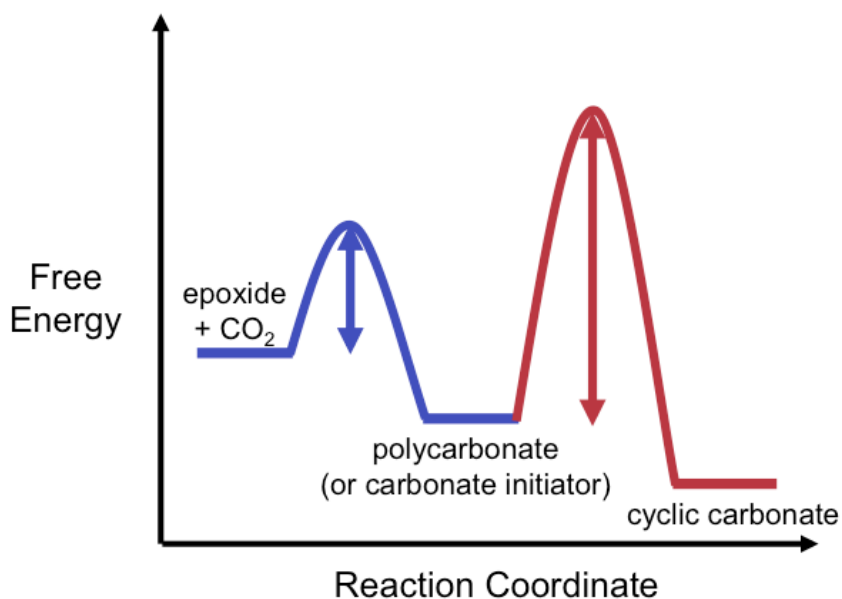


**Figure I-13.** Free energy reaction coordinate diagram for the coupling of epoxides with  $\text{CO}_2$ .

**Table I-1.** Published kinetic barriers for CO<sub>2</sub>/epoxide coupling reactions.

Epoxide	Catalyst	Cocatalyst	Activation Energy (kJ/mol)		$\Delta E_A$ , kJ/mol
			Polymer	Cyclic	
cyclohexene oxide <sup>63</sup>	(salen)CrCl	-	46.9	133.0	86.1
cyclohexene oxide <sup>64</sup>	LZn <sub>2</sub> (OAc) <sub>2</sub>	-	96.8	137.5	40.7
cyclohexene oxide <sup>65</sup>	Mg <sub>2</sub> N <sub>2</sub> O <sub>4</sub>	-	45.3	127.2	81.9
propylene oxide <sup>63</sup>	(salen)CrCl	-	67.6	100.5	32.9
propylene oxide <sup>33a,35</sup>	(salen)CoDNP	PPNDNP	34.5	88.0	53.5
styrene oxide <sup>33a</sup>	(salen)CoDNP	PPNDNP	40.4	50.7	10.3
epichlorohydrin <sup>35</sup>	(salen)CoDNP	PPNDNP	53.1	98.5	45.4

### Poly(Cyclohexene Carbonate)

For decades, CHO has been the go-to epoxide for testing new catalysts for the coupling of CO<sub>2</sub> and epoxides to form polycarbonates. Though different catalysts do display different levels of activity and/or turnover frequencies, systems are typically able to produce PCHC with a high level of selectivity (>95%). In the rare cases where cyclic byproduct is obtained from CO<sub>2</sub>/CHO coupling, the resultant material is generally the *trans*- isomer of cyclohexene carbonate. Notable exceptions include Kisch's zinc salt systems,<sup>66</sup> Darensbourg's iron/zinc double metal cyanides (DMCs),<sup>67</sup> and Williams' bimetallic iron(III) catalyst,<sup>68</sup> all of which can exclusively produce *cis*-cyclohexene carbonate under certain conditions. The difference in isomer produced by these particular systems may give clues as to the mechanism by which the byproduct was produced. Conversely, the cyclic products from the coupling of indene oxide,<sup>37</sup> and 1,4-dihydronaphthalene oxide,<sup>69</sup> and cyclopentene oxide and CO<sub>2</sub> are exclusively their corresponding *cis*-cyclic carbonate isomers.

In 2013, Darensbourg and Yeung completed a computational study in which they investigated the energetic parameters of polycarbonate backbiting reactions.<sup>70</sup> In these



studies, they determined that *cis*-CHC is thermodynamically more stable than *trans*-CHC by 4 kcal/mol, but the high transition state barrier for carbonate chain-end backbiting (via Pathways **d** and **e**, Figure I-12) prevents the accumulation of *cis*-CHC throughout the course of the reaction. *Trans*-CHC instead results from alkoxide backbiting, but the CO<sub>2</sub> present in the coupling conditions should readily insert into any alkoxide to instead form a carbonate chain end, effectively blocking these routes to cyclic carbonate production. These two opposing forces keep the production of cyclohexene carbonates to a minimum and make the cyclohexene oxide/CO<sub>2</sub> system out to give good results with a wide variety of catalysts. It is thus noteworthy that a catalyst that is good at producing poly(cyclohexene carbonate) will not necessarily also be good at producing other polycarbonates from epoxides/CO<sub>2</sub> coupling.

### **Sulfur-Containing Polymers and Cyclic (Thio)carbonates**

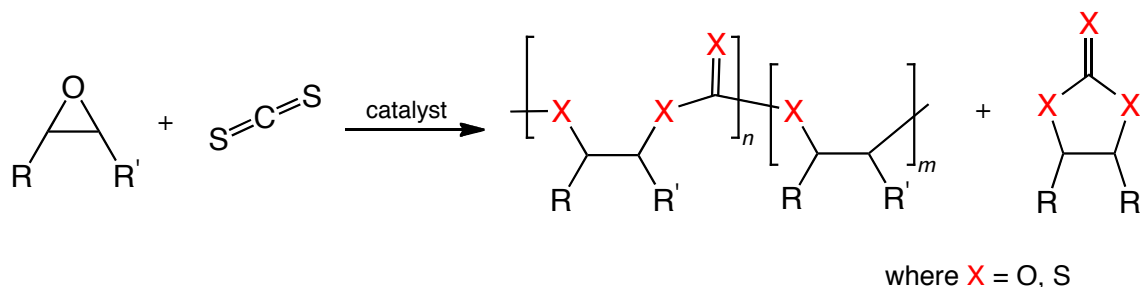
Sulfur-enriched polymers are attractive materials because of their high optical and thermal properties.<sup>71</sup> They have uses in sunglasses owing to their high refractive index<sup>72</sup> and biological systems in oxidation-response systems.<sup>73</sup> Similar to those reactions of carbon dioxide and epoxides, carbon disulfide (CS<sub>2</sub>) and cyclic thioethers can also be coupled to yield polymeric and cyclic materials.

In 1976, Soga and coworkers reported the copolymerization of ethylene sulfide and CS<sub>2</sub> utilizing various organometallic catalysts.<sup>74</sup> More recently, Nozaki et al. successfully copolymerized CS<sub>2</sub> and propylene sulfide to yield poly(propylene trithiocarbonate) and cyclic propylene trithiocarbonate utilizing (salphen)CrCl.<sup>75</sup> These

all-sulfur coupling reactions are expected to undergo similar mechanisms as the all-oxygen systems that have been previously discussed.

### Carbon Disulfide/Oxirane Coupling Reactions

Whereas it may be expected that the coupling of epoxides and thioethers would yield cyclic dithiocarbonates and polymers with a repeating  $-O-(C=S)-S-$  unit, this is typically not observed. In fact, scrambling of the oxygen and sulfur species is observed in nearly all cases of  $CS_2$ /epoxides coupling (Scheme I-3).



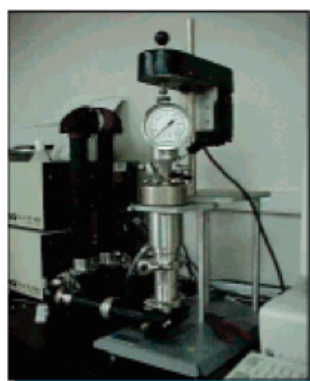
**Scheme I-3.** Generalized schematic of epoxides and  $CS_2$  coupling showing O/S scrambling.

North<sup>76</sup> and Endo<sup>77</sup> have both separately investigated the coupling of epoxides and  $CS_2$  to yield cyclic (thio)carbonates utilizing aluminum and titanium catalysts, respectively. In 2008, Zhang et al. investigated a zinc/cobalt double metal cyanide complex for the copolymerization of propylene oxide and  $CS_2$ .<sup>78</sup> The poorly defined catalyst system produced polymer and cyclic materials with large amounts of O/S scrambling. Darensbourg and Andreatta utilized the well-defined (salen)CrCl/PPNCl to further examine this process.<sup>79</sup> For the coupling of CHO and  $CS_2$ , they observed the production of oxygen-enriched polymer and sulfur-enriched cyclic species as compared

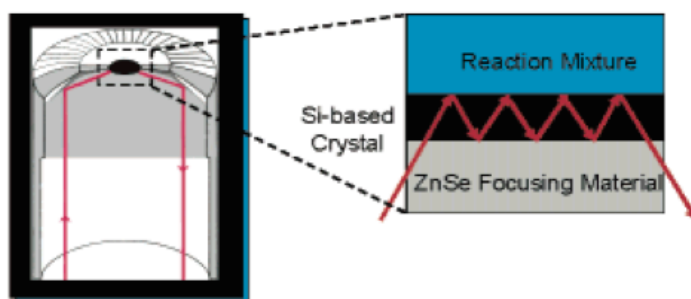
to the expected dithiocarbonate species. Several mechanisms for this process have been proposed, though it is still not well understood.

### **Physical Methods for the Characterizations of Coupling Products**

Analyses of all products were performed first utilizing  $^1\text{H}$  and FT-IR spectroscopies. When necessary,  $^{13}\text{C}$  NMR was also employed. Polycarbonate has a characteristic FT-IR  $\nu_{\text{CO}_3}$  stretch at  $1750\text{ cm}^{-1}$  while five-membered cyclic carbonates have a stretch closer to  $1810\text{ cm}^{-1}$ . For kinetic experiments, the coupling reactions were monitored utilizing in situ Attenuated Total Reflectance Infrared Spectroscopy (ATR-FTIR). The changing absorbance of the reactants and products are proportional to their concentrations, by Beer's Law, given that the path length and molar absorptivity remain constant. High-pressure experiments were conducted in a stainless steel Parr autoclave modified with a silicon composite (SiComp) ATR crystal located at the bottom of the reactor (Figure I-14). Ambient condition reactions were monitored utilizing a ReactIR ic10 reaction analysis system with a SiComp ATR crystal found at the end of a fiber optic probe (Figure I-15). In each case, IR spectra were taken at specific intervals during the course of the reaction to create three-dimensional stack plots.



Withstands 1500 psi  
(100 atm) and up to 200 °C



Schematic of *In-Situ* Probe

**Figure 1-14.** High pressure ASI® ReactIR 1000 system setup utilized by the D.J. Darensbourg labs at Texas A&M University.



**Figure I-15.** ReactIR™ ic10 system for ambient pressure measurements purchased from Mettler Toledo.

The molecular weights of purified polymer samples were determined by gel permeation chromatography in tetrahydrofuran solution. Several terms relating to molecular weight will be used through this dissertation, and they are worth defining.  $M_n$  is the number average molecular weight of a polymer (eqn I-3).  $M_w$  is the weight average molecular weight of a polymer (eqn I-4). In every case,  $M_w > M_n$ . The ratio between these two values is called the polydispersity index or PDI (eqn I-5). A broad PDI means that the polymer sample contains a broad range of molecular weights whereas a PDI of close to 1.0 means that only a narrow distribution of molecular weights exists in the sample, indicating a well-controlled polymerization by the catalyst system.

$$M_n = \left( \frac{\sum_{i=1}^n N_i M_i^2}{\sum_{i=1}^n N_i} \right) \quad (\text{I-3})$$

$$M_w = \left( \frac{\sum_{i=1}^n N_i M_i^2}{\sum_{i=1}^n N_i M_i} \right) \quad (\text{I-4})$$

$$PDI = \frac{M_w}{M_n} \quad (\text{I-5})$$

## CHAPTER II

### SYNTHESIS OF POLY(INDENE CARBONATE) FROM INDENE OXIDE AND CO<sub>2</sub>:

#### A POLYCARBONATE WITH A RIGID BACKBONE\*

##### **Introduction**

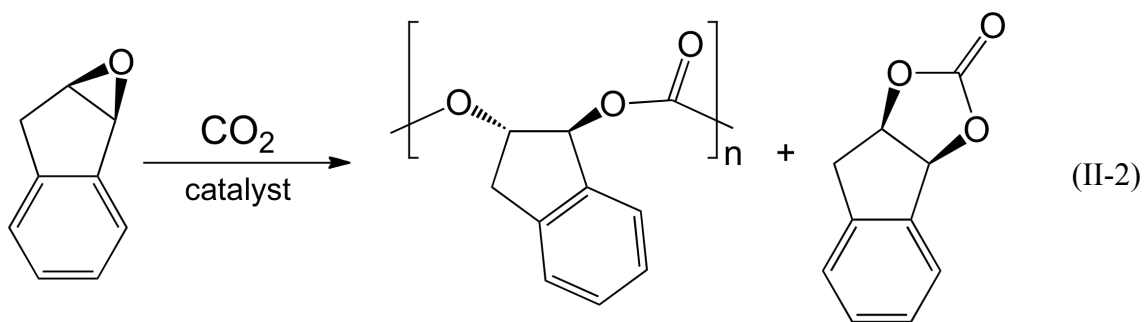
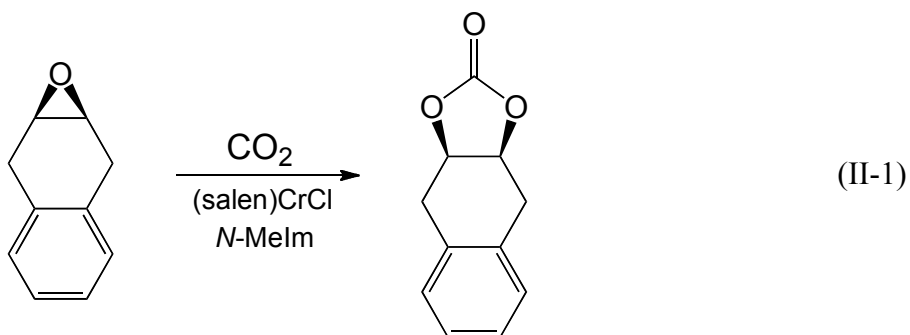
Despite the significant progress made recently in this field, the catalytic coupling of CO<sub>2</sub> and epoxides is still lacking in the production of polycarbonates with glass transition temperatures similar to that of BPA polycarbonate ( $T_g = 150$  °C). In an effort to expand upon this horizon, the D.J. Darensbourg group published a 2004 report investigating the coupling of 2,3-epoxy-1,2,3,4-tetrahydronaphthalene oxide (1,4-dihydronaphthalene oxide) and CO<sub>2</sub>.<sup>69</sup> This monomer was chosen so that the bulky benzene rings would hinder molecular rotation of the polymer backbone and therefore increase the  $T_g$ . However, 1,4-dihydronaphthalene oxide was found to couple with CO<sub>2</sub> to selectively provide the *cis*-isomer of the corresponding cyclic carbonate (eqn II-1).

In an effort to further expand upon this work, we chose to look at other bulky olefins that we could easily convert to the corresponding epoxide. Indene, consisting of fused cyclopentene and benzene rings, is a readily available olefin found in 1 wt% of coal tar.<sup>80</sup> Its primary use is in the indene-coumarone resins (ICRs) found in paints, printing inks, adhesives, rubber, etc. produced globally at about 100 000 tonnes/yr,<sup>80,81</sup>

---

\*Portions reprinted (adapted) with permission from “Synthesis of Poly(indene carbonate) from Indene Oxide and Carbon Dioxide – A Polycarbonate with a Rigid Backbone.” Darensbourg, D.J.; Wilson, S.J. *J. Am. Chem. Soc.* **2011**, *133*, 18610-18613. Copyright 2011 American Chemical Society.

and it is fairly cheap to the academic research chemist at ~\$0.11/g.<sup>82</sup> Following epoxidation to indene oxide, this monomer represents a sound choice for CO<sub>2</sub> coupling with a bulky oxirane. In this chapter, we report both the novel production of poly(indene carbonate) through the catalytic coupling of indene oxide and carbon dioxide (eqn II-2). To our knowledge, this has marked the first time that an aromatic group has been rigidly incorporated into the polymer backbone utilizing CO<sub>2</sub>/epoxides coupling.



## Experimental

**Materials and Methods.** Unless otherwise specified, all syntheses and manipulations were carried out on a double-manifold Schlenk vacuum line under an atmosphere of argon or in an argon-filled glovebox. Dichloromethane was freshly distilled over CaH<sub>2</sub>. Diethyl ether and toluene were purified by an MBraun Manual Solvent Purification system packed with Alcoa F200 activated alumina dessicant, or alternatively toluene was distilled from sodium/benzophenone and stored in an argon-filled glovebox. Indene (90+%, Alfa Aesar), and N-bromosuccinimide (Alfa Aesar) were used as received. Tetra-*n*-butylammonium bromide (Aldrich) was recrystallized from acetone/diethyl ether before use and stored in an argon-filled glovebox. PPN-2,4-dinitrophenoxide,<sup>33b</sup> all isomers of *N,N'*-bis(3,5-di-*tert*-butylsalicylidene)-1,2-cyclohexanediaminocobalt(III)-2,4-dinitrophenoxide,<sup>83</sup> and bifunctional cobalt catalysts<sup>84</sup> were prepared according to published literature procedures. In the initial coupling studies, bone-dry carbon dioxide supplied in a high-pressure cylinder and equipped with a liquid dip tube was purchased from Scott Specialty Gases. For the studies involving bifunctional cobalt catalysts, Research Grade 99.999% carbon dioxide supplied in a high-pressure cylinder and equipped with a liquid dip tube was purchased from Airgas. The CO<sub>2</sub> was further purified by passing through two steel columns packed with 4 Å molecular sieves that had been dried under vacuum at ≥ 200 °C.

**Measurements.** <sup>1</sup>H and <sup>13</sup>C NMR spectra were acquired on Unity+ 300 MHz, VXR 300 MHz, and Innova 500 MHz superconducting NMR spectrometers. Molecular weight determinations (M<sub>n</sub> and M<sub>w</sub>) were carried out with a Malvern Modular GPC



apparatus equipped with ViscoGEL I-series columns (H+L) and Model 270 dual detector comprised of RI and Light Scattering detectors. Glass transition temperatures ( $T_g$ ) were measured using a Mettler Toledo polymer DSC equipped with a liquid nitrogen cooling system and 50 mL/min purge of dry nitrogen gas. Samples (~8 mg) were weighed into 40  $\mu$ L aluminum pans and subjected to two heating cycles. The first cycle covered the range from 25 to 200  $^{\circ}$ C at 10  $^{\circ}$ C/min and was then cooled back to 0  $^{\circ}$ C at -10  $^{\circ}$ C/min. Midpoint  $T_g$  data was obtained from the second heating cycle which ranged from 0 to 300  $^{\circ}$ C at a heating rate of 5  $^{\circ}$ C/min. Thermogravimetric analyses were performed under an Ar atmosphere using a Mettler-Toledo model TGA/DSC1 STARe system. Samples were stabilized at 25  $^{\circ}$ C and heated to 500  $^{\circ}$ C at a heating rate of 10  $^{\circ}$ C/min. Onset and 50% decomposition measurements were analyzed using Mettler-Toledo STAR software version 10.00c.

**Synthesis of *trans*-2-bromo-1-indanol.** This procedure was modified from the work of Ogasawara.<sup>85</sup> Indene (60.0042 g of 90% mixture, 464.9 mmol, 1.0 eq) was dissolved in 300 mL of a 50/50 THF/water mixture at room temperature. N-bromosuccinimide (91.0285 g, 511.5 mmol, 1.1 eq) was added over the course of 5 minutes. The reaction was allowed to stir open to air for 18 h. The yellow organic layer was separated, and the aqueous layer was washed with ethyl acetate (3 x 40 mL). The combined organic layers were washed with saturated sodium sulfate (3 x 40 mL) and brine (3 x 40 mL). The solution was dried with sodium sulfate and concentrated *in vacuo*. The resulting solid was recrystallized from diethyl ether or ethanol to yield white crystalline needles (90.5052 g, 91.4% yield).  $^1\text{H}$  NMR (300 MHz,  $\text{CDCl}_3$ ):  $\delta$  7.41 (t,

1H), 7.19-7.33 (m, 3H), 5.32 (t, 1H, J = 6.0 Hz), 4.29 (q, 1H, J = 7.2, 6.0 Hz), 3.58 (dd, 1H, J = 9.0, 7.2 Hz), 3.22 (dd, 1H, J = 9.0, 7.2 Hz), 2.32 (d, 1H, J = 6.0 Hz). <sup>13</sup>C NMR (300 MHz, CDCl<sub>3</sub>): δ 139.7, 128.9, 127.6, 124.5, 124.0, 83.3, 54.4, 40.4, 29.5 ppm. Anal. Calc. for C<sub>9</sub>H<sub>9</sub>OBr: C, 50.73; H, 4.26. Found: C, 50.31; H, 4.36.

**Synthesis of Indene Oxide.** This procedure was modified from the work of Ogasawara.<sup>85</sup> In a representative procedure, *trans*-2-bromo-1-indanol (19.0726 g, 89.5 mmol, 1 eq) was dissolved in 300 mL dry Et<sub>2</sub>O or CH<sub>2</sub>Cl<sub>2</sub> at room temperature. Freshly ground sodium hydroxide powder (8.8243 g, 220.6 mmol, 2.5 eq) was added portionwise to the reaction. The flask was sealed to prevent loss of solvent, and the reaction was allowed to stir for 4 h. Water (75 mL) was added to dissolve the NaBr precipitate. The aqueous and organic layers were separated, and the organic layer was washed with saturated sodium bicarbonate (3 x 40 mL) and brine (3 x 40 mL). The resulting organic layer was dried with sodium sulfate and concentrated *in vacuo*. Depending on conversion, either an off white oil or solid is formed. The indene oxide is purified by heating to 45 °C in a sublimation apparatus under vacuum (~0.1 mmHg) over CaH<sub>2</sub> to remove any residual water. The cooling trap was flame dried before use and filled with ice during the process to induce crystallization. Sublimation is repeated to ensure purity. The resulting hygroscopic white crystalline solid is collected and immediately used or transferred into the freezer of an argon-filled glovebox. (9.5061 g, 80.4% unoptimized yield). <sup>1</sup>H NMR (300 MHz, CDCl<sub>3</sub>): δ 7.52 (d, 1H, J = 7.2 Hz), 7.12-7.30 (m, 3H, J = 7.2 Hz), 4.29 (d, 1H, J = 2.7 Hz), 4.15 (t, 1H, J = 3.0 Hz), 3.23 (d, 1H, J = 18.3 Hz), 2.99 (dd, 1H, J = 18.0, 3.0 Hz). <sup>13</sup>C NMR (125 MHz, CDCl<sub>3</sub>): δ 143.6, 140.9, 128.6, 126.3,

125.2, 59.2, 57.8, 34.7 ppm. Anal. Calc. for C<sub>9</sub>H<sub>8</sub>O: C, 81.79; H, 6.10. Found: C 81.99, H 6.30. Crystals suitable for X-ray crystallography were obtained *via* sublimation.

**Coupling Reactions of CO<sub>2</sub> and Indene Oxide.** For coupling reactions with CO<sub>2</sub>, the appropriate catalyst, cocatalyst, solvent, and indene oxide were delivered *via* injection port into a 300 mL stainless steel Parr autoclave reactor that was previously dried overnight *in vacuo* at or above 100 °C. Following reagent loading, the autoclave was then pressurized with 3.5 MPa of CO<sub>2</sub>, and the reactor was heated or cooled with an ice bath to the appropriate temperature. Unless otherwise stated, the monomer:catalyst:cocatalyst ratio was maintained at 500:1:1 for the (salen)CoY/PPNY systems and 1000:1 for the bifunctional catalysts, and the reaction was run for the corresponding reaction time. After the reaction was stopped, the autoclave was vented in a fume hood. The percent conversion to products was determined based on <sup>1</sup>H NMR integration of peaks for indene oxide, indene carbonate, oligomeric species, and poly(indene carbonate) left in the reaction solution as determined by <sup>1</sup>H NMR (In CDCl<sub>3</sub>: peaks at 4.30, 6.01, 6.01, and 6.26 ppm, respectively. In toluene-*d*<sub>8</sub>: 3.78, 4.96, 5.90, and 5.48 ppm, respectively). The polymer was twice precipitated in Et<sub>2</sub>O from a saturated CH<sub>2</sub>Cl<sub>2</sub> solution followed by two precipitations from 5% HCl in MeOH. The amounts of polycarbonate and ether linkages in the copolymer were determined by integrating the appropriate <sup>1</sup>H NMR resonances of a pure and dry sample of polymer. Anal. Calc. for (C<sub>10</sub>H<sub>8</sub>O<sub>3</sub>)<sub>*n*</sub>: C, 68.18; H, 4.58. Found: C, 68.00; H, 4.64. Peaks located at ~5.9 and ~4.7 ppm are observed in the <sup>1</sup>H NMR spectra (CDCl<sub>3</sub>) of the crude reaction mixture and remain following purification of all produced polymers. Their respective

integrations to the polycarbonate peaks remain the same both before and after polymer isolation and purification. As such, we believe them to be inherent to the poly(indene carbonate) samples. However, we believe their chemical shift to be too far downfield to be due to ether linkages within the backbone.

**Synthesis of Cyclic *cis*-Indene Carbonate.** The synthesis was followed as detailed in the coupling reactions of CO<sub>2</sub> and indene oxide with specific experimental conditions listed within the text. Solvent was removed *in vacuo*, and residual indene oxide was removed *via* sublimation. Residual catalyst was removed by filtering the solution through both activated carbon and silica gel. Clear, colorless block crystals of cyclic *cis*-indene carbonate were obtained through slow evaporation from a saturated solution in dichloromethane at 25 °C. <sup>1</sup>H NMR (300 MHz, CDCl<sub>3</sub>): δ 7.52 (d, 1H, J = 7.8 Hz), 7.36 (m, 3H, J = 7.8 Hz), 6.01 (d, 1H, J = 6.6 Hz), 5.45 (qd, 1H, J = 3.6, 6.6 Hz), 3.40 (d, 2H, J = 3.6 Hz) ppm. <sup>13</sup>C NMR (125 MHz, CDCl<sub>3</sub>): δ 154.7, 140.0, 136.4, 131.0, 128.2, 126.4, 125.6, 83.5, 79.7, 38.0 ppm. Anal. Calc. for C<sub>10</sub>H<sub>8</sub>O<sub>3</sub>: C, 68.18; H, 4.58. Found: C, 68.43; H, 4.57. Crystals suitable for X-ray diffraction were grown from a concentrated CH<sub>2</sub>Cl<sub>2</sub> solution at 25 °C.

**X-ray Crystal Study.** For the crystal structures of indene oxide and *cis*-indene carbonate, a Bausch and Lomb 10× microscope was used to identify suitable crystals. A single crystal sample was coated in mineral oil, affixed to a Nylon loop, and placed under streaming N<sub>2</sub> (110 K) in a single-crystal APEXii CCD or Bruker GADDS/Histar diffractometer. X-ray diffraction data were collected by covering a hemisphere of space upon combination of three sets of exposures. The structure was solved by direct

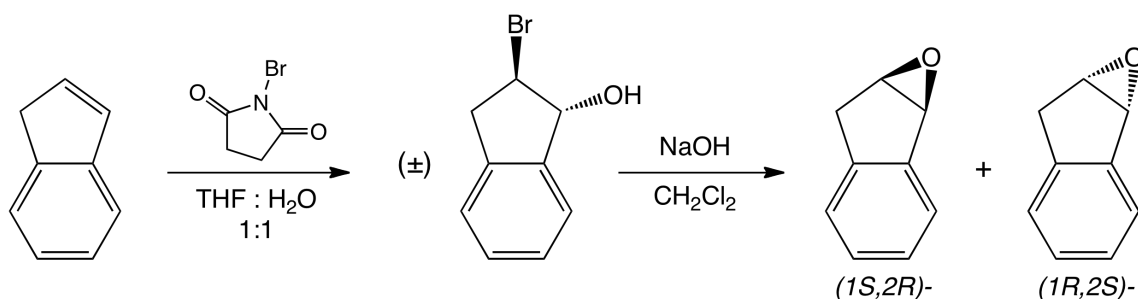
methods. H atoms were placed at idealized positions and refined with fixed isotropic displacement parameters and anisotropic displacement parameters were employed for all non-hydrogen atoms. The following programs were used: for data collection and cell refinement, APEX2;<sup>86</sup> data reductions, SAINTPLUS, version 6.63;<sup>87</sup> absorption correction, SADABS;<sup>88</sup> structure solutions, SHELXS-97;<sup>89</sup> structure refinement, SHELXL-97.<sup>90</sup>

#### **Removal of Unknown Poly/oligomeric X from Poly(Indene Carbonate)**

**Sample.** 0.1002 g poly(indene carbonate) (569  $\mu\text{mol}$ , 323 eq) was dissolved in 10 mL toluene. 0.0005 g of  $n\text{Bu}_4\text{NN}_3$  (1.76  $\mu\text{mol}$ , 1 eq) was added, and the mixture was stirred for 1 hour at 60 °C. MeOH was added to precipitate the polymer, and the solution was concentrated *in vacuo*. The precipitate was redissolved in a small amount of  $\text{CH}_2\text{Cl}_2$ , reprecipitated from MeOH, and dried under vacuum with applied heat.  $^1\text{H}$  NMR analysis of the product revealed that **X** now made up  $\ll 1$  % of the polymer sample. For the sample prior to the removal of **X**: 4% **X** by  $^1\text{H}$  NMR,  $M_n = 9700$  g/mol, PDI = 1.12,  $T_g = 138$  °C) For the sample after the removal of **X**: 0.3 % **X** by  $^1\text{H}$  NMR,  $M_n = 9700$  g/mol, PDI = 1.09,  $T_g = 136$  °C.

### **Results and Discussion**

**Synthesis of Indene Oxide.** The non-commercially available indene oxide is well known to be both acid-sensitive and labile.<sup>91</sup> On the basis of our own experimental observation of Meinwald rearrangement of indene oxide to 2-indanone when utilizing *m*CPBA as an oxidant,<sup>92</sup> the alternate stepwise synthesis through formation of the



**Scheme II-1.** Stepwise synthesis of *rac*-indene oxide. *Trans*-2-bromo-1-indanol is synthesized from indene and *N*-bromosuccinimide and followed by ring-closing by sodium hydroxide.

bromohydrin and ring-closing using NaOH was settled upon (Scheme II-1).<sup>85</sup> It should be noted that the formed 2-indanone did not impede the coupling of indene oxide and CO<sub>2</sub>. Our desire to remove it from the system involved it having a characteristic FT-IR stretch at  $\sim 1748\text{ cm}^{-1}$  which misleadingly appears at the same location as polycarbonate. Following ring-closing of the bromohydrin, purification by sublimation afforded pure *rac*-indene oxide capable of coupling with CO<sub>2</sub>. It is worth noting that indene oxide is slightly hygroscopic and must be transferred into an inert atmosphere immediately following sublimation. Excess water renders the system inactive, likely by reducing the Co(III) metal center to Co(II). Indene oxide crystals suitable for X-ray diffraction were

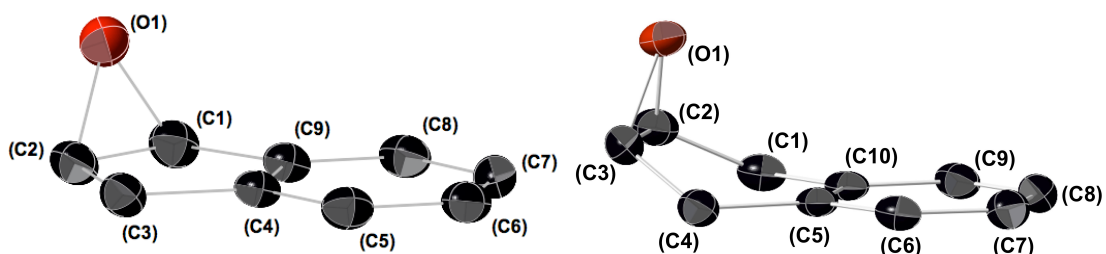


**Figure II-1.** Thermal ellipsoid representation of *(1S,2R)*-indene oxide (left) and dihydronaphthalene oxide<sup>69</sup> (right) with ellipsoids at 50% probability surfaces. Hydrogen atoms have been omitted for clarity. Bond angles and lengths are identical for the *(1R,2S)*-indene oxide enantiomer.

obtained via sublimation (Figure II-1). The fused benzene and cyclopentene rings are nearly planar, with a C8-C5-C3-C1 dihedral angle of  $1.591^\circ$ . This differs from crystals grown of 1,4-dihydronaphthalene oxide, where a distinct pucker is found within the cyclohexane ring.<sup>69</sup>

**Catalytic Synthesis of *cis*-Indene Carbonate.** On the basis of its successes with the difficult copolymerization of CO<sub>2</sub> and styrene oxide,<sup>33b</sup> we chose to initially employ *N,N'*-bis(3,5-di-*tert*-butylsalicylidene)-1,2-cyclohexanediaminocobalt(III)-2,4-dinitrophenoxide (**1**) as the catalyst along with PPN-2,4-dinitrophenoxide as cocatalyst (Figure II-2). Both resolved [(*S,S*)- or (*R,R*)-] and racemic versions of catalyst **1** were employed in this study. Indene oxide melts at  $\sim 32$ - $33^\circ\text{C}$ , and thus initial coupling reactions of neat indene oxide and CO<sub>2</sub> were performed at or above  $35^\circ\text{C}$  (Table II-1, entries 1-3).

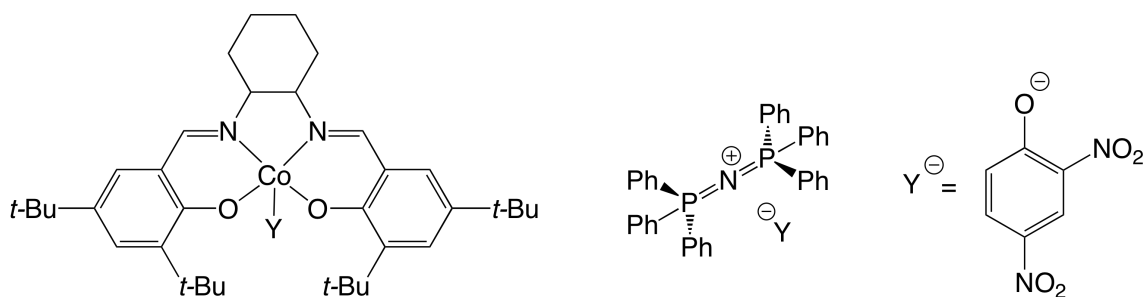


**Figure II-2.** Catalyst system for the copolymerization of indene oxide and CO<sub>2</sub>. *N,N'*-bis(3,5-di-*tert*-butylsalicylidene)-1,2-cyclohexanediaminocobalt(III)-2,4-dinitrophenoxide, (salen)CoDNP, (**1**) and PPN-2,4-dinitrophenoxide, PPN-DNP or PPNY.

**Table II-1.** Production of *cis*-indene carbonate.

Entry	Catalyst System	time (days)	T (°C)	[IO], g/mL	Pressure (MPa)	Percent Conversion <sup>a</sup>	TOF (h <sup>-1</sup> ) <sup>b</sup>
1 <sup>c</sup>	( <i>S,S</i> )-1/PPNY <sup>d</sup>	3	60	N/A	2.1	71.3	5.0
2 <sup>c</sup>	( <i>S,S</i> )-1/PPNY	3	35	N/A	3.4	11.5	0.8
3 <sup>c</sup>	<i>rac</i> -1/PPNY	3	35	N/A	2.1	5.8	0.4
4	( <i>R,R</i> )-1/PPNY	1	25	1.0	2.1	54.6	11.4
5	( <i>R,R</i> )-1/ <i>n</i> Bu <sub>4</sub> NBr	1	25	1.0	2.1	91.3	19.0

The coupling reactions were performed with catalyst/cocatalyst/epoxide = 1/1/500 molar ratio with CH<sub>2</sub>Cl<sub>2</sub> solvent in a 300 mL stainless steel Parr autoclave. (a) Determined using <sup>1</sup>H NMR spectroscopy. (b) Turnover frequency of indene oxide to indene carbonate as determined by <sup>1</sup>H NMR spectroscopy. (c) Experiment run in neat indene oxide. (d) PPN = bis(triphenylphosphine)iminium, Y = 2,4-dinitrophenoxide anion.

As expected, the increase in reaction temperature from 35 to 60 °C is mirrored by an increase in both conversion to cyclic carbonate from 5.8% to 71.3% and turnover frequency (TOF) from 0.4 to 5.0 h<sup>-1</sup>. By increasing the pressure from 2.1 to 3.4 MPa, a doubling in activity was noted at 35 °C, from 0.4 to 0.8 h<sup>-1</sup>. In the <sup>1</sup>H NMR and FT-IR spectra of the crude reaction products, no polymer formation was observed.

Following removal of residual indene oxide *in vacuo*, cyclic indene carbonate was purified by flushing a CH<sub>2</sub>Cl<sub>2</sub> solution through both activated carbon and a silica pad. Clear, colorless block crystals suitable for X-ray diffraction were grown from a concentrated CH<sub>2</sub>Cl<sub>2</sub> solution. Two unique yet similar molecules of *cis*-indene carbonate are found within the unit cell, one of which is displayed in Figure II-3. Rather than displaying near planarity in the five-membered cyclic ring as in the case of cyclopentene carbonate and *cis*-1,4-dihydronaphthalene carbonate,<sup>69</sup> the two *cis*-indene carbonate molecules have an O1-C1-C2-O2 dihedral angle of 14.187° and an O4-C11-C12-O5 angle of 8.252°, with the difference in the two molecules likely due to packing effects.



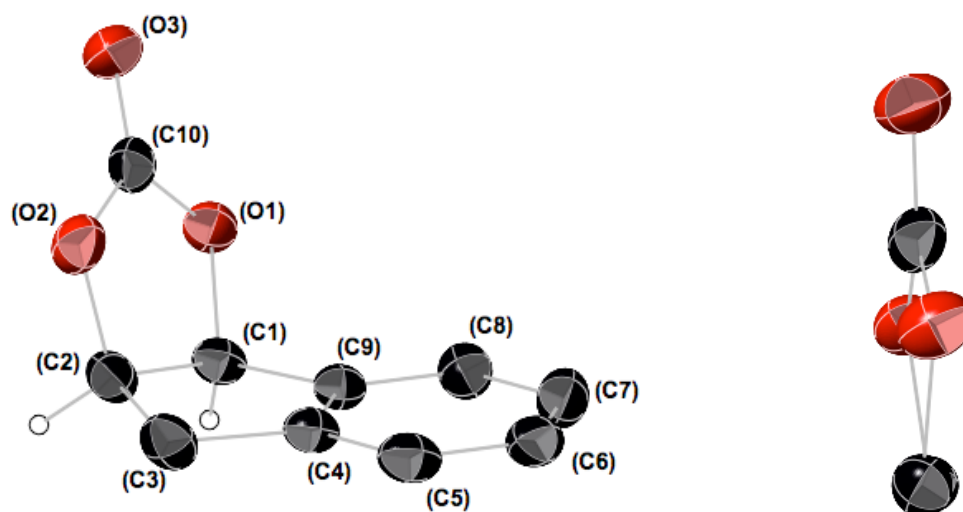


**Figure II-3.** Thermal ellipsoid representation of *cis*-indene carbonate with ellipsoids at 50% probability surfaces. All hydrogens have been omitted for clarity except H1 and H2 to display the *cis*- nature of the product. Inset image is looking down the C2-C1 bond, displaying the torsion in the five-membered cyclic ring. O1-C1-C2-O2 dihedral angle = 14.187°; O4-C11-C12-O5 dihedral angle = 8.252°

Only the *cis*- isomer of indene carbonate is produced from the coupling of CO<sub>2</sub> and indene oxide. Attempts to separately synthesize *trans*-indene carbonate from *trans*-indene-1,2-diol and ethyl chloroformate failed, likely due to the unstable nature of the *trans*- isomer. DFT calculations reveal that the *trans*-configuration is highly disfavored over the *cis*- by 21.6 kcal/mol.<sup>93</sup>

**Low Temperature Coupling Reactions.** The production of poly(styrene carbonate) from the same catalytic system was enhanced and more selective at lower temperatures.<sup>10a</sup> Thus, we decided to employ a cosolvent and study the coupling of CO<sub>2</sub> and indene oxide both at and below room temperature. Despite the potential for HCl poison in dichloromethane, CH<sub>2</sub>Cl<sub>2</sub> was chosen as the solvent due to PPNX salts'

inability to dissolve in toluene. Similar toluene-soluble  $n\text{Bu}_4\text{NX}$  cocatalysts are inherently wet with trace water. As expected,  $n\text{Bu}_4\text{NBr}$  with the better leaving group was more active than PPNY, with respective TOF of 19.0 and 11.4  $\text{h}^{-1}$  at 25 °C for cyclic carbonate production (entries 3 and 4).

When the reaction temperature was decreased further to 0 °C, the first indications of polymer formation were observed (Table II-2, entries 1-3). After 1 week of reaction at 0 °C, we were gratified to find that a 0.2 g/mL solution of indene oxide utilizing the (*S,S*)-**1**/PPNY system formed a mixture of indene carbonate and poly(indene carbonate), the latter identified by its characteristic polycarbonate FT-IR stretch at 1750  $\text{cm}^{-1}$  (entry 1).

In an effort to suppress cyclization to indene carbonate and induce further polycarbonate production, the concentration of indene oxide was increased to 1.0 g/mL. After 6 days at 0 °C, both (*S,S*)- and *rac*-**1**/PPNY afforded an ~60/40% mixture of poly(indene carbonate) and cyclic indene carbonate (entries 2 and 3, respectively). The observed low molecular weights are likely due to slow polymer growth combined with rapid, reversible chain transfer with trace water.

**Polymer Characterization.** When purified, poly(indene carbonate) is slightly off-white in color. Though the color may be due to residual cobalt remaining in the polymer, it appears to be inherent as it remains after multiple precipitations as well as filtering through activated carbon and silica gel. Each of the polymer samples has a slightly different  $T_g$ , ranging from 108 to 134 °C (Figure II-4). The differences between entries 1 and 2 (114 vs 133 °C) may be attributed to molecular weight discrepancies

between the longer-chained 7000 vs the more oligomeric 4200 g/mol sample. Similar jumps in both  $T_g$  (105 vs 134 °C) and molecular weight (7100 vs 3500 g/mol) are observed between entries 3 and 4. Bimodal GPC traces are observed, indicating that chain transfer is taking place within the reaction. Thermogravimetric analyses of the polymer samples indicate that poly(indene carbonate) is thermally stable at up to ~245 °C, with 50% degradation occurring by ~264 °C (Figure II-5).

Distinct differences in the regio- and stereoregularity of the polymer chains can be observed for polymer samples produced from different catalysts (Figure II-5). Though the peaks have not been definitively assigned, it can be seen from the carbonate region of the  $^{13}\text{C}$  NMR that the resolved (*S,S*)-**1** does display increased selectivity for specific ring-opening patterns of indene oxide over *rac*-**1**. The peaks centered at 154.5 ppm are enhanced over those centered at 154.2 ppm for (*S,S*)-**1** (green – Table II-2 entry 1, blue – Table II-2 entry 2) relative to *rac*-**1** (red – Table II-2, Entry 3). For these samples, the polymer's molecular weight appears to play a more significant role in  $T_g$  and  $T_d$  determination as compared to regio- and stereoregularity.

**Table II-2.** Production of poly(indene carbonate).

Entry	Catalyst System	time (days)	Percent Conversion <sup>a</sup>	PIC/IC <sup>a</sup>	TOF (h <sup>-1</sup> ) <sup>b</sup>	M <sub>n</sub>		PDI <sup>d</sup>	T <sub>g</sub> <sup>e</sup>	T <sub>d</sub> <sup>f</sup>	T <sub>d50</sub> <sup>g</sup>
						Theo. (g/mol) <sup>c</sup>	GPC (g/mol) <sup>d</sup>				
1 <sup>h</sup>	( <i>S,S</i> )-1/PPNY	7	17	45/55	1.1	14600	4200	1.19	114	245	262
2	( <i>S,S</i> )-1/PPNY	6	59	57/43	2.1	29600	7000	1.09	133	249	264
3	<i>rac</i> -1/PPNY	6	50	59/41	1.7	26000	7100	1.16	134	245	266
5	<i>rac</i> -1/PPNY	2	16	59/41	1.7	8300	3500	1.30	109	236	259
6	<i>rac</i> -1/ <i>n</i> Bu <sub>4</sub> NBr	2	51	0/100	4.0	-	-	-	-	-	-

The coupling reactions were performed with catalyst/cocatalyst/epoxide = 1/1/500 molar ratio in a 300 mL autoclave with indene oxide concentrations of 1.0 g/mL in CH<sub>2</sub>Cl<sub>2</sub>. Temperature and pressure were held at 0 °C and 3.4 MPa, respectively. Data regarding selectivity for carbonate linkages can be found in the Supporting Information. (a) Determined by using <sup>1</sup>H NMR spectroscopy. (b) Turnover frequency of indene oxide to products [poly(indene carbonate) and indene carbonate] as determined by <sup>1</sup>H NMR spectroscopy. (c) Theoretical M<sub>n</sub> = (M/I) x (% conversion) x (mol. wt. of indene carbonate). (d) Determined by gel permeation chromatography in THF; calibrated with narrow polystyrene standards. (e) The midpoint temperature of the major T<sub>g</sub> during the second heating using DSC. (f) Onset decomposition temperature, as determined by TGA. (g) Temperature at which 50% of the polymer's mass has been lost. (h) 0.2 g/mL indene oxide in CH<sub>2</sub>Cl<sub>2</sub>.

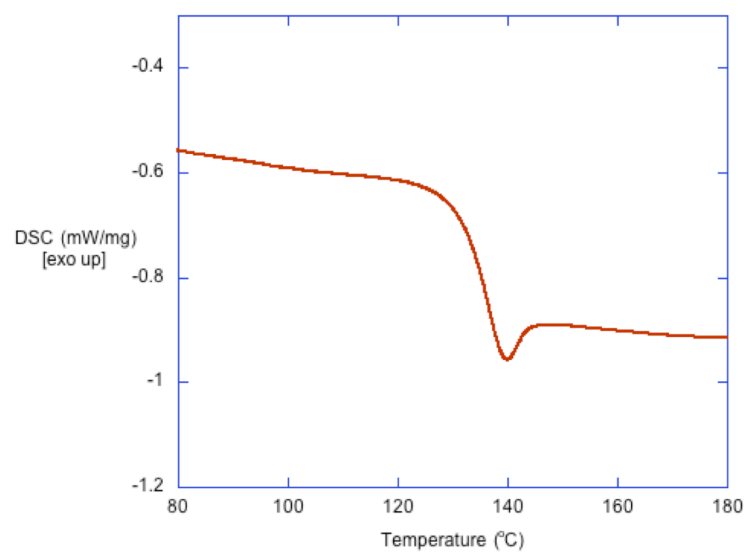


**Figure II-4.** Relevant data from the second cycle of the DSC thermogram of the polymer sample from Table II-2, entry 3.  $T_g = 134\text{ }^\circ\text{C}$ .

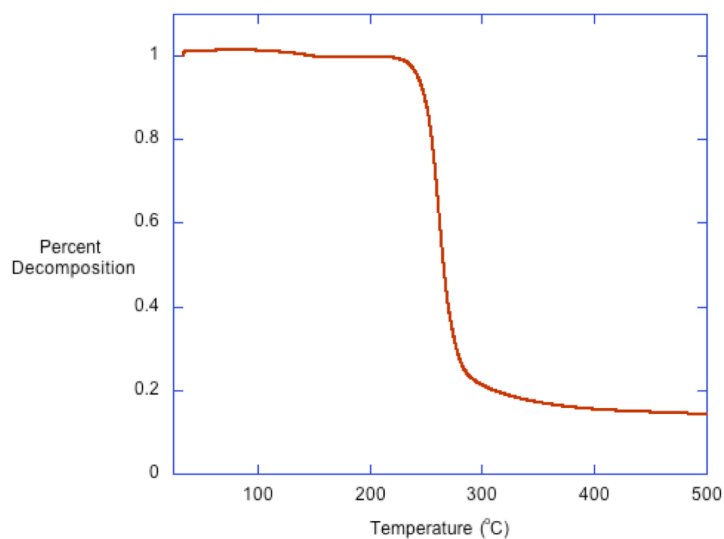


**Figure II-5.** TGA curve of polymer sample from Table II-2, entry 3.  $T_d = 245\text{ }^\circ\text{C}$ ,  $T_{d50} = 266\text{ }^\circ\text{C}$ .

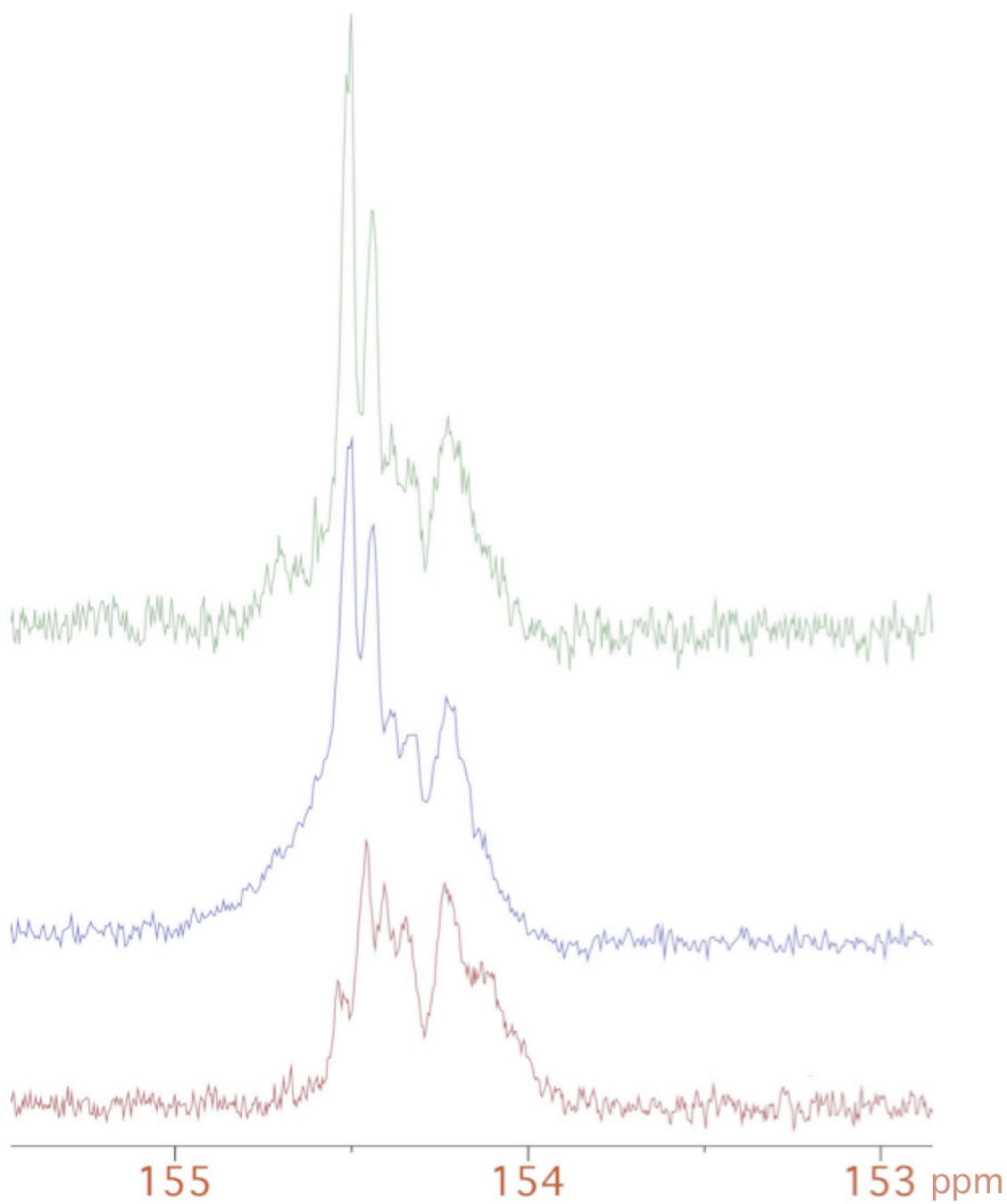


**Figure II-6.** Carbonate O-(C=O)-O peak in the <sup>13</sup>C NMR of poly(indene carbonate) samples from Table II-2 entry 1 (green), entry 2 (blue), and entry 3 (red). CDCl<sub>3</sub>, 125 MHz.

**Coupling Reactions Utilizing Bifunctional Cobalt Catalysts.** Because the molecular weight of polymers, especially those with lower molar masses, has a strong influence on the  $T_g$ , it was anticipated that copolymers of molecular weights greater than 10 000 g/mol would exceed 134 °C. Three main methods exist for increasing molecular weight:

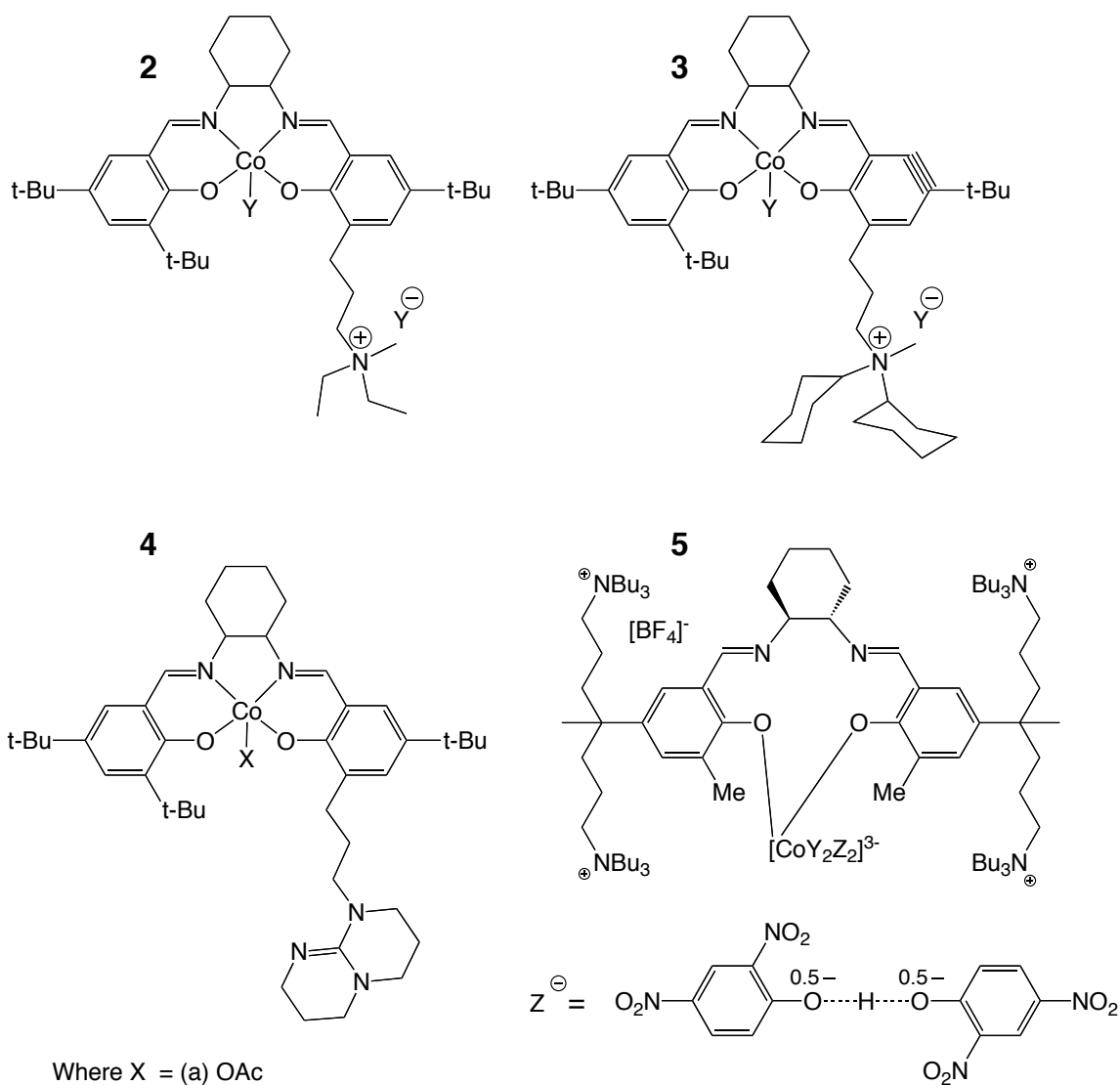
1. Decrease the temperature of the reaction to hinder backbiting to cyclic carbonate and instead favor polycarbonate production kinetically.
2. Decrease catalyst loading so as to favor longer polymer chains.
3. Utilize a more active and/or selective catalyst for the coupling reactions.

As cyclic carbonate is the thermodynamic product of the coupling reaction, lowering the reaction temperature should indeed decrease its production relative to polymer. However, the rate of polymer production would also decrease at lower temperatures, lowering the attractiveness of option (1). For (2), low catalyst/cocatalyst loadings can lead to lengthy induction periods,<sup>94</sup> though 1:1:500 (0.2 mol%) is by no means a low catalyst loading for these reactions. The Lu and Lee groups have both developed bifunctional cobalt catalysts that are highly active for poly(propylene carbonate) and poly(cyclohexene carbonate) production (3).<sup>95</sup> Thanks to a collaboration with Dr. Xiao-Bing Lu and his group from Dalian University of Technology in Dalian, China, we were able to test bifunctional catalysts **2** and **3** for the coupling of indene oxide and CO<sub>2</sub> (Figure II-7). Complexes **4** and **5** were also tested but proved to be ineffective for these particular coupling reactions.

The bifunctional nature of **2** and **3** allowed for the catalyst loading to be decreased to 1:1000 without concern for an increased induction period. Again utilizing dichloromethane as solvent, both **2** and **3** were over twice as active as the traditional catalyst/cocatalyst, with TOF of 4.7 and 4.0 h<sup>-1</sup> vs 1.9 for **1**/PPNY (Table II-3, entries 1, 2, and 5). Notably, the selectivity for polycarbonate was greatly increased for both bifunctional catalysts, with **2** producing >99% polycarbonate and **3** producing 93% polycarbonate. Despite the increase in activity and selectivity, the polymers' molecular weights remained low at 4300 and 4400 g/mol, respectively. Utilizing **2**, an increase in reaction time from 2 days to 4 days showed a corresponding increase in percent conversion from 23% to 40% and a corresponding increase in molecular weight from 4300 to 6400 g/mol (entries 2 and 3).

Though the **1**/PPNY system required dichloromethane solvent for solubility purposes, **2** and **3** are both soluble in toluene. The switch of solvent has a notable effect on polymer molecular weight for catalyst **2**, with a 1800 g/mol increase (entries 2 and 4). For **3**, toluene as solvent shows dramatic increases in conversion (43% vs 19%), activity (9.0 vs 4.0 h<sup>-1</sup>), and molecular weight (6700 vs 4400 g/mol) over the same reaction in dichloromethane (entries 6 and 5, respectively). No difference was observed in the decomposition temperatures of these longer-chained species.





Where X = (a) OAc  
 (b) NO<sub>3</sub>  
 (c) BF<sub>4</sub>

Y = 2,4-dinitrophenoxide

**Figure II-7.** Bifunctional catalysts **2** with  $-\text{NEt}_2\text{Me}$  arm (top left), **3** with  $-\text{NCy}_2\text{Me}$  arm (top right), and **4** with appended TBD group (bottom left) were generously donated by the Xiao-Bing Lu Group of Dalian University of Technology in Dalian, China. Bifunctional catalyst **5** bearing the out of pocket Co(III) metal center was generously donated by Dr. Bun Yeoul Lee of Ajou University in Suwon, South Korea.

**Table II-3.** Copolymerization of indene oxide and CO<sub>2</sub> utilizing bifunctional catalysts.

Entry	Catalyst	time (days)	T (°C)	Solvent	Percent Conversion <sup>a</sup>	% PIC <sup>a</sup>	TOF (h <sup>-1</sup> ) <sup>b</sup>	M <sub>n</sub>		PDI <sup>d</sup>	T <sub>g</sub> <sup>e</sup>	T <sub>d</sub> <sup>f</sup>	T <sub>d50</sub> <sup>g</sup>
								Theo. (g/mol) <sup>c</sup>	GPC (g/mol) <sup>d</sup>				
1 <sup>i</sup>	<i>rac</i> -1/PPNY	2	0	CH <sub>2</sub> Cl <sub>2</sub>	16	64	1.7	8300	3500	1.30	109	236	259
2	2	2	0	CH <sub>2</sub> Cl <sub>2</sub>	23	>99	4.7	40500	4300	1.10	123	-	-
3	2	4	0	CH <sub>2</sub> Cl <sub>2</sub>	40	>99	4.4	70500	6400	1.15	131	-	-
4	2	2	0	toluene	23	>99	4.4	40500	6100	1.06	126	-	-
5	3	2	0	CH <sub>2</sub> Cl <sub>2</sub>	19	93	4.0	33500	4400	1.07	122	-	-
6	3	2	0	toluene	43	>99	9.0	75700	6700	1.04	133	-	-
7	3	3	0	toluene	60	>99	8.3	106000	9700	1.12	138	239	257
8 <sup>h</sup>	3	3	0	toluene	60	>99	8.3	106000	9700	1.09	136	237	256
9	3	1	25	toluene	34	>99	7.1	59900	3900	1.09	124	-	-
10 <sup>j</sup>	3	2	25	toluene	62	>99	11.5	97200	6000	1.19	129	-	-
11 <sup>k</sup>	3	4 hours	40	toluene	4.5	0	11.3	-	-	-	-	-	-

Unless otherwise stated, the coupling reactions were performed with bifunctional catalyst/epoxide = 1/1000 molar ratio in a 300 mL autoclave with indene oxide concentrations of 1.0 g/mL in the appropriate solvent. The reactor was pressurized to 3.4 MPa before being heated/cooled to the appropriate temperature. (a) Determined by using <sup>1</sup>H NMR spectroscopy. Contains both polymer and oligomeric fractions. (b) Turnover frequency of indene oxide to products [poly(indene carbonate) and indene carbonate] as determined by <sup>1</sup>H NMR spectroscopy. (c) Theoretical M<sub>n</sub> = (M/I) x (% conversion) x (mol. wt. of indene carbonate). (d) Determined by gel permeation chromatography in THF; calibrated with narrow polystyrene standards. (e) The midpoint temperature of the major T<sub>g</sub> during the second heating using DSC. (f) Onset decomposition temperature, as determined by TGA. (g) Temperature at which 50% of the polymer's mass has been lost. (h) Sample from entry 7 was treated with *n*Bu<sub>4</sub>NN<sub>3</sub> in order to remove oligomeric X. (i) 1/1/500 molar ratio. (j) 1/890 catalyst loading. (k) 2.1 MPa.

Several reasons could exist for this change in activity. Qualitatively, indene oxide dissolves faster into dichloromethane than toluene during reaction setups. However at 0 °C and 3.4 MPa, the solubility of CO<sub>2</sub> in dichloromethane ( $X_{\text{CO}_2} = 0.69$ ) is greater than that of CO<sub>2</sub> in toluene ( $X_{\text{CO}_2} = 0.46$ ).<sup>96,97</sup> It is possible that the CO<sub>2</sub> is acting to dilute the concentration of indene oxide in solution and therefore slow the coupling reaction. The two lipophilic cyclohexyl groups in **3** may increase the solubility of the catalyst in toluene solvent, increasing the activity. Alternatively, the change to the less-polar toluene (dielectric constant 2.38 at 23 °C versus dichloromethane's 8.93 at 25 °C<sup>98</sup>) may increase ion pairing between the free polymer chain and the bifunctional catalyst.

Indeed, catalyst **3** is very active in toluene for the copolymerization of CO<sub>2</sub> and indene oxide. By increasing the reaction time to 3 days, poly(indene carbonate) was produced with molecular weight of 9700 g/mol and  $T_g$  of 138 °C (entry 7). **3** was also active at higher temperatures, producing poly(indene carbonate) with 99% selectivity even at 25 °C (entries 9-10). However, when the temperature was increased further to 40 °C, only cyclic carbonate was produced (entry 11).

**Polymer Selectivity.** There is a notable increase in poly(indene carbonate) selectivity for **2** and **3** over **1**/PPNY. This is likely due to the ability of the appended quarternary amine to electrostatically attract free polymer chains and prevent backbiting to cyclic carbonate (Figure II-8). The appended ammonium salt also keeps the stagnant polymer chains close to the metal center, allowing them to easily return to the cobalt and undergo further chain propagation.

As only the *cis*- isomer of indene carbonate is formed during the reaction, the byproduct must be forming from one of four different, though related, backbiting reactions (Figure II-9). A study of the depolymerization of poly(indene carbonate) showed that pathway **d** is unlikely to be the main route to *cis*-indene carbonate in solution. In each case investigated by Darensbourg and Wei, CO<sub>2</sub> pressure (and thereby carbonate chain end initiated) depolymerization was always slower than alkoxide-initiated. The strong base (NaHMDS, DBU)-initiated alkoxide depolymerization of poly(indene carbonate) requires high temperatures and lengthy reaction times (110 °C, 8-10 days to completion).<sup>99</sup>

If the weak base azide is instead employed to initiate depolymerization for pathway **d**, a separate radical pathway is observed. Depolymerization via pathway **a** will provide both *cis*-indene carbonate and indene oxide, the decarboxylation product. The direct coupling of CO<sub>2</sub> and indene oxide to form *cis*-indene carbonate utilizing (salen)CrCl and *n*Bu<sub>4</sub>NCl (pathway **b**) was found to proceed with  $E_A = 114.4 \pm 5.7$  kJ/mol (for further details, see Chapter III). Notably, the azide-initiated alkoxide depolymerization of poly(indene carbonate) also provides *cis*-indene carbonate as the main product, with small amounts of indene oxide also being observed. This reaction proceeds with  $E_A = 189.1 \pm 5.8$  kJ/mol, some 75 kJ/mol higher than direct, catalytic coupling of indene oxide with CO<sub>2</sub>. It can be thus inferred that most of the indene carbonate produced during the course of the reaction comes from 1:1 epoxide:CO<sub>2</sub> coupling rather than polymeric backbiting reactions.

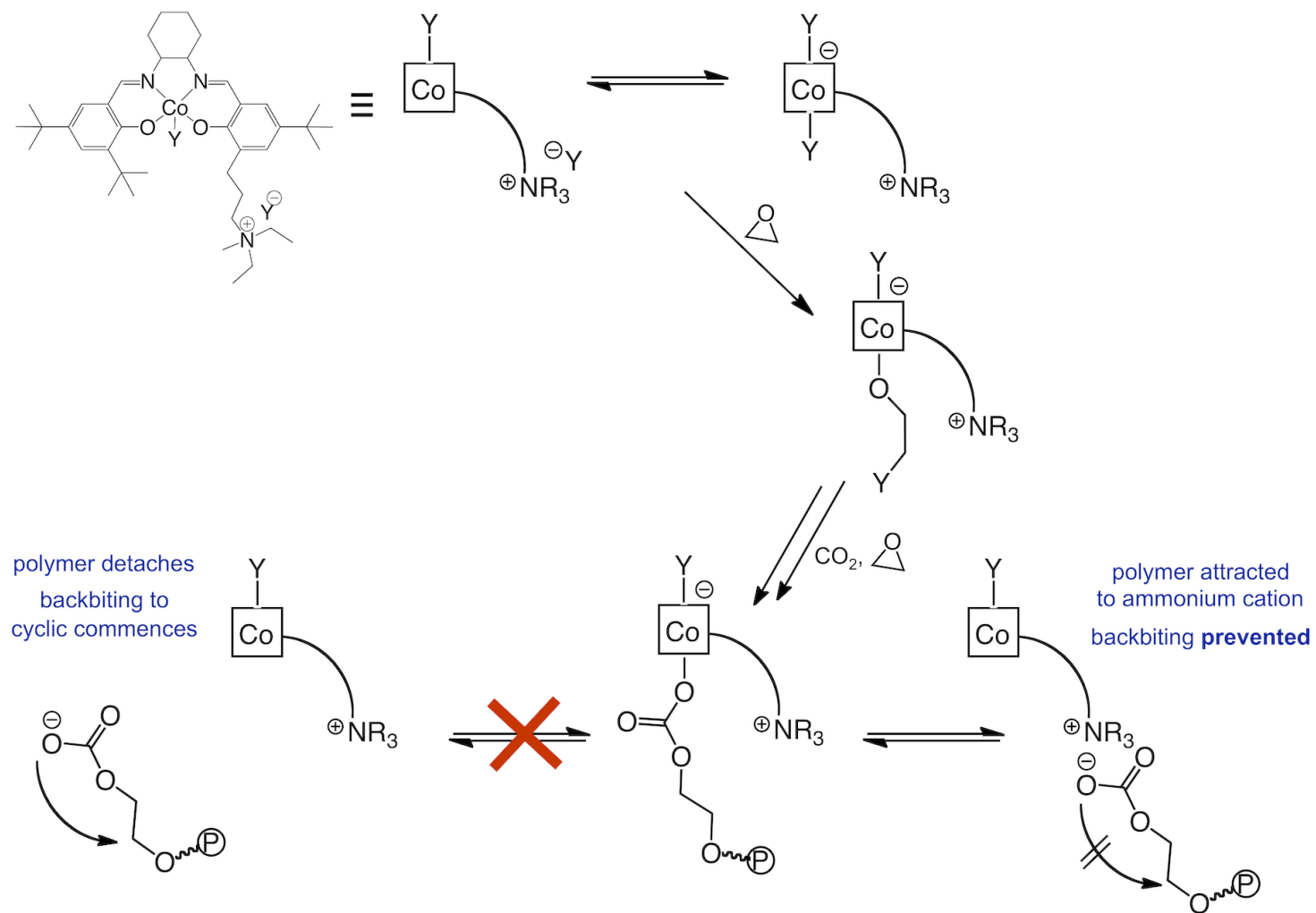


**Figure II-8.** Proposed polymerization mechanism by bifunctional catalysts. The electrostatic attraction between the free polymer anion and the ammonium salt prevents polymer backbiting to cyclic carbonate.

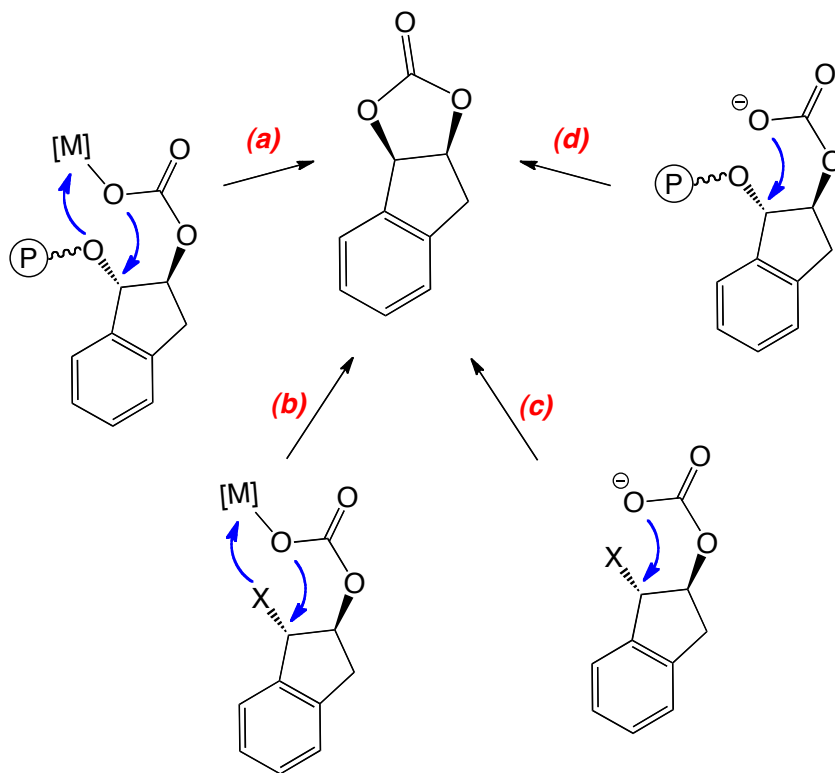


**Figure II-9.** Potential backbiting reactions for the formation of *cis*-indene carbonate.

$M_n$  vs  $T_g$ . Though  $T_g$  is often viewed as independent of polymer molecular weight, there is significance dependence for short-chained samples. Figure II-10 displays a plot of poly(indene carbonate)  $M_n$  vs  $T_g$ . There is a clear molecular weight-dependence on  $T_g$  for these chain lengths, though it is possible that a plateau will be reached around 140-145 °C, only 5-10 degrees below the  $T_g$  of BPA polycarbonate (150 °C). As displayed in Figure II-5, there does not seem to be any distinct regio- or stereoregularity within the polymer backbone. As the  $T_g$  of atactic poly(propylene carbonate) was able to be increased from 29 °C to 47 °C for completely isotactic

poly(propylene carbonate),<sup>100</sup> there is reason to believe that poly(indene carbonate) samples with higher thermal transitions are achievable through tacticity control.

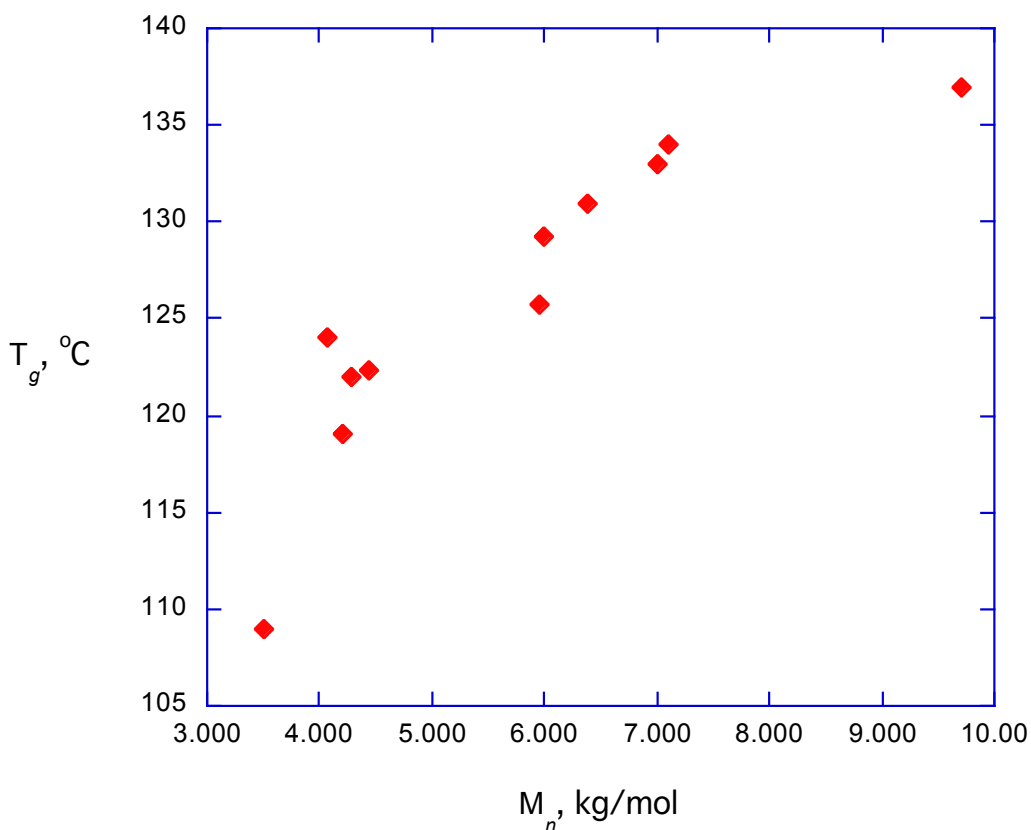


**Figure II-10.**  $M_n$  of poly(indene carbonate) vs  $T_g$  displaying dependence of the thermal transition on the molecular weight of these species.

**Additional Poly/Oligomeric Indene Carbonate Species “X.”** Following precipitation of poly(indene carbonate) from the crude reaction mixture, a separate, non-bulk polymer species can be observed by  $^1\text{H}$  and  $^{13}\text{C}$  NMR (Figures II-11 and II-12). This species, hereafter denoted as **X**, remains in a constant ratio with the polymer following not only precipitation but also column chromatography over silica and

activated carbon. Polymeric samples containing **X** do not display any unexpected FT-IR traces. As such, it is believed to be a mix of short-chain oligomers or cyclic materials.

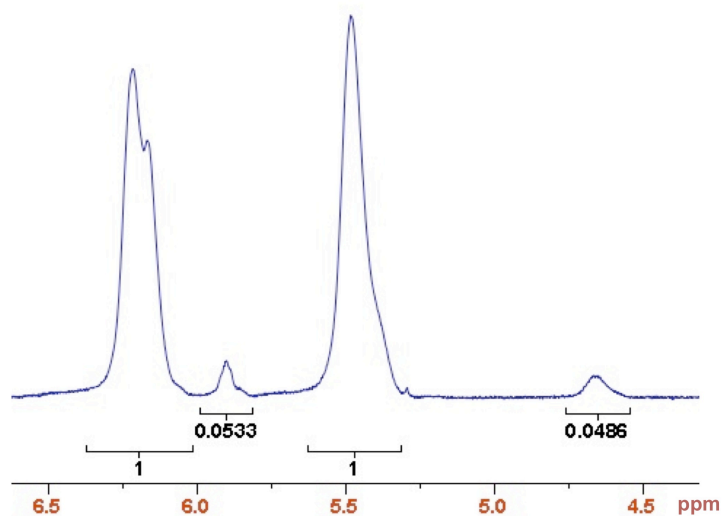


**Figure II-11.** <sup>1</sup>H NMR of purified poly(indene carbonate) sample. Bulk polymer signals can be observed at 6.2 and 5.5 ppm. **X**'s signals can be observed at 5.9 and 4.7 ppm. 500 MHz, CDCl<sub>3</sub>.

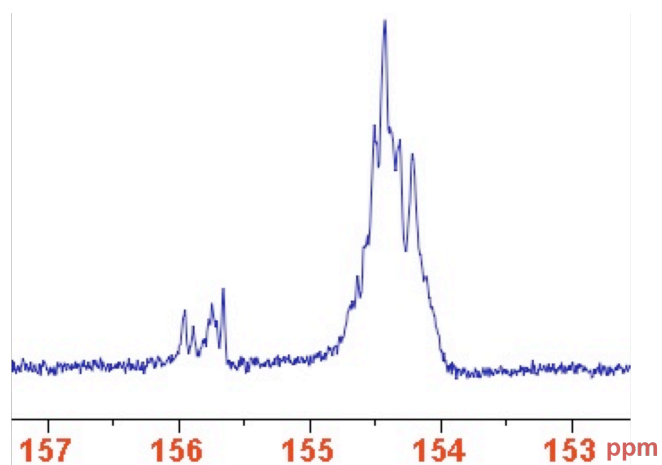


**Figure II-12.** <sup>13</sup>C NMR of the carbonate O(C=O)O purified poly(indene carbonate) sample. Bulk polymer signal can be observed at 154.4 ppm. **X** can be observed at 155.8 ppm. 125 MHz, CDCl<sub>3</sub>.



As one of the main goals of this project was to synthesize a novel polymer with a high  $T_g$ , it did not escape our notice that **X** could be acting as a plasticizer within poly(indene carbonate) and thereby be impacting the observed physical properties. By reacting a poly(indene carbonate) sample containing 4% **X** with  $n\text{Bu}_4\text{NN}_3$  for 1 hour at 60 °C, the concentration of **X** was reduced down to 0.3%, presumably by scission of the carbonate bonds. Despite the removal of **X**, the physical properties of the polymer remain the same (Table II-3, entries 7 and 8). There are no noticeable increases in  $T_g$ ,  $M_n$ , or decomposition temperatures. **X** therefore does not have an impact on these physical properties, though it may influence other properties not investigated in this report.

## Conclusions

Herein, we have reported the novel synthesis of poly(indene carbonate) from the catalytic coupling of indene oxide and  $\text{CO}_2$ . (salen)Co-(2,4-dinitrophenoxide), (salen)CoDNP, along with PPNDNP cocatalyst was able to produce poly(indene carbonate) samples with  $M_n$ s of up to 7100 g/mol and  $T_g$ s of up to 134 °C. The use of bifunctional cobalt catalysts **2** and **3** increased the molecular weights to up to 9700 g/mol, and a corresponding increase in  $T_g$  of up to 138 °C has also been realized. This polymer has the highest  $T_g$  yet reported for the coupling of  $\text{CO}_2$  and epoxides. In all cases, no polyether linkages were observed, though an oligomeric species denoted **X** always remained with the purified polymer sample. **X** does not have any impact on

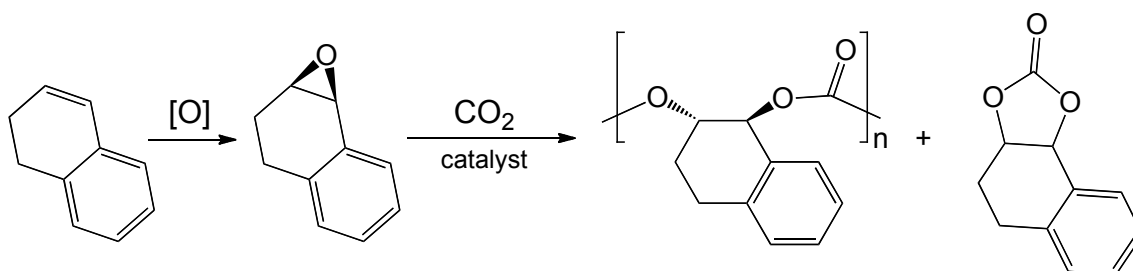
observed molecular weight,  $T_g$ , or polymer decomposition, and it can be largely removed by stirring with  $n\text{Bu}_4\text{NN}_3$  at 60 °C for 1 hour.

Though **2** and **3** were both able to produce polycarbonate with >99% selectivity, *cis*-indene carbonate byproduct was also produced during the course of the reactions with (salen)CoDNP/PPNDNP or  $n\text{Bu}_4\text{NBr}$ . The *cis*- nature of the byproduct was confirmed by X-ray crystallography. Attempts to form *trans*-indene carbonate failed, and this is likely because it is highly disfavored (enthalpy is 21.6 kcal/mol higher than *cis*-).

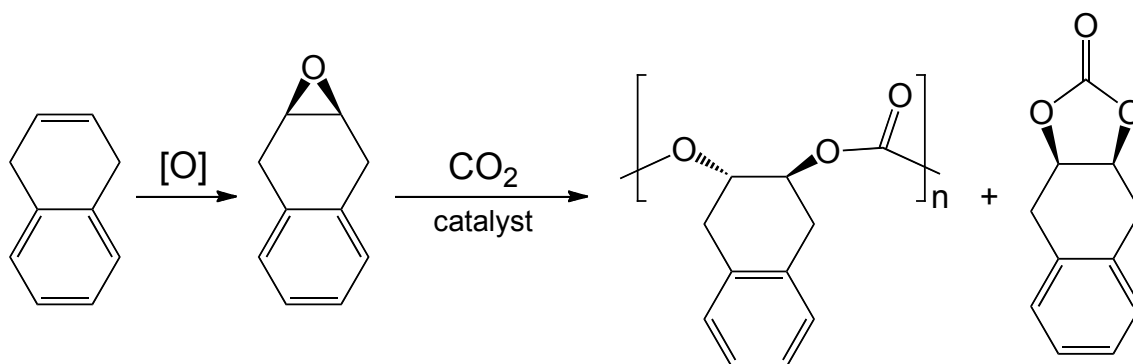
### **Future Work**

Though many achievements have been reached in this investigation, there are still many new pathways that need to be explored. Further attempts should be made to increase the chain length and therefore  $T_g$  of poly(indene carbonate). This will be best done by low catalyst loadings, low temperature, and long reaction times, as increases in temperature have also shown increases in chain transfer and decreased polymer selectivity. Indene oxide is itself a painful monomer to work with. It is not commercially available, and so it must be synthesized in the individual laboratory. However, large scale ups have been made by some pharmaceutical companies,<sup>101</sup> so it is possible to imagine production on a large scale. The bigger problem is that trace water in the system will completely inhibit polymerization, and so great care must be taken to dry the solvents, catalysts, and indene oxide prior to polymerization.

If the goal is to continue to push the limits of  $T_g$ s attainable by  $\text{CO}_2$ /epoxides copolymerization, it may be best to explore different monomers. 1,2- and 1,4-dihydronaphthalene both represent strong choices for new starting reagents, as they both contain bulky side groups along with the rigid 6-membered cyclohexene ring (Schemes II-2 and II-3, respectively). 1,2-dihydronaphthalene will likely behave similarly to indene, given their similar locations of the double bond next to the benzene ring. 1,4-



**Scheme II-2.** Idealized pathway for making poly(1,2-dihydronaphthalene carbonate).



**Scheme II-3.** Idealized pathway for making poly(1,4-dihydronaphthalene carbonate).

dihydronaphthalene has an olefin removed from the benzene ring, and it should therefore have better reactivity for polymerization with less side reactions (i.e. Meinwald rearrangement). The previous attempt to copolymerize 1,4-dihydronaphthalene oxide and CO<sub>2</sub> utilized a (salen)CrCl and *N*-methylimidazole cocatalyst, and only the *cis*- isomer of the cyclic carbonate was yielded.<sup>69</sup> There have been incredibly large leaps made in catalytic developments since 2004, and it is very likely that these new bifunctional cobalt catalysts will be capable of copolymerization of these monomers with CO<sub>2</sub>. It is believed that anthracene-derived epoxides would not only be very expensive to generate but also increase the free volume of the polymer and therefore decrease the T<sub>g</sub> relative to these indene and naphthalene-derived epoxides.

## CHAPTER III

### KINETICS OF CYCLIC CARBONATE FORMATION UTILIZING (SALEN)CrCl\*

#### Introduction

Several research groups across the globe are working diligently toward the selective production of cyclic carbonates from epoxides and CO<sub>2</sub>, whereby polycarbonate production is undesired.<sup>58-59</sup> The Darensbourg group has long been concerned with the selective production of polycarbonates from the coupling of epoxides and CO<sub>2</sub> (see Chapters I & II), trying valiantly to avoid the synthesis of the thermodynamic product, cyclic carbonates. It however came to our attention that studying the formation of cyclic carbonates themselves may give us more information regarding the mechanism(s) of their production and allow us to perhaps predict which epoxides would be good candidates for polycarbonate production over cyclic carbonates.

Cyclic carbonate can be produced via six different mechanisms (Figure III-1). Both metal-bound and metal-free alkoxide polymer chain end backbitings will produce 5-membered cyclic carbonates with *trans*- configuration (Pathways **a** and **f**, respectively). Conversely, metal-bound and metal-free polymer carbonate chain end backbiting reactions will produce cyclic carbonates with *cis*- configuration (Pathways **b** and **e**, respectively). *Cis*- cyclic carbonates can also be produced by carbonate

---

\*Portions reprinted (adapted) from “What’s New with CO<sub>2</sub>? Recent Advances in its Copolymerization with Oxiranes.” Darensbourg, D.J.; Wilson, S.J. *Green Chem.* **2012**, *14*, 2665-2671. Reproduced by permission of The Royal Society of Chemistry. <http://dx.doi.org/10.1039/c2gc35928f>.

backbiting prior to polymer propagation, i.e. immediately following initial epoxide ring-opening and CO<sub>2</sub> insertion (metal-bound Pathway **c** and metal-free Pathway **d**). In each of these cases, R and R' represent the respective side chains for the epoxide starting material. For aliphatic epoxides such as propylene and styrene oxide, no distinctions can be made between *trans*- and *cis*- cyclic carbonates, and thus we are unable to directly assign whether alkoxide or carbonate backbiting is most active. The distinction between the geometric isomers is prevalent instead for alicyclic epoxides such as cyclohexene oxide, cyclopentene oxide, and indene oxide.

Of the six potential mechanisms which can produce cyclic carbonates, only those involving carbonate backbiting (Pathways **b**, **c**, **d**, and **e**) are expected to be operational under polymerization conditions (i.e. high pressures of CO<sub>2</sub>), as it is known that CO<sub>2</sub> readily inserts into alkoxide bonds.<sup>102,103,57</sup> Pathways **a** and **f** represent sound choices for polycarbonate recycling to cyclic carbonates in the absence of CO<sub>2</sub>, and these were examined in 2012 by Darensbourg and Wei for poly(propylene carbonate), poly(epichlorohydrin carbonate), and poly(styrene carbonate).<sup>62</sup>

During the course of the polymerization reaction, it is possible that all four pathways **b-e** are operational at the same time. The goal of this project was to supplement the depolymerization studies of my labmate, Sheng-Hsuan Wei, to better assign which pathway(s) are the most prevalent during the course of the polymerization process. In knowing the activation barriers for each pathway independently, their relative activities within the reaction can then be better accessed. The kinetic barriers to direct coupling of CO<sub>2</sub> and epoxides to yield cyclic carbonates will be examined

(Pathway **c**). Indene oxide, cyclopentene oxide, styrene oxide, and 1,2-butylene oxide were all chosen because they do not form cyclic carbonates at the temperatures and conditions discussed herein (confirmed by  $^1\text{H}$  NMR and ATR-FTIR). (salen)CrCl catalyst was chosen because it has been well-researched, and  $n\text{Bu}_4\text{NCl}$  cocatalyst was chosen for its solubility in toluene.  $\text{CO}_2$  pressures of 3.4 MPa were employed in order to match the typical conditions used in polymerization reactions.<sup>104</sup> For styrene oxide/ $\text{CO}_2$  coupling reactions, attempts were also made to assign the kinetic barriers for metal-free pathway **d**.

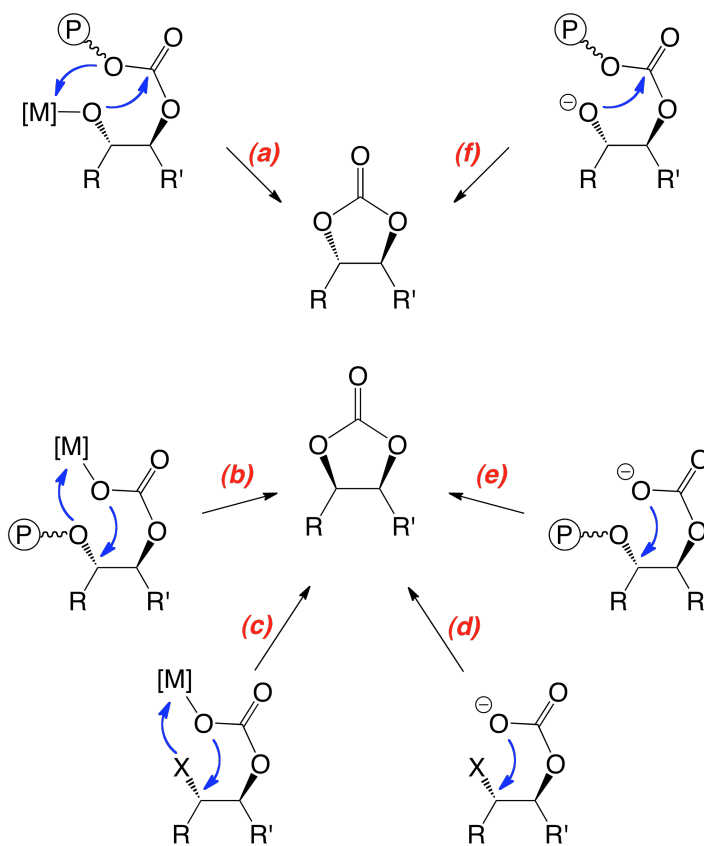


**Figure III-1.** Six potential mechanisms for *in situ* backbiting to form cyclic carbonate.

## Experimental

**Materials and Methods.** Unless otherwise specified, all syntheses and manipulations were carried out on a double-manifold Schlenk vacuum line under an atmosphere of argon or in an argon-filled glovebox. Toluene was distilled from sodium/benzophenone and stored in an argon-filled glovebox. Styrene oxide (Alfa Aesar), cyclopentene oxide (GL Biochem (Shanghai), Ltd.), and 1,2-epoxybutane (Aldrich) were stirred over CaH<sub>2</sub>, distilled, and stored in an argon-filled glovebox. Indene oxide was synthesized according to the literature procedure and stored in the glovebox freezer.<sup>37</sup> Tetra-*n*-butylammonium chloride (Aldrich) was recrystallized from acetone/diethyl ether before use and stored in an argon-filled glovebox. (*R,R*)-*N,N'*-bis(3,5-di-*tert*-butylsalicylidene)-1,2-cyclohexanediaminochromium(III) chloride, (salen)CrCl, was purchased from Strem, stored in an argon-filled glovebox, and used as received. Trimethylsilyl chloride was purchased from Acros Organics and used as received. Research Grade 99.999% carbon dioxide supplied in a high-pressure cylinder and equipped with a liquid dip tube was purchased from Airgas. The CO<sub>2</sub> was further purified by passing through two steel columns packed with 4 Å molecular sieves that had been dried under vacuum at  $\geq 200$  °C. High pressure reaction monitoring measurements were performed using an ASI ReactIR 1000 reaction analysis system with a 300 mL stainless steel Parr autoclave modified with a permanently mounted ATR crystal (SiComp) at the bottom of the reactor (purchased from Mettler Toledo). Infrared spectra were recorded on a Bruker Tensor 37 spectrometer in CaF<sub>2</sub> solution cells with a 0.1 mm path length.



**X-ray Crystal Study.** For the crystal structures of the cyclic carbonates, a Bausch and Lomb 10× microscope was used to identify suitable crystals. A single crystal sample was coated in mineral oil, affixed to a Nylon loop, and placed under streaming N<sub>2</sub> (110 K) in a single-crystal APEXii CCD or Bruker GADDS/Histar diffractometer. X-ray diffraction data were collected by covering a hemisphere of space upon combination of three sets of exposures. The structure was solved by direct methods. H atoms were placed at idealized positions and refined with fixed isotropic displacement parameters and anisotropic displacement parameters were employed for all non-hydrogen atoms. The following programs were used: for data collection and cell refinement, APEX2;<sup>86</sup> data reductions, SAINTPLUS, version 6.63;<sup>87</sup> absorption correction, SADABS;<sup>88</sup> structure solutions, SHELXS-97;<sup>89</sup> structure refinement, SHELXL-97.<sup>90</sup> Previously solved structures were obtained from the Cambridge Crystallographic Database.<sup>105</sup>

**Coupling of Cyclopentene Oxide and CO<sub>2</sub>.** 72.5 mg (salen)CrCl (114.7 μmol, 1 eq.) and 133.4 mg PPNN<sub>3</sub> (229.2 μmol, 2 eq.) were charged in a vial, dissolved in dry CH<sub>2</sub>Cl<sub>2</sub>, and allowed to stir at room temperature under argon for ~30 minutes in order to activate the catalyst. The solvent was thoroughly removed *in vacuo*, and the vial was charged with 15.0 mL dry cyclopentene oxide (171.9 mmol, 1500 eq.). The homogeneous solution was cannulated into a 300 mL stainless steel autoclave with a permanently mounted SiComp crystal. The reactor was pressurized with 3.4 MPa CO<sub>2</sub> and heated to 80 °C. The course of the reaction was monitored for 3 hours. The system was cooled to room temperature, depressurized, and both <sup>1</sup>H NMR and FT-IR spectra

were obtained of the crude reaction mixture. 56% conversion to *cis*-cyclopentene carbonate was observed from  $^1\text{H}$  NMR.

***cis*-Cyclopentene Carbonate.** Following the completion of the coupling of CPO and  $\text{CO}_2$ , the mixture was concentrated *in vacuo*, redissolved in dichloromethane, and passed through a short column of silica gel in order to remove residual catalyst and cocatalyst. Clear, slightly colored crystals were grown from slow evaporation of the resulting solution.  $^1\text{H}$  NMR (300 MHz,  $\text{CDCl}_3$ ):  $\delta$  3.39 (s, 2H), 1.94 (dd, 2H,  $J = 5.1, 7.8$  Hz), 1.45-1.54 (m, 3H), 1.23-1.34 (m, 1H) ppm.  $^{13}\text{C}$  NMR (125 MHz,  $\text{CDCl}_3$ ):  $\delta$  155.6, 82.0, 33.2, 21.6 ppm. FT-IR  $\nu_{\text{CO}_3}$  1796  $\text{cm}^{-1}$  ( $\text{CH}_2\text{Cl}_2$ ); 1838sh, 1807  $\text{cm}^{-1}$  ( $\text{C}_7\text{H}_8$ ). Anal. Calc. for  $\text{C}_6\text{H}_8\text{O}_3$ : C, 56.24; H, 6.29. Found: C, 56.22; H, 6.15.

**Coupling of cyclohexene oxide and  $\text{CO}_2$ .** 62.5 mg (salen)CrCl (98.8  $\mu\text{mol}$ , 1 eq.) and 115.0 mg PPNN<sub>3</sub> (197.7  $\mu\text{mol}$ , 2 eq.) were charged in a vial, dissolved in dry  $\text{CH}_2\text{Cl}_2$ , and allowed to stir at room temperature under argon for ~30 minutes in order to activate the catalyst. The solvent was thoroughly removed *in vacuo*, and the vial was charged with 15.0 mL dry cyclohexene oxide (148.3 mmol, 1500 eq.). The homogeneous solution was cannulated into a 300 mL stainless steel autoclave with a permanently mounted SiComp crystal. The reactor was pressurized with 3.4 MPa  $\text{CO}_2$  and heated to 80  $^\circ\text{C}$ . The course of the reaction was monitored for 3 hours. The system was cooled to room temperature, depressurized, and both  $^1\text{H}$  NMR and FT-IR spectra were obtained of the crude reaction mixture. 64% conversion to poly(cyclohexene carbonate), 0.7% conversion to *trans*-cyclohexene carbonate, 0.2% ether linkages was observable from  $^1\text{H}$  NMR.

**Poly(Cyclohexene Carbonate).** The crude reaction mixture from the coupling of CHO and CO<sub>2</sub> was added dropwise to acidified methanol (~5% HCl). The off-white polymer precipitate was collected by filtration, redissolved in dichloromethane, and reprecipitated using the same method. The resulting white solid was dried under vacuum with heating. <sup>1</sup>H NMR (300 MHz, CDCl<sub>3</sub>): δ 4.64 (br s, 2H), 2.10 (br s, 2H), 1.70 (br s, 2H), 1.23-1.55 (br m, 4H) ppm. <sup>13</sup>C NMR (75 MHz, CDCl<sub>3</sub>): broad peaks centered at δ 153.4, 29.5, 22.8 ppm. FT-IR ν<sub>CO<sub>2</sub></sub> 1850 (CH<sub>2</sub>Cl<sub>2</sub>); 1851 (C<sub>7</sub>H<sub>8</sub>). Anal. Calc. for (C<sub>7</sub>H<sub>10</sub>O<sub>3</sub>)<sub>n</sub>: C, 59.14; H, 7.09. Found: C, 59.21; H, 7.09.

**Kinetic Measurements for the Direct Coupling of SO and CO<sub>2</sub> Utilizing (salen)CrCl/*n*Bu<sub>4</sub>NCl.** In an argon-filled glovebox, 63.3 mg (salen)CrCl (0.100 mmol, 1 eq), 55.5 mg *n*Bu<sub>4</sub>NCl (0.200 mol, 2 eq), 6.00 g styrene oxide (49.9 mmol, 500 eq), and 5.22 g toluene (6 mL) were charged into a vial. The reactants were cannulated into a 300 mL stainless steel Parr autoclave modified with a permanently mounted ATR crystal (SiComp) at the bottom of the reactor. This initial mixture served as the background signal for the measurements. CO<sub>2</sub> (3.4 MPa) was charged into the system, and the reactor was heated to the desired temperature (25, 33, 43, 49 °C). Infrared spectra were taken periodically throughout the course of the reaction, and the reaction's progress was monitored through the growth of cyclic carbonate peak at 1815 cm<sup>-1</sup>. No polymer formation was ever observed at 1750 cm<sup>-1</sup>. The reaction was followed to 100% completion.

**Styrene Carbonate.** Following the completion of the coupling of SO and CO<sub>2</sub>, the mixture was concentrated *in vacuo*, redissolved in dichloromethane, and passed

through a short column of silica gel in order to remove residual catalyst and cocatalyst. Quantitative yield. Clear, slightly colored crystals were grown from slow evaporation of the resulting solution.  $^1\text{H}$  NMR (300 MHz,  $\text{CDCl}_3$ ):  $\delta$  7.40-7.48 (m, 3H,  $J = 3.6$  Hz), 7.32-7.40 (d, 2H,  $J = 3.6$  Hz), 5.68 (t, 1H,  $J = 4.8$  Hz), 4.80 (t, 1H,  $J = 4.8$  Hz), 4.34 (t, 1H,  $J = 4.8$  Hz) ppm.  $^{13}\text{C}$  NMR (125 MHz,  $\text{CDCl}_3$ ):  $\delta$  155.0, 135.9, 129.8, 129.3, 126.0, 78.1, 71.3 ppm. FT-IR  $\nu_{\text{CO}_3}$  1816, 1799sh  $\text{cm}^{-1}$  ( $\text{CH}_2\text{Cl}_2$ ); 1822, 1799sh  $\text{cm}^{-1}$  ( $\text{C}_7\text{H}_8$ ). Anal. Calc. for  $\text{C}_8\text{H}_8\text{O}_3$ : C, 65.85; H, 4.91. Found: C, 65.73; H, 5.09.

**2-chloro-1-phenylethanol.**<sup>106</sup> 6.33 g 2-chloroacetophenone (39.7 mmol, 1 eq) was dissolved in 50 mL MeOH. The solution was cooled to 0 °C, stirred vigorously, and 0.750 g sodium borohydride (19.8 mmol, 0.5 eq) was added in small portions so as to maintain the temperature at 0 °C. The solution was stirred for 30 mins at 0 °C, 30 mins at 25 °C, then recooled to 0 °C and acidified with ~10 drops of concentrated HCl. The solution was concentrated *in vacuo*, and the crude reaction products were purified by column chromatography on silica gel (4/1 hexanes/ethyl acetate) to yield a clear oil. 4.478 g, 70% yield.  $^1\text{H}$  NMR (300 MHz, toluene- $d_8$ ):  $\delta$  7.1-7.2 (m, 5H), 4.53 (t, 1H,  $J = 6.0$  Hz), 3.32 (d, 1H,  $J = 6.0$  Hz), 2.82 (br s, 1H) ppm.  $^{13}\text{C}$  NMR (125 MHz, toluene- $d_8$ ):  $\delta$  140.9, 137.5, 128.6, 128.2, 126.4, 74.2, 50.7, 20.5 ppm. Anal. Calc. for  $\text{C}_8\text{H}_9\text{ClO}$ : C, 61.35; H, 5.79.

**Kinetic Experiments for the Base-initiated Backbiting of 2-chloro-1-phenylethanol.** A 0.641 M stock solution of 2-chloro-1-phenylethanol was prepared in a 10 mL volumetric flask using 1.0035 g 2-chloro-1-phenylethanol and toluene. 1.0 mL of this solution was removed and diluted with 9.0 mL toluene (64.1 mM; 0.641 mmol, 1

eq). A bubbler was affixed, and the flask heated to the appropriate temperature (40, 50, 60 °C). A background spectrum was taken of this solution using Mettler Toledo ReactIR ic10. 99.9% CO<sub>2</sub> was bubbled into the flask until constant concentration was obtained (~20 minutes). 0.3 mL DBU (2.0 mmol, 3.1 eq) was added to the flask, the bubbler was removed, and a balloon filled with CO<sub>2</sub> was affixed to the flask so as to maintain constant pressure of 1 atm CO<sub>2</sub>. The reaction was monitored to completion by ATR FT-IR by the growth of the styrene carbonate peak at 1815 cm<sup>-1</sup>.

**NMR Experiment for the Base-initiated Backbiting of 2-chloro-1-phenylethanol.** A 1.99 M stock solution of 2-chloro-1-phenylethanol was prepared in a 10 mL volumetric flask using 3.113 g solute and toluene. 0.10 mL of this stock solution, 0.10 mL toluene-*d*<sub>8</sub>, and 0.10 mL DBU (3 equivalents) were added to a high pressure J. Young tube. A crude NMR was taken, and deprotonation was observed by the disappearance of the -OH doublet at 2.76 ppm. The methine triplet (1H) shifted downfield from 4.44 to 4.84 ppm. The methylene doublet (2H) at 3.23 ppm split into two doublets of doublets at 3.61 and 3.53 ppm, and a broad singlet corresponding to the N-H proton was also visible at 7.79 ppm. The J. Young tube was cooled in liquid nitrogen, and the argon was removed by vacuum. The tube was returned to room temperature, and CO<sub>2</sub> was added to 100 psi. Immediately upon addition of the high pressure CO<sub>2</sub>, a translucent white precipitate confirming reaction began to form on the sides of the NMR tube. Upon inverting of the solution to mix the CO<sub>2</sub>, the white precipitate continued to form very quickly, seeming to finish in less than 2 minutes. By the time the NMR scan was taken (less than 10 minutes later), complete conversion to

styrene carbonate had indeed been achieved. Only the peaks from DBU and three triplets at 5.58, 4.55, and 3.99 ppm corresponding to the methylene and methine protons of styrene carbonate were observable.

**2-chloro-2-phenylethanol.** In a 250 mL round bottomed flask, 1.00 g ZnO (12.3 mmol, 0.1 eq) and 13.35 g TMSCl (122.8 mmol, 1.0 eq) were dissolved in 150 mL CH<sub>2</sub>Cl<sub>2</sub>. The mixture was vigorously stirred under argon at 0 °C. 14.76 g styrene oxide (122.8 mmol, 1.0 eq) was added in a dropwise fashion. The cloudy white mixture slowly turned a light yellow, and at the end of addition had turned a bright canary yellow. The reaction was stirred at 0 °C for 1 hour. The argon flow was removed, and 30 mL H<sub>2</sub>O was added to the flask. The aqueous layer was acidified with 10 drops of HCl. The mixture was allowed to stir vigorously at room temperature for 1 hour. The aqueous and organic layers were separated, and the organic layer was washed sequentially with sat. NaHCO<sub>3</sub> (aq) 3 x 30 mL and sat. NaCl (aq) 3 x 30 mL. The yellow organic layer was dried over Na<sub>2</sub>SO<sub>3</sub> and concentrated *in vacuo*. It was loaded onto a silica pad, and the crude product was washed with ~ 2 L of hexanes to remove impurities. The product was flushed off of the pad with ethyl acetate, dried with Na<sub>2</sub>SO<sub>3</sub>, and concentrated *in vacuo*. Full removal of TMS-related species was not achieved, as the liquid turned green over time and extra peaks were visible in the NMR. <sup>1</sup>H NMR (300 MHz, CDCl<sub>3</sub>): δ 7.40-7.48 (m, 3H, J = 3.6 Hz), 7.32-7.40 (d, 2H, J = 3.6 Hz), 5.68 (t, 1H, J = 4.8 Hz), 4.80 (t, 1H, J = 4.8 Hz), 4.34 (t, 1H, J = 4.8 Hz) ppm. <sup>13</sup>C NMR (75 MHz, CDCl<sub>3</sub>): δ 155.0, 135.9, 129.8, 129.3, 126.0, 78.1, 71.3 ppm. Anal. Calc. for C<sub>8</sub>H<sub>8</sub>O<sub>3</sub>: C, 61.35; H, 5.79.

**2-bromo-1-phenylethanol.** 20.0 g 2-bromoacetophenone (100.4 mmol, 1 eq) was added to 50 mL MeOH. The mixture was cooled to 0 °C, stirred vigorously, and 1.96 g sodium borohydride (50.22 mmol, 0.5 eq) was added in small portions so as to maintain the temperature at 0 °C. The mixture became homogenous early in the addition process. The reaction was stirred for 1 hour at 0 °C and allowed to warm to room temperature overnight. It was returned to 0 °C and acidified with ~10 drops of concentrated HCl. The solution was concentrated *in vacuo*, and the crude reaction products were purified by column chromatography on silica gel (4/1 hexanes/ethyl acetate) to yield a pale yellow oil. 6.1861 g, 31% yield. <sup>1</sup>H NMR (300 MHz, CDCl<sub>3</sub>): δ 7.39-7.11 (m, 5H), 4.79 (dd, 1H, J = 3.6, 8.7 Hz), 3.51 (dd, 1H, J = 3.6, 10.5 Hz), 3.42 (dd, 1H, J = 8.7, 10.5 Hz), 2.75 (s, 1H) ppm. <sup>13</sup>C NMR (125 MHz, toluene-*d*<sub>8</sub>): δ 140.4, 128.7, 238.5, 126.0, 73.8, 40.1 ppm. Anal. Calc. for C<sub>8</sub>H<sub>9</sub>BrO: C, 47.79; H, 4.51. Found: C, 47.67; H, 4.60.

**Kinetic Measurements for the Direct Coupling of CPO and CO<sub>2</sub> Utilizing (salen)CrCl/*n*Bu<sub>4</sub>NCl.** In an argon-filled glovebox, 90.2 mg (salen)CrCl (0.142 mmol, 1 eq), 79.3 mg *n*Bu<sub>4</sub>NCl (0.285 mol, 2 eq), 6.00 g cyclopentene oxide (71.3 mmol, 500 eq), and 5.22 g toluene (6 mL) were charged into a vial. The reactants were cannulated into a 300 mL stainless steel Parr autoclave modified with a permanently mounted ATR crystal (SiComp) at the bottom of the reactor. This initial mixture served as the background signal for the measurements. CO<sub>2</sub> (3.4 MPa) was charged into the system, and the reactor was heated to the desired temperature (43, 53, 63, 73 °C). Infrared spectra were taken periodically throughout the course of the reaction, and the reaction's

progress was monitored through the growth of cyclic carbonate peak at  $1804\text{ cm}^{-1}$ . No activity was ever observed at  $1750\text{ cm}^{-1}$ , indicating that polymer formation did not take place or was not appreciable. The reaction was followed to 100% completion.

**Kinetic Measurements for the Direct Coupling of BO and CO<sub>2</sub> Utilizing (salen)CrCl/*n*Bu<sub>4</sub>NCl.** In an argon-filled glovebox, 10.5 mg (salen)CrCl (0.017 mmol, 1 eq), 9.2 mg *n*Bu<sub>4</sub>NCl (0.033 mmol, 2 eq), 6.00 g butylene oxide oxide (83.2 mmol, 5000 eq), and 5.22 g toluene (6.0 mL) were charged into a vial. Lower catalyst loading was employed in this reaction due to the extreme reactivity of 1,2-butylene oxide. The reactants were cannulated into a 300 mL stainless steel Parr autoclave modified with a permanently mounted ATR crystal (SiComp) at the bottom of the reactor. This initial mixture served as the background signal for the measurements. CO<sub>2</sub> (3.4 MPa) was charged into the system, and the reactor was heated to the desired temperature (69, 78, 87 °C). Infrared spectra were taken periodically throughout the course of the reaction, and the reaction's progress was monitored through the growth of cyclic carbonate peak at  $1816\text{ cm}^{-1}$ . No activity was ever observed at  $1750\text{ cm}^{-1}$ , indicating that polymer formation did not take place or was not appreciable. The reaction was followed to 100% completion.

**1,2-Butylene Carbonate.** Following the completion of the coupling of BO and CO<sub>2</sub>, the mixture was concentrated *in vacuo*, redissolved in dichloromethane, and passed through a short column of silica gel in order to remove residual catalyst and cocatalyst. Further purification by flash column chromatography (1:1 hexanes:EtAc, silica gel) yielded pure 1,2-butylene carbonate. Quantitative yield. <sup>1</sup>H NMR (300 MHz, CDCl<sub>3</sub>): δ



4.49-4.58 (m, 1H), 4.39 (dd, 1H, J = 7.7, 8.4 Hz), 3.93 (dd, 1H, J = 6.9, 8.4 Hz), 1.53-1.68 (m, 2H), 0.83 (t, 3H, J = 7.5 Hz) ppm.  $^{13}\text{C}$  NMR (75 MHz,  $\text{CDCl}_3$ ):  $\delta$  155.0, 77.9, 68.8, 26.4, 8.0 ppm. FT-IR  $\nu_{\text{CO}_3}$  1801  $\text{cm}^{-1}$  ( $\text{CH}_2\text{Cl}_2$ ); 1815  $\text{cm}^{-1}$  ( $\text{C}_7\text{H}_8$ ). Anal. Calc. for  $\text{C}_5\text{H}_8\text{O}_3$ : C, 51.72; H, 6.94. Found: C, 51.77; H, 6.96.

**Kinetic Measurements for the Direct Coupling of IO and  $\text{CO}_2$  Utilizing (salen)CrCl/*n*Bu<sub>4</sub>NCl.** In an argon-filled glovebox, 38.3 mg (salen)CrCl (0.0605 mmol, 1 eq), 33.6 mg *n*Bu<sub>4</sub>NCl (0.121 mol, 2 eq), 2.000 g indene oxide (49.9 mmol, 250 eq), and 8.7 g toluene (10.0 mL) were charged into a vial. The reactants were cannulated into a 300 mL stainless steel Parr autoclave modified with a permanently mounted ATR crystal (SiComp) at the bottom of the reactor. This initial mixture served as the background signal for the measurements.  $\text{CO}_2$  (3.4 MPa) was charged into the system, and the reactor was heated to the desired temperature (31, 41, 51, 59 °C). Infrared spectra were taken periodically throughout the course of the reaction, and the reaction's progress was monitored through the growth of the cyclic carbonate peak at 1815  $\text{cm}^{-1}$  with shoulder at 1790  $\text{cm}^{-1}$ . Lower concentrations of IO were employed in this study because the shape of the double cyclic peak would undergo noticeable changes in stretching patterns at high concentrations of indene carbonate, and higher catalyst loadings were employed in order to reduce reaction time. No polymer formation was ever observed at 1750  $\text{cm}^{-1}$ . The reaction was followed to 100% completion.

***cis*-Indene Carbonate.** Clear, off-white crystals of *cis*-indene carbonate were obtained from the reaction mixture as described in the literature.<sup>37</sup> Crystals suitable for X-ray diffraction were grown from slow evaporation of a concentrated  $\text{CH}_2\text{Cl}_2$  solution

at 25 °C. <sup>1</sup>H NMR (300 MHz, CDCl<sub>3</sub>): δ 7.52 (d, 1H, J = 7.8 Hz), 7.31-7.45 (m, 3H, J = 7.8 Hz), 6.01 (d, 1H, J = 6.6 Hz), 5.44 (qd, 1H, J = 3.6, 6.6 Hz), 3.40 (d, 2H, J = 3.6 Hz) ppm. <sup>13</sup>C NMR (125 MHz, CDCl<sub>3</sub>): δ 154.7, 140.0, 136.4, 131.0, 128.2, 126.4, 125.6, 83.5, 79.7, 38.0 ppm. FT-IR ν<sub>CO<sub>3</sub></sub> 1810sh, 1794 cm<sup>-1</sup> (CH<sub>2</sub>Cl<sub>2</sub>); 1817, 1793sh cm<sup>-1</sup> (C-<sub>7</sub>H<sub>8</sub>). Anal. Calc. for C<sub>10</sub>H<sub>8</sub>O<sub>3</sub>: C, 68.18; H, 4.58. Found: C, 68.43; H, 4.57.

## Results and Discussion

**Cyclic Carbonate Crystal Structures.** In 2003, our group initially examined the structures of cyclic carbonates in order to attempt to explain the difference in polymerizability of these two monomers with CO<sub>2</sub>. We noticed the substantial difference (~15-20°) in O-C-C-O dihedral angles between *trans*-cyclohexene carbonate (~23°) and Zn-bound (~5°) and Cd-bound (~5°) propylene carbonates.<sup>63</sup> Thus, it was initially hypothesized that the magnitude of the dihedral angle would be a good predictor of an epoxide's ease of polymerizability, whereby cyclic carbonates with large dihedral angles would be easier to polymerize while cyclic carbonates with small dihedral angles would be more likely to prefer cyclic carbonate formation. This difference in reactivity was believed to be caused by differences in the ring-closing transition state configuration. Many cyclic carbonates are crystalline at room temperature, so we have now been able to compare these solid-state parameters to look for correlations between cyclic carbonate structure and ease of copolymerization with CO<sub>2</sub> (Figure III-2 and Table III-1).

At first glance, this hypothesis appears correct. Cyclopentene oxide (*cis*-carbonate dihedral angle = 0.347°) and 1,4-dihydronaphthalene oxide (*cis*-carbonate

dihedral angle =  $2.005^\circ$ ) are well known to be difficult to copolymerize with  $\text{CO}_2$ . As previously stated, the cyclohexene oxide/ $\text{CO}_2$  copolymerization occurs readily and selectively with a wide variety of catalysts. Some of the largest dihedral angles are observed for *trans*-cyclohexene carbonate, as two different yet similar structures reveal angles of  $23.98^\circ$  and  $29.717^\circ$ .

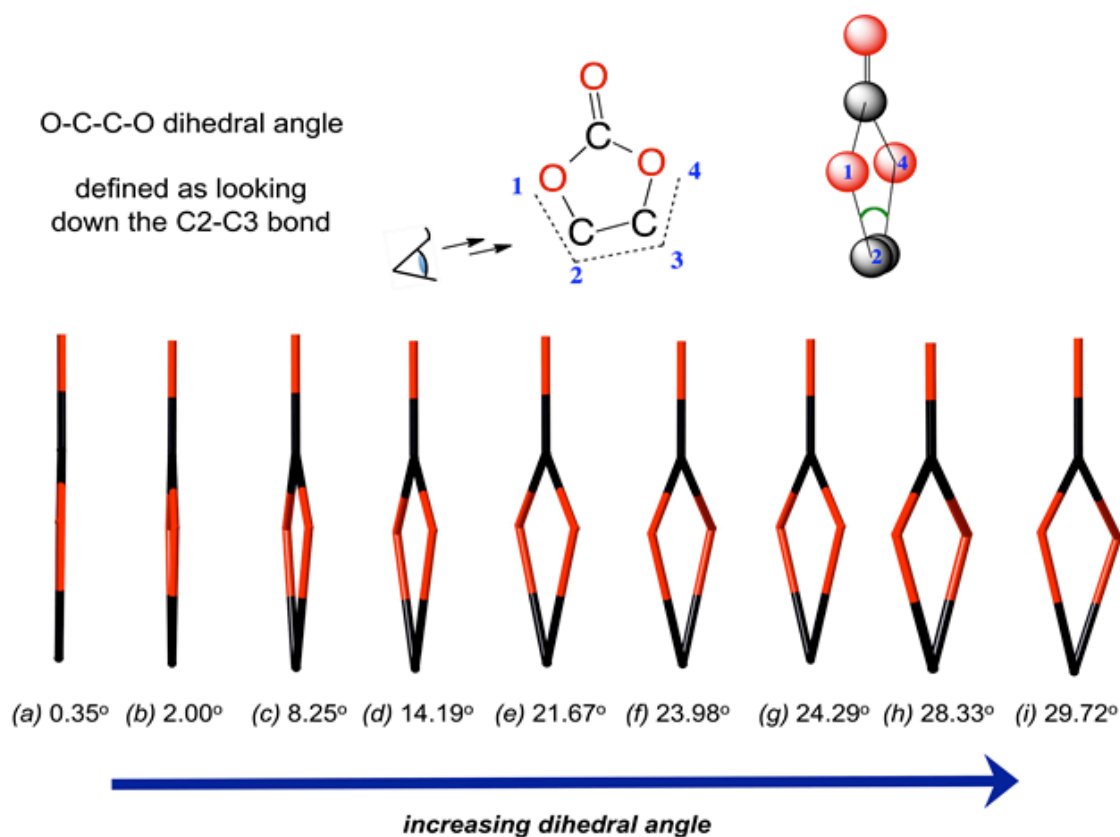


**Figure III-2.** O-C-C-O dihedral angles of various cyclic carbonates. (a) *cis*-cyclopentene carbonate –  $0.347^\circ$ , (b) *cis*-1,4-dihydronaphthalene carbonate –  $2.005^\circ$ ,<sup>69</sup> (c) *cis*-indene carbonate #1 –  $8.252^\circ$ ,<sup>37</sup> (d) *cis*-indene carbonate #2 –  $14.188^\circ$ ,<sup>37</sup> (e) styrene carbonate –  $21.667^\circ$ ,<sup>107</sup> (f) *trans*-cyclohexene carbonate –  $23.98^\circ$ ,<sup>62</sup> (g) ethylene carbonate –  $24.287^\circ$ ,<sup>107</sup> (h) ethylene carbonate –  $28.326^\circ$ ,<sup>108</sup> (i) *trans*-cyclohexene carbonate –  $29.717^\circ$ .<sup>109</sup>

**Table III-1.** X-ray crystallographic data for various cyclic carbonates.

Name	cyclopentene carbonate	1,4-dihydronaphthalene carbonate <sup>69</sup>	indene carbonate <sup>37,a</sup>		styrene carbonate <sup>107</sup>	cyclohexene carbonate <sup>107,b</sup>	ethylene carbonate <sup>107</sup>	ethylene carbonate <sup>108,c</sup>	cyclohexene carbonate <sup>109,b</sup>
<b>Empirical Formula</b>	C <sub>6</sub> H <sub>8</sub> O <sub>3</sub>	C <sub>11</sub> H <sub>10</sub> O <sub>3</sub>	C <sub>10</sub> H <sub>8</sub> O <sub>3</sub>		C <sub>9</sub> H <sub>8</sub> O <sub>3</sub>	C <sub>7</sub> H <sub>10</sub> O <sub>3</sub>	C <sub>3</sub> H <sub>4</sub> O <sub>3</sub>	C <sub>3</sub> H <sub>4</sub> O <sub>3</sub>	C <sub>7</sub> H <sub>10</sub> O <sub>3</sub>
<b>Molecular Weight, g/mol</b>	128.12	190.19	176.16		164.15	142.15	88.06	88.06	142.15
<b>Geometric Isomer</b>	<i>cis</i> -	<i>cis</i> -	<i>cis</i> -		-	<i>trans</i> -	-	-	<i>trans</i> -
<b>Crystal System</b>	<i>orthorhombic</i>	<i>monoclinic</i>	<i>monoclinic</i>		<i>orthorhombic</i>	<i>orthorhombic</i>	<i>monoclinic</i>	<i>monoclinic</i>	<i>orthorhombic</i>
<b>Space Group</b>	P2 <sub>1</sub> 2 <sub>1</sub> 2 <sub>1</sub>	P2 <sub>1</sub> /n	P12 <sub>1</sub> /c1		Pna2 <sub>1</sub>	P2 <sub>1</sub> 2 <sub>1</sub> 2 <sub>1</sub>	C2/c	C2/c	P2 <sub>1</sub> 2 <sub>1</sub> 2 <sub>1</sub>
<b>Cell Volume, Å<sup>3</sup></b>	591.90(16)	887.4(5)	1628.8(14)		776.1(5)	700.5(4)	366.80(11)	380.34	694.914
<b>Density, Mg/m<sup>3</sup></b>	1.438	1.424	1.437		1.405	1.348	1.595	1.538	1.359
<b>Goodness of Fit</b>	1.320	1.155	1.032		1.085	0.479	1.081	<i>NA</i>	<i>NA</i>
<b>R1, %</b>	4.27	4.85	3.69		2.95	3.30	3.05	25.01	3.52
<b>C=O, Å</b>	1.197(3)	1.203(2)	1.1974(18)	1.1959(18)	1.1963(14)	1.200(2)	1.1967(19)	1.150	1.193
<b>C-C, Å</b>	1.542(3)	1.550(3)	1.543(2)	1.535(2)	1.5308(18)	1.486(12)	1.513(2)	1.516	1.501
<b>O-C-C-O, deg.</b>	0.348	2.005	8.252	14.187	21.667	23.947	24.287	28.326	29.717

Data obtained from appropriate .cif files from WebCSD<sup>105</sup> and, when necessary, through modeling using CrystalMaker.<sup>110</sup> (a) Two distinct yet similar polymorphs of indene carbonate exist within the unit cell. (b) Disorder exists in the cyclohexane ring due to ring-flipping. (c) Data collected at room temperature.

Unlike the cyclic carbonates shown in Figure III-2, cyclic propylene carbonate is a liquid at room temperature, and a pure single crystal sample has not been isolated. However, propylene carbonate has been found both as a solvent as a ligand within the unit cell of other solid state structures, and the parameters in each of those cases can be found in Table III-2. We were then able to compare the structures of ten different propylene carbonate samples. The dihedral angle varied greatly in the various structures, from  $\sim 2$  to  $30^\circ$ , and these values are greatly influenced by other molecules found within the unit cell. Thus, they are not likely to directly reflect the actual nature of a pure sample of propylene carbonate. However, DFT calculations, which have long

**Table III-2.** X-ray crystallographic data for propylene carbonates.

WebCSD Family Name	O-C-C-O, deg.	C=O, Å	C-C, Å <sup>a</sup>	R1, %
RUJXOJ <sup>111</sup>	2.278	1.112	1.542	3.78
VECHUH <sup>112</sup>	3.543	1.158	1.404	5.86
HOBHUB <sup>50a,b</sup>	5.240	1.205	1.465	8.33
SEYLIR <sup>113,c</sup>	5.473	1.221	1.460	6.67
RUJXOJ <sup>111</sup>	19.951	1.212	1.366	3.78
NIDCUY <sup>114</sup>	20.218	1.185	1.387	4.87
ITECUG <sup>115</sup>	22.995	1.191	1.477	5.52
WEZLIW <sup>116</sup>	25.351	1.179	1.600	10.9
SUDMEJ <sup>117</sup>	28.870	1.209	1.533	6.9
YEFRUW <sup>118,d</sup>	30.510	1.247	1.239	5.6

For each structure, .cif files were obtained from WebCSD,<sup>105</sup> and bond angles and lengths were obtained using CrystalMaker.<sup>110</sup> (a) Distance between bridgehead carbonate carbons. (b) PC bound to zinc through carbonyl oxygen. (c) PC bound to cadmium through carbonyl oxygen. (d) According to WebCSD, disorder was observed in the propylene carbonate, but this was not apparent from the .cif file.

proven effective for the optimization of the structures of organic molecules, show the structure of propylene carbonate to have a relatively large dihedral angle of  $20.8^\circ$ .<sup>119</sup> While this does not definitively show the absence of a correlation between the dihedral angle and the ability of an epoxide monomer to be copolymerized with  $\text{CO}_2$ , we tentatively conclude that any correlation is minimal at best. We shall continue our efforts to produce single crystals of propylene carbonate at low temperature to further aid in this investigation.

**Cyclohexene Oxide vs Cyclopentene Oxide.** Until recently, cyclohexene oxide has been the go-to monomer for nearly every catalyst screening process. Researchers have typically used cyclohexene oxide as a benchmarker in order to show the viability of their catalyst for  $\text{CO}_2$ /epoxides copolymerization. Cyclohexene oxide is a cheap, easy to handle material that yields high selectivity for polycarbonate over cyclic carbonate, and many scientists have incorrectly generalized their catalyst's high selectivity for poly(cyclohexene carbonate) to be translatable to all other potential monomers. In fact, computations have shown that this low preference for carbonate chain-end backbiting is due to a high-energy (free energy barrier = 21.1 kcal/mol) chair-boat interconversion that must take place before backbiting can commence.<sup>70</sup> Additionally, the barrier for poly(cyclohexene carbonate) to undergo alkoxide backbiting to yield *trans*-cyclohexene carbonate is  $\sim 3$  kcal/mol higher than for other aliphatic polycarbonates. Thus, this high selectivity for polymer is not typical for every alicyclic system.

Indeed, the product selectivity for the coupling of  $\text{CO}_2$  with cyclohexene oxide and cyclopentene oxide with (salen)CrCl are starkly different, though the monomers

vary by only one methylene group. Whereas cyclohexene oxide and CO<sub>2</sub> will combine to form poly(cyclohexene carbonate) with 99% selectivity (>1% *trans*-cyclohexene carbonate byproduct), cyclopentene oxide and CO<sub>2</sub> will instead form *cis*-cyclopentene carbonate with 100% selectivity (Figure III-3, Scheme III-1).

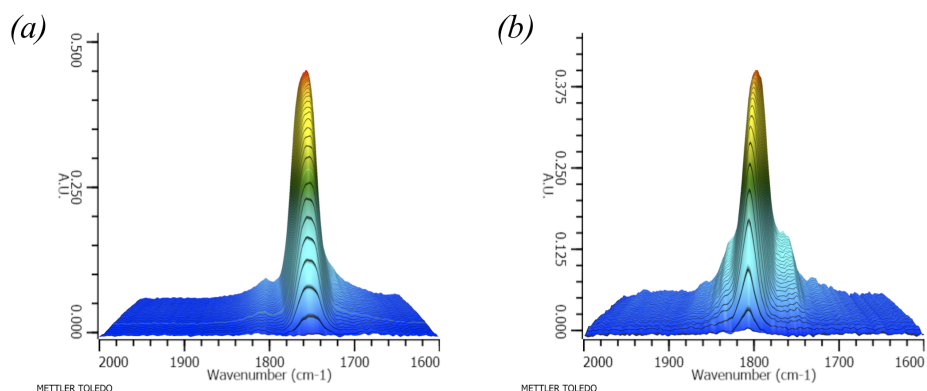
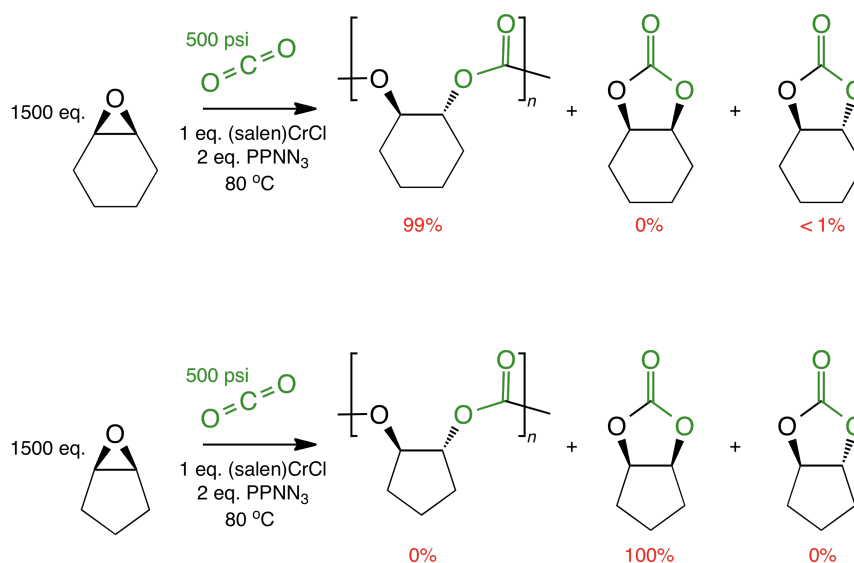


**Figure III-3.** Product growth traces for the coupling of alicyclic epoxides and CO<sub>2</sub> utilizing *in situ* ATR-FTIR spectroscopy. (a) 99% selective PCHC growth at 1750 cm<sup>-1</sup> and < 1% *trans*-CHC at 1810 cm<sup>-1</sup> as confirmed by <sup>1</sup>H NMR. (b) 100% selectivity for CPC at 1804 cm<sup>-1</sup> as confirmed by <sup>1</sup>H NMR. Reaction conditions: 500 eq. epoxide (15 mL), 1 eq. (salen)CrCl, 2 eq. PPNN<sub>3</sub>, 3.4 MPa CO<sub>2</sub>, 80 °C, 3 hours.

Indeed, the production of poly(cyclopentene carbonate) has only been published three times to date, and in each case it has been accomplished with zinc-based catalysts.<sup>28</sup> Unpublished results from Xiao-Bing Lu and Guang-Peng Wu of Dalian University in Dalian, China also document the production of poly(cyclopentene carbonate) utilizing (salen)CoDNP/PPNDNP with 60% selectivity at 60 °C.<sup>120</sup> The Darensbourg group has been able to produce poly(cyclopentene carbonate) with >99% selectivity at 50 °C utilizing bifunctional cobalt catalysts.<sup>121</sup> Attempts were made to produce *trans*-cyclopentene carbonate from *trans*-1,2-cyclopentanediol and ethyl



**Scheme III-1.** Differences in reactivity for the coupling of CO<sub>2</sub> with cyclohexene and cyclopentene oxides.

chloroformate, but these were unsuccessful. This is due to the extreme angle strain at the bridgehead carbons linking the fused 5-membered rings.<sup>70</sup> *Trans*-isomers are possible for the corresponding thiocarbonate, however (see Chapter IV).

The catalytic coupling of cyclopentene oxide and CO<sub>2</sub> to form *cis*-cyclopentene carbonate was monitored by ATR-FTIR spectroscopy at several different temperatures to obtain kinetic information. Observed rate constants ( $k_{\text{obs}}$ ) were determined from plots of  $\ln[(A_i - A_t)/A_i]$  versus time in seconds, where  $A_i$  is the absorbance of cyclic carbonate at time = infinity and  $A_t$  is the absorbance of cyclic carbonate at 1804 cm<sup>-1</sup> at time =  $t$  (Figure III-4). The activation energy,  $E_A$ , of the coupling reaction was determined from the slope of the corresponding Arrhenius plot (Figure III-5). The direct coupling of cyclopentene oxide and CO<sub>2</sub> to form *cis*-cyclopentene carbonate utilizing (salen)CrCl



has an activation barrier of  $72.9 \pm 5.2$  kJ/mol. The *cis*-nature of the product was confirmed both by  $^1\text{H}$  NMR and X-ray diffraction analysis of single crystals grown from the final product mixture (Figure III-6).

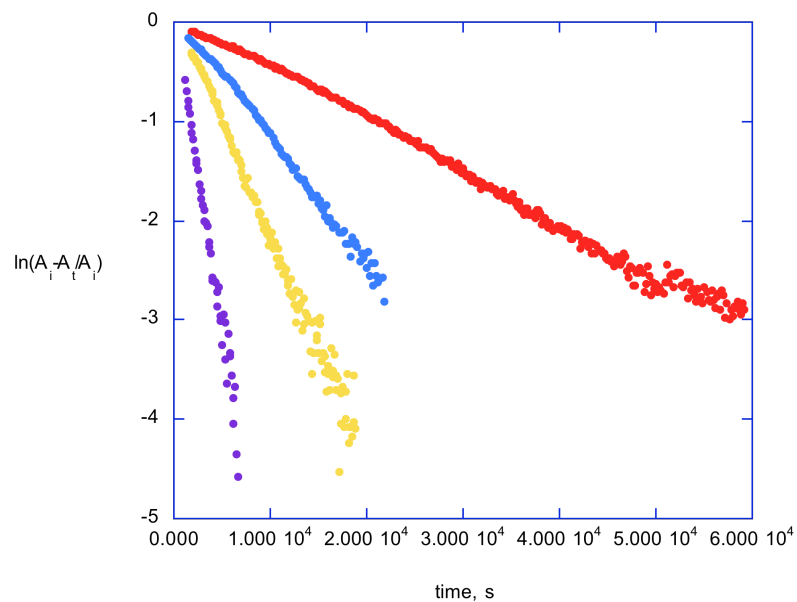


**Figure III-4.** Kinetic plots of  $\ln[(A_i - A_t)/A_i]$  vs. time for *cis*-cyclopentene carbonate production. Observed rate constants are  $5.80 \times 10^{-5} \text{ s}^{-1}$  at 43 °C (red),  $12.8 \times 10^{-5} \text{ s}^{-1}$  at 53 °C (blue),  $23.5 \times 10^{-5} \text{ s}^{-1}$  at 63 °C (yellow), and  $63.8 \times 10^{-5} \text{ s}^{-1}$  at 73 °C (purple).

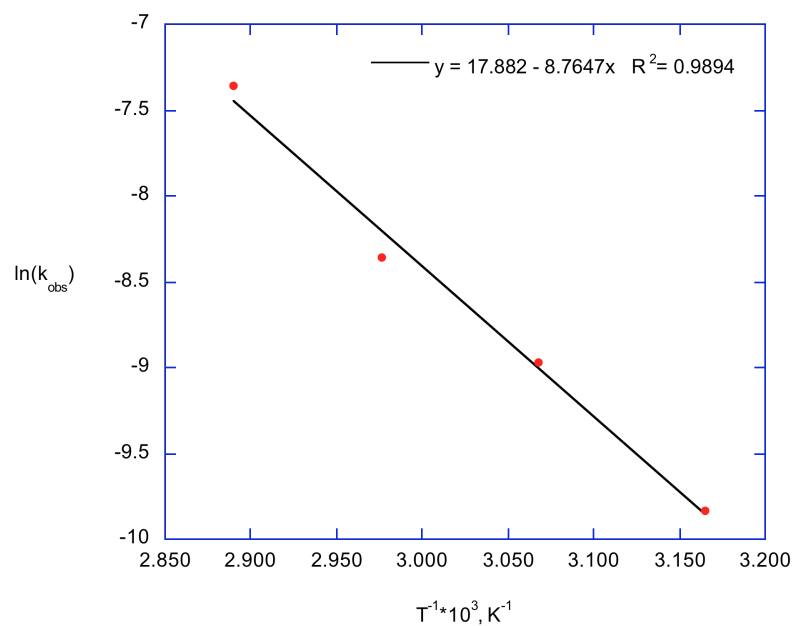


**Figure III-5.** Arrhenius plot of *cis*-cyclopentene carbonate production in the presence of (salen)CrCl/*n*Bu<sub>4</sub>NCl.  $R^2 = 0.989$ .

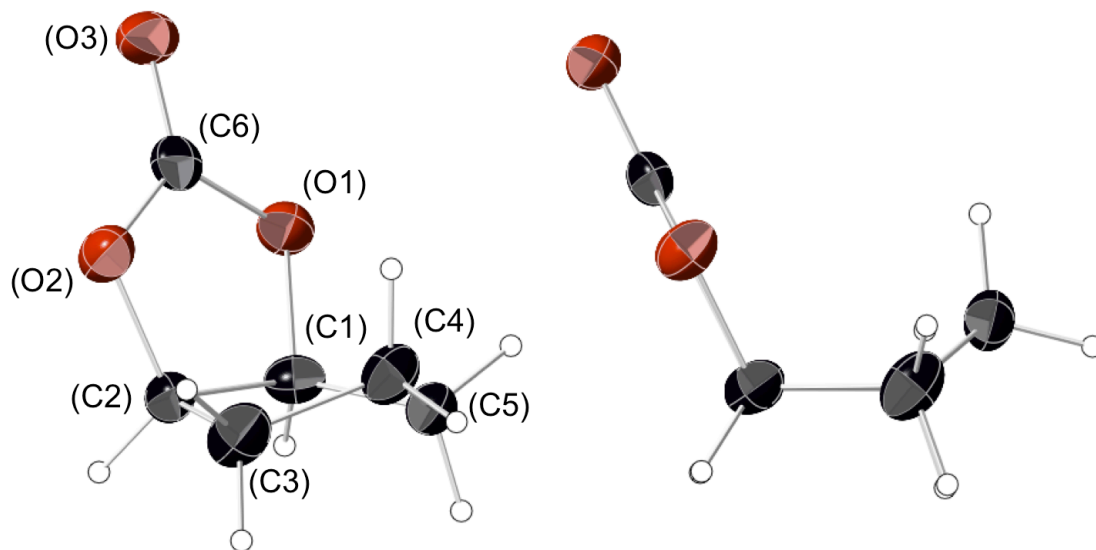


**Figure III-6.** Thermal ellipsoid representation of *cis*-cyclopentene carbonate with ellipsoids at 50% probability surfaces. At right, looking down the plane created by C2-C1-C3-C5 to show the near-planarity of the cyclic carbonate ring ( $O1-C1-C2-O2 = 0.347^\circ$ ).

**Kinetics of *cis*-Indene Carbonate Formation.** The kinetics of *cis*-indene carbonate formation from indene oxide and CO<sub>2</sub> in toluene utilizing (salen)CrCl and *n*Bu<sub>4</sub>NCl were determined utilizing ATR-FTIR. Notably, if a large amount of indene oxide was employed, the shape of the  $\nu_{\text{CO}_3}$  FT-IR stretch from indene carbonate changed over the course of the reaction (Figure III-7). Thus, the reaction was carried out in considerably lower concentrations as compared to the other studies (i.e. 2.0 g indene oxide in 10.0 mL toluene). Observed rate constants were determined (Figure III-8), and Arrhenius analysis showed that  $E_A$  for direct CO<sub>2</sub>/indene oxide coupling into *cis*-indene carbonate is  $114.4 \pm 5.7$  kJ/mol (Figure III-9). This is considerably lower than the barrier determined for the azide-assisted anionic backbiting of poly(indene carbonate),  $189.1 \pm 5.8$  kJ/mol.<sup>122</sup> No other side products (e.g. polymerization, Meinwald rearrangement to 2-indanone) were visible during the course of this reaction. Single crystals of *cis*-indene carbonate can be seen in Figure II-3. All attempts to independently synthesize *trans*-indene carbonate from *trans*-1,2-indanediol and ethyl chloroformate failed (see Chapter II).

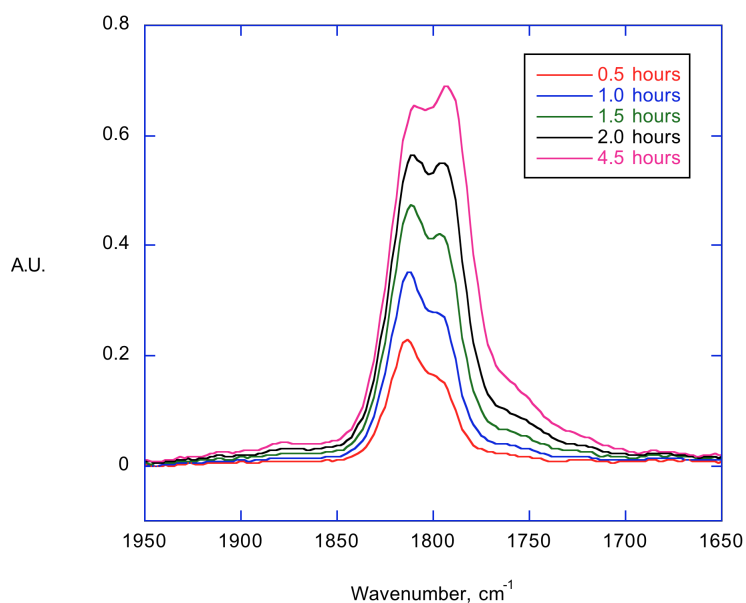


**Figure III-7.** Changing shape of *cis*-indene carbonate  $\nu_{\text{CO}_3}$  during the course of the reaction at 45 °C, 6.0 g indene oxide, 6.0 mL toluene. As the concentration of indene carbonate increases, the shoulder at 1793  $\text{cm}^{-1}$  becomes the dominant peak.

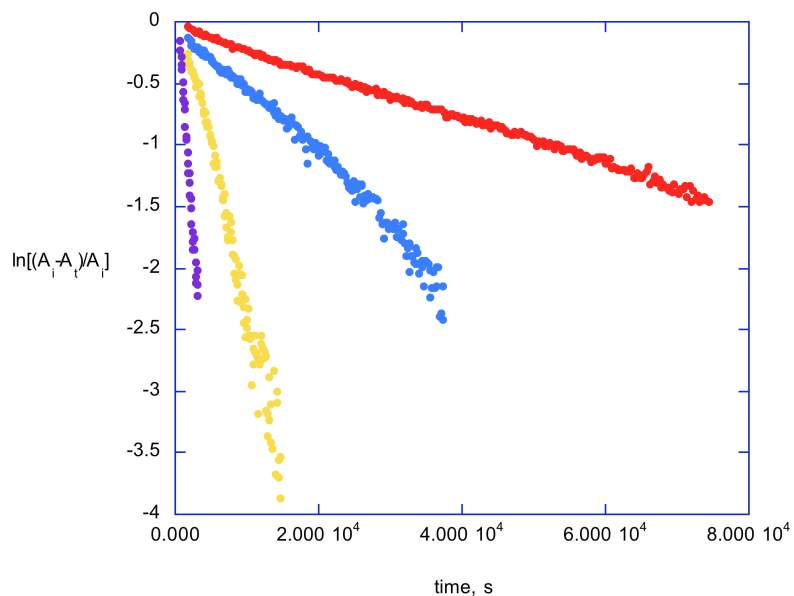


**Figure III-8.** Kinetic plots of  $\ln[(A_i - A_t)/A_t]$  vs. time for *cis*-indene carbonate production, where  $A_i$  and  $A_t$  represent the absorbance of the cyclic stretch at 1815  $\text{cm}^{-1}$  at time equals infinity and  $t$ , respectively. Observed rate constants are  $1.85 \times 10^{-5} \text{ s}^{-1}$  at 31 °C (red),  $5.66 \times 10^{-5} \text{ s}^{-1}$  at 40.5 °C (blue),  $26.0 \times 10^{-5} \text{ s}^{-1}$  at 51 °C (yellow), and  $82.6 \times 10^{-5} \text{ s}^{-1}$  at 59 °C (purple).

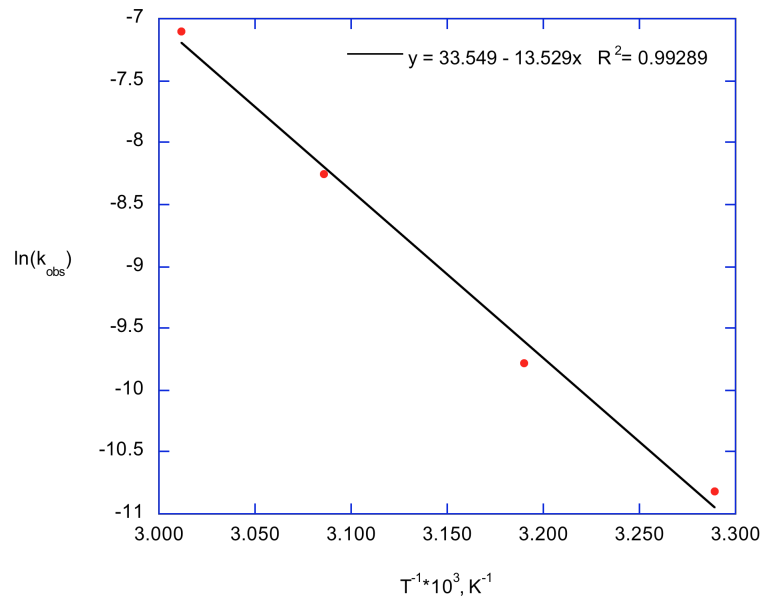


**Figure III-9.** Arrhenius plot of *cis*-indene carbonate production in the presence of (salen)CrCl/*n*Bu<sub>4</sub>NCl.  $R^2 = 0.993$ .

**Kinetics of Butylene Carbonate Formation.** Since early studies had made the distinction between alicyclic and aliphatic epoxides (that is, cyclohexene and propylene oxide, respectively), a study for the direct coupling of CO<sub>2</sub> and an aliphatic epoxide was warranted. Early attempts to directly couple propylene oxide and CO<sub>2</sub> to propylene carbonate utilizing (salen)CrCl and *n*Bu<sub>4</sub>NCl were plagued by both polymer production and high reactivity. Under the typical catalyst loadings (1:2:500 for (salen)CrCl:*n*Bu<sub>4</sub>NCl:epoxide), the Parr reactor did not have time to reach temperature equilibrium before the reaction was almost complete. Though lower catalyst loadings were attempted, concomitant polymer production still remained a problem, and a new route to determine activation parameters utilizing epoxides derived from 1,2- $\alpha$ -olefins was devised.

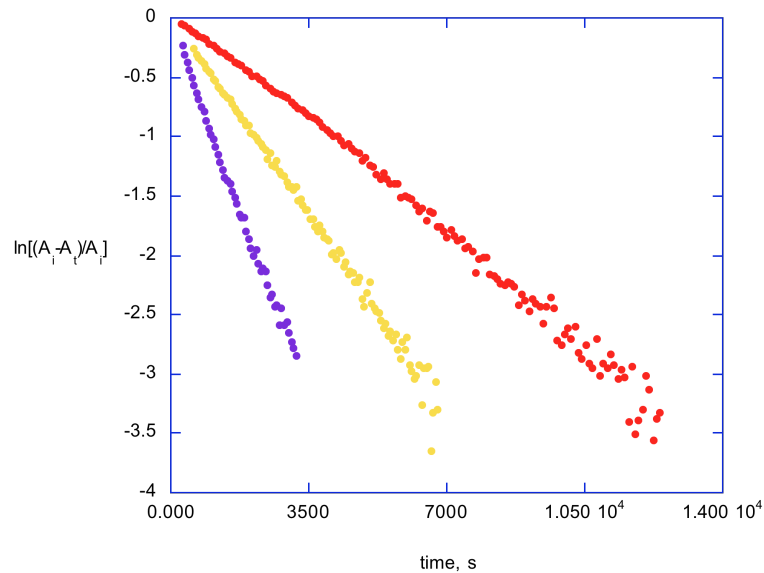


**Figure III-10.** Kinetic plots of  $\ln[(A_i - A_t)/A_i]$  vs. time for butylene carbonate production, where  $A_i$  and  $A_t$  represent the absorbance of the cyclic stretch at  $1815\text{ cm}^{-1}$  at time equals infinity and  $t$ , respectively. Observed rate constants are  $2.76 \times 10^{-4}\text{ s}^{-1}$  at  $69\text{ °C}$  (red),  $4.82 \times 10^{-5}\text{ s}^{-1}$  at  $78\text{ °C}$  (blue),  $8.64 \times 10^{-5}\text{ s}^{-1}$  at  $87\text{ °C}$  (purple).

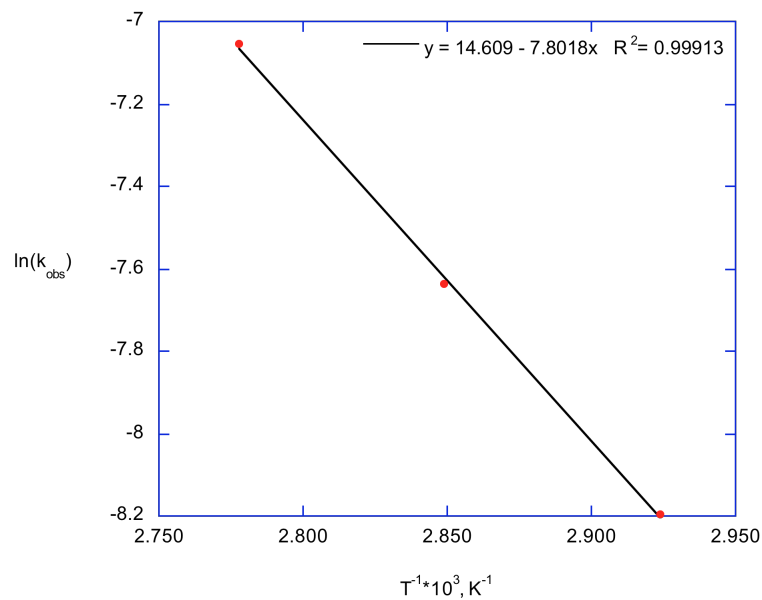


**Figure III-11.** Arrhenius plot of 1,2-butylene carbonate production in the presence of  $(\text{salen})\text{CrCl}/n\text{Bu}_4\text{NCl}$ .  $R^2 = 0.999$ .

Instead of propylene oxide, we employed 1,2-butylene oxide for the direct cyclic coupling kinetic studies. 1,2-butylene oxide has a higher boiling point (63° vs 34 °C for propylene oxide), and so the catalyst, cocatalyst, epoxide, and toluene solution could be cannulated into the Parr reactor at temperatures higher than ambient 23 °C, allowing for faster and easier temperature equilibration using the heating mantle. No polymer production was observed at 1750 cm<sup>-1</sup>, but high reactivity and short reaction times still remained a problem. As such, the catalyst loading was lowered to 1:2:5000 for these studies. The coupling of 1,2-butylene oxide and CO<sub>2</sub> was monitored at 69, 78, and 87 °C. The observed rate constants were calculated (Figure III-10), and Arrhenius analysis found the activation barrier for the direct coupling utilizing (salen)CrCl and *n*Bu<sub>4</sub>NCl to form 1,2-butylene carbonate to be 64.8 ± 2.1 kJ/mol (Figure III-11). Butylene carbonate is a liquid at room temperature, and no single crystals have yet been isolated at low temperatures.

**Kinetics of Styrene Carbonate Production.** The coupling of styrene oxide and CO<sub>2</sub> to form poly(styrene carbonate) remained elusive to researchers dating back to Inoue's initial discovery.<sup>13-14</sup> Though several low-yielding studies had existed prior to this time,<sup>32</sup> the first major advancement in the production of poly(styrene carbonate) came from the Lu and Darensbourg groups in 2010 utilizing (salen)Co(III) complexes.<sup>33b</sup> Recently, Chisholm and coworkers reported the synthesis of poly(styrene carbonate) from tetraphenylporphyrin chromium (III) complexes.<sup>34</sup>

The direct coupling of styrene carbonate from styrene oxide and CO<sub>2</sub> utilizing (salen)CrCl and *n*Bu<sub>4</sub>NCl was monitored utilizing ATR-FTIR at 25, 33, 43, and 49 °C by

the growth of the carbonate peak at  $1815\text{ cm}^{-1}$  (Figure III-12). No polymeric growth was ever observed at  $1750\text{ cm}^{-1}$ . The natural logs of the observed rate constants were plotted against the inverse of the reaction temperatures, and the  $E_A$  of the coupling reaction was determined to be  $91.2 \pm 2.7\text{ kJ/mol}$  (Figure III-13). Single crystals of styrene carbonate were grown from slow evaporation of a concentrated solution in dichloromethane (Figure III-14).

**Analysis of Styrene Carbonate Production Pathways.** In conjunction with my excellent labmate, Dr. Sheng-Hsuan Wei, I set out to complete the entire cyclic carbonate kinetics production wheel for styrene carbonate. The styrene oxide, styrene carbonate, and poly(styrene carbonate) system is an excellent model for this study. Cobalt catalysts produce PSC in a direct fashion without chain transfer, meaning that every polymer chain end has one  $-X$  group and one  $-OH$ , where  $X$  is typically 2,4-dinitrophenoxide.<sup>33b</sup> This has been confirmed both by monomodal GPC traces and MALDI-TOF. Polydispersities are also typically close to 1.0. Utilizing (salen)CrCl and onium salt cocatalysts, styrene carbonate can be selectively produced with no polycarbonate impurities (*vide supra*). Therefore, direct routes to each of the desired starting materials or products are easily achievable.

In the 2012 *Macromolecules* paper, Darensbourg and Wei determined that the  $n\text{Bu}_4\text{NN}_3$ -initiated backbiting of poly(styrene carbonate) had an activation barrier of  $46.7 \pm 2.2\text{ kJ/mol}$  utilizing *in situ* ATR-FTIR spectroscopy (Figure III-1 Pathway **a**; Scheme III-2).<sup>62</sup> The initial equilibrium between azide and hydrazoic acid as well as protonated and deprotonated polymer is expected to be similar to what is observed in



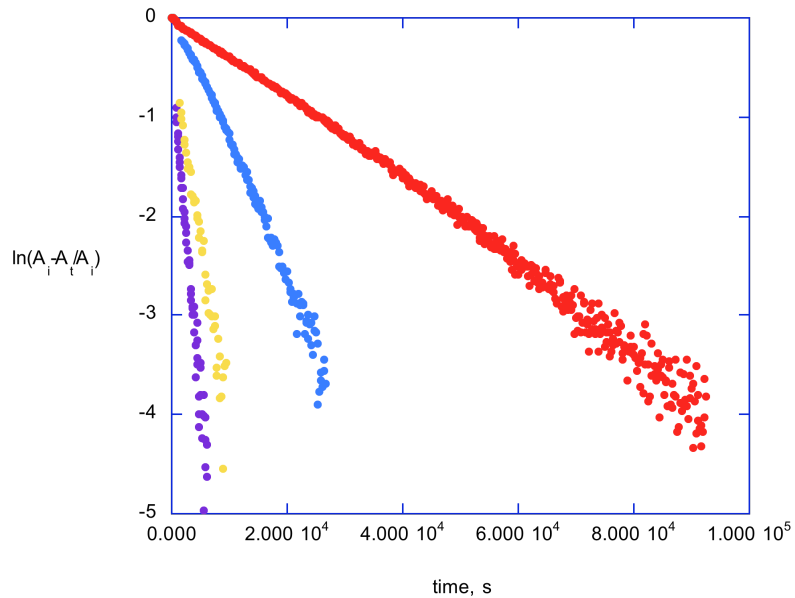


**Figure III-12.** Kinetic plots of  $\ln[(A_i - A_t)/A_t]$  vs. time for styrene carbonate production. Observed rate constants are  $4.31 \times 10^{-5} \text{ s}^{-1}$  at  $25 \text{ }^\circ\text{C}$  (red),  $13.9 \times 10^{-5} \text{ s}^{-1}$  at  $33 \text{ }^\circ\text{C}$  (blue),  $38.0 \times 10^{-5} \text{ s}^{-1}$  at  $43 \text{ }^\circ\text{C}$  (yellow), and  $66.4 \times 10^{-5} \text{ s}^{-1}$  at  $49 \text{ }^\circ\text{C}$  (purple).

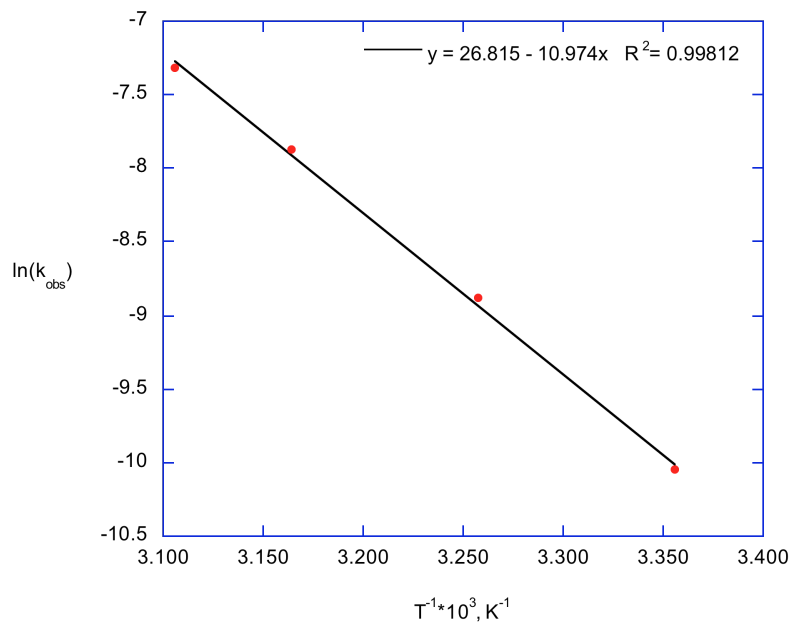


**Figure III-13.** Arrhenius plot of styrene carbonate production in the presence of  $(\text{salen})\text{CrCl}/n\text{Bu}_4\text{NCl}$ .  $R^2 = 0.998$ .

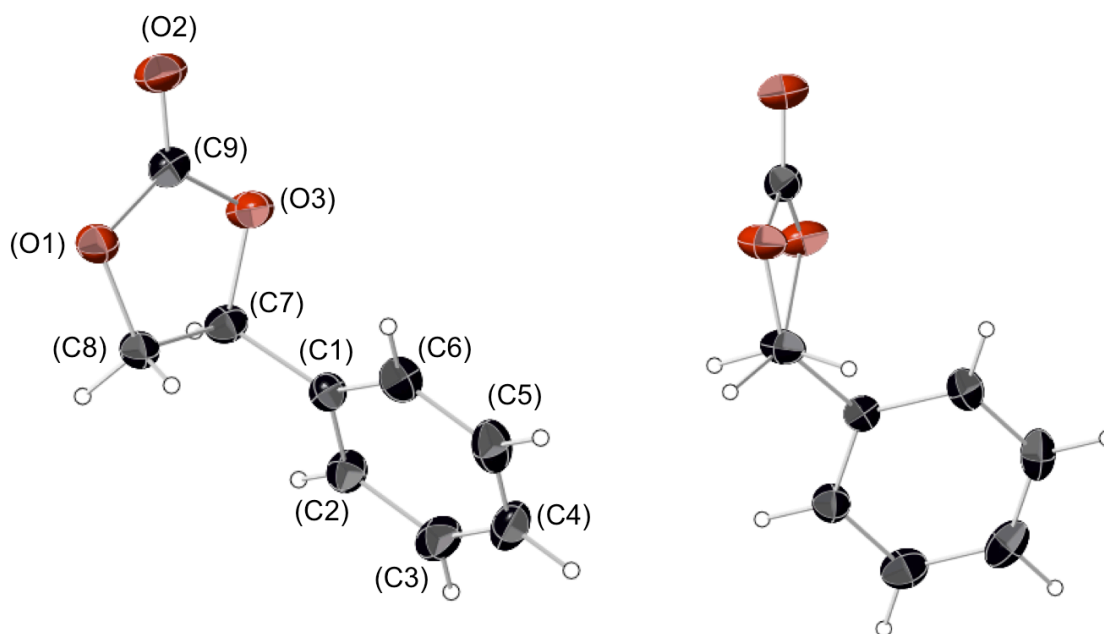
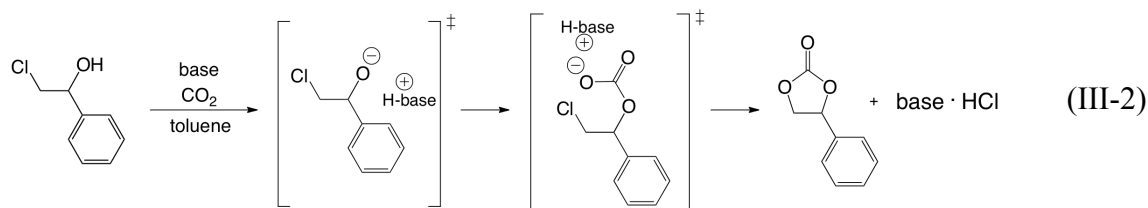
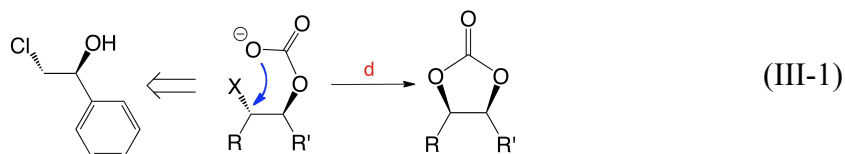


**Figure III-14.** Thermal ellipsoid representation of styrene carbonate with ellipsoids at 50% probability surfaces. At right, looking down C8-C7 bond to show torsion in the cyclic carbonate ring ( $O1-C8-C7-O3 = 21.667^\circ$ ).

chain transfer processes within the polymerization reaction. Similarly, the (salen)CrCl-assisted alkoxide backbiting of poly(styrene carbonate) was calculated to have an activation barrier of  $141.2 \pm 6.9$  kJ/mol (Figure III-1 Pathway **a**; Scheme III-3). This significantly higher barrier indicates that the chromium metal center must be acting as a capping agent that stabilizes the anion and hinders backbiting to cyclic carbonate. Finally, Dr. Wei also investigated the azide-initiated depolymerization of poly(styrene carbonate) under  $CO_2$  pressure (3.4 MPa), such that  $CO_2$  has inserted into the alkoxide bond and carbonate backbiting is instead being monitored (Figure III-1 Pathway **e**). This process was determined to have an activation barrier of  $89.2 \pm 4.6$  kJ/mol. Though it was not directly calculated, it has been inferred that poly(styrene carbonate) backbiting under  $CO_2$  pressure with added (salen)CrCl catalyst will have an even higher barrier, >>

89 kJ/mol, given that the polymer chain end should again be effectively capped by the metal center.

**Halohydrin/CO<sub>2</sub> Backbiting to Styrene Carbonate.** Figure III-1 Pathway **d** depicts the metal-free backbiting of the singly coupled ring-opened epoxide and CO<sub>2</sub>. That is, epoxide activation and ring-opening by the initiating halogen or pseudohalogen has occurred, CO<sub>2</sub> has inserted to form the carbonate bond, and the dissociated anion backbites to yield cyclic carbonate and regenerate the initiator. Following the retrosynthetic scheme shown in eqn III-1, the free backbiting reaction can be realized by the coupling of a halohydrin such as 2-chloro-1-phenylethanol and CO<sub>2</sub> in the presence of a base (eqn III-2).



2-Chloro-1-phenylethanol was synthesized from the reduction of 2-chloroacetophenone with NaBH<sub>4</sub>.<sup>106</sup> Clean, complete deprotonation of the –OH proton (2.77 ppm) can be accomplished by adding an excess (at least 1.1 eq) of the strong

organic base 1,8-diazabicyclo[5.4.0]undec-7-ene, more commonly known as DBU (Figure III-15). Downfield shifts are visible in both the methine and methylene protons. It should be noted that the deprotonated complex is stable, and no backbiting to styrene oxide is visible by  $^1\text{H}$  or  $^{13}\text{C}$  NMR.

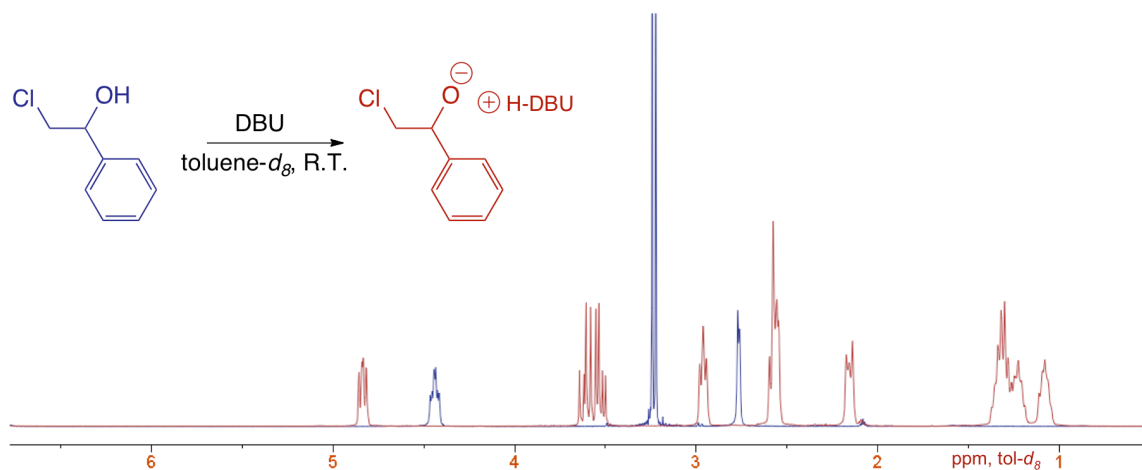


**Figure III-15.**  $^1\text{H}$  NMR of 2-chloro-1-phenylethanol (blue) and 2-chlorophenylethanol immediately following the addition of 1.4 eq DBU displaying clean, quantitative deprotonation (red). Red signals from 1-3 ppm are from DBU. Toluene- $d_8$ , 300 MHz.

Initial cyclic carbonate backbiting studies were performed under 1 atmosphere  $\text{CO}_2$ . A 64.1 mM solution of 2-chloro-1-phenylethanol in toluene was heated to the appropriate temperature (40, 50, 60  $^\circ\text{C}$ ) and saturated with  $\text{CO}_2$  (1 atm). Following saturation, the  $\text{CO}_2$  flow and bubbler were removed, and a balloon filled with  $\text{CO}_2$  was affixed to the flask so as to maintain constant  $P_{\text{CO}_2}$  at 1 atm. DBU (3.1 eq) was then injected into the reaction flask, and the growth of styrene carbonate was monitored at  $1815\text{ cm}^{-1}$ . An excess of DBU was employed to ensure that complete deprotonation of

the hydroxyl group was immediately achieved. The basic reaction setup can be seen in Figure III-16. The production of DBU•HCl white precipitate throughout the course of the reaction can also be observed. Traces of styrene carbonate production and observed rate constants can be found in Figure III-17 and Table III-3, respectively.

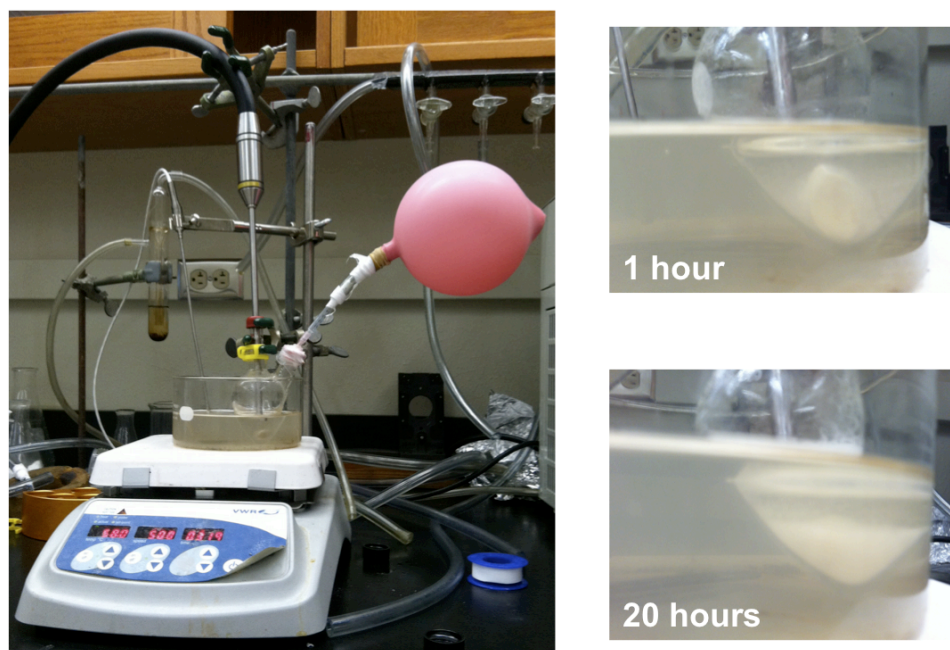


**Figure III-16.** *In situ* ATR-FTIR monitoring of the backbiting of 2-chloro-1-phenylethanol under 1 atm CO<sub>2</sub>. Inset images show the production of white DBU•HCl precipitate during the course of the reaction.

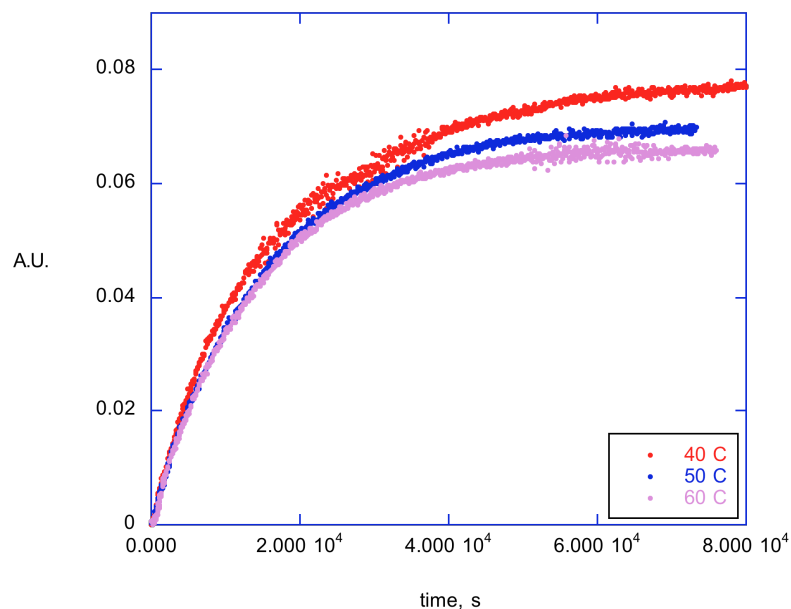


**Figure III-17.** FT-IR traces of styrene carbonate production at  $1815\text{ cm}^{-1}$  from the DBU-initiated backbiting of 2-chloro-1-phenylethanol under 1 atm  $\text{CO}_2$  pressure.

**Table III-3.** Observed first order rate constants for the DBU-initiated backbiting of 2-chloro-1-phenylethanol under 1 atm  $\text{CO}_2$  pressure.

Temperature (K)	$k_{\text{obs}}, \text{s}^{-1} \text{ } ^a$	$R^2 \text{ } ^a$
313	$5.65 \times 10^{-5}$	0.993
323	$7.07 \times 10^{-5}$	0.994
333	$7.43 \times 10^{-5}$	0.996

(a) Obtained from the plot of  $\ln[(A_i - A_t)/A_i]$  versus time.

Despite the experiments having a 20-degree temperature range, the observed first order rate constants for this process differ only slightly ( $k_{\text{obs}, 313\text{ K}} = 1.3 \times k_{\text{obs}, 333\text{ K}}$ ). Though this has not been explicitly proven, it can be imagined that the rate equation for the backbiting reaction to be

$$\text{rate} = k[2\text{-chlorophenylethanol}][\text{CO}_2] \quad (\text{III-3})$$

which, when  $k[\text{CO}_2] = k_{\text{obs}}$  (i.e. under pseudo-first order conditions) can be reduced to

$$\text{rate} = k_{\text{obs}}[2\text{-chlorophenylethanol}]. \quad (\text{III-4})$$

The rate of 2-chlorophenylethanol disappearance should be directly proportional to the rate of styrene carbonate appearance. Thus, it is

$$\text{rate} = k_{\text{obs}}[\text{styrene carbonate}] \quad (\text{III-5})$$

that is being observed for this process. Despite the  $\text{CO}_2$ -filled balloon helping to maintain constant  $\text{CO}_2$  concentration throughout the reaction, the concentration of  $\text{CO}_2$  is different at each of the investigated temperatures. While published studies exist for the mole fraction of  $\text{CO}_2$  in toluene at high pressures,<sup>97</sup> no reliable data exists for the concentrations at ambient pressures. As such, the true second-order rate constants for these reactions could not be calculated.

The DBU-initiated backbiting of 2-chloro-1-phenylethanol was then investigated under high pressures of  $\text{CO}_2$ . At high pressures, saturation behavior will have been achieved, and the reaction rate is independent of the concentration of  $\text{CO}_2$ .<sup>123</sup> In a J. Young tube at room temperature (23 °C), 0.67 M 2-chloro-1-phenylethanol solution containing 3 equivalents DBU was subjected to 0.7 MPa  $\text{CO}_2$ . Immediately following the pressurization of the tube, translucent white precipitate began to form on the outside of the tube, indicating the backbiting reaction was taking place. As the tube was inverted to move  $\text{CO}_2$  throughout the solution, rapid formation of precipitate continued to evolve. By the time a  $^1\text{H}$  NMR was taken less than 10 minutes later, the reaction was complete, and 100% production of styrene carbonate was observed (Figure III-18).

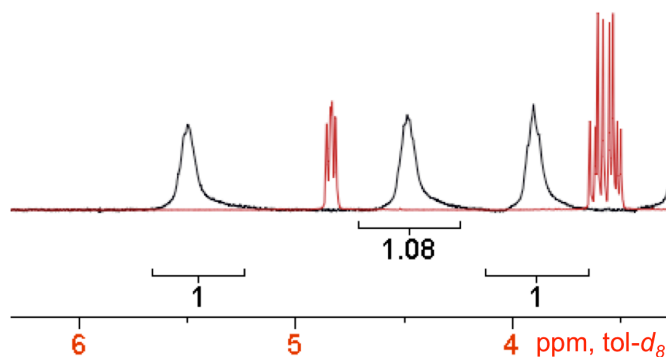


**Figure III-18.** Quantitative formation of styrene carbonate (black) after the addition of 100 psi CO<sub>2</sub> to 2-chloro-1-phenylethoxide solution (red). The reaction is estimated to have completed in less than 2 minutes.

Based on visual evidence from the production of white precipitate, the reaction was complete in less than 2 minutes.

Other halohydrins than 2-chloro-1-phenylethanol were also synthesized, including 2-bromo-1-phenylethanol and 2-chloro-2-phenylethanol. Calculations have shown that the transition state for backbiting to styrene carbonate would be lower for 2-chloro-2-phenylethanol over 2-chloro-1-phenylethanol due to stabilization from the phenyl  $\pi$ -system into the *meso*-carbon.<sup>70</sup> Since it is also accepted that bromide is a better leaving group than chloride, we believe the order of reactivity for the chloro and bromohydrin backbiting reactions to be that which is shown in Figure III-19, with 2-bromo-2-phenylethanol having the highest reactivity and the 2-chloro-1-phenylethanol employed in this study being the least reactive.



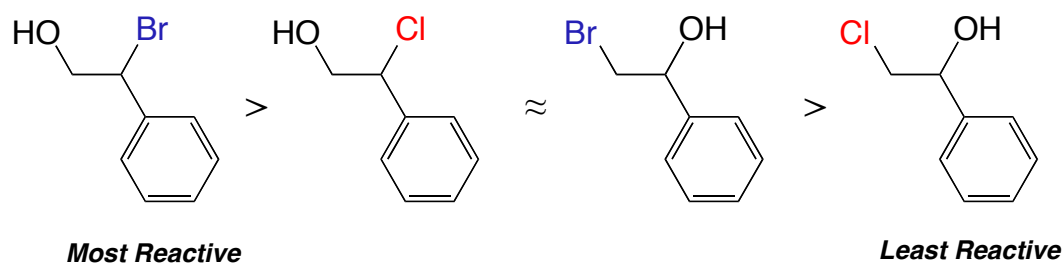


**Figure III-19.** Expected reactivity trend of bromo- and chlorohydrins for base-initiated backbiting to styrene carbonate.

## Conclusions

In this chapter, the byproduct of CO<sub>2</sub>/epoxide coupling reactions, cyclic carbonate, has been thoroughly investigated. Analysis of the crystal structures of known cyclic carbonates has revealed that little to no correlation exists between the O-C-C-O dihedral angle in the cyclic carbonate ring and the ability of the corresponding epoxide to form copolymers with CO<sub>2</sub>. There is nearly 30° range between the dihedral angles of propylene carbonates found within the unit cell of other structures, and the differences are very likely due to packing effects.

The energies of activation for the direct coupling of cyclopentene oxide, indene oxide, butylene oxide, and styrene oxide with CO<sub>2</sub> to form their corresponding cyclic carbonates were determined utilizing (salen)CrCl catalyst and *n*Bu<sub>4</sub>NCl cocatalyst. These results are summarized in Table III-4. The relative basicities between the epoxides, which are expected to provide information on the binding ability of the epoxide to the metal center,<sup>124</sup> do not provide any clear trends.

**Table III-4.** Summary of cyclic carbonate activation parameters.

<b>Cyclic Carbonate</b>	<b>E<sub>A</sub>, kJ/mol</b>	<b>Relative K<sub>b</sub><sup>a 124</sup></b>
1,2-butylene carbonate	64.8 ± 2.1	15.8
<i>cis</i> -cyclopentene carbonate	72.9 ± 5.2	15.4
styrene carbonate	91.2 ± 2.7	16.4
<i>cis</i> -indene carbonate	114.4 ± 5.7	15.2

(a) The relative K<sub>b</sub> for the corresponding epoxide as determined by Darensbourg and Chung.

Finally, the various pathways for the production of styrene carbonate were determined in conjunction with Dr. Sheng-Hsuan Wei (Figure III-20). Generally, both the chromium metal center and carbonate chain end provide stabilization against backbiting reactions (i.e. have higher free energy barriers). The DBU-initiated backbiting of 2-chloro-1-phenylethanol under CO<sub>2</sub> pressure was examined, and dependence of the reaction on CO<sub>2</sub> pressure and concentration was observed. Experimental design limitations prevented the determination of the activation parameters for Pathway **f**, though it is believed to be very low.

Notably, some mechanistic details do come to light from this analysis. For pathway **c**, the metal center must be involved in the rate-limiting step for the reaction, though it is possible that the slow step is not depicted in Figure III-20. If the CO<sub>2</sub>-inserted species were to fall off of the metal center, rapid backbiting to cyclic carbonate would occur (*vide supra*). It is possible that the cyclic carbonate stays bound to the metal following backbiting, as a similar barrier (90 kJ/mol) was calculated by Rieger for the backbiting of propylene carbonate.<sup>125</sup> Alternatively, either epoxide ring-opening or dissociation from the metal is the rate-limiting step. Whatever the slow step of the reaction may be, it is assuredly different than that of pathway **e**, despite the similar

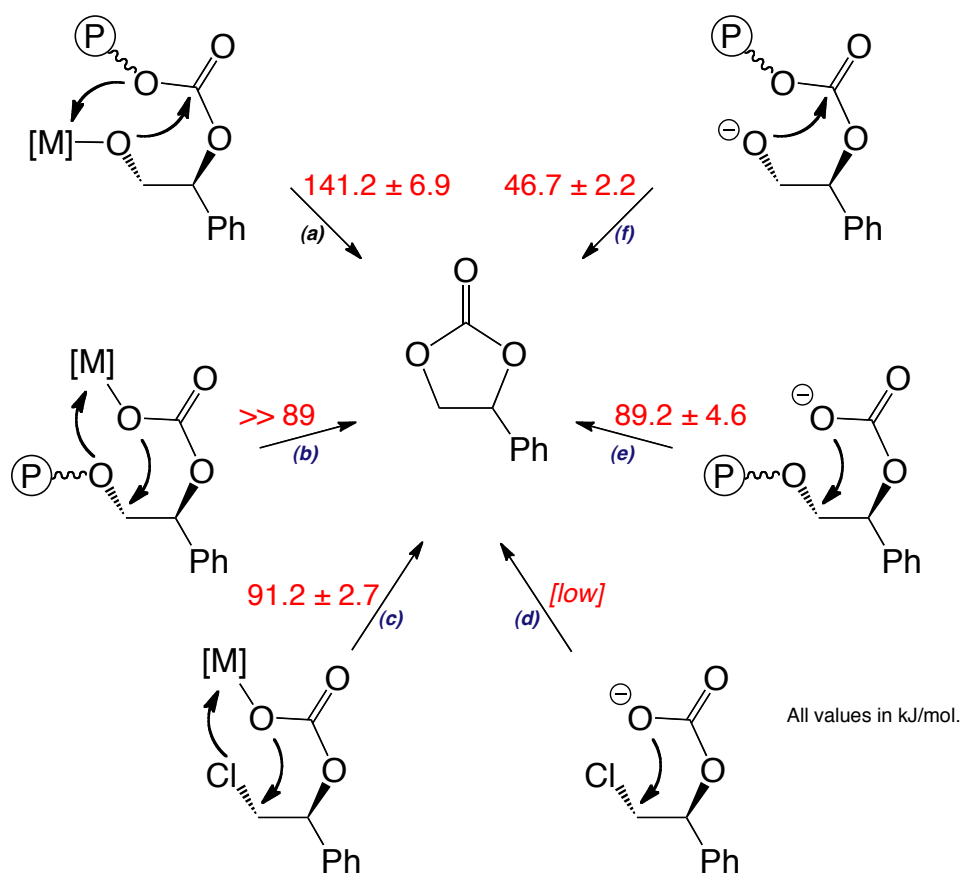


**Figure III-20.** Energies of activation for various backbiting reactions to styrene carbonate.

activation barrier.

### Future Work

As the backbiting reaction of 2-chloro-1-phenylethanol at 23 °C happened in a matter of moments, lower temperatures would be required to monitor the reaction in order to obtain rate constants and determine energy barriers. At present, we are experimentally limited by the methods we have to add base and/or CO<sub>2</sub> to the reaction. It has been observed that the addition of DBU to 2-chloro-1-phenylethanol at room

temperature under argon provides a stable, deprotonated complex. When the system is flushed with atmospheric pressure CO<sub>2</sub>, the reaction can be monitored by ATR-FTIR. However, without knowing the concentration of CO<sub>2</sub> within the system, the data is not useful. Immediately upon the addition of high pressures of CO<sub>2</sub> to the deprotonated complex at room temperature, styrene carbonate formation is observed before any monitoring can take place. The DJD ASI ReactIR2 system with the 300 mL Parr reactor cannot handle pressures below room temperature, and our ReactIR ic10 high pressure system is still undergoing troubleshooting. Even if it were fully developed, it does not have a mechanism by which DBU can be added after increased CO<sub>2</sub> pressures have been administered. Monitoring by variable temperature <sup>1</sup>H NMR may be possible, but the logistics of the reaction setup need to be carefully thought out.

## CHAPTER IV

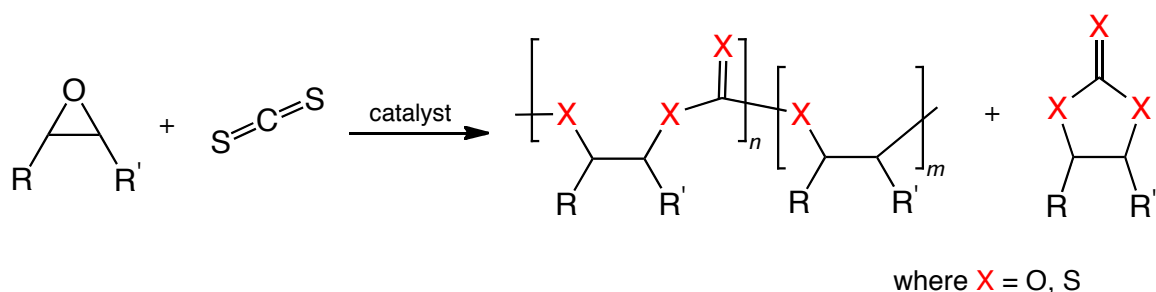
### COPOLYMERIZATION OF CYCLOPENTENE OXIDE AND CARBON

### DISULFIDE: SELECTIVITY FOR POLYMER VS. CYCLIC [THIO]CARBONATES

#### **Introduction**

While the coupling of epoxides and CO<sub>2</sub> to form polycarbonates has garnered widespread attention, the coupling of epoxides with carbon disulfide, CS<sub>2</sub>, to form polythiocarbonates has not been investigated as thoroughly. Notable studies from Endo,<sup>77</sup> North,<sup>76,126</sup> and others<sup>127</sup> have looked at the selective coupling of epoxides and CS<sub>2</sub> to form cyclic trithiocarbonate and thiocarbonate materials that have applications in materials science and biologically active systems, though polymeric coupling was not desired. In 2004, Nozaki investigated the selective coupling of propylene sulfide with CS<sub>2</sub> to yield poly(propylene trithiocarbonate) and cyclic propylene trithiocarbonate.<sup>75</sup>

In 2008, Qi and coworkers investigated the coupling of PO and CS<sub>2</sub> using a heterogeneous cobalt/iron double metal cyanide (DMC) catalyst.<sup>78</sup> The system's polymer product displayed a mix of different backbone repeat units instead of only the expected -O-(C=S)-S- dithiocarbonate repeat unit (Scheme IV-1). Oxygen and sulfur scrambling was also noted in the cyclic carbonate byproducts. The authors were able to note the presence of scrambled COS using GC-MS, though no trace of propylene sulfide was observed. It was thus hypothesized that propylene sulfide is quickly consumed in reactions with available CS<sub>2</sub>, COS, or CO<sub>2</sub> within the system. The produced



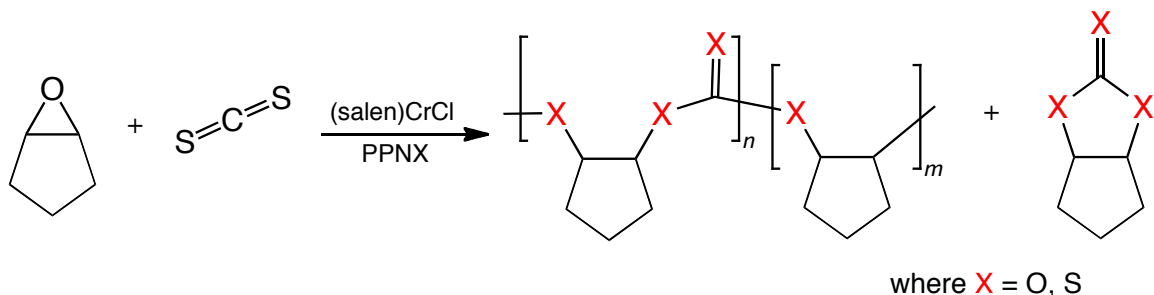
**Scheme IV-1.** Catalytic coupling of epoxides with CS<sub>2</sub> produces polycarbonate, polyether, and cyclic carbonate materials that display oxygen/sulfur scrambling.

poly[thio]carbonates had broad molecular weight distributions (PDI), varying between 1.24-3.50.

Though the structure of the DMC could be guessed with some degree of merit, Darensbourg and coworkers decided to investigate the similar coupling of cyclohexene oxide with CS<sub>2</sub> utilizing the well-known (salen)CrCl/PPNCl system, hoping that a study with a better defined catalyst/epoxide could elucidate mechanistic details.<sup>79</sup> O/S scrambling was again observed in both the polymeric and cyclic carbonates, with the polymer being oxygen enriched and the cyclics being sulfur enriched.

The work discussed in this chapter stemmed from a simple experiment meant only to occupy a few days' worth of time. As discussed in Chapter III, cyclopentene oxide couples with CO<sub>2</sub> to selectively form *cis*-cyclopentene carbonate utilizing (salen)CrCl and PPNX cocatalysts. We were hoping to quickly synthesize and isolate *cis*- and/or *trans*-cyclopentene trithiocarbonate from the coupling of cyclopentene oxide and CS<sub>2</sub> in a manner much like that of our 2009 study.<sup>79</sup> Instead of forming only cyclic

carbonates as was expected, a wide range of polymeric species displaying O/S scrambling were also produced (Scheme IV-2).



**Scheme IV-2.** Coupling of cyclopentene oxide and CS<sub>2</sub> utilizing (salen)CrCl and PPNX cocatalysts.

## Experimental

**Materials and Methods.** Unless otherwise specified, all syntheses and manipulations were carried out on a double-manifold Schlenk vacuum line under an atmosphere of argon or in an argon-filled glovebox. Following purification, materials were stored in an argon-filled glovebox prior to use unless otherwise specified. Carbon disulfide (99.9%, ACS Grade, Alfa Aesar) and cyclopentene oxide (GL Biochem (Shanghai), Ltd.) were distilled over CaH<sub>2</sub> and stored in the glovebox freezer and glovebox, respectively. (*R,R*)-*N,N'*-bis(3,5-di-*tert*-butylsalicylidene)-1,2-cyclohexanediaminochromium(III) chloride, (salen)CrCl, was purchased from Strem and used as received. Toluene was distilled from sodium/benzophenone. Toluene-*d*<sub>8</sub> (99.6% D) was purchased from Aldrich and stored over 4 Å molecular sieves. *Trans*-cyclohexene trithiocarbonate was obtained according to the literature report.<sup>79</sup> Research Grade 99.999% carbon dioxide supplied in a high-pressure cylinder and equipped with a

liquid dip tube was purchased from Airgas. The CO<sub>2</sub> was further purified by passing through two steel columns packed with 4 Å molecular sieves that had been dried under vacuum at  $\geq 200$  °C. High pressure reaction monitoring measurements were performed using an ASI ReactIR 1000 reaction analysis system with a 300 mL stainless steel Parr autoclave modified with a permanently mounted ATR crystal (SiComp) at the bottom of the reactor (purchased from Mettler Toledo). Infrared spectra were recorded on a Bruker Tensor 37 spectrometer in CaF<sub>2</sub> solution cells with a 0.1 mm path length.

Glass transition temperatures ( $T_g$ ) were measured using a Mettler Toledo polymer DSC equipped with a liquid nitrogen cooling system and 50 mL/min purge of dry nitrogen gas. Samples (~5 mg) were weighed into 40  $\mu$ L aluminum pans and subjected to two heating cycles. The first cycle covered the range from 25 to 125 °C at 10 °C/min and was then cooled back to -50 °C at -10 °C/min. Midpoint  $T_g$  data was obtained from the second heating cycle which ranged from -50 to 125 °C at a heating rate of 5 °C/min. GC-MS was performed on Ultra GC/DSQ (ThermoElectron, Waltham, MA). Rxi-5ms was used as a gas chromatographic column with dimensions of 60 m length, 0.25 mm i.d., and 0.25  $\mu$ m film thickness (Restek; Bellefonte, PA). Helium was used as a carrier gas at constant flow of 1.5 ml/min. An aliquot of 1  $\mu$ L of sample was injected in splitless mode. Transfer line and ion source were held at 250°C. The column temperature was maintained at 50 °C for 5 min and raised to 320 °C at 20 °C/min. Mass spectra were acquired in full scan mode in the range of 30-500 m/z. Additional GC-MS information can be found in Appendix D.



**Calculations.** All calculations were performed using the Gaussian 09 suite.<sup>128</sup> Geometries were fully optimized using the B3LYP functional<sup>129</sup> and the Pople-style 6-311G(2d,d,p) basis set,<sup>130</sup> as pre-defined in the composite CBS-QB3 method.<sup>131</sup> All local minima were verified by their calculated vibrational frequencies (zero imaginary frequencies). The enthalpies of the various species at their stationary points were obtained after the CBS-QB3 extrapolations.<sup>131</sup> Additional calculations information can be found in Appendix D.

**Coupling of Cyclopentene Oxide and Carbon Disulfide with PPNN<sub>3</sub> Cocatalyst.** (salen)CrCl (0.0483 g, 0.076 mmol, 1 eq) and the appropriate amount of PPNN<sub>3</sub> were added to a vial. Approximately 15 mL dry CH<sub>2</sub>Cl<sub>2</sub> was added, and the solution was allowed to stir for 15 minutes under argon to allow for catalyst activation. Following solvent removal *in vacuo*, 10.0 mL cyclopentene oxide was added to the vial, and the resulting solution was cannulated into a 300 mL stainless steel Parr reactor equipped with a permanently mounted SiComp crystal. The vial was rinsed with the appropriate amount of CS<sub>2</sub>, and the solution was injected into the reaction vessel. After 24 hours, the reactor was cooled, vented, and the contents were transferred into an Erlenmeyer flask. A sample was taken for crude <sup>1</sup>H and <sup>13</sup>C NMR analysis, and the residual solvent was removed *in vacuo*. The resulting dark red gel was dissolved in a minimal amount of CH<sub>2</sub>Cl<sub>2</sub> and added dropwise to acidified MeOH (5% HCl) to precipitate the polymer. The polymer was precipitated again from MeOH and dried in a vacuum oven. The methanol was removed from the cyclic materials. They were

redissolved in CH<sub>2</sub>Cl<sub>2</sub>, flashed through a silica pad to remove residual catalyst and cocatalyst, and concentrated *in vacuo*. A dry sample was sent for GC-MS analysis.

**Coupling of Cyclopentene Oxide and Carbon Disulfide with PPNCI Cocatalyst.** (salen)CrCl (0.0242 g, 0.0382 mmol, 1 eq) and PPNCI (0.0439 g, 0.0765 mmol, 2 eq) were added to a vial. Approximately 5 mL dry CH<sub>2</sub>Cl<sub>2</sub> was added, and the solution was allowed to stir for 15 minutes under argon to allow for catalyst activation. Following solvent removal *in vacuo*, 5.0 mL cyclopentene oxide was added to the vial, and the resulting solution was added to a 25 mL stainless steel reactor. The vial was washed with the appropriate volume of CS<sub>2</sub>, and the solution was again transferred into the reactor. The reactor was sealed and heated to 80 °C for 6 hours. Following completion, the reactor was cooled in an ice bath, vented, and the contents were transferred into an Erlenmeyer flask. A sample was taken for crude <sup>1</sup>H and <sup>13</sup>C NMR analysis, and the residual solvent was removed *in vacuo*. The resulting dark red gel was dissolved in a minimal amount of CH<sub>2</sub>Cl<sub>2</sub> and added dropwise to acidified MeOH (5% HCl) to precipitate the polymer. The polymer was precipitated again from MeOH and dried in a vacuum oven. The methanol was removed from the cyclic materials, dissolved in a CH<sub>2</sub>Cl<sub>2</sub>, and filtered through a silica pad to remove residual catalyst and cocatalyst. Polymer and cyclic materials were dried until constant mass was achieved. A dry sample of the cyclics was sent for GC-MS analysis.

***trans*-(acetylthio)-cyclopentanol.** The synthetic route of Harding and Owen<sup>132</sup> and Goodman, Benitez, and Baker<sup>133</sup> were followed starting from 20.0 g cyclopentene oxide and 20.0 g thioacetic acid. This mixture was allowed to stir for 13 days at room

temperature in a stoppered flask. The remaining thioacetic acid was removed *in vacuo*, yielding 34.776 g crude *trans*-(acetylthio)-cyclopentanol (~91% yield) as a brown liquid. The crude NMR displayed peaks of an expected pattern. The product of this reaction was used without further purification.  $^1\text{H}$  NMR (300 MHz,  $\text{CDCl}_3$ ):  $\delta$  4.09 (m, 1H), 3.54 (td, 1H,  $J = 4.7, 8.4$  Hz), 3.11 (d, 1H,  $J = 2.8$  Hz), 2.32 (s, 3H), 1.36-2.25 (m, 6H) ppm.  $^{13}\text{C}$  NMR (75 MHz,  $\text{CDCl}_3$ ):  $\delta$  198.4, 80.1, 50.8, 33.5, 30.5, 22.8 ppm.

***trans*-2-(acetylthio)-cyclopentyl acetate.** The entire 34.776 g of crude *trans*-(acetylthio)-cyclopentanol (217 mmol) was added in small portions to a stirred solution of 82.6 mg *p*-toluenesulfonic acid, monohydrate (0.43 mmol, 0.002 eq) in 70 g acetic anhydride (690 mmol). The flask heated rapidly and was sealed with a septum with an attached bubbler. Once the reaction had returned to room temperature, the septum was removed, and a glass stopper was inserted. The reaction was stirred overnight at room temperature. 100 mL dichloromethane and 100 mL sat.  $\text{NaHCO}_3$  (aq) were added to the reaction, and the aqueous and organic layers were separated. The aqueous layer was washed with dichloromethane (3 x 30 mL). The organic layers were combined and washed sequentially with sat.  $\text{NaHCO}_3$  (aq) (3 x 30 mL) and deionized water (3 x 30 mL). The organic layer was dried with  $\text{Na}_2\text{SO}_3$  and concentrated *in vacuo*. The crude NMR displayed peaks of an expected pattern. The product of this reaction was immediately used in the next step without further purification.  $^1\text{H}$  NMR (300 MHz,  $\text{CDCl}_3$ ):  $\delta$  4.98 (m, 1H), 3.71 (m, 1H), 2.26 (s, 3H), 2.23 (m, 1H), 2.02 (m, 1H), 1.99 (s, 1H), 1.45-1.83 (m, 4H) ppm.  $^{13}\text{C}$  NMR (75 MHz,  $\text{CDCl}_3$ ):  $\delta$  194.8, 170.2, 79.6, 47.3, 31.34, 31.30, 30.5, 22.5, 22.1 ppm.

**Cyclopentene Sulfide.** The resultant crude *trans*-2-(acetylthio)-cyclopentyl acetate was stirred with 300 mL 1.67 M NaOH overnight under argon at room temperature. 100 mL dichloromethane was added to the reaction mixture, and the aqueous and organic layers were separated. The aqueous layer was washed with dichloromethane (3 x 40 mL), and the combined organic layers were washed sequentially with sat. NaHCO<sub>3</sub> (aq) (3 x 40 mL) and deionized water (3 x 40 mL). The organic layer was dried with Na<sub>2</sub>SO<sub>4</sub> and concentrated *in vacuo*. The resultant brown liquid was distilled under reduced pressure to afford pure cyclopentene sulfide as a clear, colorless liquid (0.8 mmHg, 32 °C). The low boiling nature of cyclopentene sulfide meant that a large amount was found in the liquid nitrogen-cooled solvent trap. Further distillation of this material utilizing an aspirator could therefore yield a larger amount of material. 7.96 g, 33% overall yield for three steps. <sup>1</sup>H NMR (300 MHz, CDCl<sub>3</sub>): δ 3.27 (d, 2H, J = 2.4 Hz), 2.03 (dd, 2H, J = 5.7, 12.9 Hz), 1.72-1.89 (m, 2H), 1.44-1.66 (m, 2H) ppm. <sup>13</sup>C NMR (75 MHz, CDCl<sub>3</sub>): δ 41.7, 29.0, 18.1 ppm. Anal. Calc. for C<sub>5</sub>H<sub>8</sub>S: C, 59.94; H, 8.05. Found: C, 59.69; H, 7.90.

**Coupling Reactions Utilizing Cyclopentene Sulfide.** 0.25 g cyclopentene sulfide (2.5 mmol) was added to the appropriate amount of (salen)CrCl and cocatalyst in a 10 mL stainless steel reactor. When solvent was employed, the total volume of added liquid (CS<sub>2</sub> + toluene) was maintained at 1.0 mL. Reactions were run at the temperatures and for the amount of time specified in the Table. Following completion of the reaction, the reactors were cooled, vented in a fume hood, and the crude reaction products were subject to <sup>1</sup>H NMR analysis. Cyclopentene, *cis*-cyclopentene

trithiocarbonate, and cyclopentene sulfide were recognized by their characteristic  $^1\text{H}$  NMR frequencies (in  $\text{CDCl}_3$ : 5.27, 4.70, 3.24 ppm, respectively; in  $\text{C}_7\text{D}_8$ : 5.64, 3.63, 2.86, respectively).

***trans*-Cyclopentene Trithiocarbonate.** The crude reaction mixture from the coupling of  $\text{CS}_2$  and cyclopentene oxide was concentrated *in vacuo* to remove excess  $\text{CS}_2$ . The resulting mixture was dissolved in a minimal amount of dichloromethane and added dropwise to 5% HCl in MeOH. The supernatant was collected and concentrated *in vacuo*. The resulting material was purified by column chromatography (silica gel,  $\text{CH}_2\text{Cl}_2$  solvent). *Trans*-cyclopentene trithiocarbonate was eluted as a distinct yellow band. Yellow needle crystals suitable for X-ray diffraction that confirm the *trans*-designation were grown from a concentrated solution in  $\text{CH}_2\text{Cl}_2$  at room temperature.  $^1\text{H}$  NMR (300 MHz,  $\text{CDCl}_3$ ):  $\delta$  4.058 (m, 2H), 2.216 (m, 4H), 1.851 (m, 2H) ppm.  $^{13}\text{C}$  NMR (125 MHz,  $\text{CDCl}_3$ ):  $\delta$  234.7, 67.0, 26.0, 25.7 ppm. FT-IR  $\nu_{\text{CS}_3}$  1099, 1058  $\text{cm}^{-1}$  ( $\text{CH}_2\text{Cl}_2$ ). Values are in good agreement with the literature.<sup>134</sup> Anal. Calc. for  $\text{C}_6\text{H}_8\text{S}_3$ : C, 40.87; H, 4.57. Found: C, 40.92; H, 4.78.

**X-ray Crystal Study.** Yellow crystalline needles of *trans*-cyclopentene trithiocarbonate were obtained by slow evaporation of a concentrated solution in  $\text{CH}_2\text{Cl}_2$  at room temperature. For the crystal structure, a Bausch and Lomb 10 $\times$  microscope was used to identify suitable crystals. A single crystal sample was coated in mineral oil, affixed to a Nylon loop, and placed under streaming  $\text{N}_2$  (110 K) in a single-crystal APEXii CCD diffractometer. X-ray diffraction data were collected by covering a hemisphere of space upon combination of three sets of exposures. The structure was

solved by direct methods. H atoms were placed at idealized positions and refined with fixed isotropic displacement parameters and anisotropic displacement parameters were employed for all non-hydrogen atoms. The following programs were used: for data collection and cell refinement, APEX2;<sup>86</sup> data reductions, SAINTPLUS, version 6.63;<sup>87</sup> absorption correction, SADABS;<sup>88</sup> structure solutions, SHELXS-97;<sup>89</sup> structure refinement, SHELXL-97.<sup>90</sup>

***cis*-Cyclopentene Trithiocarbonate.** Following the removal of *trans*-cyclopentene trithiocarbonate, the remaining mixture of cyclic materials from the coupling of CS<sub>2</sub> and cyclopentene oxide was again subjected to column chromatography (4/1 hexanes/ethyl acetate). *Cis*-cyclopentene trithiocarbonate and *cis*-cyclopentene dithiocarbonate (SOS connectivity) eluted together. Further attempts to separate these two materials were unsuccessful. The *cis*- assignments are given due to the different <sup>1</sup>H, <sup>13</sup>C NMR, FT-IR, GC-MS traces from the known *trans*-cyclopentene trithiocarbonate, mass spectral analysis, and that these two materials were not able to be separated by any attempted physical/chemical means. <sup>1</sup>H NMR (300 MHz, CDCl<sub>3</sub>): δ 4.724 (m, 2H), 2.195 (m, 5H), 1.835 (m, 1H) ppm. <sup>13</sup>C NMR (125 MHz, CDCl<sub>3</sub>): δ 228.3, 63.6, 33.2, 24.8 ppm. FT-IR 1065 cm<sup>-1</sup> (CH<sub>2</sub>Cl<sub>2</sub>).

***cis*-Cyclopentene Dithiocarbonate (-S-(C=O)-S- Connectivity).** The crude mixture of cyclic materials from the coupling of CS<sub>2</sub> and cyclopentene oxide was purified by column chromatography (4/1 hexanes/ethyl acetate). *Cis*-cyclopentene dithiocarbonate (SOS connectivity) and *cis*-cyclopentene trithiocarbonate eluted together. Further attempts to separate these two materials were unsuccessful. The *cis*-

assignments are given due to the different  $^1\text{H}$ ,  $^{13}\text{C}$  NMR, FT-IR, GC-MS traces from the known *trans*-cyclopentene trithiocarbonate, mass spectral analysis, and that these two materials were not able to be separated by any attempted physical/chemical means. The -S-(C=O)-S connectivity was assigned because of the characteristic carbonyl stretch of the compound and mass spectral analysis showing the loss of a C=O group.  $^1\text{H}$  NMR (300 MHz,  $\text{CDCl}_3$ ):  $\delta$  4.058 (m, 2H), 2.216 (m, 4H), 1.851 (m, 2H) ppm.  $^{13}\text{C}$  NMR (125 MHz,  $\text{CDCl}_3$ ):  $\delta$  197.6, 54.5, 33.3, 24.1 ppm. FT-IR 1653  $\text{cm}^{-1}$  ( $\text{CH}_2\text{Cl}_2$ ).

**Scrambling Test Reactions with  $\text{CS}_2$ ,  $\text{CO}_2$ , and No Added Reagent.** 700 mg (4.3 mmol, 50 eq, 160 g/mol assumed molecular weight) of a purified mix of cyclic [thio]carbonates, 55.2 mg (salen)CrCl (0.087 mmol, 1 eq), and 48.6 mg  $n\text{Bu}_4\text{NCl}$  (0.175 mmol, 2 eq) were dissolved in 5.0 mL toluene. Either 0.33 g  $\text{CS}_2$  (4.3 mmol, 50 eq), 1.4 MPa  $\text{CO}_2$ , or no other reagents were added to the solution. The reaction was heated to 80  $^\circ\text{C}$  for 2 days. Following completion of the reaction, the solution was concentrated *in vacuo*, and the products were analyzed by  $^1\text{H}$  NMR and GC-MS. In each case, no differences between the starting cyclic [thio]carbonate mixture and the product [thio]carbonate mixture were discernable.

**Scrambling Test Reactions with Cyclopentene Oxide.** 34.04 mg (2.1 mmol, 50 eq, 160 g/mol assumed molecular weight) of a purified mix of cyclic [thio]carbonates, 27.6 mg (salen)CrCl (0.044 mmol, 1 eq), and 24.3 mg  $n\text{Bu}_4\text{NCl}$  (0.087 mmol, 2 eq) were dissolved in 1.16 mL cyclopentene oxide. The reaction was heated to 80  $^\circ\text{C}$  for 16 hours. Following completion of the reaction, the solution was concentrated *in vacuo*, and the products were analyzed by  $^1\text{H}$  NMR and GC-MS. Distinct shifts in

product distribution between the starting cyclic [thio]carbonate mixture and the product [thio]carbonate mixture were clearly visible.

**Scrambling of *trans*-Cyclohexene Trithiocarbonate with Cyclohexene Oxide.**

50 mg *trans*-cyclohexene trithiocarbonate (0.26 mmol, 50 eq), 6.6 mg (salen)CrCl (0.01 mmol, 1 eq), and/or 5.8 mg *n*Bu<sub>4</sub>NCl (0.02 mmol, 2 eq) were dissolved in 5.4 mL cyclohexene oxide (53 mmol, 500 eq) in a 20 mL vial. The vial was heated to 80 °C for 24 hours, and an IR spectra was taken every 3 minutes. Scrambling was observed by the growth of the cyclohexene carbonate peak at 1809 cm<sup>-1</sup>.

**Scrambling Reactions Observed by <sup>1</sup>H NMR Spectroscopy.** (a) In an argon-filled glovebox, 0.0528 g *trans*-cyclopentene trithiocarbonate (0.3 mmol, 50 eq), 0.10 mL cyclopentene oxide (1.2 mmol, 200 eq), 3.8 mg (salen)CrCl (0.006 mmol, 1 eq), 3.3 mg *n*Bu<sub>4</sub>NCl (0.012 mmol, 2 eq), and 0.30 mL toluene-*d*<sub>8</sub> were loaded into a J-Young tube. The tube was sealed, and crude <sup>1</sup>H and <sup>13</sup>C NMRs were taken. The tube was heated to 80 °C in a silicon oil bath, and the progress of the scrambling reaction was monitored over the next 48 hours by <sup>1</sup>H and <sup>13</sup>C NMR. Notably, the *trans*-cyclopentene trithiocarbonate did not fully dissolve until ~8 hours into the reaction. (b) In an argon-filled glovebox, 0.0384 g *trans*-cyclopentene trithiocarbonate (0.3 mmol, 50 eq), 0.11 mL cyclopentene oxide (1.2 mmol, 200 eq), 3.8 mg (salen)CrCl (0.006 mmol, 1 eq), 3.3 mg *n*Bu<sub>4</sub>NCl (0.012 mmol, 2 eq), and 0.29 mL toluene-*d*<sub>8</sub> were loaded into a J-Young tube. The tube was sealed, and crude <sup>1</sup>H and <sup>13</sup>C NMRs were taken. The tube was heated to 80 °C in a silicon oil bath, and the progress of the scrambling reaction was monitored over the next 48 hours by <sup>1</sup>H and <sup>13</sup>C NMR.



### Scrambling of *trans*-Cyclohexene Trithiocarbonate with Cyclopentene

**Oxide.** 50 mg *trans*-cyclohexene trithiocarbonate (0.26 mmol, 50 eq), 3.3 mg (salen)CrCl (0.0052 mmol, 1 eq), and 2.9 mg *n*Bu<sub>4</sub>NCl (0.0104 mmol, 2 eq) were dissolved in 5.7 mL cyclopentene oxide (65.4 mmol, 250 eq) in a Schlenk tube. The tube was heated to 80 °C under argon for 24 hours. The reaction was cooled and concentrated *in vacuo*. The resulting material was analyzed by <sup>1</sup>H and <sup>13</sup>C NMR as well as GC-MS.

## Results and Discussion

### Coupling of Cyclopentene Oxide and Carbon Disulfide Utilizing PPNN<sub>3</sub>.

Azide, N<sub>3</sub><sup>-</sup>, is often used as an initiator in the copolymerizations of epoxides and CO<sub>2</sub> due to its distinct  $\nu_{N_3}$  bond stretching patterns that can be monitored by infrared spectroscopy. Clear shifts in the azide stretch can be observed depending on the chemical environment (Table IV-I).<sup>135</sup>

**Table IV-1.** Azide stretching frequencies in tetrachloroethylene.<sup>135</sup>

Azide Chemical Environment	$\nu_{N_3}$ (cm <sup>-1</sup> )
free N <sub>3</sub> <sup>-</sup>	2009
singly chromium-bound X-Cr-N <sub>3</sub>	2051
doubly chromium-bound, <i>trans</i> - N <sub>3</sub> -Cr-N <sub>3</sub>	2057sh, 2047
organic R-N <sub>3</sub>	2100

Because of this valuable spectroscopic trace, bis(triphenylphosphine)iminium azide, PPNN<sub>3</sub>, was originally chosen as the cocatalyst for this investigation. Following the aforementioned coupling of CPO with CS<sub>2</sub> utilizing (salen)CrCl and PPNN<sub>3</sub>, a wide array of polymeric and cyclic [thio]carbonate materials were produced. Scrambling of the oxygen and sulfur atoms is observed in both the reactants and the products. In an effort to quickly identify the various materials produced during the coupling process, basic information including mass of produced polymer versus [thio]cyclic carbonate was not collected for these reactions. Regardless, both polymer and cyclic carbonates were produced in each case, and differences in scrambling products can be noted. These reactions were monitored utilizing ATR-FTIR, and three-dimensional stack plots and reaction profiles can be found in Appendix C. Due to the overlapping nature of the <sup>1</sup>H and FT-IR of these species, spectral assignments were difficult.

In general, peak production of the -O-(C=O)-S- polymer peak at 1712 cm<sup>-1</sup> is maximized after ~4 hours,<sup>79</sup> after which it decays away, presumably because of backbiting or rearrangement reactions. The spectral region from 1000-1400 cm<sup>-1</sup> is difficult to assign, as many different peaks are overlapping. CS<sub>2</sub> can be observed as the strong band at 1514 cm<sup>-1</sup>. The unchanging absorbance in the early stages of the reaction is caused by the saturation of CS<sub>2</sub> within the solution. Only after sufficient consumption of CS<sub>2</sub> can the absorbance change be observed. CO<sub>2</sub> production can be seen at 2338 cm<sup>-1</sup>, particularly when a limiting amount of CS<sub>2</sub> is employed in the reaction. COS production has been assigned to the peak which grows in at 2038 cm<sup>-1</sup>.<sup>136</sup> When CO<sub>2</sub> is

added to the reaction, production of *cis*-cyclopentene carbonate is achieved very quickly (see Chapter III).

Elemental analysis was performed on the purified polymer samples in order to better determine the chemical makeup (Table II-2). The hydrogen atoms were set at 8.00/repeat unit because this value should be consistent for both poly[thio]carbonate and poly[thio]ether linkages. In each case, the carbon content is significantly below the expected 6.0 for [thio]carbonate linkages, indicating a large amount of ether or thioether linkages in the polymer backbone. Indeed, when a limiting amount of CS<sub>2</sub> was employed, only 5.22 carbons exist in the idealized repeat unit, indicating that the polymer contains mostly [thio]ether linkages (entry 3). The decrease of [thio]carbonate content is mirrored by a decrease in T<sub>g</sub>, from 14.4 to -17 °C. Upon the addition of 0.7 MPa CO<sub>2</sub>, both the [thio]carbonate content and T<sub>g</sub> greatly increase, with 5.81 carbons/repeat unit and T<sub>g</sub> = 32.3 °C.

Notably, <sup>1</sup>H and <sup>13</sup>C NMRs (CDCl<sub>3</sub>) of the crude reaction mixtures each clearly display the production of cyclopentene sulfide (peaks at 3.28, 30.0 ppm) and

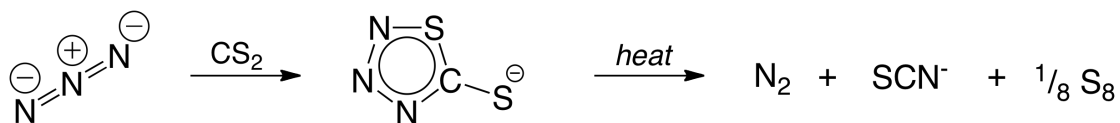
**Table IV-2.** Reaction of cyclopentene oxide with CS<sub>2</sub> with (salen)CrCl and PPNN<sub>3</sub> in a 300 mL stainless steel Parr reactor.

Entry	Equivalents PPNN <sub>3</sub>	Equivalents CS <sub>2</sub>	P <sub>CO<sub>2</sub></sub> , MPa	Polymer Repeat Unit <sup>a</sup>	T <sub>g</sub> <sup>b</sup> , °C
1	2	1500	0	C <sub>5.69</sub> H <sub>8</sub> S <sub>1.56</sub> O <sub>0.76</sub>	14.4
2	1	1500	0	C <sub>5.58</sub> H <sub>8</sub> S <sub>1.15</sub> O <sub>0.88</sub>	9.6
3	2	750	0	C <sub>5.22</sub> H <sub>8</sub> S <sub>0.80</sub> O <sub>1.22</sub>	-17.6
4	2	750	0.7	C <sub>5.81</sub> H <sub>8</sub> S <sub>1.08</sub> O <sub>1.81</sub>	32.3

Reaction conditions 9.64 g cyclopentene oxide (10.0 mL, 115 mmol, 1500 eq), 0.0483 g (salen)CrCl (0.076 mmol, 1 eq), and the appropriate amounts of PPNN<sub>3</sub>, CS<sub>2</sub>, and CO<sub>2</sub> pressure, where applicable. 80 °C, 24 h. (a) H set at 8.00 and other elements were calculated from elemental analysis of the purified polymer sample. (b) Midpoint T<sub>g</sub> from the second heating cycle utilizing Differential Scanning Calorimetry.

cyclopentene (peaks at 5.76, 32.4 ppm). At the end of the 24 hour reaction period, the cyclopentene oxide has been either completely or almost completely consumed, as evident by the disappearance of the peaks at 3.39 and 27.1 ppm in the  $^1\text{H}$  and  $^{13}\text{C}$  NMRs, respectively.

**Reaction of  $\text{N}_3^-$  with  $\text{CS}_2$ .** Though it was not known by this researcher prior to the start of this project, the facile reaction of azide with  $\text{CS}_2$  to form the 5-membered heterocyclic anion azidodithiocarbonate,  $\text{CS}_2\text{N}_3^-$ , is well defined in the literature (Scheme IV-3).<sup>137,138</sup> **NOTE:** *Azidodithiocarbonate salts and derivatives are potentially explosive, and appropriate safety precautions should be taken.* Only small quantities of the azidodithiocarbonate compounds were generated in these experiments, and they were normally generated *in situ* inside of a stainless steel Parr reactor.



**Scheme IV-3.** Reaction of azide with carbon disulfide to yield the azidodithiocarbonate anion. Upon heating, this anionic heterocycle will breakdown to dinitrogen, thiocyanate, and elemental sulfur.

As a test to confirm the presence of the  $\text{CS}_2\text{N}_3^-$  anionic heterocycle, tetrabutylammonium azide,  $n\text{Bu}_4\text{NN}_3$ , was dissolved in toluene at ambient temperature, and the characteristic free  $\text{N}_3^-$  peak was observed at  $2000\text{ cm}^{-1}$ . Upon addition of 5 equivalents of  $\text{CS}_2$ , the  $\text{N}_3^-$  peak immediately disappeared, and no distinct peaks were visible, consistent with reports that  $\text{CS}_2\text{N}_3^-$  complexes have only weak infrared

stretching patterns.<sup>139</sup>  $\text{CS}_2\text{N}_3^-$  salts and compounds are known to be thermally unstable,<sup>140</sup> and so the reaction was heated to the typical reaction temperature, 80 °C, to observe any potential decomposition. Indeed, almost immediately upon heating a sharp peak appeared at 2055  $\text{cm}^{-1}$  which indicates the formation of  $n\text{Bu}_4\text{NSCN}$  (Figure IV-1).<sup>141</sup> As such, the  $\text{CS}_2\text{N}_3^-$  heterocycle is not long-lived in the reaction medium, instead decomposing to thiocyanate,  $\text{SCN}^-$ . It is unclear at this time if  $\text{CS}_2\text{N}_3^-$  is able to initiate polymer growth prior to this decomposition.

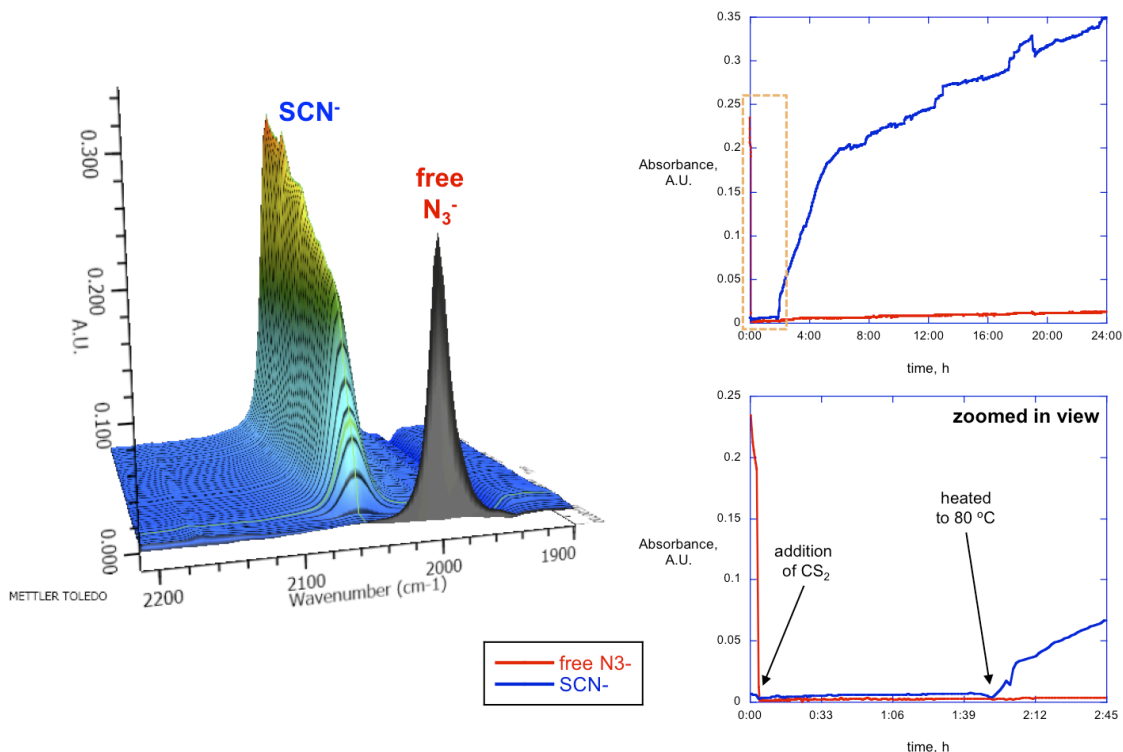


**Figure IV-1.** At left, three-dimensional stack plot of the reaction of azide ( $2000\text{ cm}^{-1}$ ) with  $\text{CS}_2$ .  $\text{CS}_2$  was added after 3 minutes. After  $\sim 2$  hours, the reaction was heated to 80 °C, and the growth of thiocyanate was observed at  $2055\text{ cm}^{-1}$ . At top right, traces of the disappearance and growth peaks of free  $\text{N}_3^-$  (red), and  $\text{SCN}^-$  (blue). Bottom right, zoomed in view from 0-2.75 hours reaction time.

### Coupling of Cyclopentene Oxide and Carbon Disulfide Utilizing PPnCl.

Due to the unclear  $\text{N}_3^-/\text{CS}_2\text{N}_3^-/\text{SCN}^-$  nature of the cocatalyst in the previous studies, it was desirable to investigate this system with the well-defined PPnCl cocatalyst. Initial ATR-FTIR monitoring of a reaction between cyclopentene oxide and  $\text{CS}_2$  revealed that peak  $-\text{O}-(\text{C}=\text{O})-\text{S}-$  polymer production at  $1712\text{ cm}^{-1}$  was achieved after 6 hours, after which it drops off quickly, presumably due to depolymerization (Figure IV-2). Thus, all subsequent reactions were monitored for this amount of time to maximize the amount of copolymerization (Table IV-3). It is currently unclear as to why the  $1712\text{ cm}^{-1}$  polymer peak begins to grow again at  $\sim 14$  hours reaction time, but it is possible that a variety of equilibrium processes may contribute to this trace.

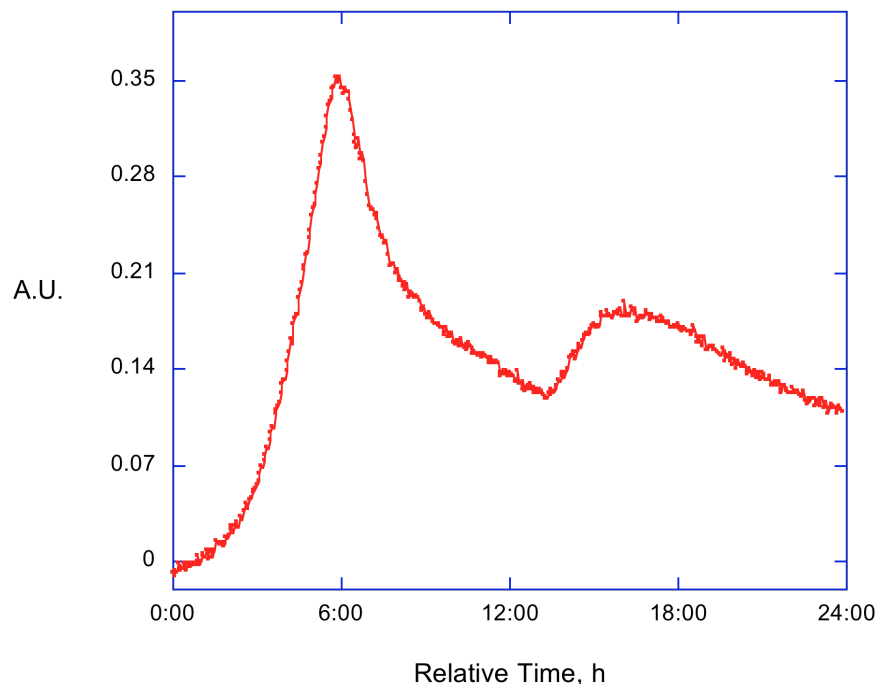


**Figure IV-2.** Trace of the  $-\text{O}-(\text{C}=\text{O})-\text{S}-$  monothiocarbonate polymer at  $1712\text{ cm}^{-1}$  displaying peak growth after 6 hours. Reaction loading is  $(\text{salen})\text{CrCl}:\text{PPnCl}:\text{cyclopentene oxide}:\text{CS}_2 = 1:2:1500:3000$ .

**Table IV-3.** Reaction of cyclopentene oxide with CS<sub>2</sub> with (salen)CrCl and PPnCl in a 25 mL stainless steel Parr reactor.

Entry	Equivalents CS <sub>2</sub> <sup>a</sup>	Mass Polymer, g <sup>b</sup>	Polymer Repeat Unit <sup>c</sup>
1	2.5	0.20	-
2	2.0	1.11	C <sub>5.92</sub> H <sub>8</sub> S <sub>1.70</sub> O <sub>1.43</sub>
3	1.5	1.27	-
4	1.0	2.04	C <sub>5.96</sub> H <sub>8</sub> S <sub>1.64</sub> O <sub>1.32</sub>
5	0.5	trace	-
6 <sup>d</sup>	1.0	0.17	-

Reaction conditions: 24.2 mg (salen)CrCl (1 eq), 43.9 mg PPnCl (2 eq), 5.0 mL cyclopentene oxide (1500 eq), 80 °C, 6 hours in a 25 mL stainless steel reactor. (a) Relative to cyclopentene oxide. (b) Mass of purified polymer sample. (c) H set at 8.00 and other elements were calculated from elemental analysis of the purified polymer sample. (d) 0.7 MPa CO<sub>2</sub> added.

As previously stated, the reaction time for those experiments with PPnCl cocatalyst was reduced to 6 hours in order to maximize the growth of the known -O-(C=O)-S- monothiocarbonate polymer product at 1712 cm<sup>-1</sup>. The largest amount of polymer was produced when equal parts cyclopentene oxide and CS<sub>2</sub> were employed (Table IV-3, entry 4). When the amount of CS<sub>2</sub> was limiting, only trace amounts of polymer were produced (entry 5), and the polymer growth was inhibited by large excesses of CS<sub>2</sub> (entry 1). The addition of 0.7 MPa CO<sub>2</sub> also prevented significant polymer growth (entry 6).

Early elemental analysis of the polymers give a consistent repeat unit of C<sub>6.0</sub>H<sub>8</sub>S<sub>1.6</sub>O<sub>1.3</sub>, indicating that there is very little [thio]ether content in the backbone of the polymer (Table IV-3, entries 2 & 4). It is therefore tentatively believed that the increased time for the 24 hour PPNN<sub>3</sub> reactions led to backbiting reactions, the loss of CS<sub>2</sub>, CO<sub>2</sub>, and COS, and corresponding increase in ether and thioether linkages in the

polymer backbone.<sup>142</sup> Full thermal and molecular weight analysis of the polymers is not yet complete, but early experiments indicate that these polymers are semicrystalline with  $T_g$  near 50 °C and  $T_m$  near 125 °C. Cyclopentene sulfide and cyclopentene are again observed in the  $^1\text{H}$  and  $^{13}\text{C}$  NMRs of the crude reaction mixture, though significant amounts of unreacted cyclopentene oxide also exist in each case.

Notably,  $^{13}\text{C}$  NMR revealed that the major [thio]carbonate component is actually at 211 ppm, caused by the the unscrambled -S-(C=S)-O- polymeric product (Figure IV-3). The infrared spectrum of the corresponding polymer shows several large peaks in the 1000-1400  $\text{cm}^{-1}$  range expected for thiones, but overlapping from the various thiocarbonates as well as C-O and C-S single bond stretches has prevented absolute assignment of peaks (Figure IV-4). The next largest contributor to the polymeric backbone is -O-(C=O)-S-, with corresponding to peaks at 169 ppm and 1712  $\text{cm}^{-1}$  in the  $^{13}\text{C}$  NMR and FT-IR, respectively. Notably, a small amount of the all-oxygen

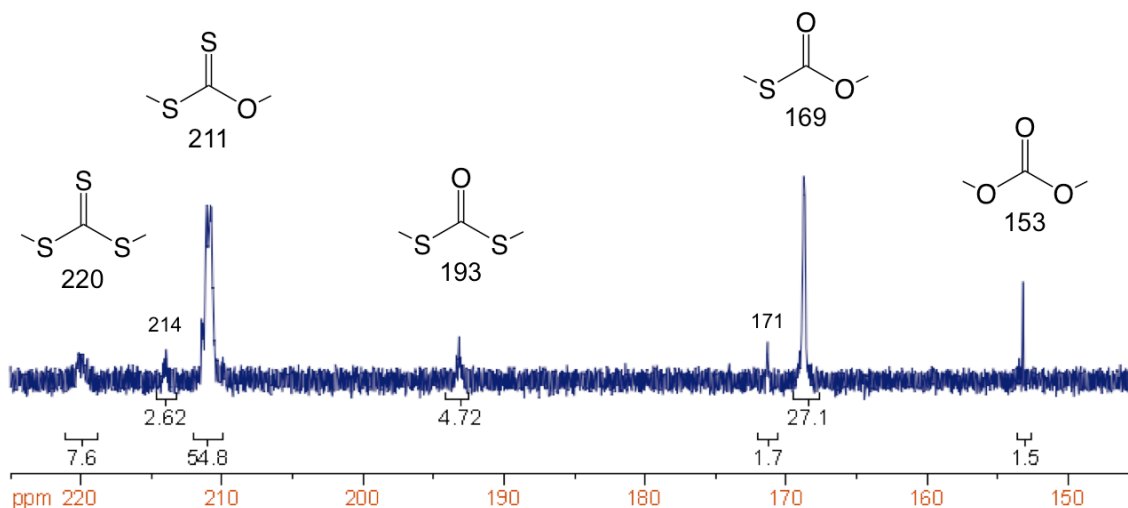


**Figure IV-3.** Carbonate region of the  $^{13}\text{C}$  NMR of poly[thio]carbonate from Table IV-3, entry 2.  $\text{CDCl}_3$ , 125 MHz.



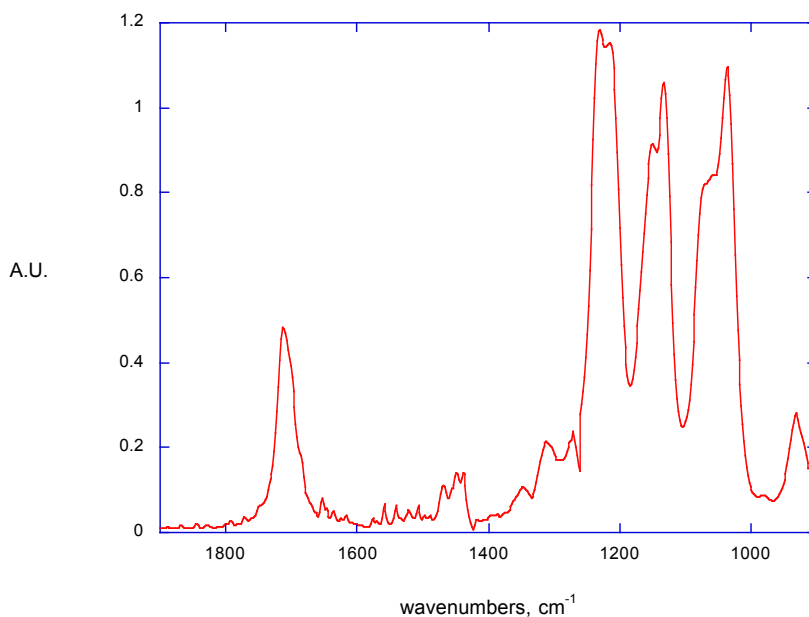


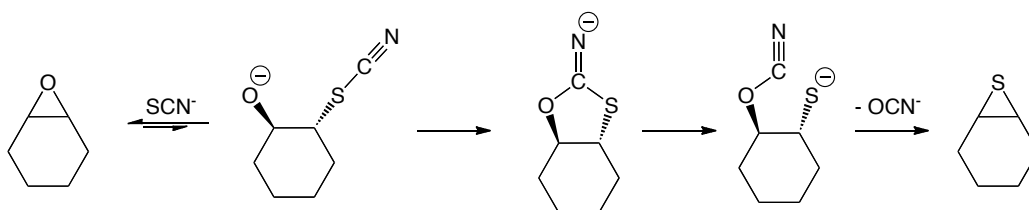
**Figure IV-4.** FT-IR of poly[thio]carbonate from Table IV-3, entry 2.  $\text{CH}_2\text{Cl}_2$  solvent.

polycarbonate can be seen both in the NMR ( $\sim 153$  ppm) and IR spectra ( $1750\text{ cm}^{-1}$ ), and other minor contributions from the trithiocarbonate ( $\sim 220$  ppm) and dithiocarbonate ( $\sim 193$  ppm) can be observed by NMR.<sup>79</sup>

**Coupling of Cyclopentene Sulfide with  $\text{CS}_2$  and  $\text{CO}_2$ .** Since the generation of cyclopentene sulfide has clearly been observed, it is believable that cyclopentene sulfide is also being consumed during the reaction. It is therefore desirable to independently determine the relative reactivity of cyclopentene sulfide with  $\text{CS}_2$  and  $\text{CO}_2$ .

Several attempts were made to synthesize cyclopentene sulfide according to recent literature reports through the reaction of cyclopentene oxide with thiourea,<sup>143</sup> potassium thiocyanate,<sup>143</sup> and ammonium thiocyanate<sup>144</sup> as sulfur sources, though none were successful. A 1951 report from van Tamelen states that thiocyanate is not effective

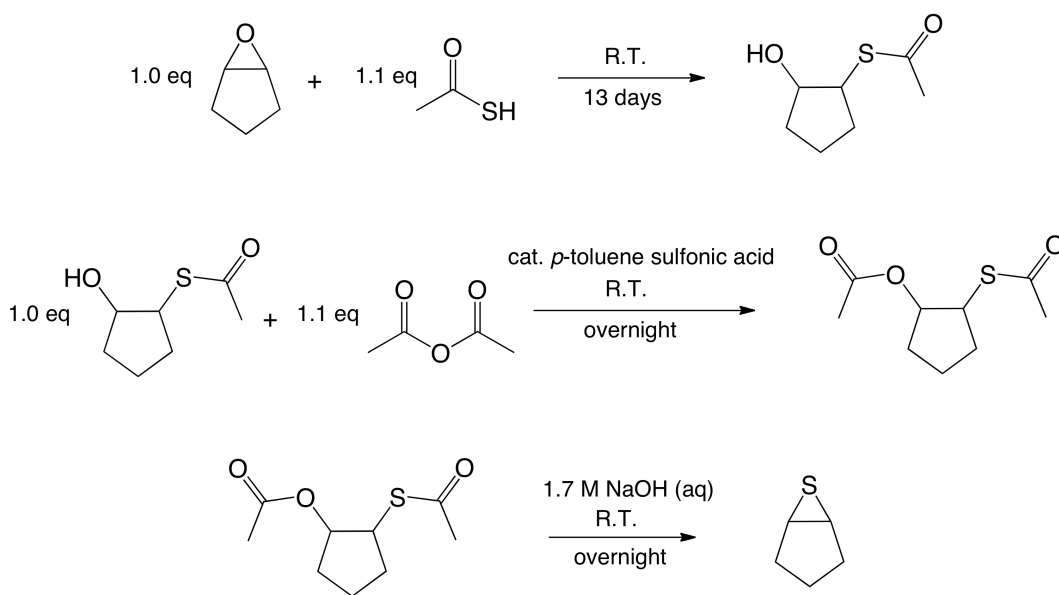
for the synthesis of cyclopentene sulfide, though identical conditions are quite effective at the synthesis of cyclohexene sulfide in a 73% yield from cyclohexene oxide (Scheme IV-4).<sup>145</sup> Indeed, the reaction between cyclopentene oxide and  $\text{SCN}^-$  does not proceed beyond the first equilibrium step, and cyclopentene oxide is the only recovered material. This is significant, as the  $\text{SCN}^-$  produced by the decomposition of  $\text{CS}_2\text{N}_3^-$  will therefore not directly react with cyclopentene oxide to form the episulfide.



**Scheme IV-4.** Thiocyanate,  $\text{SCN}^-$ , is able to convert cyclohexene oxide to cyclohexene sulfide with a 73% yield, though this same process is not effective for cyclopentene oxide to cyclopentene sulfide.<sup>145</sup>

An alternative, 15 day stepwise synthesis of cyclopentene sulfide by Harding and Owen<sup>132</sup> and Goodman, Benitez, and Baker<sup>133</sup> was instead followed (Scheme IV-5). The foul-smelling product was distilled over  $\text{CaH}_2$  under reduced pressure to yield pure cyclopentene sulfide as a clear, colorless liquid.

Several coupling studies of cyclopentene sulfide with  $\text{CS}_2$  were performed (Table IV-4). At 80 °C, the same temperature used for the coupling of cyclopentene oxide and  $\text{CS}_2$ , the reactivity of cyclopentene sulfide can be observed to be very poor, with only limited formation of *cis*-cyclopentene trithiocarbonate (Entries 1-3). A trace amount of the desulfurization product, cyclopentene, is also observed.<sup>146</sup> This desulfurization is



**Scheme IV-5.** Three step synthesis of cyclopentene sulfide.

undoubtedly the source of cyclopentene within the coupling reactions, as similar tests with cyclopentene oxide were unsuccessful. By increasing the temperature and reaction time to 110 °C and 24 h, respectively, ~20% conversion to *cis*-cyclopentene trithiocarbonate and ~40% conversion to cyclopentene is observed (Entries 4-5). Cyclopentene is the major product (36%) when only (salen)CrCl is employed, though 7% coupling products are observed (Entry 6). In the absence of both catalyst and cocatalyst, 4% desulfurization is observed with no noticeable coupling product (Entry 8). Similarly, cyclopentene sulfide remains relatively unreactive with CO<sub>2</sub> with both Cl<sup>-</sup> and N<sub>3</sub><sup>-</sup> cocatalysts (Table IV-5). It is thus apparent that cyclopentene sulfide formation is a thermodynamic sink within this reaction process. Cyclopentene sulfide is synthesized *in situ*, but it has limited further reactivity after it is generated. This lack of reactivity for the episulfide appears to be unique to the cyclopentyl derivative, as both cyclohexene

**Table IV-4.** Coupling reactions of cyclopentene sulfide with CS<sub>2</sub>.

Entry	Reaction Loading <sup>a</sup>	Cocat.	Temp, °C	t, h	cyclopentene sulfide, <sup>b</sup> %	<i>cis</i> -cyclopentene trithiocarbonate, <sup>b</sup> %	cyclopentene, <sup>b</sup> %
1	1:2:500:1000	PPNCl	80	6	98.8	0.9	0.3
2	1:2:500:1000	PPNN <sub>3</sub>	80	6	99.1	0.8	0.1
3 <sup>c</sup>	1:2:500:1000	<i>n</i> Bu <sub>4</sub> NN <sub>3</sub>	80	12	99.1	0.4	0.5
4 <sup>c</sup>	1:2:250:500	PPNCl	110	24	39	19	42
5 <sup>c</sup>	1:2:250:1000	PPNCl	110	24	39	21	39
6 <sup>c</sup>	1:0:250:1000	-	110	24	56	0.7 (6.3 <sup>d</sup> )	36
7 <sup>c</sup>	0:2:250:1000	PPNCl	110	24	86	8	6
8 <sup>c</sup>	0:0:250:500	PPNCl	110	24	96	-	4

All reactions performed in 10 mL stainless steel reactors. (a) Reaction loading refers to the relative equivalents of (salen)CrCl:cocatalyst:cyclopentene sulfide:CS<sub>2</sub> loaded into the reactor. (b) Relative product yield from crude <sup>1</sup>H NMR. (c) Toluene solvent employed; total volume of CS<sub>2</sub> + toluene = 1.0 mL. (d) Unidentified coupling products.

**Table IV-5.** Coupling reactions of cyclopentene sulfide with CO<sub>2</sub>.

Entry	Cocatalyst	cyclopentene sulfide, <sup>a</sup> %	cyclic, <sup>a,b</sup> %	cyclopentene, <sup>a</sup> %
1	PPNCl	98.1	1.3	0.6
2	<i>n</i> Bu <sub>4</sub> NN <sub>3</sub>	99.4	0.3	0.3

All reactions performed in 10 mL stainless steel reactors. 0.250 g cyclopentene sulfide (2.5 mmol, 250 eq), 1.0 mL toluene-*d*<sub>8</sub>, 6.3 mg (salen)CrCl (0.01 mmol, 1 eq), 2 equivalents of the appropriate cocatalyst, and 3.4 MPa CO<sub>2</sub> at 80 °C for 24 h. (a) Relative product yield from crude <sup>1</sup>H NMR. (b) Unidentified coupling products.

sulfide<sup>79</sup> and propylene sulfide<sup>75</sup> will effectively couple with CS<sub>2</sub> to yield poly(trithiocarbonate) and cyclic trithiocarbonate materials utilizing chromium catalysts.

**Cyclic [Thio]carbonates.** In the crude <sup>13</sup>C NMR of cyclic materials, three distinct compounds were consistently noted as the major cyclic products. Peaks at 234.7, 228.3, and 197.6 ppm (CDCl<sub>3</sub>) have been assigned to *trans*-cyclopentene trithiocarbonate, *cis*-cyclopentene trithiocarbonate, and *cis*-cyclopentene dithiocarbonate (-S-(C=O)-S- connectivity). Following purification by column chromatography, single crystals of *trans*-cyclopentene trithiocarbonate were grown and analyzed by X-ray

crystallography (Figure IV-5). The *trans*- assignment is consistent with a previous literature report.<sup>134</sup> Attempts were made to separate *cis*-cyclopentene trithiocarbonate and the -S-(C=O)-S- *cis*-cyclopentene dithiocarbonate by physical and chemical means, but these experiments were unsuccessful. When a limiting amount of CS<sub>2</sub> or added CO<sub>2</sub> was employed, *cis*-cyclopentene carbonate formation could also be clearly observed at 155.6 ppm.

Gas chromatography-mass spectrometry (GC-MS) proved a useful tool for the identification of the identities of the cyclic [thio]carbonate materials, as the GC was able

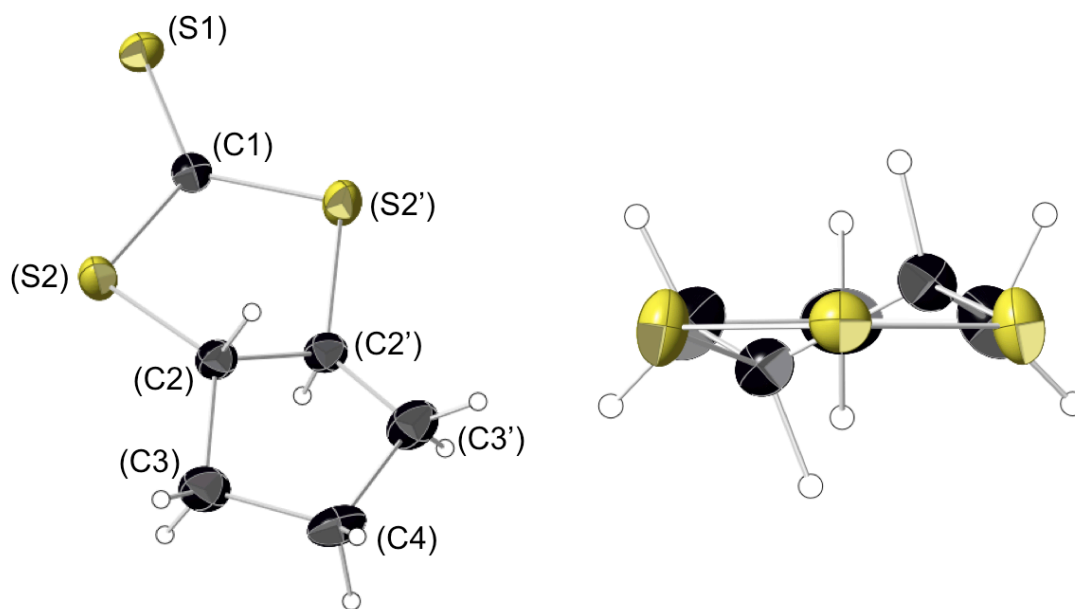


**Figure IV-5.** Thermal ellipsoid representation of *trans*-cyclopentene trithiocarbonate with ellipsoids at 50% probability surfaces. Inset image is looking down the S1-C4 plane to show torsion caused by the *trans*-configuration. S2-C2-C2'-S2' angle = 46.44°.

to separate out the various cyclic materials by their different elution times, and then mass spectrometry could be employed to identify the molecular weight of the cyclic materials. Additional information regarding the identity and spectral data of the various cyclic [thio]carbonate materials can be found in Appendix D. GC-MS analysis showed that eight of the possible twelve cyclic [thio]carbonates are produced from the coupling of CS<sub>2</sub> and cyclopentene oxide. *Cis*-cyclopentene oxide, both isomers of cyclopentene trithiocarbonate, and *cis*-cyclopentene dithiocarbonate (SOS connectivity) were each positively identified by matching traces from pure samples. Only one isomer of cyclopentene monothiocarbonate was observed. All four structural and geometric isomers of cyclopentene dithiocarbonate were observed, though only the *cis*-(-S-(C=O)-S-) connectivity was isolated. Without calibrating for the GC-MS response factor, relative concentrations of the individual cyclic carbonates were unable to be determined.

In order to better hypothesize the identity of each material, the relative enthalpies of each of the possible cyclopentene [thio]carbonate species were calculated. Slight (1-2 kcal/mol) energy differences can be observed between the *cis*-boat and *cis*-chair conformations of the cyclic systems (Figure IV-6). Generally, the *cis*- systems are lower in energy than their *trans*- counterparts. For cyclopentene carbonate, the difference is stark at ~20 kcal/mol (Figure IV-7).<sup>147</sup> This is understandable, given that only *cis*-cyclopentene carbonate has ever been isolated, and all attempts to make *trans*-cyclopentene carbonate have failed. The enthalpy difference is much smaller for

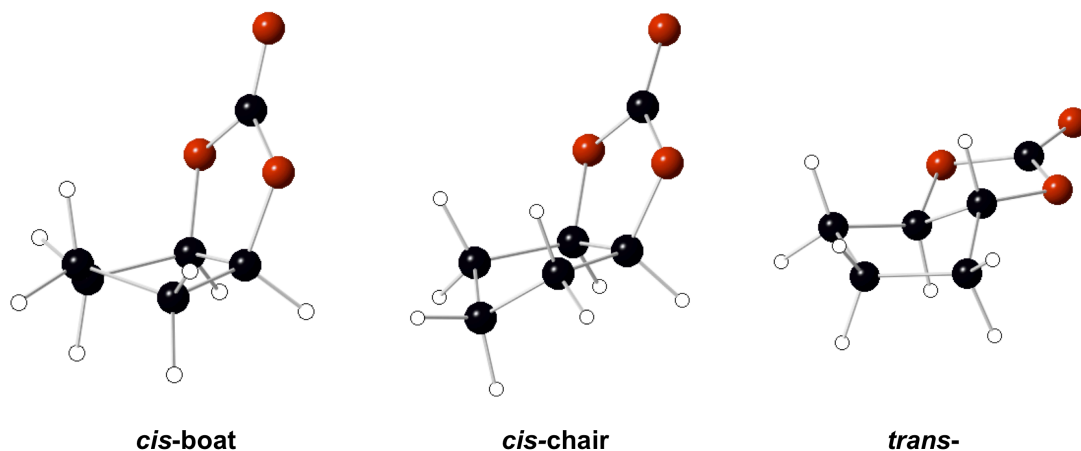


**Figure IV-6.** Calculated local minima for cyclopentene carbonate (OOO) species: *cis-boat*, *cis-chair*, and *trans-*.

cyclopentene trithiocarbonate, ~5 kcal/mol, as the larger sulfur atoms allow for a less-strain in the fused 5-membered rings (Figure IV-8). The mixed O/S species also show ~10 kcal/mol preference for the *cis-* isomers over *trans-* (Figures IV-9 and 10). Notably, there is also a large (10-25 kcal/mol) preference for the formation of the carbon-oxygen double bond over the carbon-sulfur double bond. C=O is known to be a stronger bond than C=S,<sup>148</sup> but this preference may also be due to the greater ability of the large sulfur atoms to relax the molecule and therefore reduce the strain caused by the fused 5-membered rings.

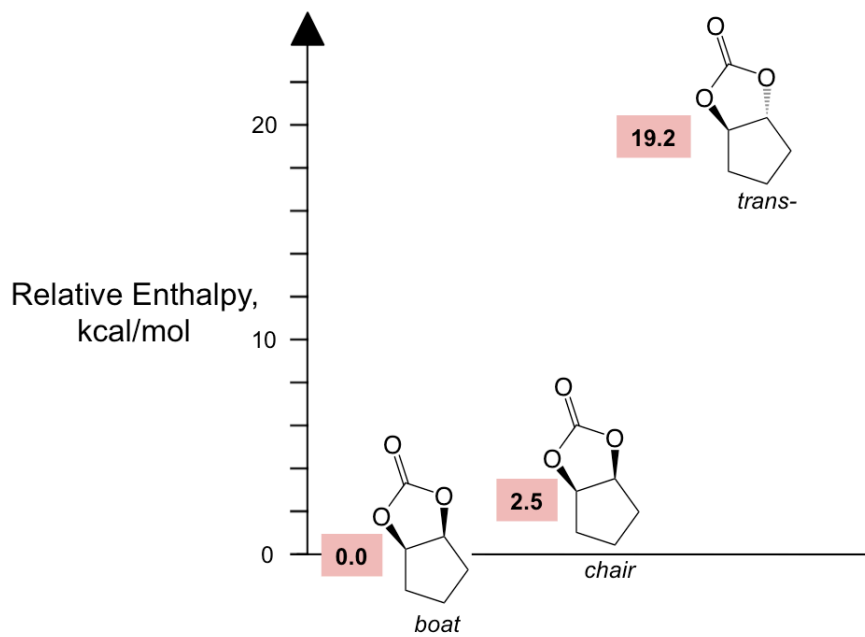


**Figure IV-7.** Calculated relative enthalpies for cyclopentene carbonate isomers in kcal/mol.<sup>147</sup>

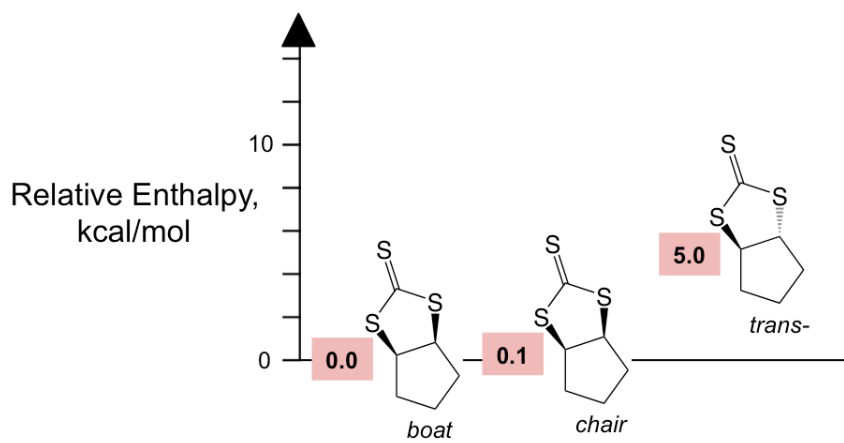


**Figure IV-8.** Calculated relative enthalpies for cyclopentene trithiocarbonate isomers in kcal/mol.<sup>147</sup>



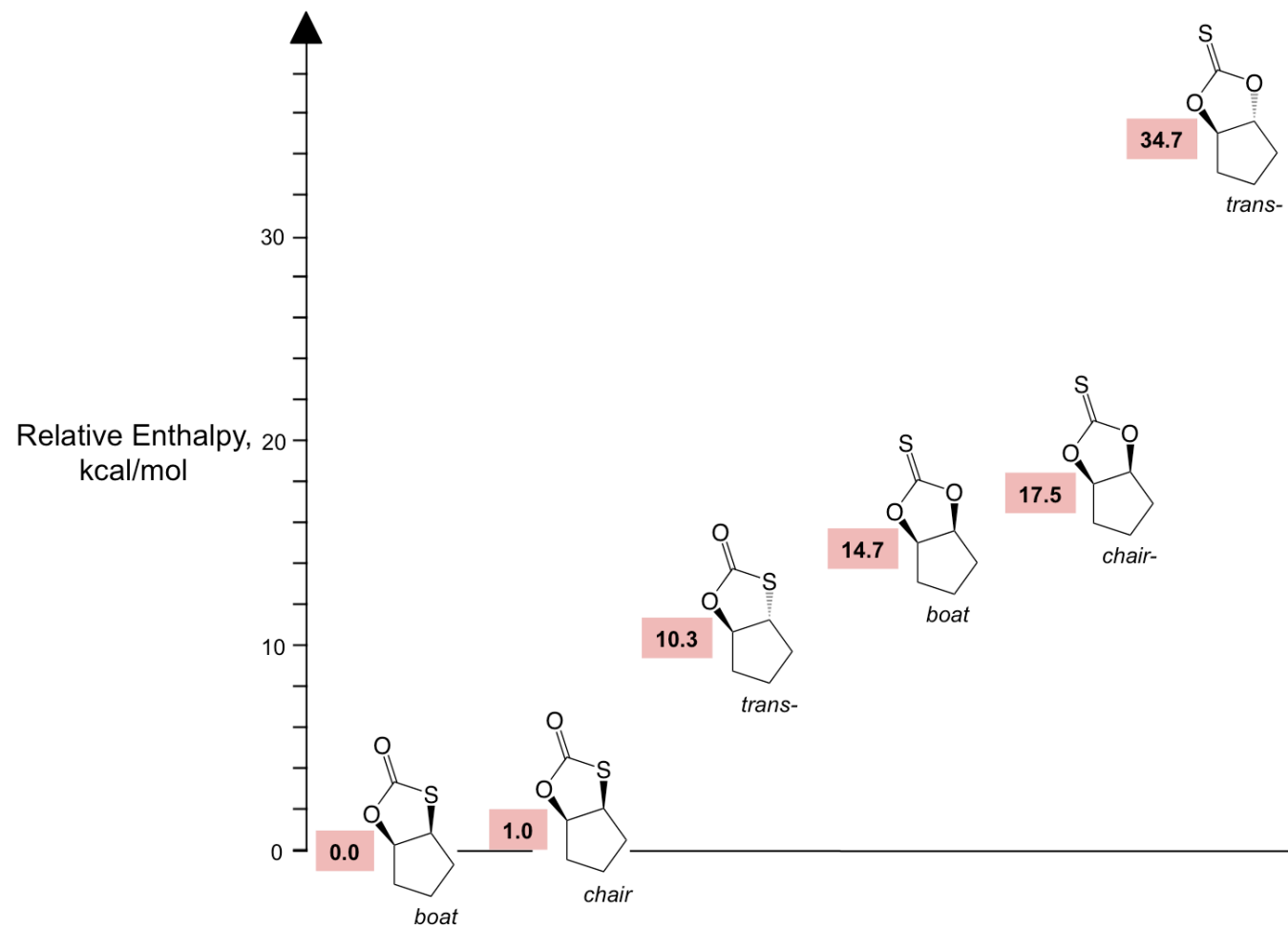


Figure IV-9. Calculated relative enthalpies for cyclopentene thiocarbonate isomers in kcal/mol.

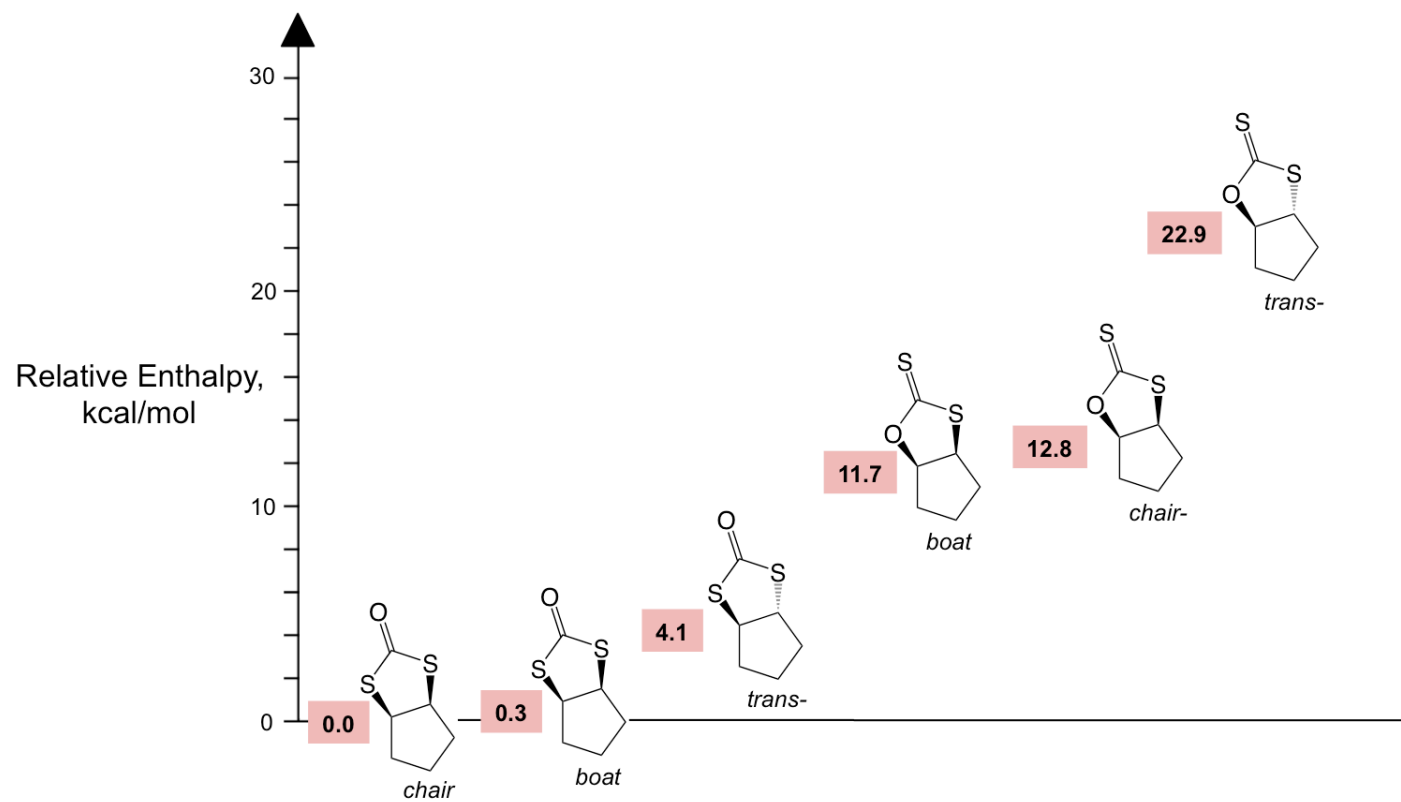


Figure IV-10. Calculated relative enthalpies for cyclopentene dithiocarbonate isomers in kcal/mol.

**Scrambling Mechanism.** Scrambling of the oxygen and sulfur atoms has been observed in both the polymer and cyclic [thio]carbonate samples. In the literature, several similar mechanisms involving the ring-opening of preformed cyclic carbonates have been proposed. In Endo's 2001 investigation of cyclic trithiocarbonate formation utilizing a titanium catalyst, scrambling was observed in the presence of excess CS<sub>2</sub>.<sup>77</sup> In our 2009 report, the Darensbourg group proposed that the insertion of CO<sub>2</sub>, COS, and CS<sub>2</sub> is reversible, and it is this reversibility that brings about the scrambling.<sup>79</sup> A similar mechanism has been proposed by North for the coupling of propylene oxide and CS<sub>2</sub> in which propylene sulfide is first eliminated and then reenters the mechanism as a new reagent.<sup>76</sup> Tetrahedral spiro intermediates have been proposed and isolated by Barbero et al. for propylene oxide/sulfide scrambling systems utilizing HBF<sub>4</sub>•Et<sub>2</sub>O,<sup>149</sup> but these were not directly observable by NMR or FT-IR in this investigation.

Several test reactions were run in order to determine the conditions necessary to induce scrambling for reactions involving cyclopentene oxide, (salen)CrCl, and an onium salt cocatalyst (Table IV-6). In three separate reactions, toluene solutions containing a mix of cyclic cyclopentene [thio]carbonates were heated to 80 °C with (salen)CrCl and *n*Bu<sub>4</sub>NCl in the presence of CO<sub>2</sub>, CS<sub>2</sub>, and a control with no other added reagents. After 48 hours, no scrambling was observed by <sup>1</sup>H NMR or GC-MS (Entries 1-3). Conversely, a solution of the same cyclic [thio]carbonates, catalyst, and cocatalyst heated to 80 °C in the presence of cyclopentene oxide displayed changes in composition, indicating scrambling had taken place (Entry 4). Further investigations revealed that the presence of (salen)CrCl catalyst was necessary to induce scrambling, though added

*n*Bu<sub>4</sub>NCl cocatalyst increased the activity (Table IV-7). Thus, the catalyst is required to activate and ring-open the epoxide, and the more nucleophilic alkoxide then attacks the [thio]carbonyl to induce scrambling (Figure IV-11). The trithiocarbonate species can be produced from the coupling of the ring-opened thiirane produced during the scrambling process and CS<sub>2</sub>. It is unlikely that cyclopentene sulfide will be separately ring-opened to undergo coupling. The possibility of spiro intermediates has not yet been ruled out at this time.

**Table IV-6.** Conditions needed for O/S scrambling utilizing a purified mix of cyclic [thio]carbonate materials utilizing (salen)CrCl and *n*Bu<sub>4</sub>NCl.

Entry	Added Reagent <sup>a</sup>	time, h	Scrambling Observed? <sup>b</sup>
1	none <sup>c</sup>	48	no
2	100 psi CO <sub>2</sub> <sup>c</sup>	48	no
3	1 eq CS <sub>2</sub> <sup>c</sup>	48	no
4	1 eq cyclopentene oxide <sup>d</sup>	16	yes

(a) Average MW of cyclic materials arbitrarily assigned to be 160 g/mol for calculations. Catalyst loading held at (salen)CrCl:*n*Bu<sub>4</sub>NCl:cyclic mix = 1:2:50. 80°C. (b) Scrambling observed by changes in the <sup>1</sup>H NMR and GC-MS traces of the starting material and reaction products. (c) 0.875 M solution in toluene. (d) 1.4 M solution.

**Table IV-7.** Conditions needed for O/S scrambling utilizing *trans*-cyclohexene trithiocarbonate and cyclohexene oxide.

Entry	Catalyst	Cocatalyst	Scrambling Observed? <sup>a</sup>
1	-	-	no
2	(salen)CrCl	-	yes, slight
3	-	<i>n</i> Bu <sub>4</sub> NCl	no
4	(salen)CrCl	<i>n</i> Bu <sub>4</sub> NCl	yes

(a) Analyzed by *in situ* ATR-FTIR spectroscopy, with scrambling being assigned by the growth of cyclohexene carbonate at 1809 cm<sup>-1</sup>.

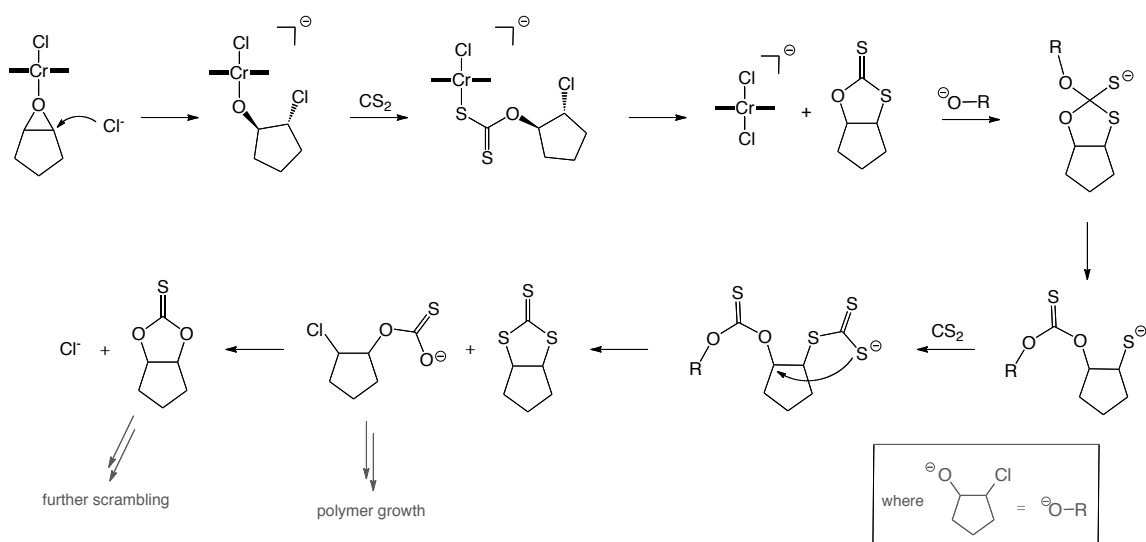


**Figure IV-11.** Proposed mechanism for scrambling in the coupling of cyclopentene oxide and  $\text{CS}_2$ .

**NMR Scrambling Studies.** In addition to being studied by ATR-FTIR, it was desirable to monitor the scrambling reactions by NMR. Figure IV-12 shows the time lapsed  $^{13}\text{C}$  NMRs for the reaction of four equivalents cyclopentene oxide with one equivalent *trans*-cyclopentene trithiocarbonate utilizing (salen)CrCl and  $n\text{Bu}_4\text{NCl}$  at  $80^\circ\text{C}$  in toluene- $d_8$ . After 15 hours, the growth of cyclopentene sulfide is clearly visible with peaks at 41.1, 29.0, and 18.3 ppm. Growth of *cis*-cyclopentene carbonate can also be clearly observed by 22.5 hours. After 48 hours, faint traces of cyclopentene can be observed at 130.7 ppm. Notably, cyclopentene oxide's signal at 56.3 ppm broadens during the course of the reaction, likely because the epoxide is undergoing reversible ring-opening and ring-closing processes. Other coupling products are visible but have not been identified. Continued experiments to identify these compounds are underway in our lab.

For completeness, the reaction of cyclopentene sulfide with *cis*-cyclopentene carbonate at 80 °C was also monitored by  $^{13}\text{C}$  NMR (Figure IV-13). The desulfurization product cyclopentene (32.7, 23.2 ppm) is the only observable product after 48 hours reaction time, indicating that either the catalyst is incapable of ring-opening the episulfide or that the thiolate is not a strong enough nucleophile to attack the carbonate. A proposed mechanism for these observed epoxide/cyclic scramblings can be seen in Figure IV-14.

**Mixed Species Scrambling.** O/S scrambling is not limited to epoxides and episulfides of the same backbone connectivity. Indeed, when *trans*-cyclohexene trithiocarbonate was reacted with cyclopentene oxide, (salen)CrCl, and *n*Bu<sub>4</sub>NCl at 80 °C, six cyclic [thio]carbonate materials were observed by  $^{13}\text{C}$  NMR and GC-MS including *cis*-cyclopentene carbonate and residual *trans*-cyclohexene trithiocarbonate. Mixed species cyclopentene thiocarbonate (SO<sub>2</sub>), cyclohexene thiocarbonate (SO<sub>2</sub>), and cyclohexene dithiocarbonate (S<sub>2</sub>O) were observed, though their exact connectivity cannot be commented on. Cyclohexene sulfide was also clearly produced during the course of the reaction. The reaction mixture was concentrated *in vacuo* prior to GC-MS and NMR analysis, so it is unclear whether cyclopentene sulfide was also generated. However, production of this thermodynamic sink is likely to have occurred.

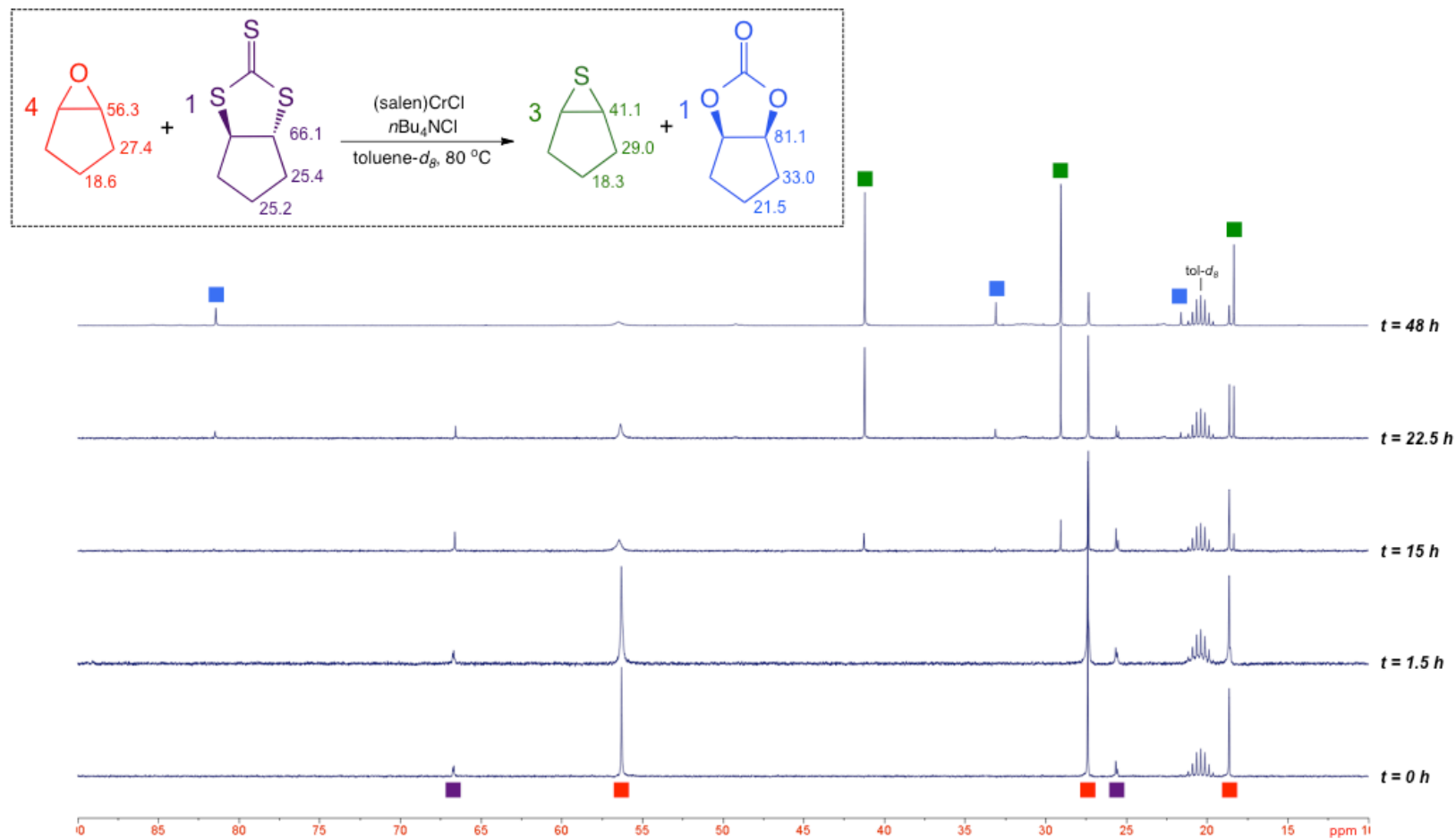


**Figure IV-12.** Time lapsed  $^{13}\text{C}$  NMR of the reaction between cyclopentene oxide (red) and *trans*-cyclopentene trithiocarbonate (purple) to produce cyclopentene sulfide (green) and *cis*-cyclopentene carbonate (blue) in toluene- $d_8$ . Broadening of cyclopentene oxide's carbon at 56.3 ppm is likely due to ring-opening and ring-closing of the epoxide.

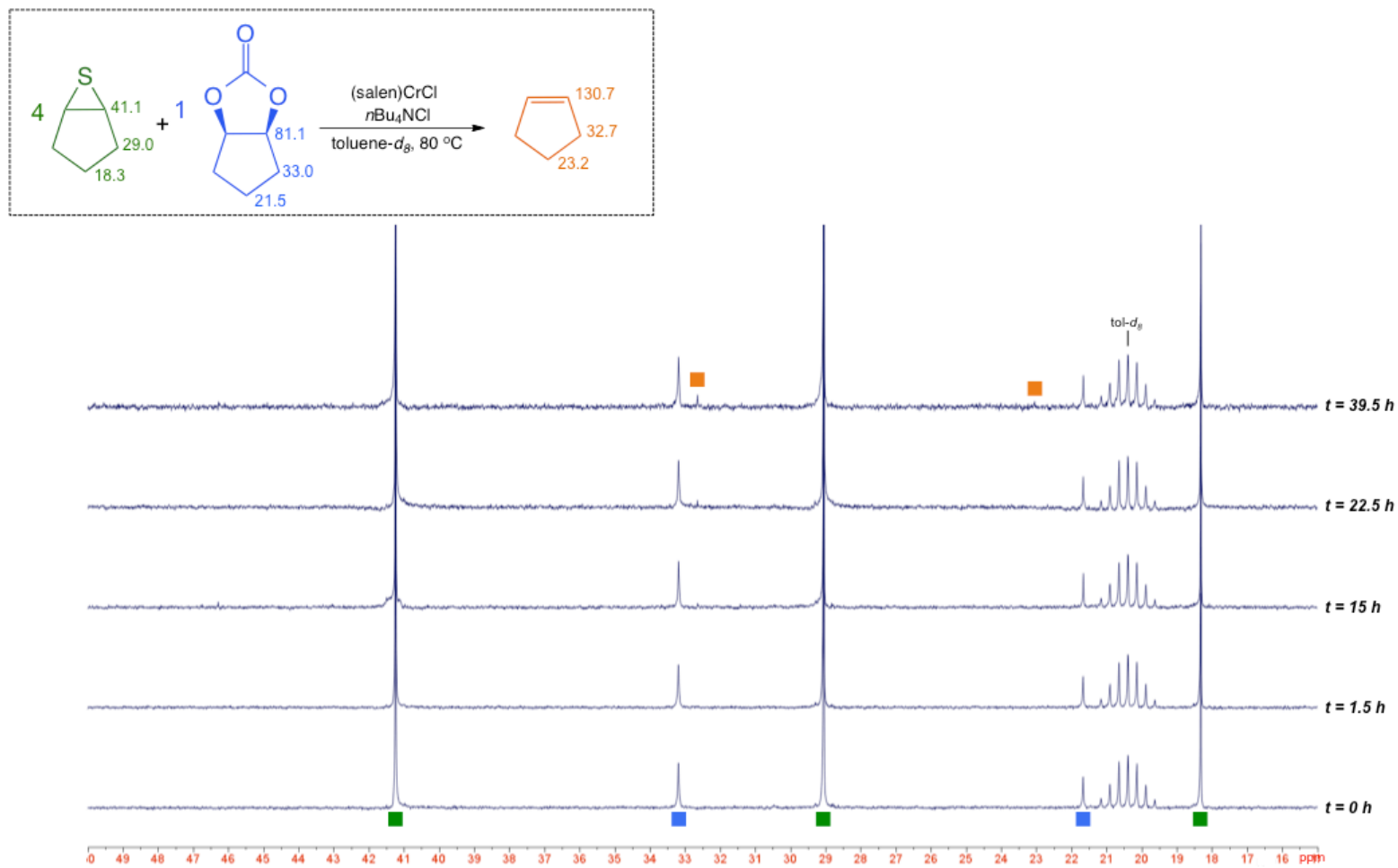


**Figure IV-13.** Time lapsed  $^{13}\text{C}$  NMR of the reaction between cyclopentene sulfide (green) and *cis*-cyclopentene carbonate (blue) in toluene- $d_8$ . Cyclopentene (orange) is the first observable product.



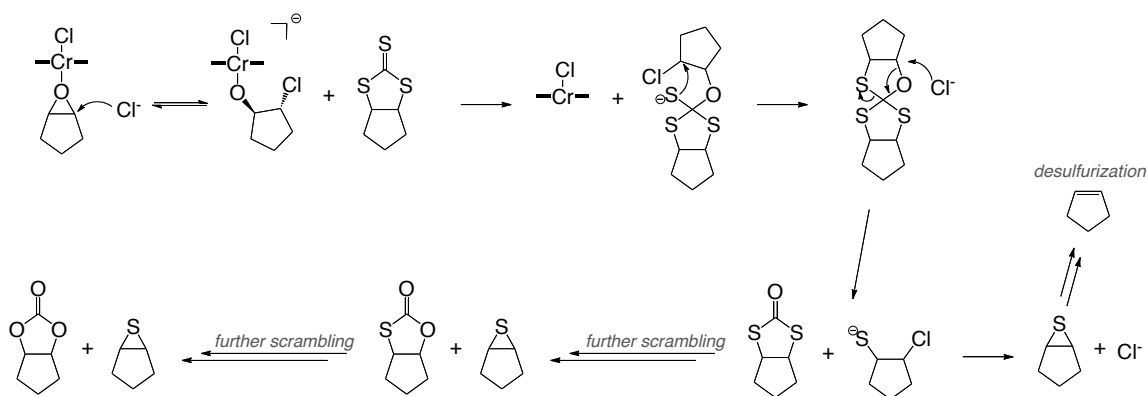


**Figure IV-14.** Proposed mechanism for observed scrambling between cyclopentene oxide and *trans*-cyclopentene trithiocarbonate.

## Conclusions

The catalytic coupling of cyclopentene oxide with carbon disulfide has been examined utilizing (salen)CrCl and onium salt cocatalysts. Scrambling of the oxygen and sulfur atoms is observable in both the polymer and cyclic carbonate products. When PPNN<sub>3</sub> is employed as cocatalyst, the temperature-sensitive five membered heterocyclic anion  $\text{CS}_2\text{N}_3^-$  is formed. It is unclear at this time whether this pseudohalogen is able to initiate the coupling reaction before decomposing to thiocyanate,  $\text{SCN}^-$ . Under certain conditions, cyclopentene sulfide is actually produced during the coupling of cyclopentene oxide and  $\text{CS}_2$ , and it is thus regarded as a thermodynamic sink for this process. The coupling of cyclopentene sulfide and both  $\text{CO}_2$  and  $\text{CS}_2$  was examined, but it was determined that cyclopentene sulfide is highly unreactive under the conditions studied in this report. Cyclopentene production can be observed from the desulfurization of cyclopentene sulfide.

The  $T_g$  of the polymers is highly dependent on the [thio]carbonate content of the polymer backbone. When a large percentage of [thio]ether is observed, the  $T_g$  drops significantly. [Thio]ether content is believed to increase with increasing reaction time, as backbiting reactions lead to the loss of  $CS_2$ ,  $COS$ , and  $CO_2$ . The largest amount of [thio]carbonate copolymer is produced utilizing (salen)CrCl and PPnCl at 80 °C for 6 hours. The major repeating units of the polymer backbone are dithiocarbonate -S-(C=S)-S- and monothiocarbonate -S-(C=O)-O-.

A wide range of cyclic [thio]carbonate materials are produced, and they have been identified utilizing NMR and GC-MS. Single crystals capable of X-ray diffraction were grown of *trans*-cyclopentene trithiocarbonate, and the S-C-C-S carbonate dihedral angle displays 46.44° of torsion. Computational analysis of the cyclic [thio]carbonates determined that, in general, the *cis*-isomers are more stable than their *trans*- counterparts by > 5 kcal/mol, and there is a 10-25 kcal/mol preference for the formation of a C=O double bond rather than C=S.

Investigations into the mechanism of O/S scrambling were also performed. It was determined that scrambling requires the presence of excess epoxide and catalyst. Added cocatalyst will greatly increase the rate of the reaction, but it is not a requirement. Two mechanisms have been proposed for the observed scrambling processes, though the exact process remains poorly understood.

## Future Work

It is known in the literature that spiroorthocarbonates<sup>150</sup> and spiroorthothiocarbonates<sup>151</sup> can be polymerized to yield polycarbonates and polythiocarbonates, respectively. As previously discussed, Barbero and coworkers were able to isolate cyclic spiro[thio]carbonate intermediates in their own propylene sulfide/propylene carbonate scrambling processes.<sup>149</sup> If similar spiro[thio]carbonate materials are involved in this study's scrambling process, it is reasonable to think that they may be undergoing polymerization in addition to the direct enchainment from cyclopentene oxide and CS<sub>2</sub>. Further experiments looking into the details of this mechanistic process is warranted. Primarily, a full kinetic analysis of the scrambling from trithiocarbonate/epoxide to carbonate/episulfide may give clues as to the mechanistic pathway(s) at work. The influence of temperature on the coupling process should also be examined.

The observed scrambling processes in the coupling of epoxides and CS<sub>2</sub> also pose an interesting question: is scrambling also occurring in the all-oxygen process? That is, in coupling reactions of CO<sub>2</sub> and epoxides, do the oxygen atoms from the reactants scramble (Figure IV-15)? While the discovery of such a scrambling process would provide only a minor mechanistic detail, it would still be interesting from a fundamental academic standpoint. C<sup>18</sup>O<sub>2</sub> could provide a valuable trace for <sup>13</sup>C NMR, FT-IR, or mass spectral assignments of scrambling.

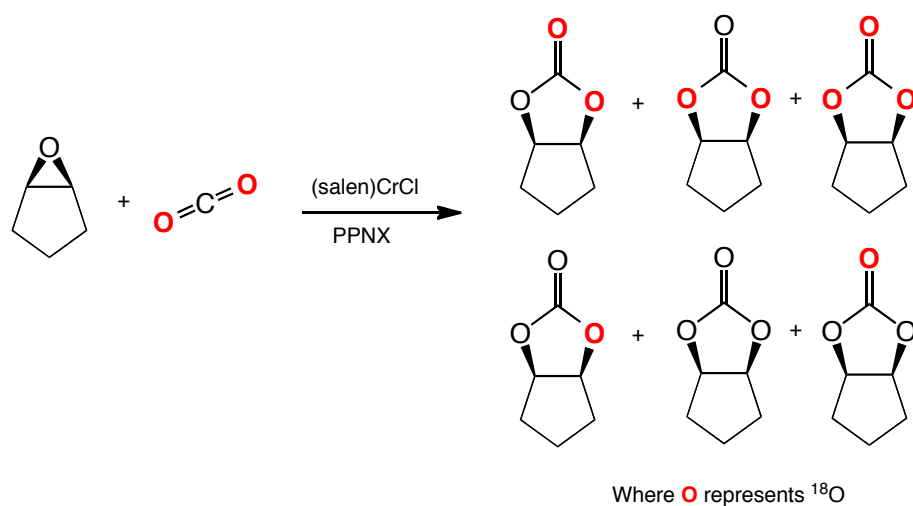
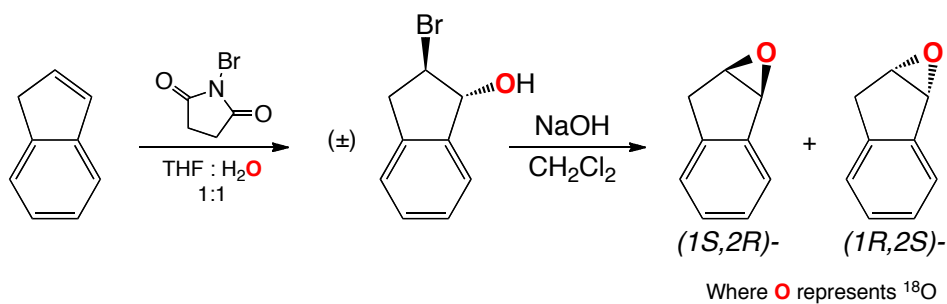


**Figure IV-16.** Proposed scrambling occurring in the coupling of  $\text{CO}_2$  and cyclopentene oxide.

Due to the high cost and limited availability of  $\text{C}^{18}\text{O}_2$ , it may be more advantageous to use epoxides labeled with  $^{18}\text{O}$ . The ring-closing of labeled halohydrins as described for the synthesis of indene oxide (Chapter II) may provide a viable route to the synthesis of these compounds. The use of a 1:1 mixture of dry THF to the relatively cheap  $\text{H}_2^{18}\text{O}$  along with *N*-bromosuccinimide should provide the labeled halohydrin, and ring-closing with base should produce the desired  $^{18}\text{O}$ -labeled epoxide (Scheme IV-6). Though indene oxide is shown, this should be possible for the general case.



**Scheme IV-6.** Proposed synthesis of  $^{18}\text{O}$ -labeled indene oxide.

It is also possible that the reactions described in this chapter are unique to the cyclopentene oxide system, as several recent papers have been able to display the unique reactivity of this alicyclic monomer (see also Chapter III). For example, it has recently been discovered that, in the presence of (salen)CrCl and  $n\text{Bu}_4\text{NN}_3$ , *cis*-cyclopentene carbonate will decarboxylate to yield small amounts of cyclopentene oxide at 110 °C.<sup>152</sup> Furthermore, cyclopentene sulfide's lack of reactivity toward  $\text{CS}_2$  and  $\text{CO}_2$  is not shared by cyclohexene sulfide<sup>79</sup> or propylene sulfide.<sup>75</sup> This stark difference in reactivity could greatly influence the products produced in these coupling reactions.

## CHAPTER V

### SUMMARY AND CONCLUSIONS

Since Inoue's remarkable discovery in 1969, the study of the catalytic coupling of oxiranes with CO<sub>2</sub> has been steadily growing as a viable alternative to traditional diol/phosgene polycondensations for the production of polycarbonates. Indeed, several companies including Empower Materials, Novomer, and SK Energy now have commercial processes for the production of poly(propylene carbonate), poly(ethylene carbonate), poly(cyclohexene carbonate), and copolymers of those materials. Despite the many advances made in this field, there has not been a great deal of work exploring the reactivity of epoxides other than cyclohexene oxide and propylene oxide. In this dissertation, the catalytic coupling of CO<sub>2</sub> and CS<sub>2</sub> with a variety of previously un- or underexplored epoxides has been discussed.

In Chapter II, the novel copolymerization of indene oxide with CO<sub>2</sub> to produce poly(indene carbonate) was discussed. Indene oxide was synthesized in a stepwise process from indene, a readily available starting material used commercially for the production of indene-coumarone resins found in paints and rubber. With the use of (salen)Co-2,4-dinitrophenoxide, (salen)CoY, and PPN-2,4-dinitrophenoxide, PPNY, in dichloromethane solvent, poly(indene carbonate) samples were produced with ~60% selectivity over *cis*-indene carbonate at 0 °C. Molecular weights of up to 7000 g/mol were achieved with corresponding glass transition temperatures of up to 134 °C. The use of both cobalt as the metal center and 2,4-dinitrophenoxide as the anionic initiator is

believed to be necessary in order to avoid buildup of cyclic carbonate materials, as  $n\text{Bu}_4\text{NBr}$  with the good bromide leaving group yielded only cyclic carbonate materials under similar conditions.

Despite these achievements, the (salen)CoY/PPNY system was plagued with poor reactivity and constrained to use at 0 °C. The bifunctional salen cobalt systems **2** and **3** popularized by the Xiao-Bing Lu group proved to be highly effective for this particular copolymerization process. These catalysts achieved molecular weights of up to 9700 g/mol and >99% selectivity for polymer. The activity of the bifunctional catalysts was greatly increased over that of the (salen)CoY/PPNY system, with TOF increasing from  $\sim 2 \text{ h}^{-1}$  to  $\sim 4.5 \text{ h}^{-1}$  under similar conditions. Switching cosolvents from dichloromethane to toluene also saw a large jump in activity for catalyst **3** bearing a quarternary  $-\text{NCy}_2\text{Me}^+$  group, reaching TOF of  $9 \text{ h}^{-1}$ . Catalyst **3** could also function at room temperature while still producing poly(indene carbonate) with >99% selectivity.

In addition to the expected long-chain polymeric product, a separate byproduct denoted **X** was also observed in all of the produced polymer samples. It was determined that **X** did not have a major impact on polymer molecular weight,  $T_g$ , or  $T_d$ . The identity of this species is still unknown, though experiments are underway in order to determine its exact structure. At present, we believe it to be an oligomeric, perhaps cyclic, indene carbonate sample.

Cyclic carbonates and the pathways of their production were discussed in Chapter III. Crystal structures of various cyclic carbonates were found utilizing the Cambridge Crystallographic Database, and their parameters were analyzed to determine

if any trends existed. Particular attention was paid to the O-C-C-O carbonate dihedral angle, as previous reports had suggested that there was a correlation between this angle and polymer/cyclic carbonate selectivity. The small angles of *cis*-cyclopentene carbonate and 1,4-dihydronaphthalene carbonate (0.347 and 2.005°, respectively) and the large angle observed for *trans*-cyclohexene carbonate (~27°) seem to support this hypothesis. However, the nearly 30° range observed for propylene carbonates found crystallized within the structures of other systems seems to discredit this notion. Any correlation appears minimal at best.

The differences in activity between cyclohexene oxide, which prefers to make poly(cyclohexene carbonate), and cyclopentene oxide, which prefers to make *cis*-cyclopentene carbonate, were highlighted. Kinetic activation barriers were determined for the direct coupling of cyclopentene oxide, indene oxide, butylene oxide, and styrene oxide with CO<sub>2</sub> to yield their corresponding cyclic carbonates utilizing (salen)CrCl and *n*Bu<sub>4</sub>NCl. The reactions were monitored utilizing *in situ* ATR-FTIR by the growth of the cyclic carbonate peak near 1810 cm<sup>-1</sup>. No polymer formation was observed in any of the cases at 1750 cm<sup>-1</sup>. This was also confirmed by <sup>1</sup>H NMR. Observed rate constants were determined at a range of temperatures, and activation barriers were determined. The E<sub>A</sub>'s increased in the order of 1,2-butylene carbonate (64.8 kJ/mol) < *cis*-cyclopentene carbonate (72.9 kJ/mol) < styrene carbonate (91.2 kJ/mol) < *cis*-indene carbonate (114.4 kJ/mol). No clear trend was observed that corresponds to this order. The solid state structures of *cis*-cyclopentene carbonate, styrene carbonate, and *cis*-indene carbonate were each obtained by X-ray crystallography.



An attempt was made to clearly define the activation parameters for each of the six different cyclic carbonate production pathways for the styrene oxide/CO<sub>2</sub> system in conjunction with the work of my labmate, Dr. Sheng-Hsuan Wei. Previous studies in the literature have not distinguished which pathway(s) are the most likely under polymerization conditions, instead saying that cyclic carbonates came from polycarbonate or “carbonate initiators.” Dr. Wei was able to calculate the barriers for metal-assisted alkoxide polycarbonate backbiting (141.2 kJ/mol), azide-assisted alkoxide polycarbonate backbiting (46.7 kJ/mol), and azide-assisted carbonate polycarbonate backbiting (89.2 kJ/mol). The halohydrin 2-chloro-1-phenylethanol was synthesized, and the DBU-initiated backbiting of this compound under CO<sub>2</sub> was monitored utilizing *in situ* ATR-FTIR. Experimental difficulties including CO<sub>2</sub> pressure-dependence and temperature control prevented the determination of the activation barrier for this process, though it is believed to be much lower than 90 kJ/mol. This study does however demonstrate that anionic initiators should be poor leaving groups in order to stop the direct coupling of CO<sub>2</sub> and epoxides to make polycarbonates. Carbonate backbiting requires a larger energy input than alkoxide backbiting, and the catalyst’s metal center is able to stabilize the anionic polymer chain and hinder backbiting to cyclic carbonate.

In Chapter IV, the catalytic coupling of cyclopentene oxide with CS<sub>2</sub> to yield poly[thio]carbonates and cyclic [thio]carbonates was discussed. O/S scrambling was observed in each of the examined experiments. When PPNN<sub>3</sub> was employed as cocatalyst, the heterocyclic CS<sub>2</sub>N<sub>3</sub><sup>-</sup> was formed. Thermal decomposition of this pseudohalogen to SCN<sup>-</sup> was observable by ATR-FTIR. The polymers produced from

these day-long reactions showed a wide range of  $T_g$ 's (-17.6 - 32.3 °C) that were highly dependent on the relative amounts of [thio]ether linkages in the polymer backbone. Those systems with higher poly[thio]carbonate linkages also displayed higher  $T_g$ 's.

When the cocatalyst was switched to PPnCl, the reaction time was also lowered to 6 hours in order to maximize the growth of the polymer peak at 1712  $\text{cm}^{-1}$ . After this time, this peak steadily drops off, presumably because of decomposition or backbiting reactions. Early thermal analysis of these polymers indicate that they are semicrystalline in nature, though this increase in crystallinity is not believed to be due to the cocatalyst, as a similar drop in the peak at 1712  $\text{cm}^{-1}$  can be observed after four hours in similar reactions with PPnN<sub>3</sub>. These polymers have limited [thio]ether content.

Separately, cyclopentene sulfide was isolated, and it was found to be highly unreactive toward both CS<sub>2</sub> and CO<sub>2</sub> under the examined conditions. In addition to small amounts of coupling to form cyclic materials, the desulfurization product cyclopentene was also observed. Indeed, cyclopentene sulfide and cyclopentene could be observed in the crude NMRs of each CS<sub>2</sub>/cyclopentene oxide coupling reaction, though the low boiling nature of cyclopentene sulfide meant that it was removed during the reaction workup.

Eight of the possible twelve different cyclopentene [thio]carbonates were produced during the coupling reactions, as identified by GC-MS. The solid-state structure of *trans*-cyclopentene trithiocarbonate was obtained. Computational analysis of the cyclic materials revealed that the *cis*- isomers were typically lower in energy than their *trans*- counterparts (5-20 kcal/mol, relative enthalpies). When a choice can be

made, there is also a 10-20 kcal/mol preference to form the C=O rather than the C=S double bond. Enthalpic differences are generally smaller when sulfur atoms are found at the bridgehead carbons, as their larger size allows for relaxation of the strained fused 5-membered rings.

The mechanism of the coupling and scrambling reactions were studied in depth. It was determined that excess epoxide and catalyst are both required to induce scrambling between cyclic carbonate mixtures. Added onium salt cocatalyst will greatly increase the rate of the scrambling reaction. Scrambling is not limited to epoxides and cyclic carbonates with the same side chains, as *trans*-cyclohexene trithiocarbonate and cyclopentene oxide were scrambled to form a mixture of cyclic cyclohexene and cyclopentene [thio]carbonates, cyclohexene sulfide, and presumably cyclopentene sulfide as well. It has been hypothesized that similar scrambling may be taking place in the all-oxygen system from CO<sub>2</sub>/epoxides coupling.

Though the individual projects discussed in this thesis varied greatly, they all serve the same purpose of expanding the utility of the transition metal-catalyzed coupling of oxiranes with CO<sub>2</sub> and CS<sub>2</sub>. Though the field is generally limited to the production of poly(propylene carbonate) and poly(cyclohexene carbonate), it is important to continue to push the barrier and explore new monomers in order to fully explore the utility of this process. Global concerns about carbon emissions, particularly CO<sub>2</sub>, from man-made processes are steadily increasing, and the increasing CO<sub>2</sub> levels are unlikely to change anytime soon. The coupling of CO<sub>2</sub> and epoxides to yield polycarbonates serves as a fantastic way to give value to a waste material and to produce

value-added polymeric materials in the process (Figure IV-1). The catalytic coupling of  $\text{CS}_2$  and epoxides can also provide interesting sulfur-containing polymers with complicated mechanisms that certainly warrant further study. I hope that my small contributions to this field help to spawn new discoveries and to guide the next group of researchers in their scientific pursuits.

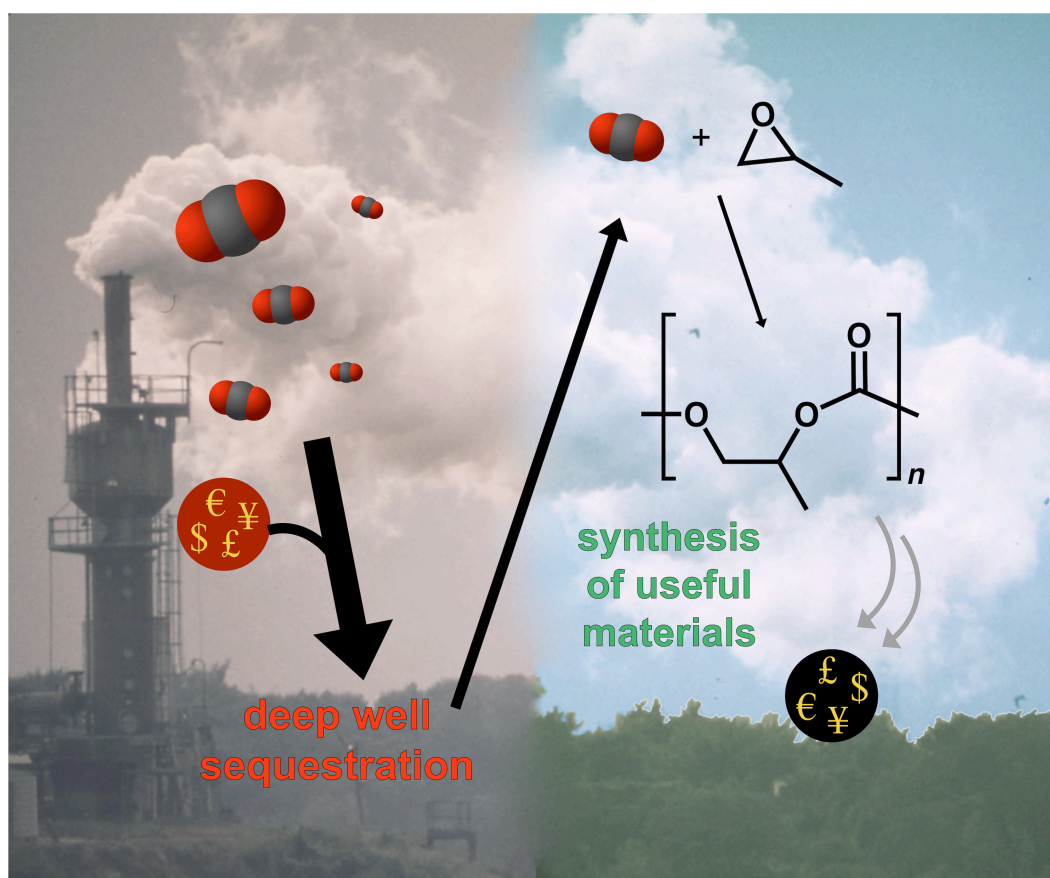


**Figure V-1.** Idealized representation for atmospheric  $\text{CO}_2$  sequestration and use as a starting material for the production of value-added polycarbonates.

## REFERENCES

1. Stevens, M. P., *Polymer Chemistry: An Introduction*. 3rd ed.; Oxford University Press: New York, New York, 1999.
2. Odian, G., *Principles of Polymerization*. 4th ed.; John Wiley & Sons, Inc.: Hoboken, New Jersey, 2004.
3. IHS Chemical 2012 World Polycarbonate and ABS Analysis. [www.press.ihs.com/press-release/commodities-pricing-cost/after-major-downturn-global-demand-polycarbonate-growing-again](http://www.press.ihs.com/press-release/commodities-pricing-cost/after-major-downturn-global-demand-polycarbonate-growing-again) (accessed 3.19.2013).
4. Phosgene MSDS from sigmaldrich.com. Last updated 10.29.2012. Accessed 3.19.2013.
5. vom Saal Fs, M. J. *JAMA* **2008**, *300*, 1353-1355.
6. Fukuoka, S.; Tojo, M.; Hachiya, H.; Aminaka, M.; Hasegawa, K. *Polym. J.* **2007**, *39*, 91.
7. Fan, G.; Zhao, H.; Duan, Z.; Fang, T.; Wan, M.; He, L. *Catal. Sci. Technol.* **2011**, *1*, 1138-1141.
8. Aresta, M., Carbon Dioxide Utilization: Greening Both the Energy and Chemical Industry: An Overview. In *Utilization of Greenhouse Gases*, American Chemical Society: 2003; Vol. 852, pp 2-39.
9. Sakakura, T.; Choi, J.-C.; Yasuda, H. *Chem. Rev.* **2007**, *107*, 2365-2387.
10. Pagani, G. 5573734, 1996.
11. Carbon Recycling International. <http://www.carbonrecycling.is/> (accessed 3.25.2013).
12. Lindsey, A. S.; Jeskey, H. *Chem. Rev.* **1957**, *57*, 583-620.
13. Inoue, S.; Koinuma, H.; Tsuruta, T. *Makromol. Chem.* **1969**, *130*, 210.
14. Inoue, S.; Koinuma, H.; Tsuruta, T. *J. Polym. Sci., Part B* **1969**, *7*, 287.
15. Empower Materials: Home. [www.empowermaterials.com](http://www.empowermaterials.com) (accessed 3.25.2013).
16. Novomer: Coating Resins. [www.novomer.com/?action=CO2\\_coatings](http://www.novomer.com/?action=CO2_coatings) (accessed 3.25.2013).

17. Zhong, X.; Dehghani, F. *Green Chem.* **2012**, *14*, 2523-2533.
18. Novomer: Carbon Dioxide, [www.novomer.com/?action=CO2](http://www.novomer.com/?action=CO2) (accessed 3.25.2013).
19. Ok, M.-A.; Jeon, M. In *Properties of poly(propylene carbonate) produced via SK Energy's Greenpol™ Technology*, ANTEC, 2011.
20. Lee, B. Y.; Cyriac, A. *Nat. Chem.* **2011**, *3*, 505-507.
21. Aschenbrenner, N.; Kunze, K. Green Polymer Made of CO<sub>2</sub> from Exhaust Gases. [www.siemens.com/innovation/en/news/2012/e\\_inno\\_1213\\_2.htm](http://www.siemens.com/innovation/en/news/2012/e_inno_1213_2.htm) (accessed 6.5.2012).
22. Seong, J. E.; Na, S. J.; Cyriac, A.; Kim, B. W.; Lee, B. Y. *Macromolecules* **2010**, *43*, 903.
23. (a) Nakano, K.; Kamada, T.; Nozaki, K. *Angew. Chem., Int. Ed.* **2006**, *45*, 7274; (b) Okada, A.; Kikuchi, S.; Yamada, T. *Chem. Lett.* **2011**, *40*, 209-211.
24. Zhang, H.; Grinstaff, M. W. *J. Am. Chem. Soc.* **2013**, *135*, 6806-6809.
25. Geschwind, J.; Frey, H. *Macromolecules* **2013**, *46*, 3280-3287.
26. Darensbourg, D. J.; Rodgers, J. L.; Fang, C. C. *Inorg. Chem.* **2003**, *42*, 4498.
27. Kim, J. G.; Cowman, C. D.; LaPointe, A. M.; Wiesner, U.; Coates, G. W. *Macromolecules* **2011**, *44*, 1110.
28. (a) Cannarsa, M. J.; Sun, H.-N.; Kesling, H. S. J. EP0321207A1, 6.21.1989; (b) Cheng, M.; Darling, N. A.; Lobkovsky, E. B.; Coates, G. W. *Chem. Commun.* **2000**, 2007-2008; (c) Nozaki, K.; Nakano, K.; Hiyama, T. *J. Am. Chem. Soc.* **1999**, *121*, 11008-11009; (d) Kim, I.; Yi, M. J.; Lee, K. J.; Park, D.-W.; Kim, B. U.; Ha, C.-S. *Catal. Today* **2006**, *111*, 292-296.
29. (a) Lu, X.-B.; Wu, G.-P. unpublished observations. (b) Darensbourg, D.J.; Chung, W.-C. unpublished observations.
30. Byrne, C. M.; Allen, S. D.; Lobkovsky, E. B.; Coates, G. W. *J. Am. Chem. Soc.* **2004**, *126*, 11404-11405.
31. Wu, G.-P.; Ren, W.-M.; Luo, Y.; Li, B.; Zhang, W.-Z.; Lu, X.-B. *J. Am. Chem. Soc.* **2012**, *134*, 5682-5688.
32. (a) Allen, S. D.; Byrne, C. M.; Coates, G. W.; Bozell, J.; Patel, M., *Feedstocks for the Future: Renewables for the Production of Chemicals and Materials*.

- 2006; Vol. 921, p 116; (b) Lee, Y. B.; Shin, E. J.; Yoo, J. Y. *J. Korean Int. Eng. Chem.* **2008**, *19*, 133; (c) Zou, Z. Q.; Ji, W. D.; Luo, J. X.; Zhang, M.; Chen, L. B. *Polym. Mater. Sci. Eng.* **2010**, *26*, 1.
33. (a) Wu, G. P.; Wei, S. H.; Ren, W. M.; Lu, X. B.; Li, B.; Zu, Y. P.; Darensbourg, D. J. *Energy Environ. Sci.* **2011**, *4*, 5084; (b) Wu, G. P.; Wei, S. H.; Lu, X. B.; Ren, W. M.; Darensbourg, D. J. *Macromolecules* **2010**, *43*, 9202; (c) Wu, G.-P.; Darensbourg, D. J.; Lu, X.-B. *J. Am. Chem. Soc.* **2012**, *134*, 17739-17745; (d) Wu, G.-P.; Xu, P.-X.; Zu, Y.-P.; Ren, W.-M.; Lu, X.-B. *J. Poly. Sci., Part A: Polym. Chem.* **2013**, *51*, 874-879; (e) Lu, X.-B.; Ren, W.-M.; Wu, G.-P. *Acc. Chem. Res.* **2012**, *45*, 1721-1735.
34. Harrold, N. D.; Li, Y.; Chisholm, M. H. *Macromolecules* **2013**, *46*, 692-698.
35. Wu, G.-P.; Wei, S.-H.; Ren, W.-M.; Lu, X.-B.; Xu, T.-Q.; Darensbourg, D. J. *J. Am. Chem. Soc.* **2011**, *133*, 15191-15199.
36. Wu, G.-P.; Xu, P.-X.; Lu, X.-B.; Zu, Y.-P.; Wei, S.-H.; Ren, W.-M.; Darensbourg, D. J. *Macromolecules* **2013**, *46*, 2128-2133.
37. Darensbourg, D. J.; Wilson, S. J. *J. Am. Chem. Soc.* **2011**, *133*, 18610-18613.
38. Darensbourg, D. J.; Yarbrough, J. C. *J. Am. Chem. Soc.* **2002**, *124*, 6335.
39. Darensbourg, D. J.; Mackiewicz, R. M.; Phelps, A. L.; Billodeaux, D. R. *Acc. Chem. Res.* **2004**, *37*, 836.
40. Darensbourg, D. J.; Moncada, A. I.; Choi, W.; Reibenspies, J. H. *J. Am. Chem. Soc.* **2008**, *130*, 6523-6533.
41. Darensbourg, D. J.; Phelps, A. L. *Inorg. Chem.* **2005**, *44*, 4622.
42. (a) Cheng, M.; Moore, D. R.; Reczek, J. J.; Chamberlain, B. M.; Lobkovsky, E. B.; Coates, G. W. *J. Am. Chem. Soc.* **2001**, *123*, 8738; (b) Moore, D. R.; Cheng, M.; Lobkovsky, E. B.; Coates, G. W. *Angew. Chem. Int. Ed.* **2002**, *41*, 2599; (c) Moore, D. R.; Cheng, M.; Lobkovsky, E. B.; Coates, G. W. *J. Am. Chem. Soc.* **2003**, *125*, 11911.
43. Klaus, S.; Vagin, S. I.; Lehenmeier, M. W.; Deglmann, P.; Brym, A. K.; Rieger, B. *Macromolecules* **2011**, *44*, 9508-9516.
44. (a) Bok, T.; Yun, H.; Lee, B. Y. *Inorg. Chem.* **2006**, *45*, 4228-4237; (b) Lee, B. Y.; Kwon, H. Y.; Lee, S. Y.; Na, S. J.; Han, S.-i.; Yun, H.; Lee, H.; Park, Y.-W. *J. Am. Chem. Soc.* **2005**, *127*, 3031-3037.

45. (a) Kember, M. R.; Knight, P. D.; Reung, P. T. R.; Williams, C. K. *Angew. Chem., Int. Ed.* **2009**, *48*, 931; (b) Kember, M. R.; White, A. J. P.; Williams, C. K. *Inorg. Chem.* **2009**, *48*, 9535; (c) Kember, M. R.; White, A. J. P.; Williams, C. K. *Macromolecules* **2010**, *43*, 2291; (d) Kember, M. R.; Williams, C. K. *J. Am. Chem. Soc.* **2012**, *134*, 15676-15679.
46. Cyriac, A.; Lee, S. H.; Varghese, J. K.; Park, E. S.; Park, J. H.; Lee, B. Y. *Macromolecules* **2010**, *43*, 7398-7401.
47. Cyriac, A.; Lee, S. H.; Varghese, J. K.; Park, J. H.; Jeon, J. Y.; Kim, S. J.; Lee, B. Y. *Green Chem.* **2011**, *13*, 3469-3475.
48. Inoue, S. *J. Poly. Sci., Part A: Polym. Chem.* **2000**, *38*, 2861-2871.
49. (a) Lu, X.-B.; Shi, L.; Wang, Y.-M.; Zhang, R.; Zhang, Y.-J.; Peng, X.-J.; Zhang, Z.-C.; Li, B. *J. Am. Chem. Soc.* **2006**, *128*, 1664-1674; (b) Lu, X. B.; Wang, Y. *Angew. Chem. Int. Ed.* **2004**, *43*, 3574; (c) Cohen, C. T.; Chu, T.; Coates, G. W. *J. Am. Chem. Soc.* **2005**, *127*, 10869; (d) Cohen, C. T.; Coates, G. W. *J. Polym. Sci., Part A: Polym. Chem.* **2006**, *44*, 5182.
50. (a) Darensbourg, D. J.; Holtcamp, M. W.; Struck, G. E.; Zimmer, M. S.; Niezgodna, S. A.; Rainey, P.; Roberston, J. B.; Draper, J. D.; Riebenspies, J. H. *J. Am. Chem. Soc.* **1999**, *121*, 107; (b) Lehenmeier, M. W.; Bruckmeier, C.; Klaus, S.; Dengler, J. E.; Deglmann, P.; Ott, A.-K.; Rieger, B. *Chem. Eur. J.* **2011**, *17*, 8858-8869.
51. S, S.; Min, J. K.; Seong, J. E.; Na, S. J.; Lee, B. Y. *Angew. Chem. Int. Ed.* **2008**, *47*, 7306-7309.
52. Na, S. J.; S, S.; Cyriac, A.; Kim, B. E.; Yoo, J.; Kang, Y. K.; Han, S. J.; Lee, C.; Lee, B. Y. *Inorg. Chem.* **2009**, *48*, 10455-10465.
53. Yoo, J.; Na, S. J.; Park, H. C.; Cyriac, A.; Lee, B. Y. *Dalton Trans.* **2010**, *39*, 2622-2630.
54. Ren, W. M.; Liu, Z. W.; Wen, Y. Q.; Zhang, R.; Lu, X. B. *J. Am. Chem. Soc.* **2009**, *131*, 11509.
55. Darensbourg, D.J.; Wilson, S.J. unpublished observations.
56. Cyriac, A.; Jeon, J. Y.; Varghese, J. K.; Park, J. H.; Choi, S. Y.; Chung, Y. K.; Lee, B. Y. *Dalton Trans.* **2012**, *41*, 1444-1447.
57. Elmas, S.; Subhani, M. A.; Vogt, H.; Leitner, W.; Muller, T. E. *Green Chem.* **2013**, *15*, 1356-1360.



58. North, M.; Pasquale, R.; Young, C. *Green Chem.* **2010**, *12*, 1514-1539.
59. Sun, J.; Fujita, S.-i.; Arai, M. *J. Organomet. Chem.* **2005**, *690*, 3490-3497.
60. North, M.; Pasquale, R. *Angew. Chem. Int. Ed.* **2009**, *48*, 2946-2948.
61. Darensbourg, D. J.; Wilson, S. J. *Green Chem.* **2012**, *14*, 2665.
62. Darensbourg, D. J.; Wei, S.-H. *Macromolecules* **2012**, *45*, 5916-5922.
63. Darensbourg, D. J.; Yarbrough, J. C.; Ortiz, C.; Fang, C. C. *J. Am. Chem. Soc.* **2003**, *125*, 7586.
64. Jutz, F.; Buchard, A.; Kember, M. R.; Fredriksen, S. B.; Williams, C. K. *J. Am. Chem. Soc.* **2011**, *133*, 17395-17405.
65. Xiao, Y.; Wang, Z.; Ding, K. *Macromolecules* **2005**, *39*, 128-137.
66. Dümler, W.; Kisch, H. *Chem. Ber.* **1990**, *123*, 277-283.
67. Darensbourg, D. J.; Adams, M. J.; Yarbrough, J. C.; Phelps, A. L. *Inorg. Chem.* **2003**, *42*, 7809-7818.
68. Buchard, A.; Kember, M. R.; Sandeman, K. G.; Williams, C. K. *Chem. Commun.* **2011**, *47*, 212.
69. Darensbourg, D. J.; Fang, C. C.; Rodgers, J. L. *Organometallics* **2004**, *23*, 924.
70. Darensbourg, D. J.; Yeung, A. D. *Macromolecules* **2012**, *46*, 83-95.
71. Ochiai, B.; Endo, T. *Prog. Polym. Sci.* **2005**, *30*, 183-215.
72. Marianucci, E.; Berti, C.; Pilati, F.; Manaresi, P.; Guaita, M.; Chiantore, O. *Polymer* **1994**, *35*, 1564-1566.
73. Vo, C. D.; Kilcher, G.; Tirelli, N. *Macromol. Rapid Commun.* **2009**, *30*, 299-315.
74. Soga, K.; Imamura, H.; Sato, M.; Ikeda, S. *J. Poly. Sci., Part A: Polym. Chem.* **1976**, *14*, 677-684.
75. Nakano, K.; Tatsumi, G.; Nozaki, K. *J. Am. Chem. Soc.* **2007**, *129*, 15116-15117.
76. Clegg, W.; Harrington, R. W.; North, M.; Villuendas, P. *J. Org. Chem.* **2010**, *75*, 6201-6207.

77. Motokuchō, S.; Takeuchi, D.; Sanda, F.; Endo, T. *Tetrahedron* **2001**, *57*, 7149-7152.
78. Zhang, X.-H.; Liu, F.; Sun, X.-K.; Chen, S.; Du, B.-Y.; Qi, G.-R.; Wan, K. M. *Macromolecules* **2008**, *41*, 1587-1590.
79. Darensbourg, D. J.; Andreatta, J. R.; Jungman, M. J.; Reibenspies, J. H. *Dalton Trans.* **2009**, *0*, 8891-8899.
80. Weissermel, K.; Arpe, H. J., *Industrial Organic Chemistry*. 4th ed.; WILEY-VCH VERLAG GMBH & CO.: Weinheim, Germany, 2003.
81. Richardson, T. L.; Lokensgard, E., *Industrial Plastics: Theory & Applications*. Delmar Publications: Clifton Park, NY, 2004.
82. Price from acros.be. (accessed 2.28.2013).
83. Lu, X. B.; Shi, L.; Wang, Y. M.; Zhang, R.; Zhang, Y. J.; Peng, X. J.; Zhang, Z. C.; Li, B. *J. Am. Chem. Soc.* **2006**, *128*, 1664.
84. Ren, W. M.; Zhang, X.; Liu, Y.; Li, J. F.; Wang, H.; Lu, X. B. *Macromolecules* **2010**, *43*, 1396.
85. Takahashi, M.; Ogasawara, K. *Synthesis* **1996**, *8*, 954.
86. *APEX2*, 2009.7-0; Bruker AXS Inc.: Madison, WI, 2007.
87. *SAINTPLUS: Program for Reduction of Area Detector Data*, 6.63; Bruker AXS Inc.: Madison, WI, 2007.
88. Sheldrick, G. M. *SADABS: Program for Absorption Correction of Area Detector Frames*, Bruker AXS Inc.: Madison, WI, 2001.
89. Sheldrick, G. M. *SHELXS-97: Program for Crystal Structure Solution*, Universitat Gottingen: Gottingen, Germany, 1997.
90. Sheldrick, G. M., *SHELXL-97: Program for Crystal Structure Refinement*. Universitat Gottingen: Gottingen, Germany, 1997.
91. Whalen, D. L.; Ross, A. M. *J. Am. Chem. Soc.* **1976**, *98*, 7859.
92. Meinwald, J.; Labana, S. S.; Chadha, M. S. *J. Am. Chem. Soc.* **1963**, *85*, 582.
93. Calculations performed by Andrew Yeung.
94. Liu, J.; Ren, W.-M.; Liu, Y.; Lu, X.-B. *Macromolecules* **2013**, *46*, 1343-1349.

95. Lu, X. B.; Darensbourg, D. J. *Chem. Soc. Rev.* **2012**, *41*, 1462.
96. Vega Gonzalez, A.; Tufeu, R.; Subra, P. *J. Chem. Eng. Data* **2002**, *47*, 492-495.
97. Yang, Z.; Li, M.; Peng, B.; Lin, M.; Dong, Z. *J. Chem. Eng. Data* **2012**, *57*, 1305-1311.
98. Dielectric constants obtained from sigmaaldrich.com (accessed 4.25.2013).
99. Darensbourg, D. J.; Wei, S.-H.; Wilson, S. J. *Macromolecules* **2013**, *46*, 3228-3233.
100. Ren, W. M.; Liu, Y.; Wu, G. P.; Liu, J.; Lu, X. B. *J. Polym. Sci., Part A: Polym. Chem.* **2011**, *49*, 4894.
101. Senanayake, C. H. *Aldrichim. Acta* **1998**, *31*, 3-15.
102. Heston, B. O.; Dermer, O. C.; Woodside, J. A. *Proc. Okla. Acad. Sci.* **1943**, *23*, 67-68.
103. Darensbourg, D. J.; Sanchez, K. M.; Rheingold, A. L. *J. Am. Chem. Soc.* **1987**, *109*, 290-292.
104. Darensbourg, D. J. *Chem. Rev.* **2007**, *107*, 2388.
105. Fletcher, D. A.; McMeeking, R. F.; Parkin, D. *J. Chem. Inf. Comput. Sci.* **1996**, *36*, 746-749.
106. Hiratake, J.; Inagaki, M.; Nishioka, T.; Oda, J. *J. Org. Chem.* **1988**, *53*, 6130-6133.
107. Darensbourg, D. J.; Wei, S. H. *unpublished results*.
108. Brown, C. J. *Acta Crystallogr.* **1954**, *7*, 92-96.
109. Darensbourg, D. J.; Lewis, S. J.; Rodgers, J. L.; Yarbrough, J. C. *Inorg. Chem.* **2003**, *42*, 581.
110. *Images and video generated using CrystalMaker®: a crystal and molecular structures program for Mac and Windows. CrystalMaker Software Ltd, Oxford, England ([www.crystallmaker.com](http://www.crystallmaker.com)).*
111. Shibata, A.; Yamaguchi, T.; Ito, T. *Inorg. Chim. Acta* **1997**, *265*, 197-204.
112. Bertolasi, V.; Bortolini, O.; Fantin, G.; Fogagnolo, M.; Pretto, L. *Tetrahedron: Asymmetry* **2006**, *17*, 308-312.

113. Darensbourg, D. J.; Niezgoda, S. A.; Draper, J. D.; Reibenspies, J. H. *J. Am. Chem. Soc.* **1998**, *120*, 4690-4698.
114. Preetz, W.; Uttecht, J.-G. *Z. Naturforsch., B: Chem. Sci.* **1998**, *53*, 93-100.
115. Hasegawa, Y.; Takahashi, K.; Kume, S.; Nishihara, H. *Chem. Commun.* **2011**, *47*, 6846-6848.
116. Shklover, V.; Eremenko, I. L.; Berke, H.; Nesper, R.; Zakeeruddin, S. M.; Nazeeruddin, M. K.; Grätzel, M. *Inorg. Chim. Acta* **1994**, *219*, 11-21.
117. Perchenek, N.; Simon, A. *Z. Anorg. Allg. Chem.* **1993**, *619*, 98-102.
118. Okamoto, K.-i.; Kirchhoff, J. R.; Heineman, W. R.; Deutsch, E.; Heeg, M. J. *Polyhedron* **1993**, *12*, 749-757.
119. The structure of propylene carbonate was optimized in the gas phase at the B3LYP/6-311++G(2d,p) level of theory by Andrew Yeung.
120. Lu, X.-B.; Wu, G.-P. unpublished results.
121. Darensbourg, D.J.; Chung, W.C. unpublished results.
122. Darensbourg, D.; Wei, S. H.; Wilson, S. J. *Macromolecules* **2013**, submitted.
123. Jordan, R. B., *Reaction Mechanisms of Inorganic and Organic Systems*. 3rd ed.; Oxford University Press: New York, NY, 2007.
124. Darensbourg, D. J.; Chung, W.-C. *Polyhedron* **2013**, *58*, 139-143.
125. Luinstra, G. A.; Haas, G. R.; Molnar, F.; Bernhart, V.; Eberhardt, R.; Rieger, B. *Chem.—Eur. J.* **2005**, *11*, 6298.
126. North, M.; Villuendas, P. *Synlett* **2010**, 623.
127. (a) Durden, J. A.; Stansbury, H. A.; Catlette, W. H. *J. Am. Chem. Soc.* **1960**, *82*, 3082-3084; (b) Taguchi, Y.; Yasumoto, M.; Shibuya, I.; Suhara, Y. *Bull. Chem. Soc. Jpn.* **1989**, *62*, 474-478; (c) Taguchi, Y.; Yanagiya, K.; Shibuya, I.; Suhara, Y. *Bull. Chem. Soc. Jpn.* **1988**, *61*, 921-925.
128. Frisch, M. J.; Trucks, G. W.; Schlegel, H. B.; Scuseria, G. E.; Robb, M. A.; Cheeseman, J. R.; Scalmani, G.; Barone, V.; Mennucci, B.; Petersson, G. A.; Nakatsuji, H.; Caricato, M.; Li, X.; Hratchian, H. P.; Izmaylov, A. F.; Bloino, J.; Zheng, G.; Sonnenberg, J. L.; Hada, M.; Ehara, M.; Toyota, K.; Fukuda, R.; Hasegawa, J.; Ishida, M.; Nakajima, T.; Honda, Y.; Kitao, O.; Nakai, H.; Vreven, T.; Montgomery, J. A.; Peralta, J. E.; Ogliaro, F.; Bearpark, M.; Heyd, J. J.;

- Brothers, E.; Kudin, K. N.; Staroverov, V. N.; Kobayashi, R.; Normand, J.; Raghavachari, K.; Rendell, A.; Burant, J. C.; Iyengar, S. S.; Tomasi, J.; Cossi, M.; Rega, N.; Millam, J. M.; Klene, M.; Knox, J. E.; Cross, J. B.; Bakken, V.; Adamo, C.; Jaramillo, J.; Gomperts, R.; Stratmann, R. E.; Yazyev, O.; Austin, A. J.; Cammi, R.; Pomelli, C.; Ochterski, J. W.; Martin, R. L.; Morokuma, K.; Zakrzewski, V. G.; Voth, G. A.; Salvador, P.; Dannenberg, J. J.; Dapprich, S.; Daniels, A. D.; Farkas; Foresman, J. B.; Ortiz, J. V.; Cioslowski, J.; Fox, D. J. *Gaussian 09, Revision B.01*, Gaussian Inc.: Wallingford CT, 2009.
129. (a) Becke, A. D. *J. Chem. Phys.* **1993**, *98*, 5648-5652; (b) Lee, C.; Yang, W.; Parr, R. G. *Phys. Rev. B: Condens. Matter* **1988**, *37*, 785-789; (c) Vosko, S. H.; Wilk, L.; Nusair, M. *Can. J. Phys.* **1980**, *58*, 1200-1211.
130. Krishnan, R.; Binkley, J. S.; Seeger, R.; Pople, J. A. *J. Chem. Phys.* **1980**, *72*, 650-654.
131. (a) Montgomery, J. A.; Frisch, M. J.; Ochterski, J. W.; Petersson, G. A. *J. Chem. Phys.* **1999**, *110*, 2822-2827; (b) Montgomery, J. A.; Frisch, M. J.; Ochterski, J. W.; Petersson, G. A. *J. Chem. Phys.* **2000**, *112*, 6532-6542.
132. Harding, J. S.; Owen, L. N. *Journal of the Chemical Society (Resumed)* **1954**, *0*, 1528-1536.
133. Goodman, L.; Benitez, A.; Baker, B. R. *J. Am. Chem. Soc.* **1958**, *80*, 1680-1686.
134. Iqbal, S. M.; Owen, L. N. *J. Chem. Soc.* **1960**, 1030-1036.
135. Darensbourg, D. J.; Moncada, A. I. *Inorg. Chem.* **2008**, *47*, 10000-10008.
136. (a) Zander, R.; Rinsland, C. P.; Farmer, C. B.; Namkung, J.; Norton, R. H.; Russell, J. M. *J. Geophys. Res.* **1988**, *93*, 1669-1678; (b) Margoshes, M.; Fillwalk, F.; Fassel, V. A.; Rundle, R. E. *J. Chem. Phys.* **1954**, *22*, 381-382.
137. Perman, C. A.; Gleason, W. B. *Acta Crystallogr., Sect. C: Cryst. Struct. Commun.* **1991**, *47*, 1018-1021.
138. Lieber, E.; Oftedahl, E.; Rao, C. N. R. *J. Org. Chem.* **1963**, *28*, 194-199.
139. Crawford, M.-J.; Klapötke, T. M.; Mayer, P.; Vogt, M. *Inorg. Chem.* **2004**, *43*, 1370-1378.
140. Sommer, F. *Ber. Dtsch. Chem. Ges.* **1915**, *48*, 1833-1841.
141. Bailey, P. J.; Bell, N. L.; Nichol, G. S.; Parsons, S.; White, F. *Inorg. Chem.* **2012**, *51*, 3677-3689.

142. Darensbourg, D. J.; Bottarelli, P.; Andreatta, J. R. *Macromolecules* **2007**, *40*, 7727.
143. Das, B.; Reddy, V. S.; Krishnaiah, M. *Tetrahedron Lett.* **2006**, *47*, 8471-8473.
144. Wu, L.; Yang, L.; Fang, L.; Yang, C.; Yan, F. *Phosphorus, Sulfur Silicon Relat. Elem.* **2010**, *185*, 2159-2164.
145. van Tamelen, E. E. *J. Am. Chem. Soc.* **1951**, *73*, 3444-3448.
146. The "lost" sulfur may be going to form elemental sulfur or be adding to other materials within the reaction. GC-MS analysis reveals that several cyclopentene-based systems with multiple sulfurs are created, though their exact structures have not been determined.
147. Darensbourg, D. J.; Yeung, A. D.; Wei, S.-H. *Green Chem.* **2013**, *15*, 1578-1583.
148. Hadad, C. M.; Rablen, P. R.; Wiberg, K. B. *J. Org. Chem.* **1998**, *63*, 8668-8681.
149. Barbero, M.; Degani, I.; Dughera, S.; Fochi, R.; Piscopo, L. *J. Chem. Soc., Perkin Trans. 1* **1996**, 289.
150. Eick, J. D.; Byerley, T. J.; Chappell, R. P.; Chen, G. R.; Bowles, C. Q.; Chappelow, C. C. *Dent. Mater.* **1993**, *9*, 123-127.
151. (a) Takata, T.; Kanamaru, M.; Endo, T. *Macromolecules* **1997**, *30*, 6721-6726;  
(b) Takata, T.; Endo, T. *Macromolecules* **1988**, *21*, 2314-2318.
152. Darensbourg, D. J.; Wei, S. H. *manuscript in preparation* **2013**.

## APPENDIX A

### COPYRIGHT INFORMATION AND PERMISSIONS



RightsLink®

Home

Create Account

Help



ACS Publications  
High quality. High impact.

**Title:** Synthesis of Poly(indene carbonate) from Indene Oxide and Carbon Dioxide—A Polycarbonate with a Rigid Backbone

**Author:** Donald J. Darensbourg and Stephanie J. Wilson

**Publication:** Journal of the American Chemical Society

**Publisher:** American Chemical Society

**Date:** Nov 1, 2011

Copyright © 2011, American Chemical Society

User ID
<input type="text"/>
Password
<input type="text"/>
<input type="checkbox"/> Enable Auto Login
<input type="button" value="LOGIN"/>
<a href="#">Forgot Password/User ID?</a>
<b>If you're a copyright.com user</b> , you can login to RightsLink using your copyright.com credentials. Already a <b>RightsLink user</b> or want to <a href="#">learn more?</a>

#### PERMISSION/LICENSE IS GRANTED FOR YOUR ORDER AT NO CHARGE

This type of permission/license, instead of the standard Terms & Conditions, is sent to you because no fee is being charged for your order. Please note the following:

- Permission is granted for your request in both print and electronic formats, and translations.
- If figures and/or tables were requested, they may be adapted or used in part.
- Please print this page for your records and send a copy of it to your publisher/graduate school.
- Appropriate credit for the requested material should be given as follows: "Reprinted (adapted) with permission from (COMPLETE REFERENCE CITATION). Copyright (YEAR) American Chemical Society." Insert appropriate information in place of the capitalized words.
- One-time permission is granted only for the use specified in your request. No additional uses are granted (such as derivative works or other editions). For any other uses, please submit a new request.

Message (My Domain)

**From:** "CONTRACTS-COPYRIGHT (shared)" <Contracts-Copyright@rsc.org>  
**Subject:** RE: Dissertation Copyright - Texas A&M University  
**Date:** Sat, 16 Mar 2013 07:24:37 +0000  
**To:** Stephanie Wilson <stephanie.wilson@mail.chem.tamu.edu>

Dear Stephanie

The Royal Society of Chemistry hereby grants permission for the use of the material specified below in the work described and in all subsequent editions of the work for distribution throughout the world, in all media including electronic and microfilm. You may use the material in conjunction with computer-based electronic and information retrieval systems, grant permissions for photocopying, reproductions and reprints, translate the material and to publish the translation, and authorize document delivery and abstracting and indexing services. The Royal Society of Chemistry is a signatory to the STM Guidelines on Permissions (available on request).

Please note that if the material specified below or any part of it appears with credit or acknowledgement to a third party then you must also secure permission from that third party before reproducing that material.

Please ensure that the published article carries a credit to The Royal Society of Chemistry in the following format:

[Original citation] – Reproduced by permission of The Royal Society of Chemistry

and that any electronic version of the work includes a hyperlink to the article on the Royal Society of Chemistry website. The recommended form for the hyperlink is <http://dx.doi.org/10.1039/DOI> suffix, for example in the link <http://dx.doi.org/10.1039/b110420a> the DOI suffix is 'b110420a'. To find the relevant DOI suffix for the RSC paper in question, go to the Journals section of the website and locate your paper in the list of papers for the volume and issue of your specific journal. You will find the DOI suffix quoted there.

Regards

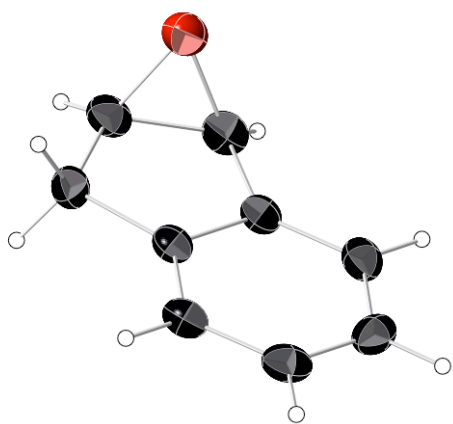
Gill Cockhead  
Publishing Contracts & Copyright Executive

Gill Cockhead (Mrs), Publishing Contracts & Copyright Executive  
Royal Society of Chemistry, Thomas Graham House  
Science Park, Milton Road, Cambridge CB4 0WF, UK  
Tel +44 (0) 1223 432134, Fax +44 (0) 1223 423623  
<http://www.rsc.org>

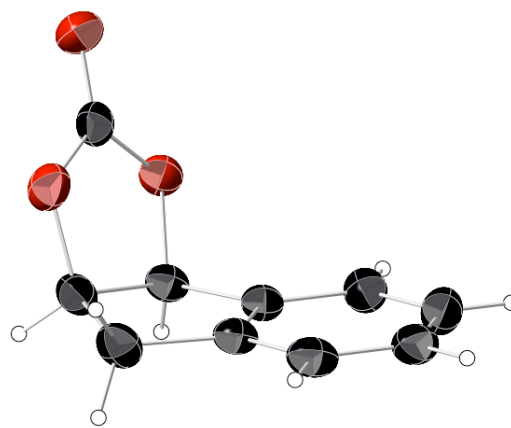


APPENDIX B

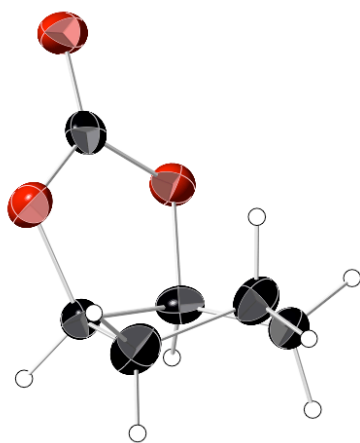
TABLES OF CRYSTALLOGRAPHIC DATA



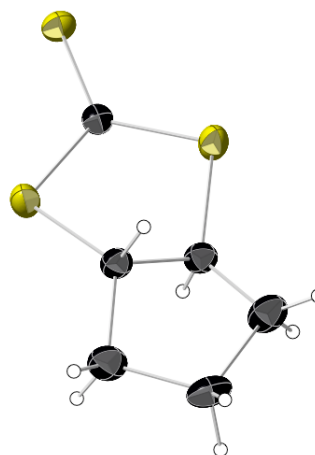
**indene oxide**



***cis*-indene carbonate**



***cis*-cyclopentene carbonate**



***trans*-cyclopentene triiocarbonate**

**Table B-1.** Crystal data and structure refinement for indene oxide.

Identification code	indene oxide	
Empirical formula	C <sub>9</sub> H <sub>8</sub> O	
Formula weight	132.15	
Temperature	110(2) K	
Wavelength	1.54178 $\approx$	
Crystal system	Monoclinic	
Space group	P 21/c	
Unit cell dimensions	a = 7.0295(9) $\approx$	$\alpha = 90^\circ$ .
	b = 8.2003(10) $\approx$	$\beta = 103.520(7)^\circ$ .
	c = 11.7634(16) $\approx$	$\gamma = 90^\circ$ .
Volume	659.30(15) $\approx^3$	
Z	4	
Density (calculated)	1.331 Mg/m <sup>3</sup>	
Absorption coefficient	0.679 mm <sup>-1</sup>	
F(000)	280	
Crystal size	0.14 x 0.13 x 0.13 mm <sup>3</sup>	
Theta range for data collection	6.48 to 60.15 $^\circ$ .	
Index ranges	-7 $\leq$ h $\leq$ 7, -9 $\leq$ k $\leq$ 8, -13 $\leq$ l $\leq$ 13	
Reflections collected	4975	
Independent reflections	975 [R(int) = 0.0373]	
Completeness to theta = 60.15 $^\circ$	99.7 %	
Absorption correction	Semi-empirical from equivalents	
Max. and min. transmission	0.9170 and 0.9110	
Refinement method	Full-matrix least-squares on F <sup>2</sup>	
Data / restraints / parameters	975 / 0 / 92	
Goodness-of-fit on F <sup>2</sup>	1.214	
Final R indices [I $\geq$ 2 $\sigma$ (I)]	R1 = 0.0582, wR2 = 0.1362	
R indices (all data)	R1 = 0.0614, wR2 = 0.1392	
Extinction coefficient	0.094(8)	
Largest diff. peak and hole	0.341 and -0.567 e. $\approx^3$	

**Table B-2.** Atomic coordinates ( $\times 10^4$ ) and equivalent isotropic displacement parameters ( $\approx 2 \times 10^3$ ) for indene oxide.  $U(\text{eq})$  is defined as one third of the trace of the orthogonalized  $U^{ij}$  tensor.

C(1)	3673(3)	2449(2)	-228(2)	30(1)
C(2)	2138(3)	3525(2)	7(2)	31(1)
C(3)	2931(3)	4471(2)	1113(2)	28(1)
C(4)	5000(3)	3829(2)	1529(2)	24(1)
C(5)	6405(3)	4252(2)	2520(2)	28(1)
C(6)	8251(3)	3541(2)	2707(2)	31(1)
C(7)	8686(3)	2427(2)	1921(2)	31(1)
C(8)	7278(3)	1986(2)	926(2)	29(1)
C(9)	5439(3)	2694(2)	741(2)	24(1)
O(1)	2023(2)	1786(2)	201(1)	34(1)

**Table B-3.** Bond lengths [ $\approx$ ] and angles [ $\infty$ ] for indene oxide

C(1)-C(2)	1.470(3)	C(1)-C(2)-C(3)	109.40(17)
C(1)-O(1)	1.472(3)	O(1)-C(2)-H(2)	119.8
C(1)-C(9)	1.490(3)	C(1)-C(2)-H(2)	119.8
C(1)-H(1)	1.0000	C(3)-C(2)-H(2)	119.8
C(2)-O(1)	1.450(2)	C(2)-C(3)-C(4)	103.51(16)
C(2)-C(3)	1.506(3)	C(2)-C(3)-H(3A)	111.1
C(2)-H(2)	1.0000	C(4)-C(3)-H(3A)	111.1
C(3)-C(4)	1.516(3)	C(2)-C(3)-H(3B)	111.1
C(3)-H(3A)	0.9900	C(4)-C(3)-H(3B)	111.1
C(3)-H(3B)	0.9900	H(3A)-C(3)-H(3B)	109.0
C(4)-C(5)	1.384(3)	C(5)-C(4)-C(9)	120.04(18)
C(4)-C(9)	1.398(3)	C(5)-C(4)-C(3)	128.78(19)
C(5)-C(6)	1.393(3)	C(9)-C(4)-C(3)	111.16(17)
C(5)-H(4)	0.9500	C(4)-C(5)-C(6)	118.90(19)
C(6)-C(7)	1.384(3)	C(4)-C(5)-H(4)	120.5
C(6)-H(5)	0.9500	C(6)-C(5)-H(4)	120.5
C(7)-C(8)	1.392(3)	C(7)-C(6)-C(5)	120.92(19)
C(7)-H(6)	0.9500	C(7)-C(6)-H(5)	119.5
C(8)-C(9)	1.387(3)	C(5)-C(6)-H(5)	119.5
C(8)-H(7)	0.9500	C(6)-C(7)-C(8)	120.57(19)
		C(6)-C(7)-H(6)	119.7
C(2)-C(1)-O(1)	59.04(13)	C(8)-C(7)-H(6)	119.7
C(2)-C(1)-C(9)	107.00(17)	C(9)-C(8)-C(7)	118.48(19)
O(1)-C(1)-C(9)	111.71(16)	C(9)-C(8)-H(7)	120.8
C(2)-C(1)-H(1)	121.1	C(7)-C(8)-H(7)	120.8
O(1)-C(1)-H(1)	121.1	C(8)-C(9)-C(4)	121.08(19)
C(9)-C(1)-H(1)	121.1	C(8)-C(9)-C(1)	130.04(18)
O(1)-C(2)-C(1)	60.58(12)	C(4)-C(9)-C(1)	108.87(17)
O(1)-C(2)-C(3)	113.20(16)	C(2)-O(1)-C(1)	60.38(13)

---

**Table B-4.** Anisotropic displacement parameters ( $\approx 2 \times 10^3$ ) for indene oxide. The anisotropic displacement factor exponent takes the form:  $-2\pi^2 [ h^2 a^{*2} U^{11} + \dots + 2 h k a^* b^* U^{12} ]$

	U11	U22	U33	U23	U13	U12
C(1)	34(1)	28(1)	25(1)	0(1)	3(1)	-1(1)
C(2)	31(1)	25(1)	34(1)	6(1)	0(1)	2(1)
C(3)	29(1)	22(1)	34(1)	4(1)	9(1)	2(1)
C(4)	28(1)	19(1)	27(1)	4(1)	7(1)	-2(1)
C(5)	34(1)	23(1)	26(1)	-1(1)	7(1)	-5(1)
C(6)	31(1)	28(1)	29(1)	6(1)	0(1)	-7(1)
C(7)	26(1)	28(1)	38(1)	12(1)	7(1)	2(1)
C(8)	34(1)	23(1)	32(1)	2(1)	13(1)	2(1)
C(9)	29(1)	20(1)	24(1)	2(1)	6(1)	-2(1)
O(1)	31(1)	29(1)	39(1)	-1(1)	4(1)	-2(1)

**Table B-5.** Hydrogen coordinates ( $\times 10^4$ ) and isotropic displacement parameters ( $\approx 2 \times 10^3$ ) for indene oxide.

	x	y	z	U(eq)
H(1)	3793	2237	-1046	36
H(2)	1189	4053	-658	37
H(3A)	2153	4262	1699	34
H(3B)	2932	5657	954	34
H(4)	6114	5014	3064	33
H(5)	9227	3826	3383	37
H(6)	9955	1958	2062	37
H(7)	7571	1218	387	34

**Table B-6.** Torsion angles [ $^{\circ}$ ] for indene oxide.

---

C(9)-C(1)-C(2)-O(1)	-105.53(16)
O(1)-C(1)-C(2)-C(3)	106.31(17)
C(9)-C(1)-C(2)-C(3)	0.8(2)
O(1)-C(2)-C(3)-C(4)	63.4(2)
C(1)-C(2)-C(3)-C(4)	-2.0(2)
C(2)-C(3)-C(4)-C(5)	-178.95(19)
C(2)-C(3)-C(4)-C(9)	2.7(2)
C(9)-C(4)-C(5)-C(6)	0.6(3)
C(3)-C(4)-C(5)-C(6)	-177.61(18)
C(4)-C(5)-C(6)-C(7)	-0.2(3)
C(5)-C(6)-C(7)-C(8)	-0.2(3)
C(6)-C(7)-C(8)-C(9)	0.2(3)
C(7)-C(8)-C(9)-C(4)	0.2(3)
C(7)-C(8)-C(9)-C(1)	-179.55(18)
C(5)-C(4)-C(9)-C(8)	-0.6(3)
C(3)-C(4)-C(9)-C(8)	177.90(17)
C(5)-C(4)-C(9)-C(1)	179.16(17)
C(3)-C(4)-C(9)-C(1)	-2.3(2)
C(2)-C(1)-C(9)-C(8)	-179.30(19)
O(1)-C(1)-C(9)-C(8)	117.9(2)
C(2)-C(1)-C(9)-C(4)	0.9(2)
O(1)-C(1)-C(9)-C(4)	-61.8(2)
C(3)-C(2)-O(1)-C(1)	-99.97(19)
C(9)-C(1)-O(1)-C(2)	97.36(18)

---

**Table B-7.** Crystal data and structure refinement for *cis*-indene carbonate.

Identification code	<i>cis</i> -indene carbonate	
Empirical formula	C <sub>10</sub> H <sub>8</sub> O <sub>3</sub>	
Formula weight	176.16	
Temperature	293(2) K	
Wavelength	0.71073 $\approx$	
Crystal system	Monoclinic	
Space group	P12(1)/c1	
Unit cell dimensions	a = 8.780(5) $\approx$	$\alpha = 90^\circ$ .
	b = 11.000(6) $\approx$	$\beta = 98.066(6)^\circ$ .
	c = 17.033(9) $\approx$	$\gamma = 90^\circ$ .
Volume	1628.8(14) $\approx^3$	
Z	8	
Density (calculated)	1.437 Mg/m <sup>3</sup>	
Absorption coefficient	0.107 mm <sup>-1</sup>	
F(000)	736	
Crystal size	.25 x .12 x .12 mm <sup>3</sup>	
Theta range for data collection	2.21 to 26.22 $^\circ$ .	
Index ranges	-10 $\leq$ h $\leq$ 10, -13 $\leq$ k $\leq$ 13, -21 $\leq$ l $\leq$ 21	
Reflections collected	16508	
Independent reflections	3265 [R(int) = 0.0403]	
Completeness to theta = 26.22 $^\circ$	99.4 %	
Absorption correction	Semi-empirical from equivalents	
Max. and min. transmission	0.9848 and 0.6617	
Refinement method	Full-matrix least-squares on F <sup>2</sup>	
Data / restraints / parameters	3265 / 0 / 235	
Goodness-of-fit on F <sup>2</sup>	1.032	
Final R indices [I > 2 $\sigma$ (I)]	R1 = 0.0369, wR2 = 0.0885	
R indices (all data)	R1 = 0.0466, wR2 = 0.0951	
Largest diff. peak and hole	0.213 and -0.189 e. $\approx^3$	

**Table B-8.** Atomic coordinates ( $\times 10^4$ ) and equivalent isotropic displacement parameters ( $\approx 2 \times 10^3$ ) for *cis*-indene carbonate. U(eq) is defined as one third of the trace of the orthogonalized  $U^{ij}$  tensor.

	x	y	z	U(eq)
C(1)	5715(2)	1577(1)	1378(1)	27(1)
C(2)	6687(2)	771(1)	1992(1)	31(1)
C(3)	7459(2)	-194(1)	1538(1)	34(1)
C(4)	7253(2)	277(1)	697(1)	28(1)
C(5)	7899(2)	-151(1)	53(1)	36(1)
C(6)	7537(2)	414(2)	-674(1)	38(1)
C(7)	6532(2)	1396(2)	-765(1)	38(1)
C(8)	5874(2)	1825(1)	-124(1)	32(1)
C(9)	6248(2)	1260(1)	605(1)	26(1)
C(10)	7404(2)	2770(1)	2174(1)	31(1)
C(11)	2188(2)	4705(1)	9264(1)	26(1)
C(12)	886(2)	4236(1)	8634(1)	27(1)
C(13)	-182(2)	3450(1)	9056(1)	27(1)
C(14)	608(2)	3377(1)	9900(1)	24(1)
C(15)	142(2)	2740(1)	10532(1)	28(1)
C(16)	1063(2)	2768(1)	11262(1)	31(1)
C(17)	2428(2)	3426(1)	11367(1)	32(1)
C(18)	2884(2)	4083(1)	10743(1)	29(1)
C(19)	1958(2)	4055(1)	10014(1)	24(1)
C(20)	3231(2)	3640(1)	8319(1)	30(1)
O(1)	6156(1)	2808(1)	1628(1)	30(1)
O(2)	7817(1)	1623(1)	2374(1)	37(1)
O(3)	8083(1)	3647(1)	2451(1)	43(1)
O(4)	3586(1)	4331(1)	8967(1)	30(1)
O(5)	1716(1)	3502(1)	8127(1)	33(1)
O(6)	4170(1)	3180(1)	7967(1)	42(1)



**Table B-9.** Bond lengths [ $\approx$ ] and angles [ $\infty$ ] for *cis*-indene carbonate.

C(1)-O(1)	1.4557(18)	C(18)-H(14)	0.9300
C(1)-C(9)	1.500(2)	C(20)-O(6)	1.1974(18)
C(1)-C(2)	1.535(2)	C(20)-O(5)	1.3335(19)
C(1)-H(1)	0.9800	C(20)-O(4)	1.3401(18)
C(2)-O(2)	1.4505(19)		
C(2)-C(3)	1.526(2)	O(1)-C(1)-C(9)	111.66(11)
C(2)-H(2)	0.9800	O(1)-C(1)-C(2)	103.83(11)
C(3)-C(4)	1.510(2)	C(9)-C(1)-C(2)	104.55(12)
C(3)-H(3A)	0.9700	O(1)-C(1)-H(1)	112.1
C(3)-H(3B)	0.9700	C(9)-C(1)-H(1)	112.1
C(4)-C(5)	1.387(2)	C(2)-C(1)-H(1)	112.1
C(4)-C(9)	1.390(2)	O(2)-C(2)-C(3)	110.62(13)
C(5)-C(6)	1.383(2)	O(2)-C(2)-C(1)	102.26(11)
C(5)-H(4)	0.9300	C(3)-C(2)-C(1)	107.53(12)
C(6)-C(7)	1.390(2)	O(2)-C(2)-H(2)	112.0
C(6)-H(5)	0.9300	C(3)-C(2)-H(2)	112.0
C(7)-C(8)	1.387(2)	C(1)-C(2)-H(2)	112.0
C(7)-H(6)	0.9300	C(4)-C(3)-C(2)	103.83(12)
C(8)-C(9)	1.386(2)	C(4)-C(3)-H(3A)	111.0
C(8)-H(7)	0.9300	C(2)-C(3)-H(3A)	111.0
C(10)-O(3)	1.1959(18)	C(4)-C(3)-H(3B)	111.0
C(10)-O(1)	1.3358(19)	C(2)-C(3)-H(3B)	111.0
C(10)-O(2)	1.3432(19)	H(3A)-C(3)-H(3B)	109.0
C(11)-O(4)	1.4518(17)	C(5)-C(4)-C(9)	119.87(14)
C(11)-C(19)	1.502(2)	C(5)-C(4)-C(3)	128.77(14)
C(11)-C(12)	1.543(2)	C(9)-C(4)-C(3)	111.35(12)
C(11)-H(8)	0.9800	C(6)-C(5)-C(4)	119.21(15)
C(12)-O(5)	1.4518(17)	C(6)-C(5)-H(4)	120.4
C(12)-C(13)	1.527(2)	C(4)-C(5)-H(4)	120.4
C(12)-H(9)	0.9800	C(5)-C(6)-C(7)	120.74(14)
C(13)-C(14)	1.509(2)	C(5)-C(6)-H(5)	119.6
C(13)-H(10B)	0.9700	C(7)-C(6)-H(5)	119.6
C(13)-H(10A)	0.9700	C(8)-C(7)-C(6)	120.37(15)
C(14)-C(19)	1.390(2)	C(8)-C(7)-H(6)	119.8
C(14)-C(15)	1.393(2)	C(6)-C(7)-H(6)	119.8
C(15)-C(16)	1.385(2)	C(9)-C(8)-C(7)	118.66(15)
C(15)-H(11)	0.9300	C(9)-C(8)-H(7)	120.7
C(16)-C(17)	1.390(2)	C(7)-C(8)-H(7)	120.7
C(16)-H(12)	0.9300	C(8)-C(9)-C(4)	121.15(13)
C(17)-C(18)	1.389(2)	C(8)-C(9)-C(1)	128.22(13)
C(17)-H(13)	0.9300	C(4)-C(9)-C(1)	110.62(12)
C(18)-C(19)	1.386(2)	O(3)-C(10)-O(1)	124.33(14)

O(3)-C(10)-O(2)	123.84(14)	C(16)-C(15)-C(14)	118.98(14)
O(1)-C(10)-O(2)	111.83(12)	C(16)-C(15)-H(11)	120.5
O(4)-C(11)-C(19)	112.53(11)	C(14)-C(15)-H(11)	120.5
O(4)-C(11)-C(12)	104.07(11)	C(15)-C(16)-C(17)	120.73(14)
C(19)-C(11)-C(12)	104.93(11)	C(15)-C(16)-H(12)	119.6
O(4)-C(11)-H(8)	111.6	C(17)-C(16)-H(12)	119.6
C(19)-C(11)-H(8)	111.6	C(18)-C(17)-C(16)	120.57(13)
C(12)-C(11)-H(8)	111.6	C(18)-C(17)-H(13)	119.7
O(5)-C(12)-C(13)	110.96(12)	C(16)-C(17)-H(13)	119.7
O(5)-C(12)-C(11)	102.46(11)	C(19)-C(18)-C(17)	118.52(14)
C(13)-C(12)-C(11)	107.84(11)	C(19)-C(18)-H(14)	120.7
O(5)-C(12)-H(9)	111.7	C(17)-C(18)-H(14)	120.7
C(13)-C(12)-H(9)	111.7	C(18)-C(19)-C(14)	121.24(13)
C(11)-C(12)-H(9)	111.7	C(18)-C(19)-C(11)	128.26(13)
C(14)-C(13)-C(12)	104.32(11)	C(14)-C(19)-C(11)	110.49(12)
C(14)-C(13)-H(10B)	110.9	O(6)-C(20)-O(5)	124.16(14)
C(12)-C(13)-H(10B)	110.9	O(6)-C(20)-O(4)	123.68(14)
C(14)-C(13)-H(10A)	110.9	O(5)-C(20)-O(4)	112.13(12)
C(12)-C(13)-H(10A)	110.9	C(10)-O(1)-C(1)	109.43(11)
H(10B)-C(13)-H(10A)	108.9	C(10)-O(2)-C(2)	110.50(11)
C(19)-C(14)-C(15)	119.93(13)	C(20)-O(4)-C(11)	109.69(11)
C(19)-C(14)-C(13)	111.95(12)	C(20)-O(5)-C(12)	110.87(11)
C(15)-C(14)-C(13)	128.13(13)		

---

**Table B-10.** Anisotropic displacement parameters ( $\approx 2 \times 10^3$ ) for *cis*-indene carbonate. The anisotropic displacement factor exponent takes the form:  $-2p^2 [ h^2 a^* U^{11} + \dots + 2 h k a^* b^* U^{12} ]$

	U11	U22	U33	U23	U13	U12
C(1)	28(1)	22(1)	33(1)	-1(1)	7(1)	-1(1)
C(2)	37(1)	26(1)	31(1)	3(1)	10(1)	0(1)
C(3)	40(1)	25(1)	39(1)	4(1)	8(1)	5(1)
C(4)	28(1)	23(1)	34(1)	-2(1)	7(1)	-3(1)
C(5)	36(1)	28(1)	45(1)	-7(1)	13(1)	0(1)
C(6)	38(1)	44(1)	35(1)	-11(1)	15(1)	-8(1)
C(7)	35(1)	49(1)	29(1)	1(1)	3(1)	-7(1)
C(8)	28(1)	36(1)	33(1)	3(1)	2(1)	1(1)
C(9)	22(1)	26(1)	30(1)	-1(1)	4(1)	-3(1)
C(10)	39(1)	32(1)	24(1)	0(1)	8(1)	-1(1)
C(11)	28(1)	20(1)	31(1)	-2(1)	5(1)	1(1)
C(12)	31(1)	25(1)	26(1)	0(1)	2(1)	5(1)
C(13)	24(1)	31(1)	26(1)	-3(1)	2(1)	2(1)
C(14)	24(1)	23(1)	26(1)	-4(1)	3(1)	6(1)
C(15)	26(1)	27(1)	31(1)	-2(1)	8(1)	2(1)
C(16)	38(1)	30(1)	27(1)	3(1)	11(1)	9(1)
C(17)	35(1)	36(1)	23(1)	-4(1)	0(1)	11(1)
C(18)	27(1)	29(1)	31(1)	-7(1)	1(1)	1(1)
C(19)	26(1)	20(1)	26(1)	-4(1)	4(1)	3(1)
C(20)	37(1)	26(1)	28(1)	3(1)	10(1)	-3(1)
O(1)	35(1)	23(1)	32(1)	0(1)	4(1)	2(1)
O(2)	46(1)	32(1)	30(1)	1(1)	-4(1)	3(1)
O(3)	57(1)	38(1)	35(1)	-9(1)	6(1)	-12(1)
O(4)	29(1)	32(1)	30(1)	-2(1)	6(1)	-3(1)
O(5)	34(1)	39(1)	28(1)	-8(1)	8(1)	-5(1)
O(6)	45(1)	45(1)	42(1)	-4(1)	22(1)	-1(1)

**Table B-11.** Hydrogen coordinates ( $\times 10^4$ ) and isotropic displacement parameters ( $\approx 2 \times 10^3$ ) for *cis*-indene carbonate.

	x	y	z	U(eq)
H(1)	4610	1435	1367	32
H(2)	6071	409	2369	37
H(3A)	8540	-272	1747	41
H(3B)	6963	-977	1567	41
H(4)	8569	-810	110	43
H(5)	7970	133	-1108	46
H(6)	6299	1768	-1257	45
H(7)	5194	2478	-183	39
H(8)	2141	5589	9326	32
H(9)	331	4905	8341	33
H(10B)	-1188	3824	9032	33
H(10A)	-301	2648	8818	33
H(11)	-774	2303	10465	33
H(12)	765	2341	11686	37
H(13)	3041	3426	11859	38
H(14)	3791	4532	10814	35

**Table B-12.** Crystal data and structure refinement for *cis*-cyclopentene carbonate.

Identification code	<i>cis</i> -cyclopentene carbonate	
Empirical formula	C <sub>6</sub> H <sub>8</sub> O <sub>3</sub>	
Formula weight	128.12	
Temperature	110(2) K	
Wavelength	1.54178 $\approx$	
Crystal system	Orthorhombic	
Space group	P <sub>2</sub> <sub>1</sub> <sub>2</sub> <sub>1</sub> <sub>2</sub> <sub>1</sub>	
Unit cell dimensions	a = 6.4789(11) $\approx$	$\alpha = 90^\circ$ .
	b = 9.0621(14) $\approx$	$\beta = 90^\circ$ .
	c = 10.0814(15) $\approx$	$\gamma = 90^\circ$ .
Volume	591.90(16) $\approx^3$	
Z	4	
Density (calculated)	1.438 Mg/m <sup>3</sup>	
Absorption coefficient	0.984 mm <sup>-1</sup>	
F(000)	272	
Crystal size	0.49 x 0.12 x 0.12 mm <sup>3</sup>	
Theta range for data collection	6.57 to 60.04 $^\circ$ .	
Index ranges	-6 $\leq$ h $\leq$ 7, -9 $\leq$ k $\leq$ 10, -11 $\leq$ l $\leq$ 11	
Reflections collected	4638	
Independent reflections	870 [R(int) = 0.0511]	
Completeness to theta = 60.04 $^\circ$	98.3 %	
Absorption correction	Semi-empirical from equivalents	
Max. and min. transmission	0.8910 and 0.6441	
Refinement method	Full-matrix least-squares on F <sup>2</sup>	
Data / restraints / parameters	870 / 0 / 83	
Goodness-of-fit on F <sup>2</sup>	1.320	
Final R indices [I $\geq$ 2 $\sigma$ (I)]	R1 = 0.0427, wR2 = 0.1012	
R indices (all data)	R1 = 0.0443, wR2 = 0.1031	
Absolute structure parameter	-0.1(3)	
Extinction coefficient	0.139(9)	
Largest diff. peak and hole	0.395 and -0.400 e. $\approx^3$	

**Table B-13.** Atomic coordinates ( $\times 10^4$ ) and equivalent isotropic displacement parameters ( $\approx 2 \times 10^3$ ) for *cis*-cyclopentene carbonate. U(eq) is defined as one third of the trace of the orthogonalized  $U_{ij}$  tensor.

	x	y	z	U(eq)
C(1)	8406(3)	9149(2)	6572(2)	26(1)
C(2)	9283(3)	8008(2)	7558(2)	28(1)
C(3)	7894(4)	8071(3)	8774(2)	35(1)
C(4)	5866(3)	8666(3)	8246(2)	30(1)
C(5)	6558(3)	9840(2)	7255(2)	26(1)
C(6)	8149(3)	6821(2)	5683(2)	26(1)
O(1)	7763(2)	8249(2)	5452(1)	29(1)
O(2)	9011(2)	6610(2)	6872(2)	30(1)
O(3)	7738(2)	5851(2)	4923(2)	36(1)

**Table B-14.** Bond lengths [ $\approx$ ] and angles [ $\infty$ ] for *cis*-cyclopentene carbonate.

C(1)-O(1)	1.454(3)	C(3)-C(2)-C(1)	106.05(17)
C(1)-C(5)	1.517(3)	O(2)-C(2)-H(2)	112.2
C(1)-C(2)	1.542(3)	C(3)-C(2)-H(2)	112.2
C(1)-H(1)	1.0000	C(1)-C(2)-H(2)	112.2
C(2)-O(2)	1.455(3)	C(4)-C(3)-C(2)	104.05(18)
C(2)-C(3)	1.521(3)	C(4)-C(3)-H(3A)	110.9
C(2)-H(2)	1.0000	C(2)-C(3)-H(3A)	110.9
C(3)-C(4)	1.517(3)	C(4)-C(3)-H(3B)	110.9
C(3)-H(3A)	0.9900	C(2)-C(3)-H(3B)	110.9
C(3)-H(3B)	0.9900	H(3A)-C(3)-H(3B)	109.0
C(4)-C(5)	1.526(3)	C(3)-C(4)-C(5)	102.90(18)
C(4)-H(4A)	0.9900	C(3)-C(4)-H(4A)	111.2
C(4)-H(4B)	0.9900	C(5)-C(4)-H(4A)	111.2
C(5)-H(5A)	0.9900	C(3)-C(4)-H(4B)	111.2
C(5)-H(5B)	0.9900	C(5)-C(4)-H(4B)	111.2
C(6)-O(3)	1.197(3)	H(4A)-C(4)-H(4B)	109.1
C(6)-O(2)	1.336(3)	C(1)-C(5)-C(4)	103.96(16)
C(6)-O(1)	1.338(3)	C(1)-C(5)-H(5A)	111.0
		C(4)-C(5)-H(5A)	111.0
O(1)-C(1)-C(5)	110.99(18)	C(1)-C(5)-H(5B)	111.0
O(1)-C(1)-C(2)	103.33(17)	C(4)-C(5)-H(5B)	111.0
C(5)-C(1)-C(2)	105.94(18)	H(5A)-C(5)-H(5B)	109.0
O(1)-C(1)-H(1)	112.0	O(3)-C(6)-O(2)	124.2(2)
C(5)-C(1)-H(1)	112.0	O(3)-C(6)-O(1)	123.9(2)
C(2)-C(1)-H(1)	112.0	O(2)-C(6)-O(1)	111.93(18)
O(2)-C(2)-C(3)	110.10(18)	C(6)-O(1)-C(1)	110.69(17)
O(2)-C(2)-C(1)	103.44(17)	C(6)-O(2)-C(2)	110.61(15)

**Table B-15.** Anisotropic displacement parameters ( $\approx 2 \times 10^3$ ) for *cis*-cyclopentene carbonate. The anisotropic displacement factor exponent takes the form:  $-2p^2 [h^2 a^2 U^{11} + \dots + 2 h k a^* b^* U^{12}]$

	U11	U22	U33	U23	U13	U12
C(1)	29(1)	24(1)	26(1)	-2(1)	-1(1)	-6(1)
C(2)	25(1)	30(1)	28(1)	-7(1)	-7(1)	4(1)
C(3)	50(2)	31(1)	23(1)	1(1)	-1(1)	7(1)
C(4)	31(1)	27(1)	31(1)	-3(1)	8(1)	0(1)
C(5)	28(1)	21(1)	29(1)	-2(1)	-3(1)	2(1)
C(6)	17(1)	32(1)	29(1)	-4(1)	3(1)	1(1)
O(1)	32(1)	29(1)	24(1)	-2(1)	-4(1)	2(1)
O(2)	37(1)	27(1)	27(1)	-3(1)	-3(1)	6(1)
O(3)	28(1)	39(1)	40(1)	-17(1)	2(1)	-4(1)

**Table B-16.** Hydrogen coordinates ( $\times 10^4$ ) and isotropic displacement parameters ( $\approx 2 \times 10^3$ ) for *cis*-cyclopentene carbonate.

	x	y	z	U(eq)
H(1)	9459	9902	6312	32
H(2)	10761	8205	7782	33
H(3A)	7707	7077	9163	42
H(3B)	8476	8736	9457	42
H(4A)	5027	9104	8965	36
H(4B)	5057	7881	7803	36
H(5A)	5449	10060	6609	31
H(5B)	6953	10763	7715	31



**Table B-17.** Torsion angles [ $^{\circ}$ ] for *cis*-cyclopentene carbonate.

---

O(1)-C(1)-C(2)-O(2)	-0.3(2)
C(5)-C(1)-C(2)-O(2)	116.44(17)
O(1)-C(1)-C(2)-C(3)	-116.22(19)
C(5)-C(1)-C(2)-C(3)	0.6(2)
O(2)-C(2)-C(3)-C(4)	-87.2(2)
C(1)-C(2)-C(3)-C(4)	24.1(2)
C(2)-C(3)-C(4)-C(5)	-39.5(2)
O(1)-C(1)-C(5)-C(4)	86.6(2)
C(2)-C(1)-C(5)-C(4)	-24.9(2)
C(3)-C(4)-C(5)-C(1)	40.0(2)
O(3)-C(6)-O(1)-C(1)	178.9(2)
O(2)-C(6)-O(1)-C(1)	0.1(2)
C(5)-C(1)-O(1)-C(6)	-112.99(19)
C(2)-C(1)-O(1)-C(6)	0.2(2)
O(3)-C(6)-O(2)-C(2)	-179.18(19)
O(1)-C(6)-O(2)-C(2)	-0.3(2)
C(3)-C(2)-O(2)-C(6)	113.39(19)
C(1)-C(2)-O(2)-C(6)	0.4(2)

---

**Table B-18.** Crystal data and structure refinement for *trans*-cyclopentene trithiocarbonate.

Identification code	<i>trans</i> -cyclopentene trithiocarbonate	
Empirical formula	C <sub>6</sub> H <sub>8</sub> S <sub>3</sub>	
Formula weight	176.30	
Temperature	110(2) K	
Wavelength	0.71073 $\approx$	
Crystal system	Orthorhombic	
Space group	Pnma	
Unit cell dimensions	a = 13.053(3) $\approx$	$\alpha = 90^\circ$ .
	b = 9.571(2) $\approx$	$\beta = 90^\circ$ .
	c = 6.0856(15) $\approx$	$\gamma = 90^\circ$ .
Volume	760.2(3) $\approx^3$	
Z	4	
Density (calculated)	1.540 Mg/m <sup>3</sup>	
Absorption coefficient	0.879 mm <sup>-1</sup>	
F(000)	368	
Crystal size	0.39 x 0.10 x 0.10 mm <sup>3</sup>	
Theta range for data collection	3.12 to 26.00 $^\circ$ .	
Index ranges	-16 $\leq$ h $\leq$ 16, -11 $\leq$ k $\leq$ 11, -7 $\leq$ l $\leq$ 7	
Reflections collected	7231	
Independent reflections	789 [R(int) = 0.0626]	
Completeness to theta = 26.00 $^\circ$	100.0 %	
Absorption correction	None	
Max. and min. transmission	0.9173 and 0.7256	
Refinement method	Full-matrix least-squares on F <sup>2</sup>	
Data / restraints / parameters	789 / 2 / 52	
Goodness-of-fit on F <sup>2</sup>	1.123	
Final R indices [I > 2 $\sigma$ (I)]	R1 = 0.0249, wR2 = 0.0718	
R indices (all data)	R1 = 0.0275, wR2 = 0.0727	
Largest diff. peak and hole	0.309 and -0.317 e. $\approx^3$	

**Table B-19.** Atomic coordinates ( $\times 10^4$ ) and equivalent isotropic displacement parameters ( $\approx 2 \times 10^3$ ) for *trans*-cyclopentene trithiocarbonate.  $U(\text{eq})$  is defined as one third of the trace of the orthogonalized  $U^{\text{ij}}$  tensor.

	x	y	z	U(eq)
S(1)	1631(1)	2500	1020(1)	23(1)
S(2)	2971(1)	4041(1)	4129(1)	27(1)
C(1)	2491(2)	2500	3006(4)	19(1)
C(3)	4445(1)	3811(2)	7735(3)	32(1)
C(4)	4909(2)	2500	8881(4)	32(1)
C(2)	3968(3)	3164(4)	5698(6)	22(1)
C(2')	3564(3)	3247(4)	6442(6)	22(1)

**Table B-20.** Bond lengths [ $\approx$ ] and angles [ $\infty$ ] for *trans*-cyclopentene trithiocarbonate.

S(1)-C(1)	1.650(2)	C(2')-C(3)-H(3A)	86.1
S(2)-C(1)	1.7415(13)	C(2)-C(3)-H(3A)	111.5
S(2)-C(2')	1.777(4)	C(4)-C(3)-H(3A)	111.5
S(2)-C(2)	1.820(4)	C(2')-C(3)-H(3B)	131.3
C(1)-S(2)#1	1.7415(13)	C(2)-C(3)-H(3B)	111.5
C(3)-C(2')	1.494(4)	C(4)-C(3)-H(3B)	111.5
C(3)-C(2)	1.519(4)	H(3A)-C(3)-H(3B)	109.3
C(3)-C(4)	1.558(2)	C(3)#1-C(4)-C(3)	107.26(19)
C(3)-H(3A)	0.9900	C(3)#1-C(4)-H(4A)	110.3
C(3)-H(3B)	0.9900	C(3)-C(4)-H(4A)	110.3
C(4)-C(3)#1	1.558(2)	C(3)#1-C(4)-H(4B)	110.3
C(4)-H(4A)	0.9900	C(3)-C(4)-H(4B)	110.3
C(4)-H(4B)	0.9900	H(4A)-C(4)-H(4B)	108.5
C(2)-H(2)	1.0551	C(3)-C(2)-S(2)	122.2(3)
C(2')-C(2)#1	1.518(4)	C(3)-C(2)-H(2)	109.6
C(2')-H(2')	1.0246	S(2)-C(2)-H(2)	111.7
		C(3)-C(2')-C(2)#1	102.2(3)
C(1)-S(2)-C(2')	96.06(14)	C(3)-C(2')-S(2)	126.7(3)
C(1)-S(2)-C(2)	94.17(14)	C(2)#1-C(2')-S(2)	107.2(3)
C(2')-S(2)-C(2)	22.41(12)	C(3)-C(2')-H(2')	110.1
S(1)-C(1)-S(2)	122.16(6)	C(2)#1-C(2')-H(2')	104.5
S(1)-C(1)-S(2)#1	122.16(6)	S(2)-C(2')-H(2')	104.2
S(2)-C(1)-S(2)#1	115.69(13)		
C(2')-C(3)-C(2)	26.85(15)		
C(2')-C(3)-C(4)	104.1(2)		
C(2)-C(3)-C(4)	101.3(2)		

---

Symmetry transformations used to generate equivalent atoms:  
 #1  $x, -y+1/2, z$

**Table B-21.** Anisotropic displacement parameters ( $\approx 2 \times 10^3$ ) for *cpttc*. The anisotropic displacement factor exponent takes the form:  $-2p^2 [ h^2 a^2 U^{11} + \dots + 2 h k a^* b^* U^{12} ]$

	U <sup>11</sup>	U <sup>22</sup>	U <sup>33</sup>	U <sup>23</sup>	U <sup>13</sup>	U <sup>12</sup>
S(1)	21(1)	27(1)	22(1)	0	-5(1)	0
S(2)	31(1)	19(1)	32(1)	-3(1)	-11(1)	2(1)
C(1)	16(1)	21(1)	19(1)	0	4(1)	0
C(3)	28(1)	37(1)	32(1)	-8(1)	-8(1)	1(1)
C(4)	27(1)	49(2)	21(1)	0	-6(1)	0
C(2)	21(2)	25(1)	21(2)	-1(1)	-2(1)	2(1)
C(2')	21(2)	25(1)	21(2)	-1(1)	-2(1)	2(1)

**Table B-22.** Hydrogen coordinates ( $\times 10^4$ ) and isotropic displacement parameters ( $\approx 2 \times 10^3$ ) for *trans*-cyclopentene trithiocarbonate.

	x	y	z	U(eq)
H(3A)	3922	4267	8670	39
H(3B)	4981	4499	7348	39
H(4A)	5665	2500	8730	39
H(4B)	4736	2500	10464	39
H(2)	4551	2770	4669	76(14)
H(2')	2966	3011	7469	44(12)

**Table B-23.** Torsion angles [ $^{\circ}$ ] for *trans*-cyclopentene trithiocarbonate.

---

C(2')-S(2)-C(1)-S(1)	167.11(19)
C(2)-S(2)-C(1)-S(1)	-170.47(19)
C(2')-S(2)-C(1)-S(2)#1	-12.40(19)
C(2)-S(2)-C(1)-S(2)#1	10.02(19)
C(2')-C(3)-C(4)-C(3)#1	14.0(3)
C(2)-C(3)-C(4)-C(3)#1	-13.4(3)
C(2')-C(3)-C(2)-S(2)	61.1(5)
C(4)-C(3)-C(2)-S(2)	160.1(3)
C(1)-S(2)-C(2)-C(3)	-156.5(3)
C(2')-S(2)-C(2)-C(3)	-60.7(5)
C(2)-C(3)-C(2')-C(2)#1	51.4(5)
C(4)-C(3)-C(2')-C(2)#1	-35.8(3)
C(2)-C(3)-C(2')-S(2)	-71.1(5)
C(4)-C(3)-C(2')-S(2)	-158.3(3)
C(1)-S(2)-C(2')-C(3)	155.6(3)
C(2)-S(2)-C(2')-C(3)	69.4(5)
C(1)-S(2)-C(2')-C(2)#1	35.2(2)
C(2)-S(2)-C(2')-C(2)#1	-51.0(5)

---

Symmetry transformations used to generate equivalent atoms:

#1  $x, -y+1/2, z$

## APPENDIX C

### THREE-DIMENSIONAL STACK PLOTS AND REACTION PROFILES FOR THE COUPLING OF CYCLOPENTENE OXIDE AND CS<sub>2</sub> UTILIZING PPNN<sub>3</sub>

Typical reaction setup: (salen)CrCl (0.0483 g, 0.076 mmol, 1 eq) and the appropriate amount of PPNN<sub>3</sub> were added to a vial. Approximately 15 mL dry CH<sub>2</sub>Cl<sub>2</sub> was added, and the solution was allowed to stir for 15 minutes under argon to allow for catalyst activation. Following solvent removal *in vacuo*, 10.0 mL cyclopentene oxide was added to the vial, and the resulting solution was cannulated into a 300 mL stainless steel Parr reactor equipped with a permanently mounted SiComp crystal. A background spectrum was taken. The vial was rinsed with the appropriate amount of CS<sub>2</sub>, and the solution was injected into the reaction vessel. The reactor was heated to 80 °C, and the reaction was monitored for 24 hours. Relevant peaks were chosen for the traces depicted in Figures C-7 through C-11.

In the following tables and figures, reaction loadings refer to the relative amounts of (salen)CrCl : PPNN<sub>3</sub> : cyclopentene oxide : CS<sub>2</sub>. That is, 1:2:1500:3000 refers to a reaction containing 1 equivalent (salen)CrCl, 2 equivalents PPNN<sub>3</sub>, 1500 equivalents cyclopentene oxide, and 3000 equivalents CS<sub>2</sub>.

In general, peak production of the -O-(C=O)-S- polymer peak at 1712 cm<sup>-1</sup> (dark green) is maximized after ~4 hours. The peak at 1057 cm<sup>-1</sup> (red) has tentatively been assigned to *trans*-cyclopentene trithiocarbonate, although the large amount of overlap in that region may mean that this assignment is incorrect. Whatever the identity, peak production typically occurs at ~4 hours. When a limiting amount of CS<sub>2</sub> is employed, it is quickly consumed (1514 cm<sup>-1</sup>, orange). In the other reactions, the absorbance holds at ~0.85 A.U. until the concentration is lowered enough for a concentration change to be observed. CO<sub>2</sub> (2338 cm<sup>-1</sup>, pink) is often produced during the course of the reaction, particularly when limiting amounts of CS<sub>2</sub> are employed. COS (2038 cm<sup>-1</sup>, lime green) is

also sometimes observed. When CO<sub>2</sub> is added to the reaction, *cis*-cyclopentene carbonate production is very quickly achieved (1806 cm<sup>-1</sup>, black).

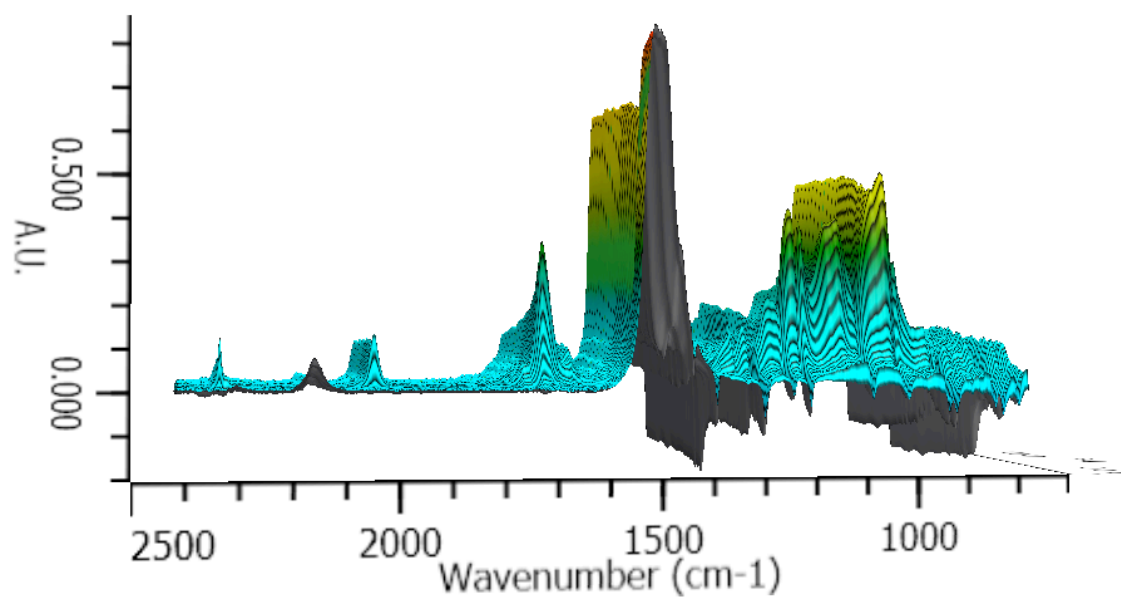


**Figure C-1.** Three dimensional stack plot of FT-IR scans for the coupling of cyclopentene oxide and CS<sub>2</sub>. Reaction loading 1:2:1500:3000.

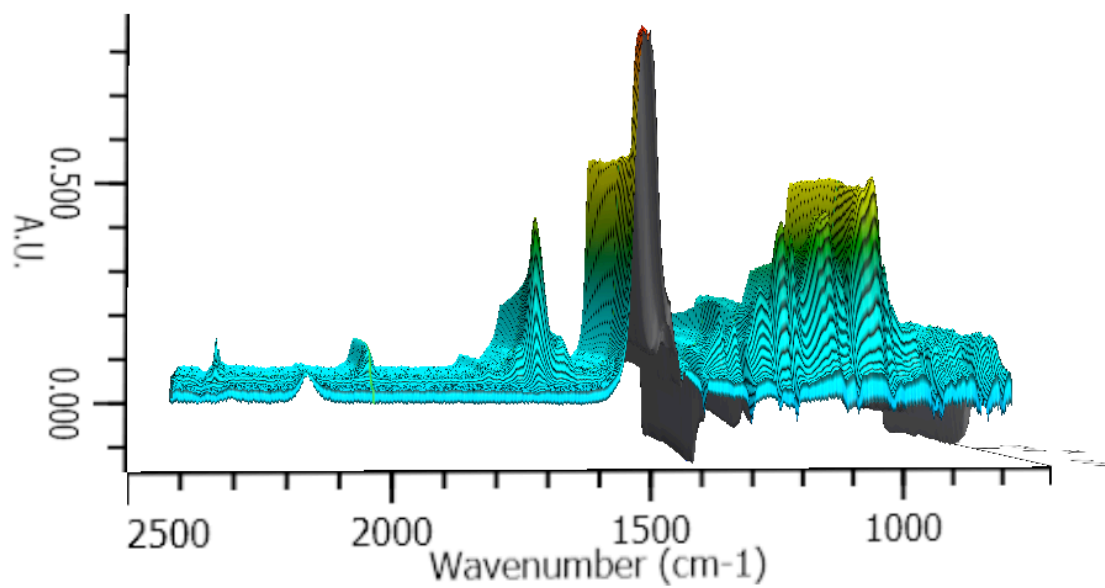


**Figure C-2.** Three dimensional stack plot of FT-IR scans for the coupling of cyclopentene oxide and CS<sub>2</sub>. Reaction loading 1:2:1500:1500.

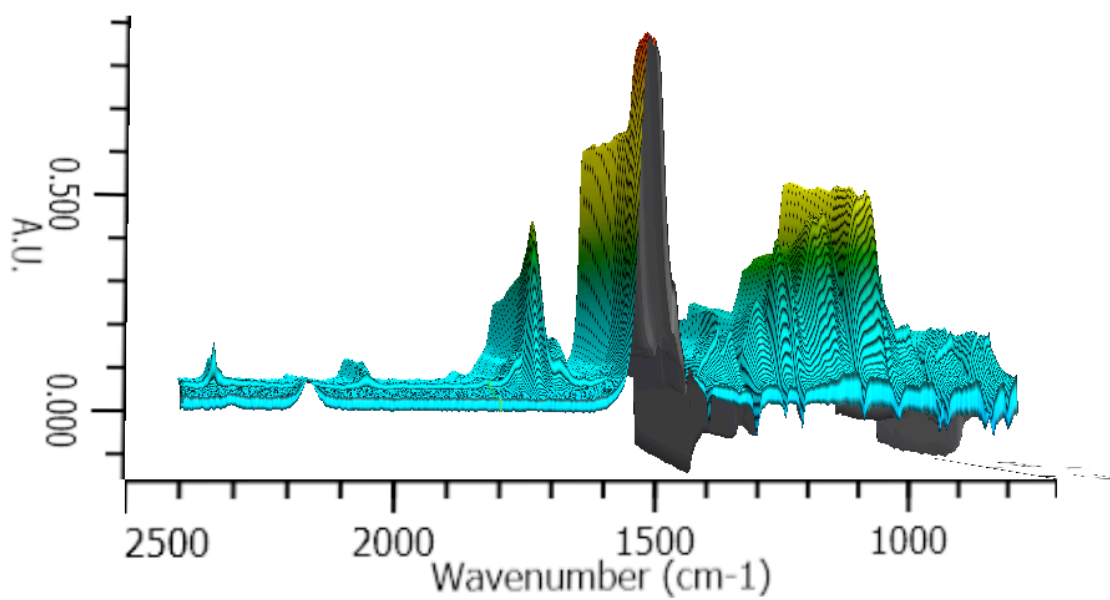


**Figure C-3.** Three dimensional stack plot of FT-IR scans for the coupling of cyclopentene oxide and CS<sub>2</sub>. Reaction loading 1:1:1500:1500.



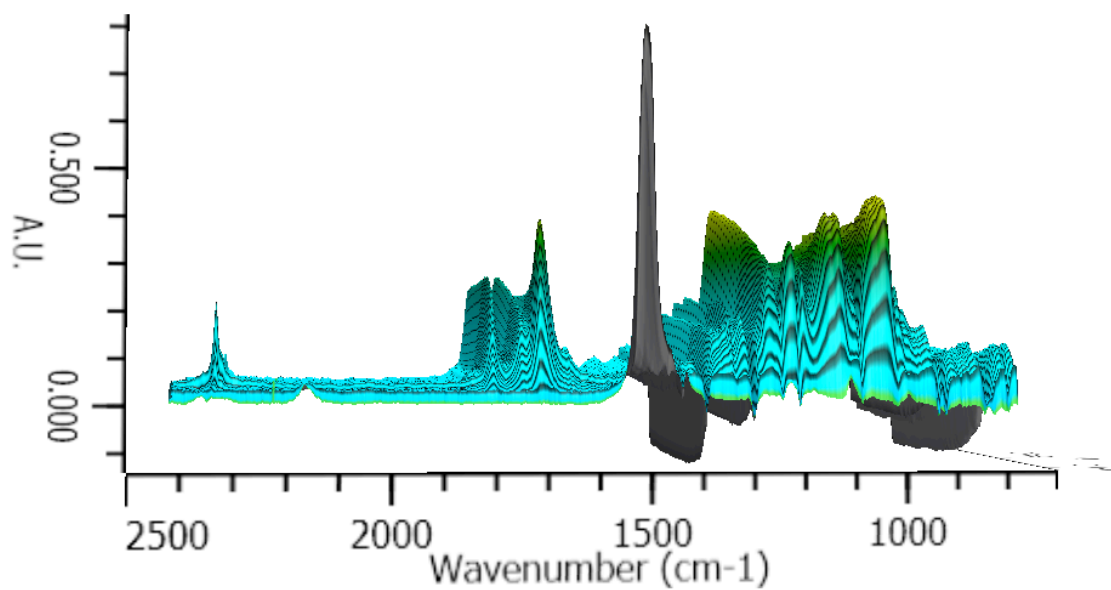


**Figure C-4.** Three dimensional stack plot of FT-IR scans for the coupling of cyclopentene oxide and CS<sub>2</sub>. Reaction loading 1:2:1500:750.

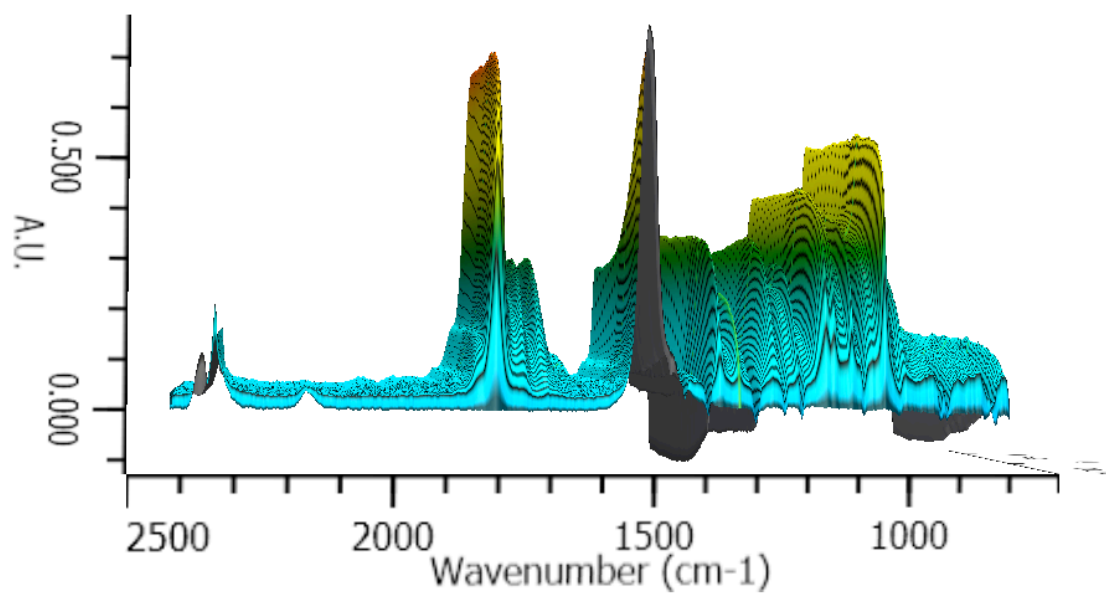


**Figure C-5.** Three dimensional stack plot of FT-IR scans for the coupling of cyclopentene oxide and CS<sub>2</sub>. Reaction loading 1:2:1500:750 + 0.7 MPa CO<sub>2</sub>.

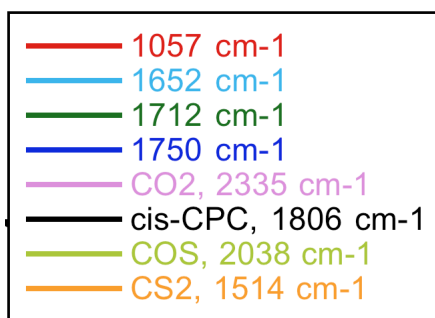


**Figure C-6.** Legend for traces of cyclopentene oxide/CS<sub>2</sub> coupling reactions.

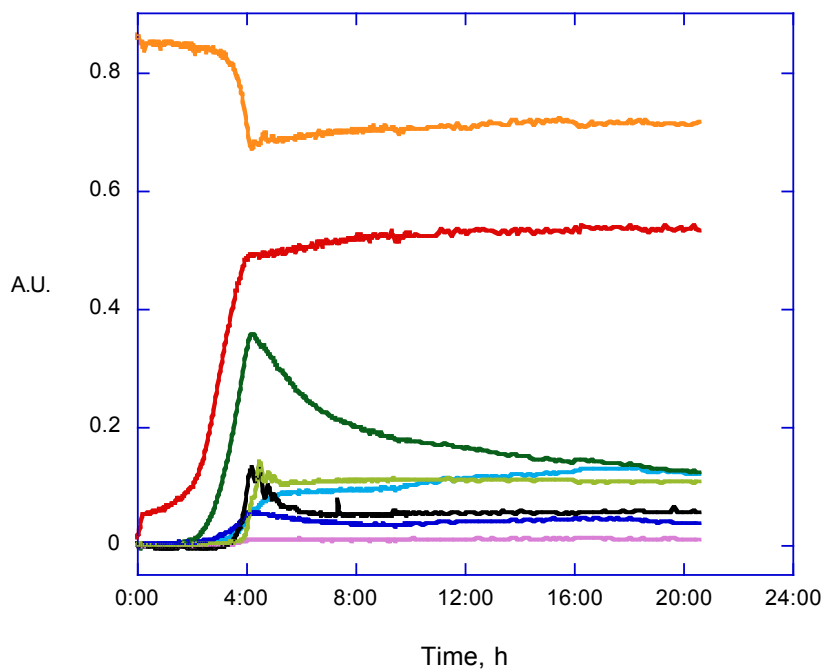


**Figure C-7.** FT-IR trace for reaction loading 1:2:1500:3000.

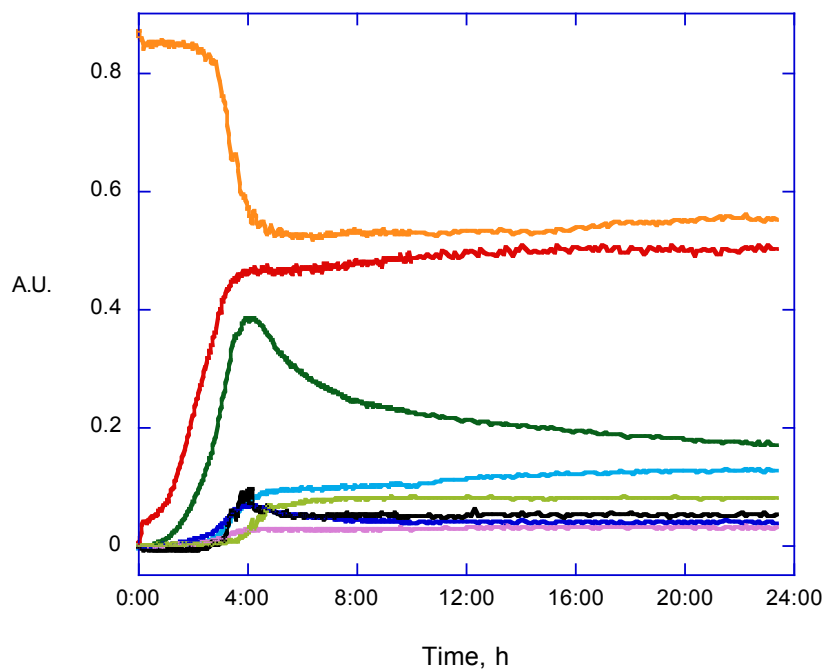


**Figure C-7.** FT-IR trace for reaction loading 1:2:1500:1500.

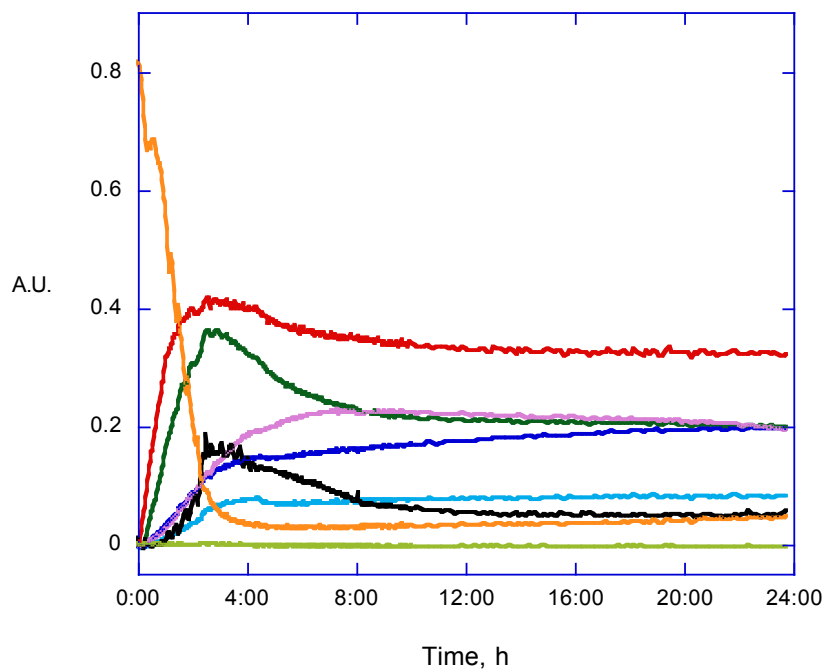


**Figure C-7.** FT-IR trace for reaction loading 1:2:1500:750.

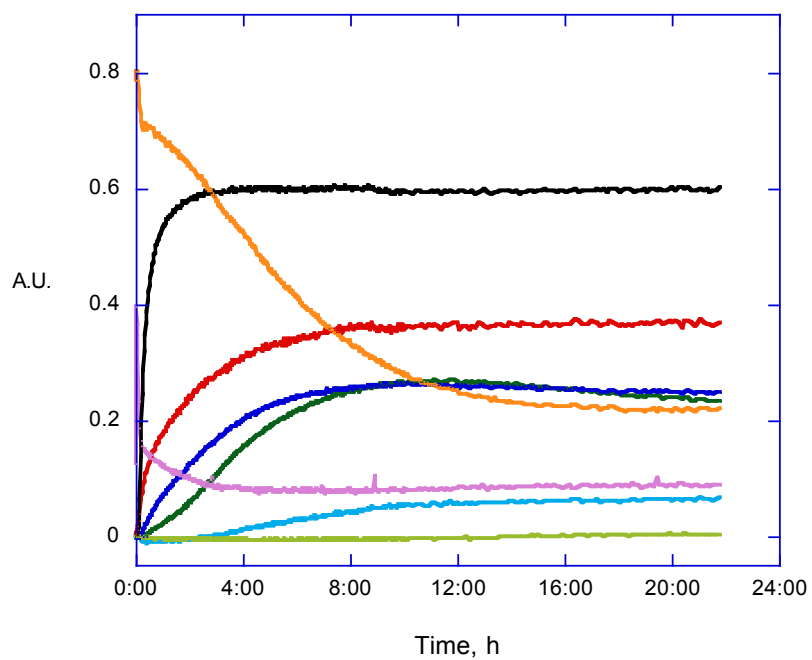


**Figure C-7.** FT-IR trace for reaction loading 1:2:1500:750 + 0.7 MPa CO<sub>2</sub>.

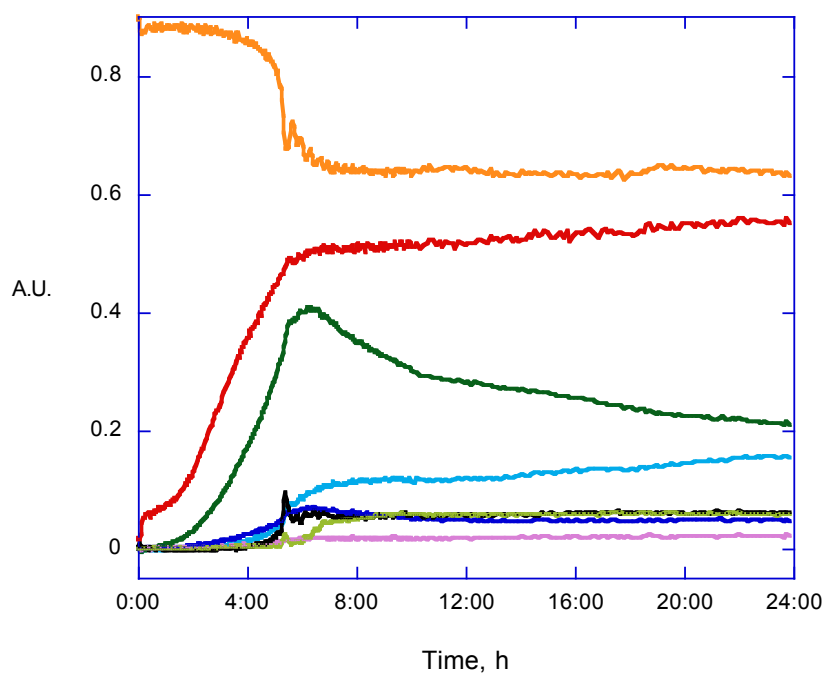


**Figure C-7.** FT-IR trace for reaction loading 1:1:1500:1500.

## APPENDIX D

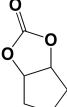
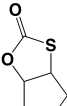
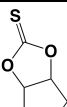
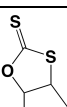
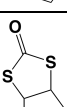
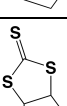
### SUPPLEMENTARY DATA FOR CYCLIC [THIO]CARBONATES

#### DISCUSSED IN CHAPTER IV

**Materials and Methods.** NMR shielding tensors were obtained using the Gauge-Independent Atomic Orbital (GIAO) method. NMR and IR data reported here were obtained by calculations using B3LYP/6-311+G(2d,p)-optimized geometries by Andrew Yeung.

GC-MS was performed on Ultra GC/DSQ (ThermoElectron, Waltham, MA). Rxi-5ms was used as a gas chromatographic column with dimensions of 60 m length, 0.25 mm i.d., and 0.25  $\mu\text{m}$  film thickness (Restek; Bellefonte, PA). Helium was used as a carrier gas at constant flow of 1.5 ml/min. An aliquot of 1  $\mu\text{L}$  of sample was injected in splitless mode. Transfer line and ion source were held at 250°C. The column temperature was maintained at 50 °C for 5 min and raised to 320 °C at 20 °C/min. Mass spectra were acquired in full scan mode in the range of 30-500 m/z. Calculated relative enthalpies of the cyclic [thio]carbonate materials can be found in Figures IV-7 through IV-10.

**Table D-1.** Calculated parameters of cyclic cyclopentene [thio]carbonates.

Cyclic [thio]carbonate family	Isomer <sup>a</sup>	Relative Enthalpy, kJ/mol <sup>b</sup>	C=X <sup>13</sup> C NMR, ppm <sup>c</sup>	IR C=X, cm <sup>-1</sup>	IR C=X (scaled), cm <sup>-1 d,e</sup>
	<i>cis</i> -boat	0.0	160.6	1871	1807
	<i>cis</i> -chair	2.5	160.3	1873	1809
	<i>trans</i> -	19.2	164.4	1890	1826
	<i>cis</i> -boat	0.0	178.8	1812	1750
	<i>cis</i> -chair	1.0	178.0	1814	1752
	<i>trans</i> -	10.3	182.3	1833	1771
	<i>cis</i> -boat	14.7	200.0	1289	1245
	<i>cis</i> -chair	17.5	199.4	1299	1255
	<i>trans</i> -	34.7	207.1	1301	1257
	<i>cis</i> -boat	11.7	222.5	1211	1170
	<i>cis</i> -chair	12.8	221.3	1225	1183
	<i>trans</i> -	22.9	228.8	1194	1153
	<i>cis</i> -boat	0.0	205.5	1748	1689
	<i>cis</i> -chair	0.3	204.4	1754	1694
	<i>trans</i> -	4.1	208.8	1772	1712
	<i>cis</i> -boat	0.0	244.2	1068	1032
	<i>cis</i> -chair	0.1	242.9	1073	1037
	<i>trans</i> -	5.0	250.8	1072	1036

(a) As defined in Figure X. (b) CBS-QB3, gas phase. (c) ± 5 ppm, gas phase.  
(d) Strongest vibration presented. Vibrations are strongly coupled to cyclopentane ring. (e) IR frequencies scaled by 0.966 as recommended by NIST.

**Table D-2.** GC-MS data for cyclic cyclopentene [thio]carbonates.

Elution Time, min.	X <sub>3</sub> Type	Known Identity	Notable m/z
12.26	O <sub>3</sub>	<i>cis</i> -cyclopentene carbonate	128, 99, 83, 56, 55, 41
13.18	SO <sub>2</sub>	not determined, but likely -O-(C=S)-O- (m/z of C=S is 44)	144, 100, 85, 71, 67, 66
13.96	S <sub>2</sub> O	-	160, 136, 100, 85, 71, 67, 66
14.19	S <sub>2</sub> O	<i>cis</i> -cyclopentene dithiocarbonate (-S-(C=O)-S-)	160, 132, 99, 85, 71, 67, 66
14.68	S <sub>2</sub> O	-	160, 147, 100, 85, 71, 67, 66
14.76	S <sub>2</sub> O	-	160, 144, 99, 85, 71, 67, 66
15.69	S <sub>3</sub>	<i>trans</i> -cyclopentene trithiocarbonate	176, 134, 108, 100, 85, 71, 67
15.88	S <sub>3</sub>	<i>cis</i> -cyclopentene trithiocarbonate	176, 174, 132, 108, 100, 85, 71, 67, 66, 45

**Table D-2.** GC-MS data for cyclic cyclohexene [thio]carbonates.

Elution Time, min.	X <sub>3</sub> Type	Known Identity	Notable m/z
13.13	O <sub>3</sub>	<i>trans</i> -cyclohexene carbonate	142, 98, 69, 58, 41
14.66 <sup>a</sup>	S <sub>2</sub> O	-	174, 114, 99, 81, 73, 67
15.37	S <sub>2</sub> O	-	174, 114, 99, 81, 73, 67
16.32	S <sub>2</sub> O	<i>trans</i> -cyclohexene trithiocarbonate	190, 81, 80, 73

(a) Co-elutes with m/z = 219 (identity unknown).

**Table D-3.** GC-MS data for other notable materials.

Elution Time, min.	Known Identity	Notable m/z
8.50	cyclopentene sulfide	100, 85, 67
10.42	cyclohexene sulfide	114, 99, 81, 79
13.26 <sup>a</sup>	cyclopentene sulfide•S <sub>2</sub>	164
13.66 <sup>a</sup>	(C <sub>5</sub> H <sub>8</sub> ) <sub>2</sub> S	170
15.13 <sup>a</sup>	cyclopentene sulfide•S <sub>3</sub>	196

(a) Unidentified materials containing multiple sulfurs. These species likely form at the same time as cyclopentene.

## APPENDIX E

### VITA

Stephanie Jo Wilson was born to Mary Jo and Richard Wilson in Terre Haute, Indiana. She received her high school degree from Terre Haute South Vigo High School in May 2004 and enrolled in the University of Southern Indiana in August of the same year. At USI, Stephanie was a four-year starter for the volleyball team and was named to the CoSIDA Second-Team All American team in 2007. She graduated *summa cum laude* from USI in May 2009 with a B.S. in Chemistry (ACS Certified) and a minor in Mathematics. Stephanie joined the Donald J. Darensbourg research group at Texas A&M University in July 2009. In August 2013, Stephanie received her Ph.D. in Inorganic Chemistry from TAMU. She began her independent academic career as an Assistant Professor of Chemistry at Rose-Hulman Institute of Technology in Terre Haute, Indiana in August 2013.



